Urania
Jurnal Ilmiah Daur Bahan Bakar Nuklir

Beranda jurnal: http://jurnal.batan.go.id/index.php/urania/

THE EFFECT OF TIME IN THE ANODIZING PROCESS ON THE COATING CHARACTERISTICS AND CORROSION BEHAVIOR OF ZIRCONIUM METAL

Manogari Sianturi[1*], Fajar Al Afghani[2], Frisca Ronauli Batubara[3], Sri Rahmadani[4], Romi Saputra[1]

[1]Department of Physics Education, Faculty of Teacher Training and Education, Universitas Kristen Indonesia, Jakarta 13630, Indonesia
[2]Research Center and Technology for Nuclear Material and Radioactive Waste – BRIN Kawasan Sains dan Teknologi B.J. Habibie, Bld. 720, Tangerang Selatan, Banten 15314
[3]Department of Physiology, Faculty of Medicine, Universitas Kristen Indonesia, Jakarta 13630, Indonesia
[4]Mechanical Engineering, Faculty of Engineering, Computer, and Design, Nusa Putra University, Sukabumi, Jawa Barat 43152, Indonesia
*Corresponding Author: manogari.sianturi@uki.ac.id

ABSTRAK

Zirkonium dan paduannya merupakan material standar untuk kelongsong bahan bakar nuklir pada Pressurized Water Reactor (PWR) karena memiliki penampang lintang serapan neutron yang rendah, sifat mekanik yang unggul, serta ketahanan korosi yang baik dalam lingkungan air bersuhu tinggi. Namun, kondisi operasi PWR memberikan lingkungan yang sangat berat sehingga dapat menurunkan integritas kelongsong seiring waktu, termasuk melalui proses oksidasi, hidriding, serta kerusakan mekanik seperti goresan atau penyok yang dapat terjadi selama operasi pengisian ulang bahan bakar. Cacat permukaan tersebut dapat bertindak sebagai lokasi inisiasi korosi terlokalisasi yang berpotensi mengompromikan penghalang penahanan primer.Penelitian ini menyelidiki efektivitas anodisasi elektrokimia sebagai teknik modifikasi permukaan untuk meningkatkan kinerja zirkonium. Proses anodisasi dilakukan pada tegangan konstan sebesar 30 V dengan variasi waktu 10, 15, dan 20 menit. Karakteristik permukaan yang dihasilkan dievaluasi menggunakan Mikroskop Optik, Mikroskop Digital untuk analisis kekasaran permukaan, serta X-Ray Diffraction (XRD). Keandalan mekanik dinilai melalui pengujian kekerasan mikro Vickers, sedangkan perilaku korosi dipelajari dalam larutan NaCl 3,5% menggunakan metode Open Circuit Potential (OCP), Potentiodynamic Polarization (PDP), dan Electrochemical Impedance Spectroscopy (EIS).Hasil penelitian menunjukkan bahwa peningkatan waktu anodisasi secara signifikan memperbaiki kualitas permukaan, ditunjukkan dengan penurunan nilai kekasaran rata-rata Ra dari 0,53 µm (10 menit) menjadi 0,24 µm (20 menit). Analisis XRD mengonfirmasi terbentuknya lapisan oksida ZrO_2 yang bersifat kristalin. Pengujian elektrokimia memperlihatkan peningkatan ketahanan korosi yang signifikan, di mana rapat arus korosi i_{corr} menurun hingga dua orde magnitudo dari 12,93 x 10^{-9} A/cm^2 pada substrat menjadi 0,19 x 10^{-9} A/cm^2 pada spesimen yang dianodisasi selama 20 menit. Penelitian ini menyimpulkan bahwa perlakuan anodisasi selama 20 menit pada tegangan 30 V mampu menghasilkan lapisan oksida yang kuat, halus, dan sangat tahan terhadap korosi, sehingga berpotensi efektif dalam memitigasi degradasi pada aplikasi kelongsong bahan bakar nuklir.

Kata kunci: Zirkonium, Anodisasi, Ketahanan Korosi, Kelongsong Nuklir, PWR, Modifikasi Permukaan.

ABSTRACT

Zirconium and its alloys are the standard material for nuclear fuel cladding in Pressurized Water Reactors (PWR) due to their low neutron absorption cross-section, excellent mechanical properties, and good corrosion resistance in high-temperature water. However, the operational environment of a PWR imposes severe conditions that can degrade the cladding integrity over time, including oxidation, hydriding, and mechanical damage such as scratching or denting during fuel refueling operations. These surface defects can act as initiation sites for localized corrosion, potentially compromising the primary containment barrier. This study investigates the effectiveness of electrochemical anodizing as a surface modification technique to enhance the performance of Zirconium. The anodizing process was conducted at a constant voltage of 30 V with varying durations of 10, 15, and 20 minutes. The resulting surface characteristics were evaluated using Optical Microscopy, Digital Microscopy for roughness analysis, and X-Ray Diffraction (XRD). Mechanical reliability was assessed via Vickers Microhardness testing, while corrosion behavior was studied in a 3.5% NaCl solution using Open Circuit Potential (OCP), Potentiodynamic Polarization (PDP), and Electrochemical Impedance Spectroscopy (EIS). The results demonstrated that increasing the anodizing time significantly improved the surface quality, reducing the arithmetic mean roughness Ra from 0.53 µm (10 min) to 0.24µm (20 min). XRD analysis confirmed the formation of a crystalline ZrO_2 oxide layer. Electrochemical tests revealed a substantial enhancement in corrosion resistance; the corrosion current density i_{corr} decreased by two orders of magnitude from 12.93 x 10^{-9} A/cm^2 for the substrate to 0.19 x 10^{-9} A/cm^2 for the 20-minute anodized specimen. The study concludes that a 20-minute anodizing treatment at 30 V produces a robust, smooth, and highly corrosion-resistant oxide layer suitable for mitigating degradation in nuclear fuel cladding applications.

Keywords: Zirconium, Anodizing, Corrosion Resistance, Nuclear Cladding, PWR, Surface Modification.

INTRODUCTION

Zirconium (Zr) and its alloys, such as Zircaloy-4 and Zirlo, are the materials of choice for nuclear fuel cladding in light water reactors (LWR), particularly Pressurized Water Reactors (PWR). This selection is driven by Zirconium's unique combination of properties: an exceptionally low thermal neutron capture cross-section (0.18 barn), which ensures efficient neutron economy, good thermal conductivity, and adequate mechanical strength at elevated temperatures [1, 2]. As the first barrier in the defense-in-depth strategy, the cladding must hermetically seal radioactive fission products preventing their release into the primary coolant.

Despite these advantages, Zirconium cladding faces formidable challenges during its service life. The aggressive operating environment, characterized by high-pressure water (approx. 15.5 MPa) and high temperatures (approx. 300-350°C), promotes waterside corrosion and hydrogen pickup [3, 4]. The oxidation of zirconium ($Zr+2H_2O \rightarrow ZrO_2 +2H_2$) not only thins the structural wall but also generates hydrogen, a fraction of which diffuses into the metal matrix, leading to hydride precipitation and embrittlement [5]. Furthermore, beyond steady-state operation, the cladding is subjected to mechanical stress during fuel handling and refueling processes. Physical contact with grid spacers or other assemblies can cause surface scratches, fretting, or dents. These surface imperfections significantly increase local roughness and can serve as stress concentration points or preferential sites for pitting corrosion, accelerating material degradation [6, 7].

Extending the operational life of fuel assemblies and enhanced safety margins, particularly for high-burnup regimes, surface modification techniques have gained attention. The goal is to create a protective surface layer that is harder than the substrate to resist mechanical damage and more chemically stable to inhibit corrosion [8]. Among various techniques such as physical vapor deposition (PVD) or laser surface treatment, electrochemical anodizing stands out due to its simplicity, cost-effectiveness, and ability to form a uniform, adherent oxide film (ZrO2) even on complex geometries [9].

Anodizing promotes the growth of a thickened oxide layer that acts as a passivating barrier. While the natural oxide film on Zirconium is protective, it is thin and liable to breakdown. Anodic films, depending on process parameters like voltage,

DOI: https://doi.org/10.17146/urania.20xx.xx.x.xxxx

p ISSN: 0852-4777
e ISSN: 2528-0473

electrolyte, and time, can be engineered to be thicker and more compact [10, 11]. Recent studies have focused on the voltage effects, but the influence of anodizing duration—specifically in the transition from initial film formation to steady-state growth—on the micro-roughness and electrochemical impedance of the surface remains an area for optimization [12].

This study aims to systematically evaluate the effect of anodizing time (10, 15, and 20 minutes) at a fixed potential of 30 V on the surface characteristics and corrosion behavior of Zirconium. We hypothesize that extending the anodizing duration will not only increase the oxide thickness but also reduce surface roughness through a leveling effect, thereby providing superior corrosion resistance in aggressive chloride environments.

METHODOLOGY

The Substrate material used was commercial purity Zirconium metal, cut into coupon specimens with dimensions of $10 mm \times 10 mm$. The samples were mounted in epoxy resin to expose a single working surface area. Prior to anodizing, the surfaces were mechanically polished using a sequence of Silicon Carbide (SiC) abrasive papers with grit sizes of 500, 800, 1200, and 2000. This step was crucial to remove the heterogeneous native oxide layer and standardize the initial surface roughness. After polishing, the samples were ultrasonically cleaned in acetone and rinsed with demineralized water to remove any particulate residues.

The anodizing process was carried out in a two-electrode electrochemical cell at room temperature. The Zirconium specimen served as the anode, while a high-purity platinum sheet was used as the cathode to ensure chemical inertness. The electrolyte was a specific aqueous solution tailored for compact film growth (typically phosphate/ammonium based). Phosphoric acid (H_3PO_4) at a concentration of 30 g/L is used as the electrolyte for the anodization process. Measuring the phosphoric acid with an analytical balance and combining it with distilled water in a beaker is the first step in the electrolyte production process. When the solution is ready to be employed as an anodizing medium on zirconium metal substrates, it is mixed with a magnetic stirrer until it dissolves uniformly.

A DC power supply was used to apply a constant voltage of 30 V. The anodizing duration varied as the experimental parameter: 10 minutes (Zr-10), 15 minutes (Zr-15), and 20 minutes (Zr-20). Post-anodizing, samples were rinsed and dried in air. A digital multimeter (DMM) was used to monitor the voltage and current during the anodization process. The solution was kept at room temperature to prevent localized heating that would result in non-uniform oxidation. The voltage source was turned off, and the specimen was removed from the electrolyte solution after the anodization period was complete. A hair dryer was used to dry any leftover electrolyte after it had been cleansed with distilled water. All anodized specimens were kept in a closed container, and silica gel was added to regulate the humidity in the storage area prior to testing for corrosion resistance, hardness, and surface morphology examination.

Surface morphology and visual appearance were documented using an Optical Microscope and a high-resolution Digital Microscope. The surface roughness parameters, Arithmetic Mean Roughness (Ra) and Ten-Point Mean Roughness (Rz), were quantified to evaluate the smoothing effect of the treatment. The surface morphology study was supported by microstructural findings. The samples' surface and texture were examined using scanning electron microscopy (SEM) at an accelerating voltage of 15 kV, which provided precise topographical information on the zirconium dioxide (ZrO_2) layer. Porosity, fractures, oxide layer thickness, and surface features that matched each time variation were observed using SEM examination. Additionally, the elemental composition of the coating was determined using Energy Dispersive Spectroscopy (EDS), with a focus on the distribution of phosphorus and oxygen to validate the creation of the ZrO_2 layer and potential interactions with the H_3PO_4 electrolyte. For additional examination, elemental mapping and spectra were both obtained.

The crystalline structure of the anodic oxide layers was analyzed using X-Ray Diffraction (XRD) with Cu-Kα radiation. To assess the resistance to mechanical damage, Vickers Microhardness testing was performed using a load of 300 gf with a dwell time of 15 seconds; five indentations were made per sample to obtain an average value.

Corrosion performance was evaluated in a 3.5% NaCl solution, chosen to simulate an aggressive corrosive environment that accelerates pitting attack. A standard three-electrode cell was employed, consisting of the Zr specimen (working electrode), an Ag/AgCl reference electrode, and a graphite counter electrode. The measurements were conducted using a Potentiostat/Galvanostat with the following sequence:

1. Open Circuit Potential (OCP): Monitored for 3600 seconds until a stable potential was reached.
2. Potentiodynamic Polarization (PDP): Scanned from -250 mV to +250 mV relative to OCP at a scan rate of 1 mV/s to determine Tafel parameters E_{corr} and i_{corr}.

RESULTS AND DISCUSSION

Surface Morphology and Roughness

Analysis Visual inspection of the samples immediately after anodizing revealed a distinct coloration of the surface. As shown in Figure 1, the surface color shifted from the metallic silver of the substrate to uniform hues of gold and blue. This phenomenon is attributed to the interference of light within the transparent anodic oxide film (ZrO_2), where the perceived color is directly related to the film thickness governed by the anodizing duration [13].

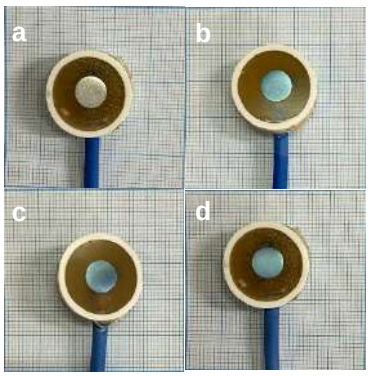

Figure 1. Color of zirconium oxide with various anodizing time of a) Zr, b) Zr-10, c) Zr-15, and d) Zr-20 minutes

Microstructural analysis via optical microscopy (Figure 2) and SEM (Figure 3) indicated a significant improvement in surface texture. The non-anodized substrate exhibited polishing lines and surface irregularities. However, post-anodizing, these features were progressively smoothed.

The anodization of Zr metal at 10 minutes produced a comparatively uneven surface morphology in Figure 2a. A coating of zirconium oxide had developed at that point, although it was not yet uniformly distributed. The 3D profile data (Figure 2b) revealed that the oxide layer was still in its early phases of formation, resulting in a very rough surface roughness. The duration of anodization was extended to 15 minutes (Figure 2c). Compared to Zr-10, the resulting zirconium oxide layer became more homogeneous, thick, and continuous. This result was also confirmed from the 3D profile of Figure 2d. Figure 2e shows the anodization of Zr metal with a process time of 20 minutes. Increasing the anodization time contributed to the growth and stability of the zirconium oxide layer formed on the metal surface. The layer was more uniform, dense, and surface defects were significantly reduced. The relevant results are confirmed by Figure 2f.

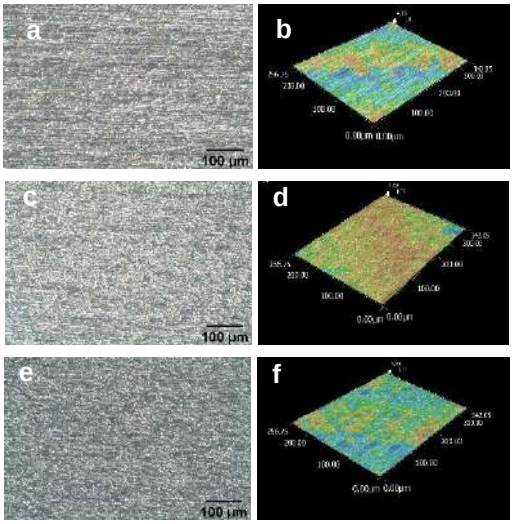

g

Specimen	Surface Roughness	
	Ra	Rz
Zr-10	0.53	4.35
Zr-15	0.34	4.98
Zr-20	0.24	2.34

Figure 2. Microstructural analysis via optical microscopy (a,c,e), 3D profile (b,d,f), and surface roughness value (g) of (a,b) Zr-anodized 10 minutes, (c,d) Zr-anodized 15 minutes, and (e,f) Zr-anodized 20 minutes.

Quantitative roughness data presented in Figure 2g and Figure 2 (b,d,f) confirm this observation. The average roughness (Ra) decreased from 0.53 µm for the Zr-10

DOI: https://doi.org/10.17146/urania.20xx.xx.x.xxxx

specimen to 0.34 μm for Zr-15, and finally to 0.24 μm for Zr-20. This trend suggests a "leveling mechanism" where the oxide grows preferentially in the microscopic valleys of the metal surface, effectively reducing the peak-to-valley height [14]. A smoother surface is highly advantageous for nuclear cladding as it reduces the friction coefficient during fuel rod insertion and minimizes the surface area available for corrosive attack.

Figure 3. Surface view SEM images and the corresponding EDS area mapping of zirconium anodized under different duration processes. The surfaces of all the specimens were quite homogeneous and devoid of significant cracks. Increasing the anodization time prevented any significant morphological changes at the micrometer scale. For every modification in anodization time, the elemental mapping findings on the zirconium oxide layer's surface revealed an equitable distribution of elements. The anodized metal surface was dominated by Zr and O elements.

The zirconium substrate, whose composition decreased as the anodization duration increased, provided the Zr element. The O element showed that an oxide layer had formed during the anodization processes. The composition of the O element increased as the anodization duration increased, indicating the thickening and expansion of the zirconium oxide layer (ZrO_2). The increase in the O element was formed from 44.66 at% for the Zr-10 specimen, 53.12 at% for the Zr-15 specimen, and the highest for the Zr-20 specimen, namely 54.33 at%. The P element was also found throughout the layer's surface in addition to these primary components. The phosphate-based electrolyte used during the anodizing process is the source of the phosphorus, which is present in trace levels (around 1-2 at%) but is dispersed rather uniformly.

Crystalline Structure and Microhardness the XRD patterns shown in Figure 4 display sharp diffraction peaks corresponding to Zirconium Oxide (ZrO_2). The analysis suggests the presence of a cubic crystalline phase, which is notable as anodic films formed at lower voltages are often amorphous. The formation of this crystalline phase contributes to the chemical stability of the coating [15]. Diffraction peaks for the zirconium (Zr) and zirconium oxide (ZrO_2) phases were detected on all anodized specimens. The ZrO_2 peak's formation indicates that the anodization procedure was effective in generating an oxide layer on the zirconium substrate's surface. The ZrO_2 diffraction peak's clarity tended to rise with increasing anodization time, especially in the Zr-20 specimen, which showed the maximum peak intensity. This suggests that extended anodization durations encourage the formation of an oxide layer that is thicker and/or more crystalline. In the meantime, peaks from the Zr phase were still identified, suggesting that the relatively tiny oxide layer thickness allowed X-rays to proceed toward the substrate. In general, the XRD data confirm that different anodization times affect the zirconium oxide layer’s growth and crystal properties.

Mechanical integrity was evaluated via Vickers microhardness (HV). As detailed in Table 1, the hardness values were relatively stable across the anodized samples: 144.41±8.99 HV (10 min), 144.66±7.84 HV (15 min), and 142.88±6.96 HV (20 min). Although the macroscopic hardness did not show a drastic increase compared to the substrate (likely due to the indentation depth exceeding the thin oxide layer thickness), the presence of the hard ceramic ZrO_2 skin provides essential resistance against superficial scratching and fretting wear, which are critical precursors to cladding failure [16].

Table 1. Average and Standar Deviation (STDV) for Microhardness of Zr-Anodized under different duration process

Specimen	HV					Average	Standard Deviasi
	1	2	3	4	5		
Zr-10	150.97	138.23	140.08	158.57	134.19	144.41	8.99
Zr-15	156.89	142.93	138.07	149.92	135.5	144.66	7.84
Zr-20	155.79	144.39	137.77	136.86	139.61	142.88	6.96

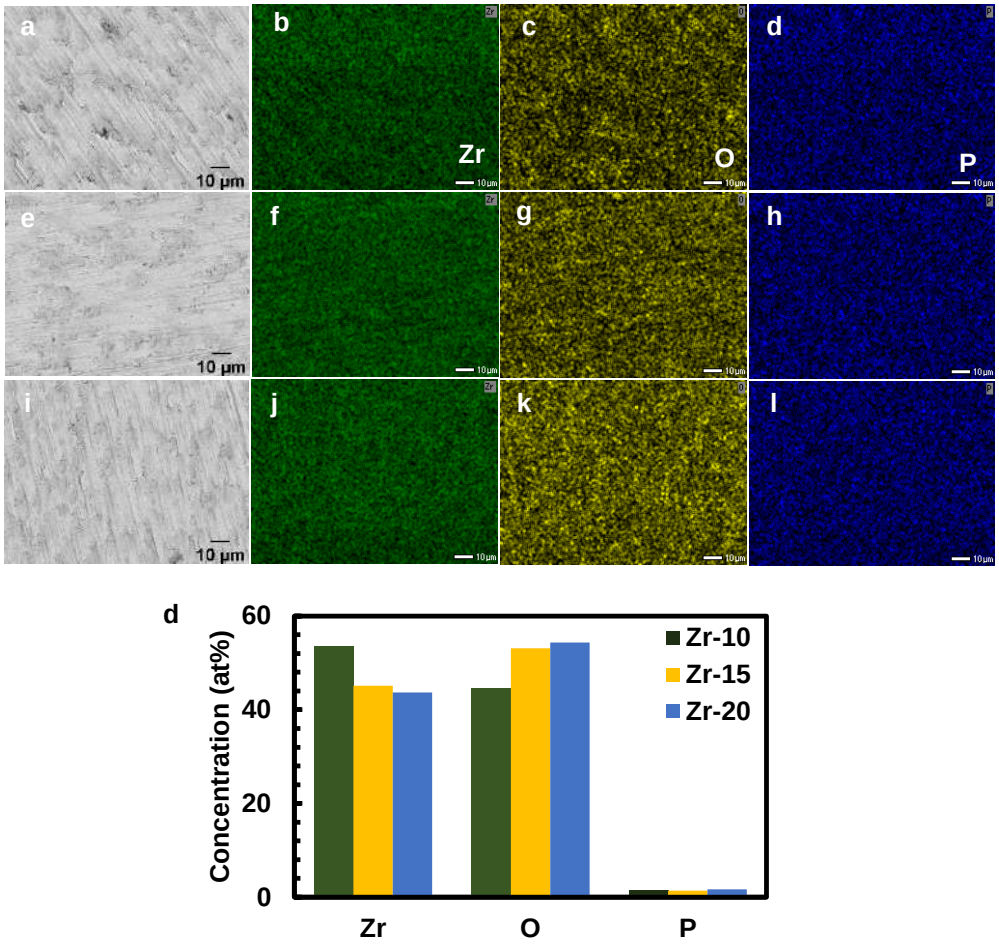

Figure 3. Surface view SEM images and the corresponding EDS area mapping of zirconium anodized of (a-d) Zr-10, (e-h) Zr-15, and (i-l) Zr-20 minutes

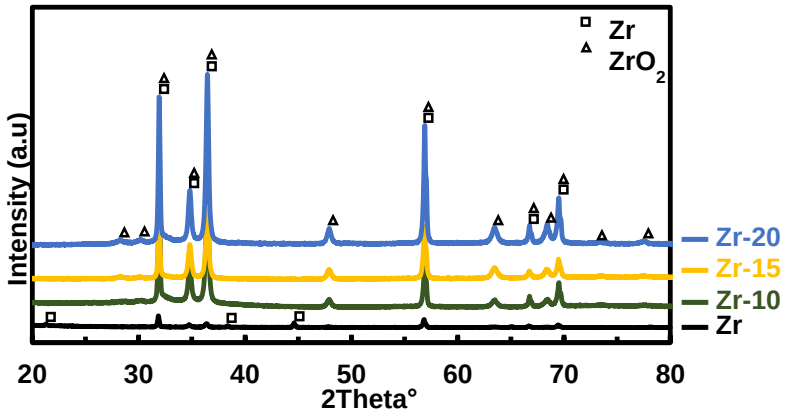

Figure 4. XRD pattern of zirconium oxide (ZrO_2)

DOI: https://doi.org/10.17146/urania.20xx.xx.x.xxxx

Electrochemical Corrosion Behavior

The corrosion resistance was comprehensively analyzed using OCP, PDP, and EIS techniques. Open Circuit Potential (OCP): Figure 5 illustrates the OCP evolution. All anodized specimens exhibited more positive (noble) potentials compared to the bare substrate. The Zr-20 sample showed the most noble potential, stabilizing at a higher value, which indicates a thermodynamic tendency to resist spontaneous corrosion reactions in the electrolyte [17]. During the test, pure zirconium (Zr) specimens had the most negative and comparatively steady potential values, suggesting more potential for corrosion. All the specimens indicated a potential change in a more positive direction immediately after the anodization process, which suggests that the formation of a zirconium oxide layer had increased electrochemical stability. Zr-20, Zr-15, and Zr-10 were the anodized specimens with the most positive and consistent OCP values while the test. This suggests that extending the anodization duration increases the material's resistance to corrosion and creates a more protective oxide layer. The formation of a rather stable passive layer on the zirconium surface is also shown by the stability of the OCP curves over an extended test time.

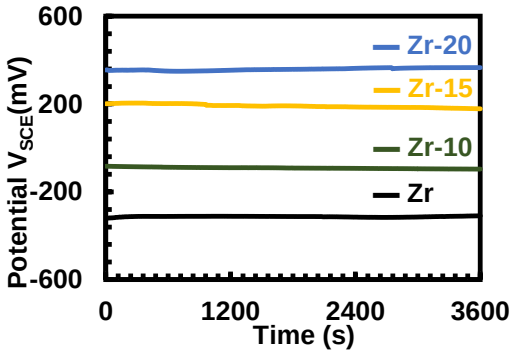

Figure 5. Average of OCP curves for zirconium substrate and zirconium-anodized at 30 V

Potentiodynamic Polarization (PDP): The Tafel polarization curves in Figure 6 demonstrate a clear shift in corrosion kinetics. The electrochemical parameters summarized in Table 2 show a dramatic reduction in corrosion current density (i_{corr}). The substrate exhibited an i_{corr} of 12.93 × 10^{-9}A/cm^2. In contrast, the Zr-20 specimen exhibited an i_{corr} of 0.19 × 10^{-9}A/cm^2. This reduction by nearly two orders of magnitude confirms that the thicker oxide layer formed at 20 minutes acts as an effective barrier, blocking the diffusion of chloride ions (Cl^-) and oxygen to the metal interface [18, 19].

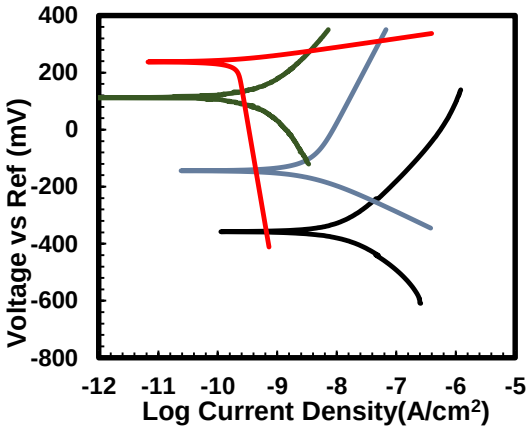

Figure 6. Average of PDP curves for zirconium substrate and zirconium-anodised at 30 V

Figure 6 presents the potentiodynamic polarization (PDP) curves of anodized and pure zirconium. These curves illustrate the relationship between the voltage across a reference electrode and the log current density, which is used to assess corrosion behavior and electrochemical reaction kinetics. Pure zirconium exhibits poor corrosion resistance, indicated by its limited passivation range and relatively high corrosion current density. In contrast, anodized specimens show a shift in corrosion potential to more positive values and a decrease in corrosion current density. Compared to Zr-15 and Zr-10, the Zr-20 specimen shows the biggest passivation area and the lowest current density. The Zr-20 specimen exhibits the lowest current density and the largest passivation region compared to Zr-15 and Zr-10. This suggests that the zirconium oxide layer that develops over extended anodization durations successfully prevents charge transfer and reduces the rate of corrosion.

Table 2. PDP Parameter of Zr-Anodized under different duration process

Specimen	E_{corr} (mV)	i_{corr} (10^{-9}A/cm^2)	β_{Anodic} (mV/Decade)	$\beta_{Catodic}$ (mV/Decade)
Zr	-346 ± 88	12.93 ± 2.89	399 ± 350	275 ± 152
Zr-10	-114 ± 94	2.57 ± 1.12	599± 461	198 ± 122
Zr-15	113 ± 98	1.10 ± 0.82	275 ± 201	363 ± 262
Zr-20	233 ± 74	0.19 ± 0.04	275 ± 201	363 ± 262

CONCLUSIONS

The effect of anodizing duration on the surface characteristics and corrosion behavior of Zirconium was successfully investigated. The following conclusions are drawn:

1. Surface Improvement: Increasing the anodizing time from 10 to 20 minutes at 30 V results in a progressively smoother surface. The Zr-20 specimen achieved the lowest roughness (Ra= 0.24 µm), reducing friction and potential pit initiation sites.
2. Oxide Formation: The process forms a stable, crystalline ZrO_2 layer, as confirmed by XRD and the observation of interference colors.
3. Corrosion Resistance: The 20-minute anodized coating offers superior corrosion protection in chloride environments. It reduced the corrosion rate i_{corr} by approximately 98% compared to the bare substrate and significantly increased the polarization resistance.
4. Application Viability: The study confirms that a 20-minute anodizing treatment is an effective, low-cost method to enhance the durability of Zirconium nuclear fuel cladding, potentially extending the safety margins against corrosion and mechanical degradation in PWR environments.

ACKNOWLEDGEMENT

We would like to thank our gratitude to the Universitas Kristen Indonesia (UKI) through the UKI Institute for Research and Community Service (LPPM) for funding this research.

REFERENCES

[1] Motta, A. T., Couet, A., & Comstock, R. J. (2015). Corrosion of Zirconium Alloys Used for Nuclear Fuel Cladding. Annual Review of Materials Research, 45, 311-343.

[2] Duan, Z., Yang, H., Satoh, Y., & Murakami, K. (2017). Oxidation behavior of zirconium alloys in a simulated nuclear reactor primary coolant. Journal of Nuclear Materials, 485, 147-158.

[3] Terrani, K. A. (2018). Accident tolerant fuel cladding development: Promise, status, and challenges. Journal of Nuclear Materials, 501, 13-30.

[4] Gong, W., & Yun, D. (2022). A review on the corrosion behavior of zirconium alloys in supercritical water. Corrosion Science, 208, 110620.

[5] Yilmazbayhan, A., Motta, A. T., & Comstock, R. J. (2021). Hydride morphology and embrittlement in Zircaloy-4 cladding. Journal of Nuclear Materials, 545, 152646.

[6] Liu, J., & Li, Q. (2023). Fretting wear behavior of zirconium alloy cladding tubes. Wear, 522, 204689.

[7] Kim, H. G., & Kim, I. H. (2020). Oxidation behavior of zirconium alloy claddings in high temperature steam. Nuclear Engineering and Technology, 52(4), 808-815.

[8] Suresh, S., & Sharma, A. (2021). Surface modification of zirconium alloys for biomedical and nuclear applications: A review. Surface and Coatings Technology, 405, 126666.

[9] Verma, R., & Kumar, S. (2022). Electrochemical anodization of zirconium: Growth mechanism and properties. Electrochimica Acta, 412, 140135.

DOI: https://doi.org/10.17146/urania.20xx.xx.x.xxxx

[10] Cheng, Y., & Matykina, E. (2021). Formation of nanotubular oxide layers on Zirconium alloys by anodization. Corrosion Science, 182, 109289.

[11] Ali, F., & Al-Hajri, M. (2023). Effect of voltage and electrolyte composition on the morphology of anodic zirconium oxide. Materials Chemistry and Physics, 295, 127087.

[12] Wang, L., Zhang, Y., & Wu, X. (2024). Time-dependent growth kinetics of anodic films on zirconium in phosphate electrolytes. Journal of Electrochemical Society, 171(2), 021504.

[13] Diamanti, M. V., & Pedeferri, M. P. (2020). Color production on zirconium by anodizing: Interference and absorption effects. Color Research & Application, 45(3), 456-464.

[14] Thompson, G. E. (2019). Porous anodic oxide films: Formation, growth and applications. Thin Solid Films, 685, 34-45.

[15] Zhao, X., & Xu, H. (2022). Phase transformation in anodic zirconia films: From amorphous to crystalline. Scripta Materialia, 210, 114421.

[16] Obbard, E. G., & Burr, P. A. (2021). Mechanical properties of zirconium oxide scales: A review. Journal of Nuclear Materials, 557, 153255.

[17] McCafferty, E. (2020). Introduction to Corrosion Science (2nd ed.). Springer.

[18] Zhang, B., & Frankel, G. S. (2022). Corrosion mechanisms of zirconium alloys in chloride-containing environments. Corrosion, 78(5), 412-425.

[19] Li, T., & Wang, F. (2023). Improvement of pitting corrosion resistance of Zr alloys by anodic oxidation. Applied Surface Science, 610, 155567.

[20] Orazem, M. E., & Tribollet, B. (2017). Electrochemical Impedance Spectroscopy. Wiley.

Bukti Korespondensi dengan pihak Editor Jurnal

Tangkap Layar dengan Reviewer Jurnal Urania

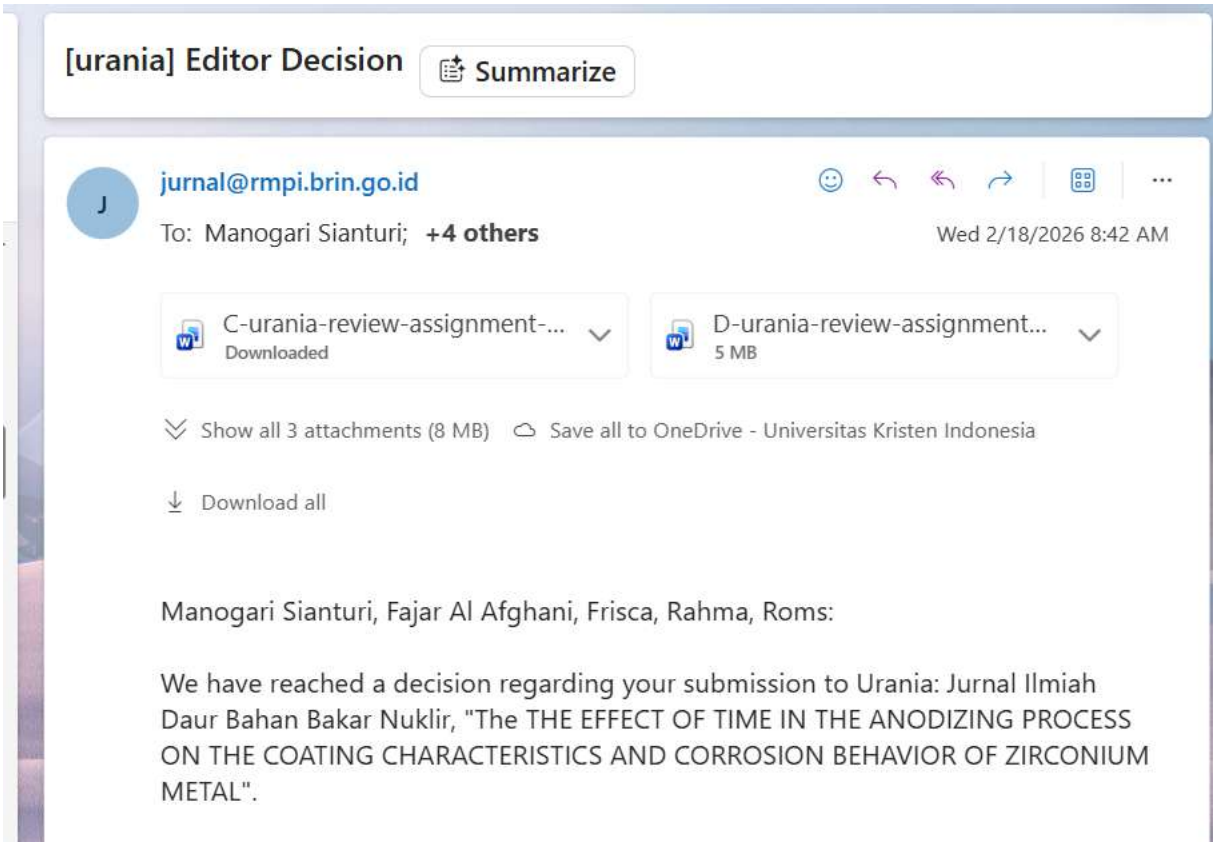

[urania] Editor Decision

Summarize

Our decision is: Revisions Required

Reviewer A:
Recommendation: Revisions Required

Reviewer B:

The novelty is overstated implicitly; anodization of zirconium for corrosion resistance is well established. What aspect of this study goes beyond existing anodization-time studies on zirconium?

[urania] Editor Decision

Summarize

How does the achieved corrosion performance compare quantitatively with previously reported anodized Zr systems? Explicitly identify what previous studies did not quantify.

How can barrier properties (blocking the diffusion of chloride ions) be claimed without impedance-based resistance values?
Does the hardness measurement truly reflect the oxide layer or the substrate? How uniform is the oxide thickness across the surface?
Which ZrO_2 polymorph (monoclinic/tetragonal/cubic) dominates? Please performed the Scherrer analysis! This will help discussion the corrosion and hardness properties.

In conclusion, acknowledge of study limitations, its overgeneralization toward nuclear reactor conditions.

Recommendation: Revisions Required

[urania] Editor Decision

Summarize

Reviewer C:

The manuscript presents an interesting study about anodization on zirconium and is generally well-structured. However, several revisions are required to improve the clarity, technical accuracy, and overall quality of the work before it can be considered for publication.

Detailed comments, queries, and suggested edits have been embedded directly into the manuscript file.

Please revise the document accordingly, ensuring that each comment is addressed systematically in the manuscript.

Recommendation: Revisions Required

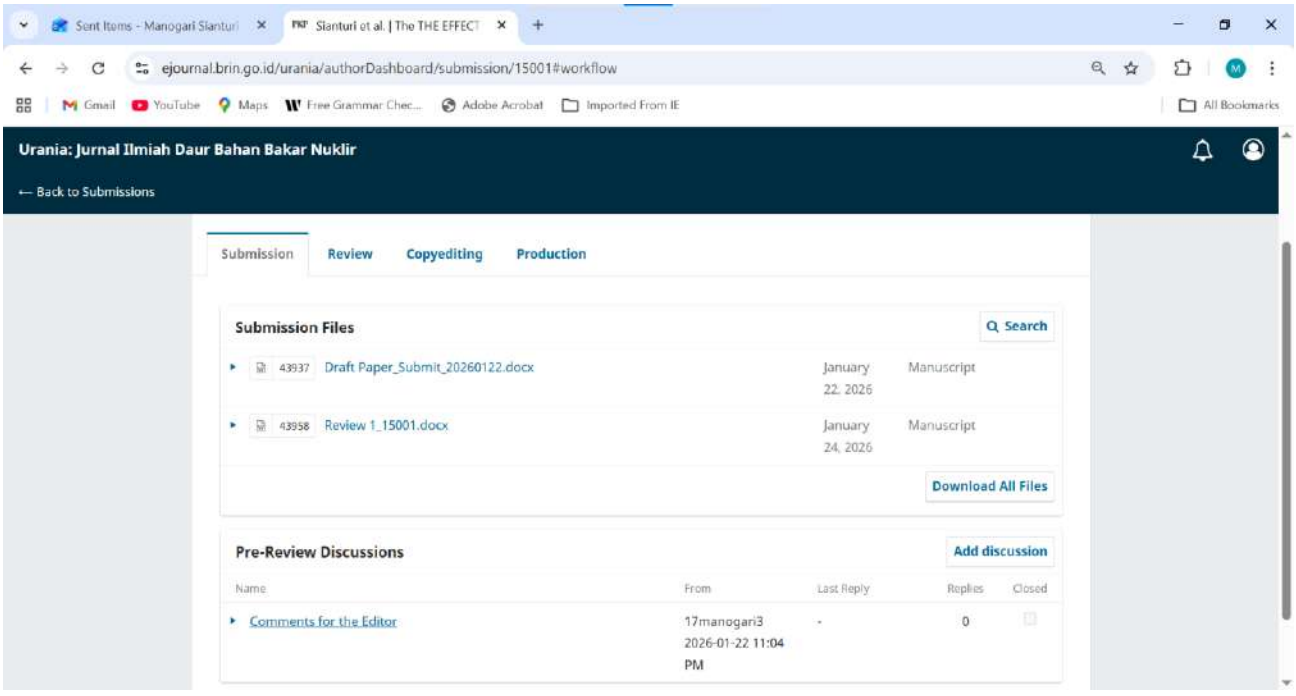

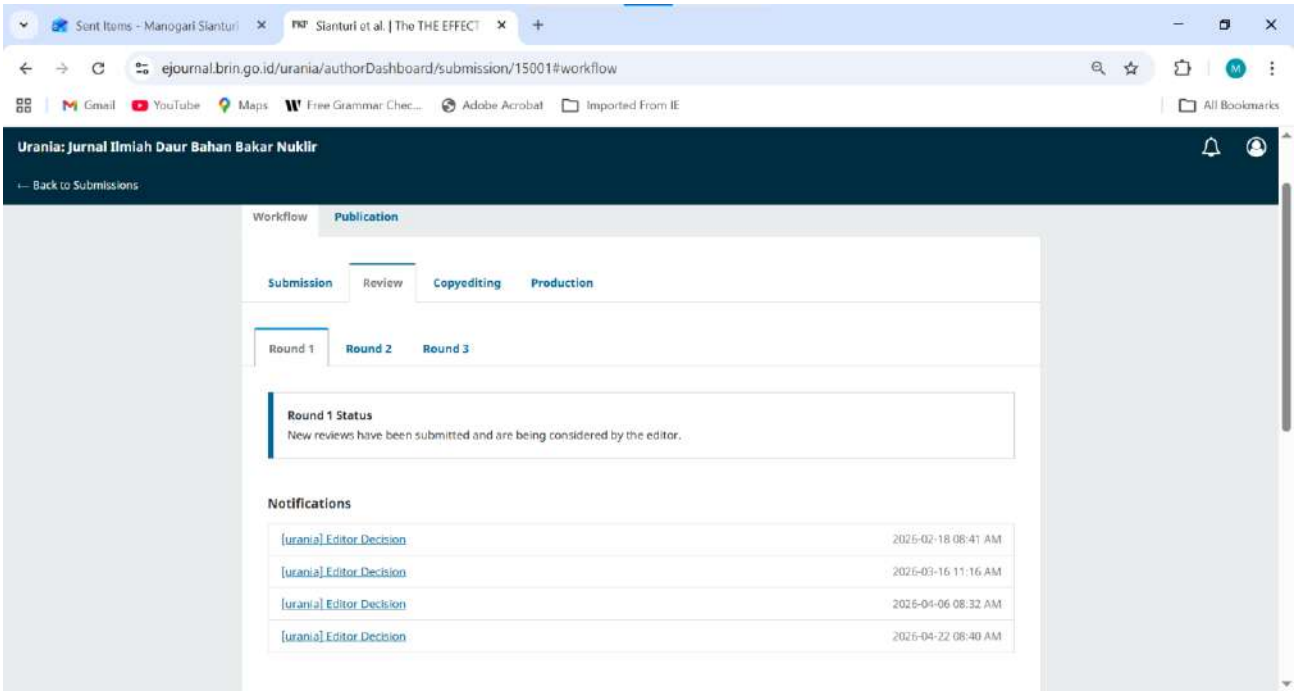
Sent Items - Manogari Silanturi
Silanturi et al. | The THE EFFECT
ejournal.brin.go.id/urania/authorDashboard/submission/15001#workflow
Gmail
YouTube
Maps
Free Grammar Chec...
Adobe Acrobat
Imported From IE
All Bookmarks
Urania: Jurnal Ilmiah Daur Bahan Bakar Nuklir
← Back to Submissions
Workflow
Publication
Submission
Review
Copyediting
Production
Round 1
Round 2
Round 3
Round 1 Status
New reviews have been submitted and are being considered by the editor.
Notifications
[urania] Editor Decision 2026-02-18 08:41 AM
[urania] Editor Decision 2026-03-16 11:16 AM
[urania] Editor Decision 2026-04-06 08:32 AM
[urania] Editor Decision 2026-04-22 08:40 AM

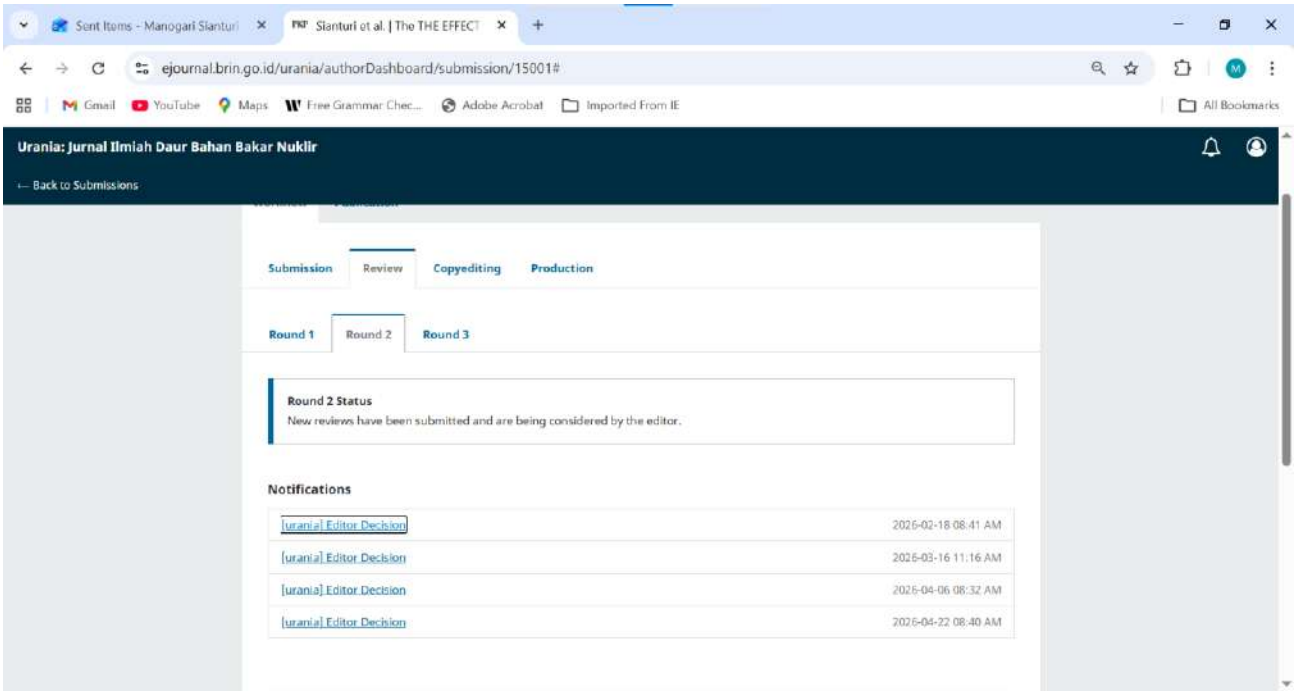
Sent Items - Manogari Silanturi
Silanturi et al. | The THE EFFECT
ejournal.brin.go.id/urania/authorDashboard/submission/15001#
Gmail
YouTube
Maps
Free Grammar Chec...
Adobe Acrobat
Imported From IE
All Bookmarks
Urania: Jurnal Ilmiah Daur Bahan Bakar Nuklir
← Back to Submissions
Submission
Review
Copyediting
Production
Round 1
Round 2
Round 3
Round 2 Status
New reviews have been submitted and are being considered by the editor.
Notifications
[urania] Editor Decision 2026-02-18 08:41 AM
[urania] Editor Decision 2026-03-16 11:16 AM
[urania] Editor Decision 2026-04-06 08:32 AM
[urania] Editor Decision 2026-04-22 08:40 AM

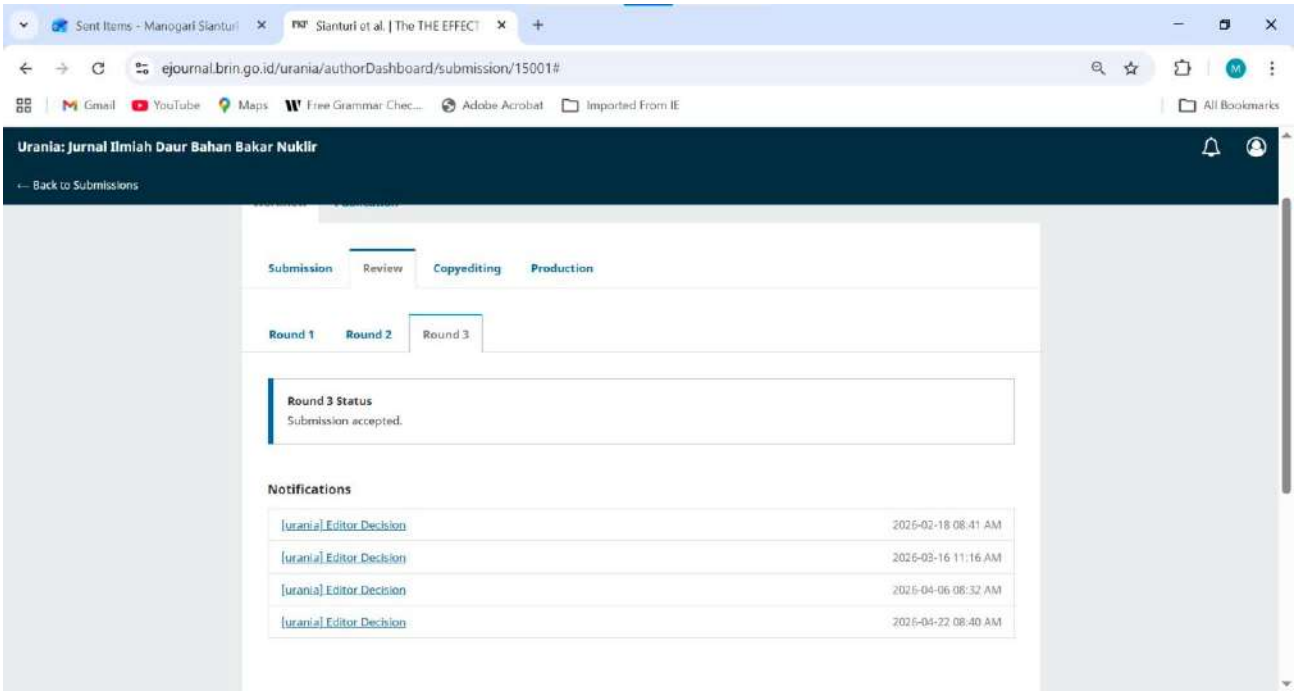
Sent Items - Manogari Sianturi
Sianturi et al. | The THE EFFECT
ejournal.brin.go.id/urania/authorDashboard/submission/15001#
Gmail
YouTube
Maps
Free Grammar Chec...
Adobe Acrobat
Imported From IE
All Bookmarks
Urania: Jurnal Ilmiah Daur Bahan Bakar Nuklir
← Back to Submissions
Submission
Review
Copyediting
Production
Round 1
Round 2
Round 3
Round 3 Status
Submission accepted.
Notifications
[urania] Editor Decision
2026-02-18 08:41 AM
[urania] Editor Decision
2026-03-16 11:16 AM
[urania] Editor Decision
2026-04-06 08:32 AM
[urania] Editor Decision
2026-04-22 08:40 AM

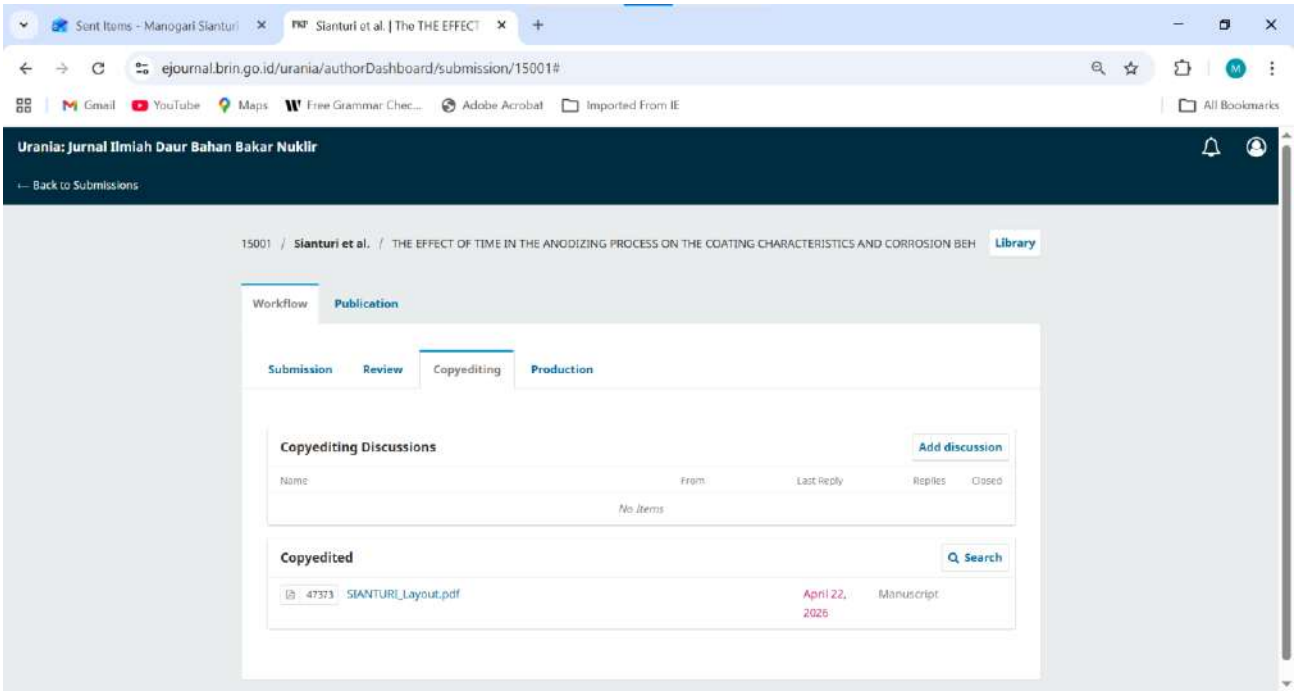
Sent Items - Manogari Sianturi
Sianturi et al. | The THE EFFECT
ejournal.brin.go.id/urania/authorDashboard/submission/15001#
Gmail
YouTube
Maps
Free Grammar Chec...
Adobe Acrobat
Imported From IE
All Bookmarks
Urania: Jurnal Ilmiah Daur Bahan Bakar Nuklir
← Back to Submissions
15001 / Sianturi et al. / THE EFFECT OF TIME IN THE ANODIZING PROCESS ON THE COATING CHARACTERISTICS AND CORROSION BEH
Library
Workflow
Publication
Submission
Review
Copyediting
Production
Copyediting Discussions
Add discussion
Name
From
Last Reply
Replies
Closed
No Items
Copyedited
Search
47373
SIANTURI_Layout.pdf
April 22, 2026
Manuscript

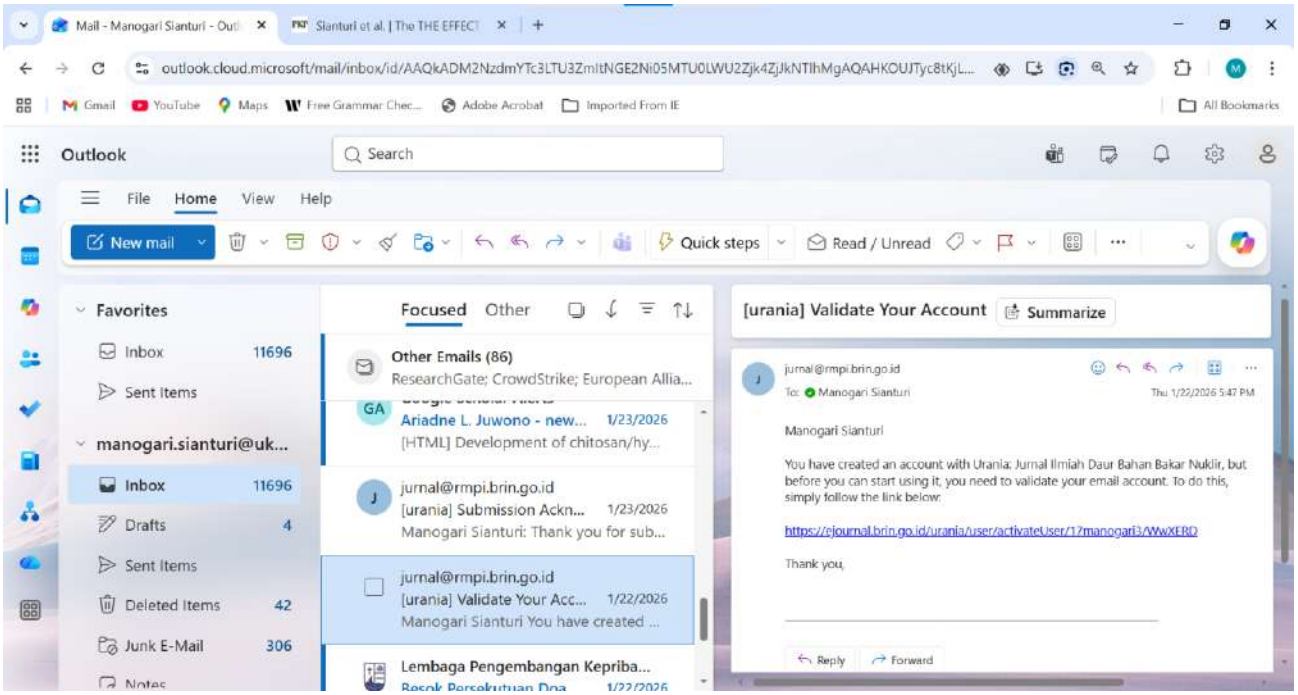
Mail - Manogari Sianturi - Outl
Sianturi et al. | The THE EFFECT
outlook.cloud.microsoft/mail/inbox/id/AAQkADM2NzdmYTc3LTU3ZmItNGE2Ni05MTU0LWU2Zjk4ZjJkNTlhMgAQAHKOUJTyc8tKjL...
Gmail
YouTube
Maps
Free Grammar Chec...
Adobe Acrobat
Imported From IE
All Bookmarks
Outlook
Search
File
Home
View
Help
New mail
Quick steps
Read / Unread
Favorites
Inbox 11696
Sent Items
manogari.sianturi@uk...
Inbox 11696
Drafts 4
Sent Items
Deleted Items 42
Junk E-Mail 306
Notes
Focused
Other
Other Emails (86)
ResearchGate; CrowdStrike; European Allia...
Ariadne L. Juwono - new... 1/23/2026
[HTML] Development of chitosan/hy...
jurnal@rmpi.brin.go.id
[urania] Submission Ackn... 1/23/2026
Manogari Sianturi: Thank you for sub...
jurnal@rmpi.brin.go.id
[urania] Validate Your Acc... 1/22/2026
Manogari Sianturi You have created ...
Lembaga Pengembangan Kepriba...
[urania] Validate Your Account
Summarize
jurnal@rmpi.brin.go.id
To: Manogari Sianturi
Thu 1/22/2026 5:47 PM
Manogari Sianturi
You have created an account with Urania: Jurnal Ilmiah Daur Bahan Bakar Nuklir, but before you can start using it, you need to validate your email account. To do this, simply follow the link below:
https://ejournal.brin.go.id/urania/user/activateUser/17manogari3/AWwXERD
Thank you,
Reply
Forward

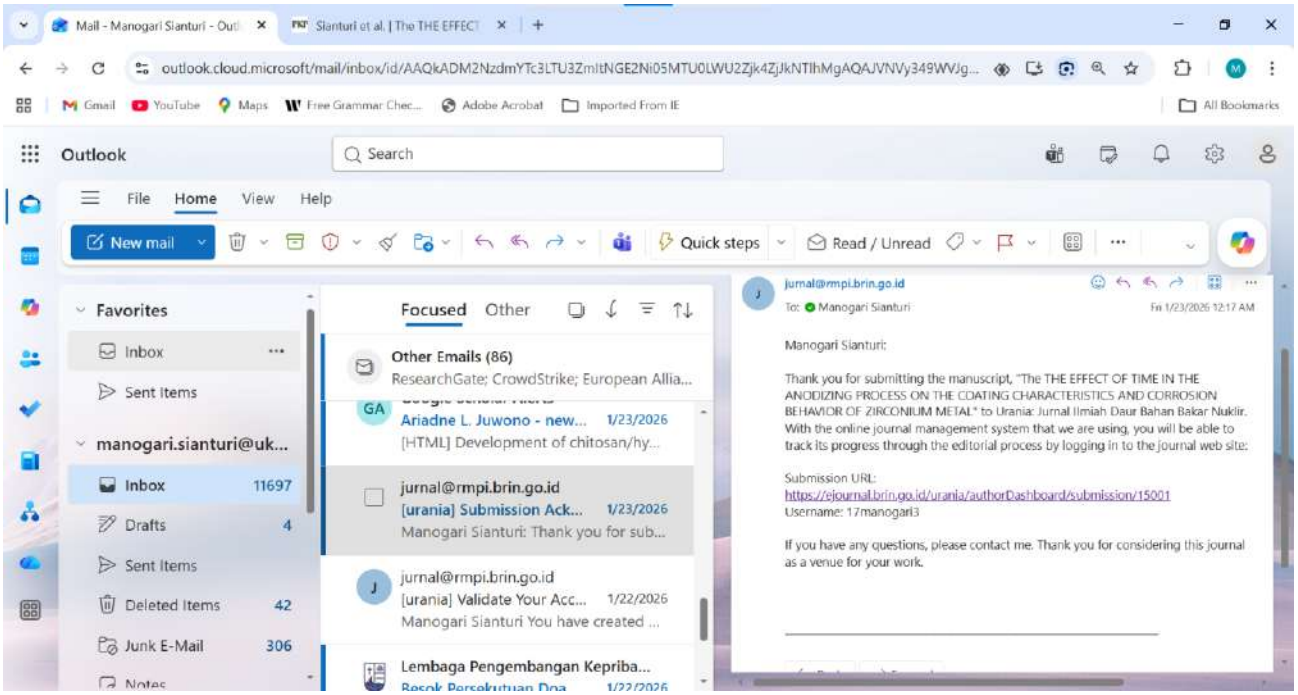
Mail - Manogari Sianturi - Outl
Sianturi et al. | The THE EFFECT
outlook.cloud.microsoft/mail/inbox/id/AAQkADM2NzdmYTc3LTU3ZmItNGE2Ni05MTU0LWU2Zjk4ZjJkNTlhMgAQAJVNVy349WVJg...
Gmail
YouTube
Maps
Free Grammar Chec...
Adobe Acrobat
Imported From IE
All Bookmarks
Outlook
Search
File
Home
View
Help
New mail
Quick steps
Read / Unread
Favorites
Inbox
Sent Items
manogari.sianturi@uk...
Inbox 11697
Drafts 4
Sent Items
Deleted Items 42
Junk E-Mail 306
Notes
Focused
Other
Other Emails (86)
ResearchGate; CrowdStrike; European Allia...
Ariadne L. Juwono - new... 1/23/2026
[HTML] Development of chitosan/hy...
jurnal@rmpi.brin.go.id
[urania] Submission Ack... 1/23/2026
Manogari Sianturi: Thank you for sub...
jurnal@rmpi.brin.go.id
[urania] Validate Your Acc... 1/22/2026
Manogari Sianturi You have created ...
Lembaga Pengembangan Kepriba...
jurnal@rmpi.brin.go.id
To: Manogari Sianturi
Fri 1/23/2026 12:17 AM
Manogari Sianturi:
Thank you for submitting the manuscript, "The THE EFFECT OF TIME IN THE ANODIZING PROCESS ON THE COATING CHARACTERISTICS AND CORROSION BEHAVIOR OF ZIRCONIUM METAL" to Urania: Jurnal Ilmiah Daur Bahan Bakar Nuklir. With the online journal management system that we are using, you will be able to track its progress through the editorial process by logging in to the journal web site:
Submission URL:
https://ejournal.brin.go.id/urania/authorDashboard/submission/15001
Username: 17manogari3
If you have any questions, please contact me. Thank you for considering this journal as a venue for your work.

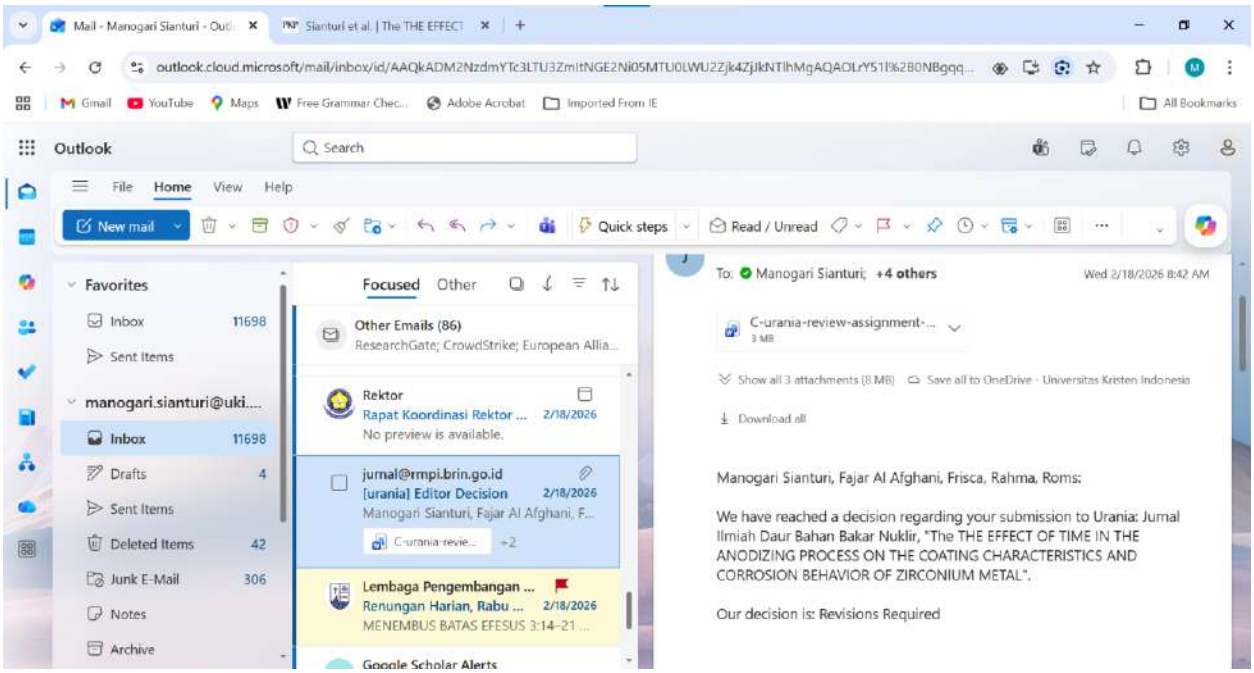
Mail - Manogari Sianturi - Outl
Sianturi et al. | The THE EFFECT
outlook.cloud.microsoft/mail/inbox/id/AAQkADM2NzdmYTc3LTU3ZmItNGE2Ni05MTU0LWU2Zjk4ZjJkNTlhMgAQAOLrY51l%2B0NBgqq...
Gmail
YouTube
Maps
Free Grammar Chec...
Adobe Acrobat
Imported From IE
All Bookmarks
Outlook
Search
File
Home
View
Help
New mail
Quick steps
Read / Unread
Favorites
Inbox 11698
Sent Items
manogari.sianturi@uki....
Inbox 11698
Drafts 4
Sent Items
Deleted Items 42
Junk E-Mail 306
Notes
Archive
Focused
Other
Other Emails (86)
ResearchGate; CrowdStrike; European Allia...
Rektor
Rapat Koordinasi Rektor ... 2/18/2026
No preview is available.
jurnal@rmpi.brin.go.id
[urania] Editor Decision 2/18/2026
Manogari Sianturi, Fajar Al Afghani, F...
C-urania-revie... +2
Lembaga Pengembangan ...
Renungan Harian, Rabu ... 2/18/2026
MENEMBUS BATAS EFESUS 3:14-21 ...
Google Scholar Alerts
To: Manogari Sianturi; +4 others
Wed 2/18/2026 8:42 AM
C-urania-review-assignment-...
3 MB
Show all 3 attachments (8 MB)
Save all to OneDrive - Universitas Kristen Indonesia
Download all
Manogari Sianturi, Fajar Al Afghani, Frisca, Rahma, Roms:
We have reached a decision regarding your submission to Urania: Jurnal Ilmiah Daur Bahan Bakar Nuklir, "The THE EFFECT OF TIME IN THE ANODIZING PROCESS ON THE COATING CHARACTERISTICS AND CORROSION BEHAVIOR OF ZIRCONIUM METAL".
Our decision is: Revisions Required

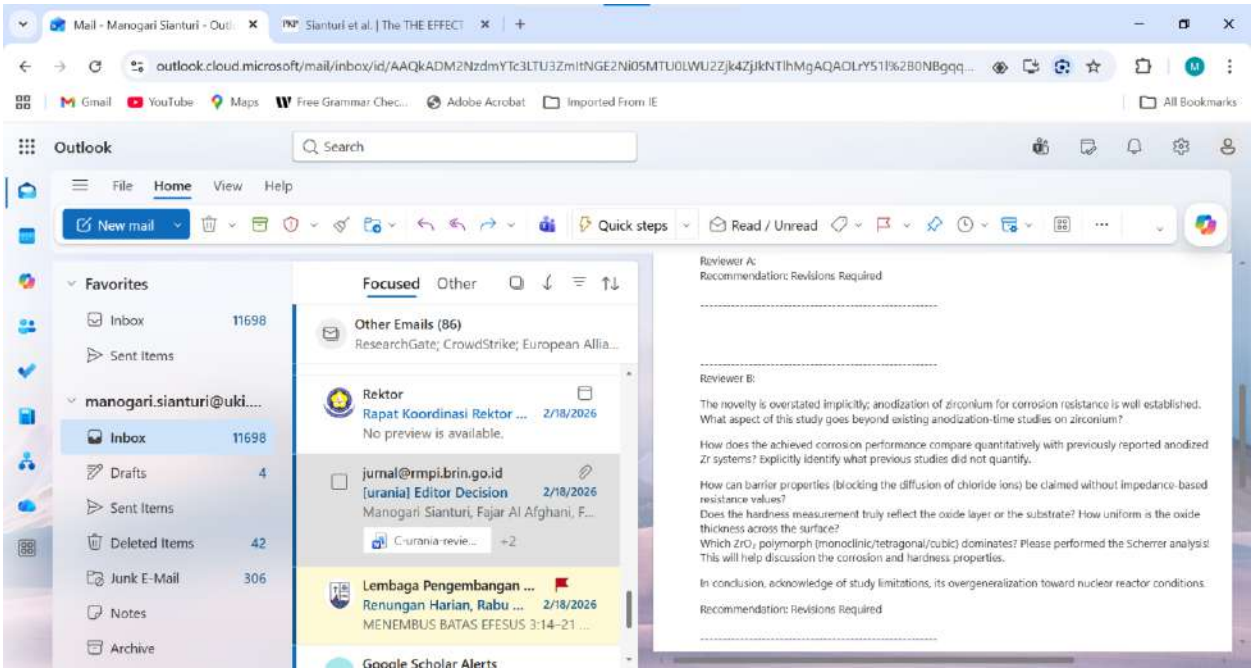
Mail - Manogari Sianturi - Outl
Sianturi et al. | The THE EFFECT
outlook.cloud.microsoft/mail/inbox/id/AAQkADM2NzdmYTc3LTU3ZmItNGE2Ni05MTU0LWU2Zjk4ZjJkNTlhMgAQAOLrY51l%2B0NBgqq...
Gmail
YouTube
Maps
Free Grammar Chec...
Adobe Acrobat
Imported From IE
All Bookmarks
Outlook
Search
File
Home
View
Help
New mail
Quick steps
Read / Unread
Favorites
Inbox 11698
Sent Items
manogari.sianturi@uki....
Inbox 11698
Drafts 4
Sent Items
Deleted Items 42
Junk E-Mail 306
Notes
Archive
Focused
Other
Other Emails (86)
ResearchGate; CrowdStrike; European Allia...
Rektor
Rapat Koordinasi Rektor ... 2/18/2026
No preview is available.
jurnal@rmpi.brin.go.id
[urania] Editor Decision 2/18/2026
Manogari Sianturi, Fajar Al Afghani, F...
C-urania-revie... +2
Lembaga Pengembangan ...
Renungan Harian, Rabu ... 2/18/2026
MENEMBUS BATAS EFESUS 3:14-21 ...
Google Scholar Alerts
Reviewer A:
Recommendation: Revisions Required
Reviewer B:
The novelty is overstated implicitly; anodization of zirconium for corrosion resistance is well established. What aspect of this study goes beyond existing anodization-time studies on zirconium?
How does the achieved corrosion performance compare quantitatively with previously reported anodized Zr systems? Explicitly identify what previous studies did not quantify.
How can barrier properties (blocking the diffusion of chloride ions) be claimed without impedance-based resistance values?
Does the hardness measurement truly reflect the oxide layer or the substrate? How uniform is the oxide thickness across the surface?
Which ZrO_2 polymorph (monoclinic/tetragonal/cubic) dominates? Please performed the Scherrer analysis! This will help discussion the corrosion and hardness properties.
In conclusion, acknowledge of study limitations, its overgeneralization toward nuclear reactor conditions.
Recommendation: Revisions Required

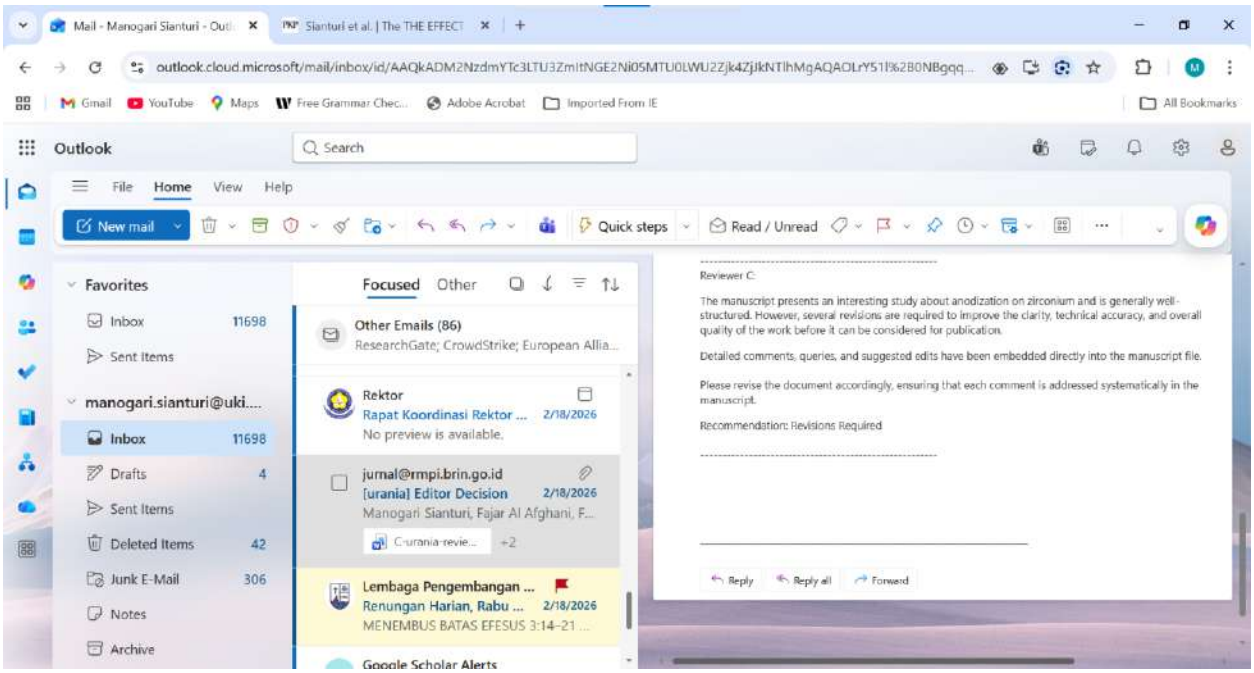
Mail - Manogari Sianturi - Out
Sianturi et al. | The THE EFFECT
outlook.cloud.microsoft/mail/inbox/id/AAQkADM2NzdmYTc3LTU3ZmItNGE2Ni05MTU0LWU2Zjk4ZjJkNTlhMgAQAOLrY51l%2B0NBgqq...
Gmail
YouTube
Maps
Free Grammar Chec...
Adobe Acrobat
Imported From IE
All Bookmarks
Outlook
Search
File
Home
View
Help
New mail
Quick steps
Read / Unread
Favorites
Inbox 11698
Sent Items
manogari.sianturi@uki....
Inbox 11698
Drafts 4
Sent Items
Deleted Items 42
Junk E-Mail 306
Notes
Archive
Focused
Other
Other Emails (86)
ResearchGate; CrowdStrike; European Allia...
Rektor
Rapat Koordinasi Rektor ... 2/18/2026
No preview is available.
jurnal@rmpi.brin.go.id
[urania] Editor Decision 2/18/2026
Manogari Sianturi, Fajar Al Afghani, F...
C-urania-revie...
+2
Lembaga Pengembangan ...
Renungan Harian, Rabu ... 2/18/2026
MENEMBUS BATAS EFESUS 3:14-21 ...
Google Scholar Alerts
Reviewer C:
The manuscript presents an interesting study about anodization on zirconium and is generally well-structured. However, several revisions are required to improve the clarity, technical accuracy, and overall quality of the work before it can be considered for publication.
Detailed comments, queries, and suggested edits have been embedded directly into the manuscript file.
Please revise the document accordingly, ensuring that each comment is addressed systematically in the manuscript.
Recommendation: Revisions Required
Reply
Reply all
Forward

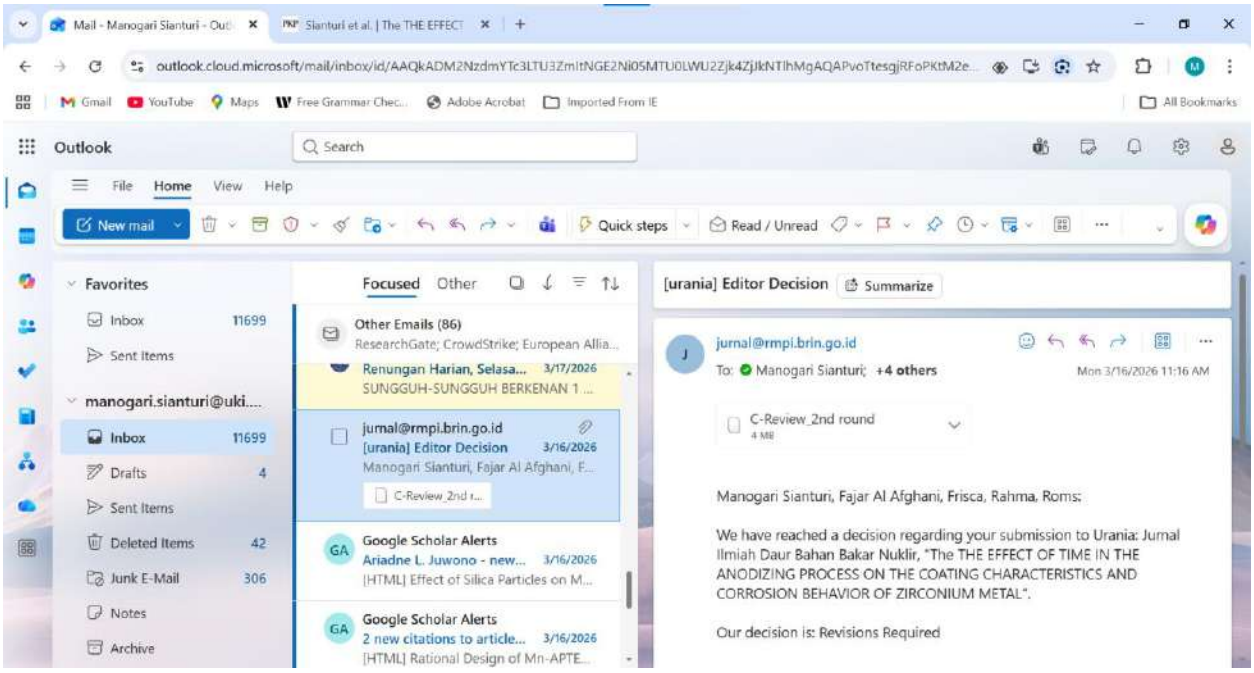
Mail - Manogari Sianturi - Out
Sianturi et al. | The THE EFFECT
outlook.cloud.microsoft/mail/inbox/id/AAQkADM2NzdmYTc3LTU3ZmItNGE2Ni05MTU0LWU2Zjk4ZjJkNTlhMgAQAPvoTtesgjRFoPKtM2e...
Gmail
YouTube
Maps
Free Grammar Chec...
Adobe Acrobat
Imported From IE
All Bookmarks
Outlook
Search
File
Home
View
Help
New mail
Quick steps
Read / Unread
Favorites
Inbox 11699
Sent Items
manogari.sianturi@uki....
Inbox 11699
Drafts 4
Sent Items
Deleted Items 42
Junk E-Mail 306
Notes
Archive
Focused
Other
Other Emails (86)
ResearchGate; CrowdStrike; European Allia...
Renungan Harian, Selasa... 3/17/2026
SUNGGUH-SUNGGUH BERKENAN 1 ...
jurnal@rmpi.brin.go.id
[urania] Editor Decision 3/16/2026
Manogari Sianturi, Fajar Al Afghani, F...
C-Review_2nd r...
Google Scholar Alerts
Ariadne L. Juwono - new... 3/16/2026
[HTML] Effect of Silica Particles on M...
Google Scholar Alerts
2 new citations to article... 3/16/2026
[HTML] Rational Design of Mn-APTE...
[urania] Editor Decision
Summarize
jurnal@rmpi.brin.go.id
To: Manogari Sianturi; +4 others
Mon 3/16/2026 11:16 AM
C-Review_2nd round
4 MB
Manogari Sianturi, Fajar Al Afghani, Frisca, Rahma, Roms:
We have reached a decision regarding your submission to Urania: Jurnal Ilmiah Daur Bahan Bakar Nuklir, "The THE EFFECT OF TIME IN THE ANODIZING PROCESS ON THE COATING CHARACTERISTICS AND CORROSION BEHAVIOR OF ZIRCONIUM METAL".
Our decision is: Revisions Required

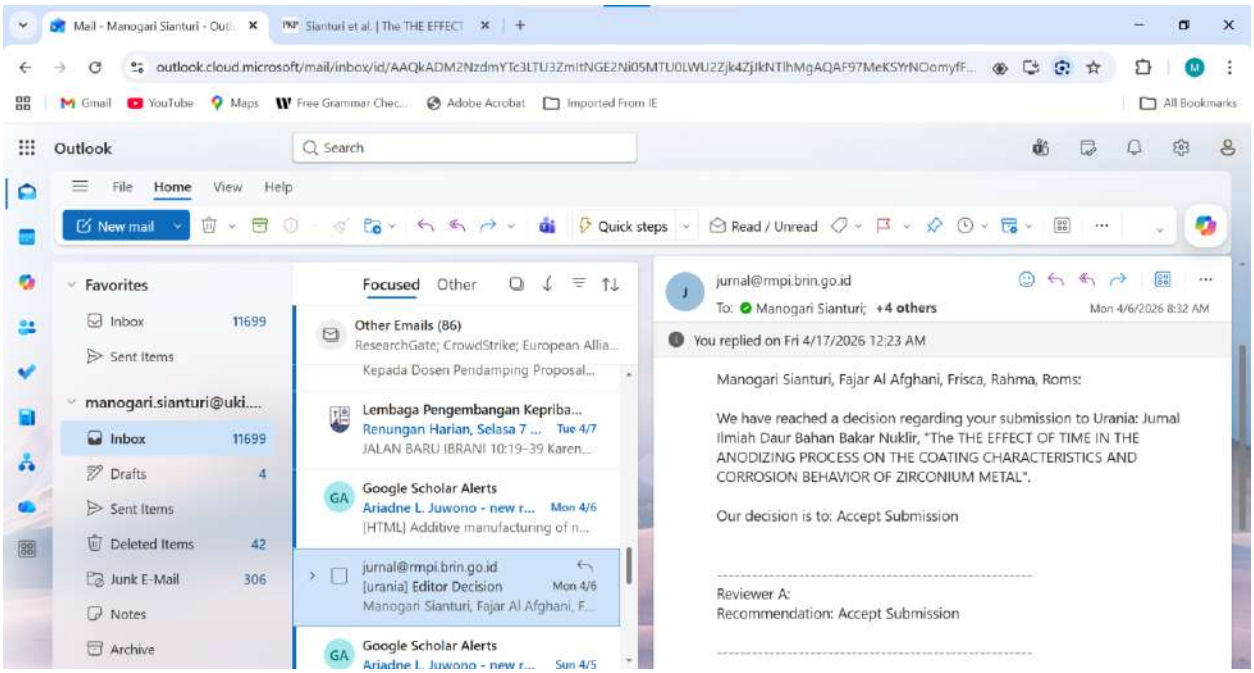
Mail - Manogari Sianturi - Outl
Sianturi et al. | The THE EFFECT
outlook.cloud.microsoft/mail/inbox/id/AAQkADM2NzdmYTc3LTU3ZmItNGE2Ni05MTU0LWU2Zjk4ZjJkNTlhMgAQAF97MeKSYrNCOmyfF...
Gmail
YouTube
Maps
Free Grammar Chec...
Adobe Acrobat
Imported From IE
All Bookmarks
Outlook
Search
File
Home
View
Help
New mail
Quick steps
Read / Unread
Favorites
Inbox 11699
Sent Items
manogari.sianturi@uki....
Inbox 11699
Drafts 4
Sent Items
Deleted Items 42
Junk E-Mail 306
Notes
Archive
Focused
Other
Other Emails (86)
ResearchGate; CrowdStrike; European Allia...
Kepada Dosen Pendamping Proposal...
Lembaga Pengembangan Kepriba...
Renungan Harian, Selasa 7 ... Tue 4/7
JALAN BARU IBRANI 10:19-39 Karen...
Google Scholar Alerts
Ariadne L. Juwono - new r... Mon 4/6
[HTML] Additive manufacturing of n...
jurnal@rmpi.brin.go.id
[urania] Editor Decision Mon 4/6
Manogari Sianturi, Fajar Al Afghani, F...
Google Scholar Alerts
Ariadne L. Juwono - new r... Sun 4/5
jurnal@rmpi.brin.go.id
To: Manogari Sianturi; +4 others
Mon 4/6/2026 8:32 AM
You replied on Fri 4/17/2026 12:23 AM
Manogari Sianturi, Fajar Al Afghani, Frisca, Rahma, Roms:
We have reached a decision regarding your submission to Urania: Jurnal Ilmiah Daur Bahan Bakar Nuklir, "The THE EFFECT OF TIME IN THE ANODIZING PROCESS ON THE COATING CHARACTERISTICS AND CORROSION BEHAVIOR OF ZIRCONIUM METAL".
Our decision is to: Accept Submission
Reviewer A:
Recommendation: Accept Submission

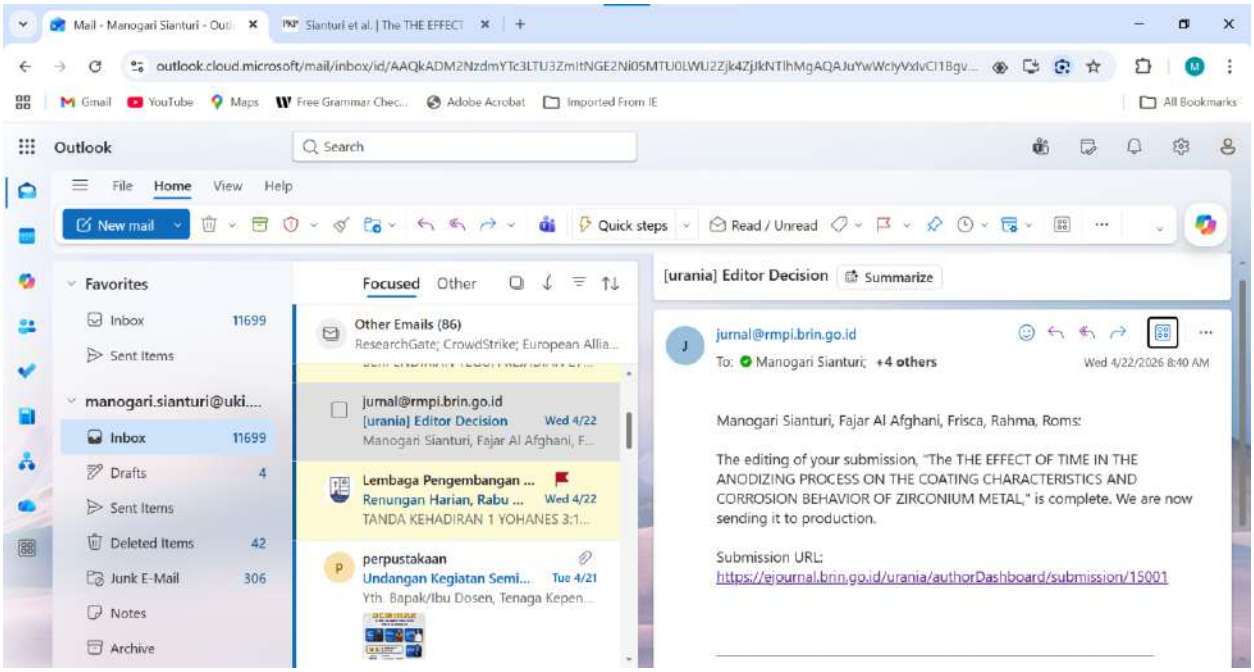
Mail - Manogari Sianturi - Outl
Sianturi et al. | The THE EFFECT
outlook.cloud.microsoft/mail/inbox/id/AAQkADM2NzdmYTc3LTU3ZmItNGE2Ni05MTU0LWU2Zjk4ZjJkNTlhMgAQAJuYwWcIyVxlvCI1Bgv...
Gmail
YouTube
Maps
Free Grammar Chec...
Adobe Acrobat
Imported From IE
All Bookmarks
Outlook
Search
File
Home
View
Help
New mail
Quick steps
Read / Unread
Favorites
Inbox 11699
Sent Items
manogari.sianturi@uki....
Inbox 11699
Drafts 4
Sent Items
Deleted Items 42
Junk E-Mail 306
Notes
Archive
Focused
Other
Other Emails (86)
ResearchGate; CrowdStrike; European Allia...
jurnal@rmpi.brin.go.id
[urania] Editor Decision Wed 4/22
Manogari Sianturi, Fajar Al Afghani, F...
Lembaga Pengembangan ...
Renungan Harian, Rabu ... Wed 4/22
TANDA KEHADIRAN 1 YOHANES 3:1...
perpustakaan
Undangan Kegiatan Semi... Tue 4/21
Yth. Bapak/Ibu Dosen, Tenaga Kepen...
[urania] Editor Decision
Summarize
jurnal@rmpi.brin.go.id
To: Manogari Sianturi; +4 others
Wed 4/22/2026 8:40 AM
Manogari Sianturi, Fajar Al Afghani, Frisca, Rahma, Roms:
The editing of your submission, "The THE EFFECT OF TIME IN THE ANODIZING PROCESS ON THE COATING CHARACTERISTICS AND CORROSION BEHAVIOR OF ZIRCONIUM METAL," is complete. We are now sending it to production.
Submission URL:
https://ejournal.brin.go.id/urania/authorDashboard/submission/15001

Urania
Jurnal Ilmiah Daur Bahan Bakar Nuklir

Beranda jurnal: http://jurnal.batan.go.id/index.php/urania/

THE EFFECT OF TIME IN THE ANODIZING PROCESS ON THE COATING CHARACTERISTICS AND CORROSION BEHAVIOR OF ZIRCONIUM METAL

ABSTRAK

Zirkonium dan paduannya merupakan material standar untuk kelongsong bahan bakar nuklir pada Pressurized Water Reactor (PWR) karena memiliki penampang lintang serapan neutron yang rendah, sifat mekanik yang unggul, serta ketahanan korosi yang baik dalam lingkungan air bersuhu tinggi. Namun, kondisi operasi PWR memberikan lingkungan yang sangat berat sehingga dapat menurunkan integritas kelongsong seiring waktu, termasuk melalui proses oksidasi, hidriding, serta kerusakan mekanik seperti goresan atau penyok yang dapat terjadi selama operasi pengisian ulang bahan bakar. Cacat permukaan tersebut dapat bertindak sebagai lokasi inisiasi korosi terlokalisasi yang berpotensi mengompromikan penghalang penahanan primer.Penelitian ini menyelidiki efektivitas anodisasi elektrokimia sebagai teknik modifikasi permukaan untuk meningkatkan kinerja zirkonium. Proses anodisasi dilakukan pada tegangan konstan sebesar 30 V dengan variasi waktu 10, 15, dan 20 menit. Karakteristik permukaan yang dihasilkan dievaluasi menggunakan Mikroskop Optik, Mikroskop Digital untuk analisis kekasaran permukaan, serta X-Ray Diffraction (XRD). Keandalan mekanik dinilai melalui pengujian kekerasan mikro Vickers, sedangkan perilaku korosi dipelajari dalam larutan NaCl 3,5% menggunakan metode Open Circuit Potential (OCP), Potentiodynamic Polarization (PDP), dan Electrochemical Impedance Spectroscopy (EIS).Hasil penelitian menunjukkan bahwa peningkatan waktu anodisasi secara signifikan memperbaiki kualitas permukaan, ditunjukkan dengan penurunan nilai kekasaran rata-rata Ra dari 0,53 µm (10 menit) menjadi 0,24 µm (20 menit). Analisis XRD mengonfirmasi terbentuknya lapisan oksida ZrO_2 yang bersifat kristalin. Pengujian elektrokimia memperlihatkan peningkatan ketahanan korosi yang signifikan, di mana rapat arus korosi i_{corr} menurun hingga dua orde magnitudo dari 12,93 x 10^{-9} A/cm^2 pada substrat menjadi 0,19 x 10^{-9} A/cm^2 pada spesimen yang dianodisasi selama 20 menit. Penelitian ini menyimpulkan bahwa perlakuan anodisasi selama 20 menit pada tegangan 30 V mampu menghasilkan lapisan oksida yang kuat, halus, dan sangat tahan terhadap korosi, sehingga berpotensi efektif dalam memitigasi degradasi pada aplikasi kelongsong bahan bakar nuklir.

Kata kunci: Zirkonium, Anodisasi, Ketahanan Korosi, Kelongsong Nuklir, PWR, Modifikasi Permukaan.

ABSTRACT

Zirconium and its alloys are the standard material for nuclear fuel cladding in Pressurized Water Reactors (PWR) due to their low neutron absorption cross-section, excellent mechanical properties, and good corrosion resistance in high-temperature water. However, the operational environment of a PWR imposes severe conditions that can degrade the cladding integrity over time, including oxidation, hydriding, and mechanical damage such as scratching or denting during fuel refueling operations. These surface defects can act as initiation sites for localized corrosion, potentially compromising the primary containment barrier. This study investigates the effectiveness of electrochemical anodizing as a surface modification technique to enhance the performance of Zirconium. The anodizing process was conducted at a constant voltage of 30 V with varying durations of 10, 15, and 20 minutes. The resulting surface characteristics were evaluated using Optical Microscopy, Digital Microscopy for roughness analysis, and X-Ray Diffraction (XRD). Mechanical reliability was assessed via Vickers Microhardness testing, while corrosion behavior was studied in a 3.5% NaCl solution using Open Circuit Potential (OCP), Potentiodynamic Polarization (PDP), and Electrochemical Impedance Spectroscopy (EIS). The results demonstrated that increasing the anodizing time significantly improved the surface quality, reducing the arithmetic mean roughness Ra from 0.53 µm (10 min) to 0.24µm (20 min). XRD analysis confirmed the formation of a crystalline ZrO_2 oxide layer. Electrochemical tests revealed a substantial enhancement in corrosion resistance; the corrosion current density i_{corr} decreased by two orders of magnitude from 12.93 x 10^{-9} A/cm^2 for the substrate to 0.19 x 10^{-9} A/cm^2 for the 20-minute anodized specimen. The study concludes that a 20-minute anodizing treatment at 30 V produces a robust, smooth, and highly corrosion-resistant oxide layer suitable for mitigating degradation in nuclear fuel cladding applications.

Keywords: Zirconium, Anodizing, Corrosion Resistance, Nuclear Cladding, PWR, Surface Modification.

Commented [MOU1]: There is no EIS data and analysis in the manuscript

INTRODUCTION

Zirconium (Zr) and its alloys, such as Zircaloy-4 and Zirlo, are the materials of choice for nuclear fuel cladding in light water reactors (LWR), particularly Pressurized Water Reactors (PWR). This selection is driven by Zirconium's unique combination of properties: an exceptionally low thermal neutron capture cross-section (0.18 barn), which ensures efficient neutron economy, good thermal conductivity, and adequate mechanical strength at elevated temperatures [1, 2]. As the first barrier in the defense-in-depth strategy, the cladding must hermetically seal radioactive fission products preventing their release into the primary coolant.

Despite these advantages, Zirconium cladding faces formidable challenges during its service life. The aggressive operating environment, characterized by high-pressure water (approx. 15.5 MPa) and high temperatures (approx. 300-350°C), promotes waterside corrosion and hydrogen pickup [3, 4]. The oxidation of zirconium ($Zr + 2H_2O \rightarrow ZrO_2 + 2H_2$) not only thins the structural wall but also generates hydrogen, a fraction of which diffuses into the metal matrix, leading to hydride precipitation and embrittlement [5]. Furthermore, beyond steady-state operation, the cladding is subjected to mechanical stress during fuel handling and refueling processes. Physical contact with grid spacers or other assemblies can cause surface scratches, fretting, or dents. These surface imperfections significantly increase local roughness and can serve as stress concentration points or preferential sites for pitting corrosion, accelerating material degradation [6, 7].

Extending the operational life of fuel assemblies and enhanced safety margins, particularly for high-burnup regimes, surface modification techniques have gained attention. The goal is to create a protective surface layer that is harder than the substrate to resist mechanical damage and more chemically stable to inhibit corrosion [8]. Among various techniques such as physical vapor deposition (PVD) or laser surface treatment, electrochemical anodizing stands out due to its simplicity, cost-effectiveness, and ability to form a uniform, adherent oxide film (ZrO2) even on complex geometries [9].

Commented [MOU2]: ZrO_2

Anodizing promotes the growth of a thickened oxide layer that acts as a passivating barrier. While the natural oxide film on Zirconium is protective, it is thin and liable to breakdown. Anodic films, depending on process parameters like voltage,

Commented [MOU3]: what is the advantage of anodizing method compared to PVD?

DOI: https://doi.org/10.17146/urania.20xx.xx.x.xxxx

electrolyte, and time, can be engineered to be thicker and more compact [10, 11]. Recent studies have focused on the voltage effects, but the influence of anodizing duration—specifically in the transition from initial film formation to steady-state growth—on the micro-roughness and electrochemical impedance of the surface remains an area for optimization [12].

This study aims to systematically evaluate the effect of anodizing time (10, 15, and 20 minutes) at a fixed potential of 30 V on the surface characteristics and corrosion behavior of Zirconium. We hypothesize that extending the anodizing duration will not only increase the oxide thickness but also reduce surface roughness through a leveling effect, thereby providing superior corrosion resistance in aggressive chloride environments.

METHODOLOGY

The sSubstrate material used was commercial purity Zirconium metal, cut into coupon specimens with dimensions of $10 mm \times 10 mm$. The samples were mounted in epoxy resin to expose a single working surface area. Prior to anodizing, the surfaces were mechanically polished using a sequence of Silicon Carbide (SiC) abrasive papers with grit sizes of 500, 800, 1200, and 2000. This step was crucial to remove the heterogeneous native oxide layer and standardize the initial surface roughness. After polishing, the samples were ultrasonically cleaned in acetone and rinsed with demineralized water to remove any particulate residues.

The anodizing process was carried out in a two-electrode electrochemical cell at room temperature. The Zirconium specimen served as the anode, while a high-purity platinum sheet was used as the cathode to ensure chemical inertness. The electrolyte was a specific aqueous solution tailored for compact film growth (typically phosphate/ammonium based). Phosphoric acid (H_3PO_4) at a concentration of 30 g/L is used as the electrolyte for the anodization process. Measuring the phosphoric acid with an analytical balance and combining it with distilled water in a beaker is the first step in the electrolyte production process. When the solution is ready to be employed as an anodizing medium on zirconium metal substrates, it is mixed with a magnetic stirrer until it dissolves uniformly.

A DC power supply was used to apply a constant voltage of 30 V. The anodizing duration varied as the experimental parameter: 10 minutes (Zr-10), 15 minutes (Zr-15), and 20 minutes (Zr-20). Post-anodizing, samples were rinsed and dried in air. A digital multimeter (DMM) was used to monitor the voltage and current during the anodization process. The solution was kept at room temperature to prevent localized heating that would result in non-uniform oxidation. The voltage source was turned off, and the specimen was removed from the electrolyte solution after the anodization period was complete. A hair dryer was used to dry any leftover electrolyte after it had been cleansed with distilled water. All anodized specimens were kept in a closed container, and silica gel was added to regulate the humidity in the storage area prior to testing for corrosion resistance, hardness, and surface morphology examination.

Surface morphology and visual appearance were documented using an Optical Microscope and a high-resolution Digital Microscope. The surface roughness parameters, Arithmetic Mean Roughness (Ra) and Ten-Point Mean Roughness (Rz), were quantified to evaluate the smoothing effect of the treatment. The surface morphology study was supported by microstructural findings. The samples' surface and texture were examined using scanning electron microscopy (SEM) at an accelerating voltage of 15 kV, which provided precise topographical information on the zirconium dioxide (ZrO_2) layer. Porosity, fractures, oxide layer thickness, and surface features that matched each time variation were observed using SEM examination. Additionally, the elemental composition of the coating was determined using Energy Dispersive Spectroscopy (EDS), with a focus on the distribution of phosphorus and oxygen to validate the creation of the ZrO_2 layer and potential interactions with the H_3PO_4 electrolyte. For additional examination, elemental mapping and spectra were both obtained.

The crystalline structure of the anodic oxide layers was analyzed using X-Ray Diffraction (XRD) with Cu-Kα radiation. To assess the resistance to mechanical damage, Vickers Microhardness testing was performed using a load of 300 gf with a dwell time of 15 seconds; five indentations were made per sample to obtain an average value.

Commented [MOU8]: was the current response of the power supply being recorded?

Commented [MOU4]: Please strengthen the introduction and literature review sections regarding the anodization of Zirconium (Zr) for nuclear cladding applications.

Commented [MOU5]: Please revised this writing

Commented [MOU6]: Please define the area of exposed surface (in cm^2)

Commented [MOU9]: There is no data of porosity and oxide thickness in the Result section.
It would be better to provide oxide thickness data using cross-sectional SEM or thickness gauge measurement to confirm the effect of anodizing time variations.

Commented [MOU10]: Please provide the ZrO2 formation and H3PO4 incorporation reaction in the Result section.

Commented [MOU7]: Are there references for this compact film growth setup? Since anodization coating layer can also be nanoporous/nanotubular.

Corrosion performance was evaluated in a 3.5% NaCl solution, chosen to simulate an aggressive corrosive environment that accelerates pitting attack. A standard three-electrode cell was employed, consisting of the Zr specimen (working electrode), an Ag/AgCl reference electrode, and a graphite counter electrode. The measurements were conducted using a Potentiostat/Galvanostat with the following sequence:

1. Open Circuit Potential (OCP): Monitored for 3600 seconds until a stable potential was reached.
2. Potentiodynamic Polarization (PDP): Scanned from -250 mV to +250 mV relative to OCP at a scan rate of 1 mV/s to determine Tafel parameters E_{corr} and i_{corr}.

RESULTS AND DISCUSSION

Surface Morphology and Roughness Analysis

~~Analysis~~ Visual inspection of the samples immediately after anodizing revealed a distinct coloration of the surface. As shown in Figure 1, the surface color shifted from the metallic silver of the substrate to uniform hues of gold and blue. This phenomenon is attributed to the interference of light within the transparent anodic oxide film (ZrO_2), where the perceived color is directly related to the film thickness governed by the anodizing duration [13].

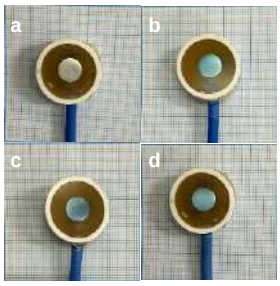

Figure 1. Color of zirconium oxide with various anodizing time of a) Zr, b) Zr-10, c) Zr-15, and d) Zr-20 minutes

Microstructural analysis via optical microscopy (Figure 2) and SEM (Figure 3) indicated a significant improvement in surface texture. The non-anodized substrate exhibited polishing lines and surface irregularities. However, post-anodizing, these features were progressively smoothed.

The anodization of Zr metal at 10 minutes produced a comparatively uneven surface morphology in Figure 2a. A coating of zirconium oxide had developed at that point, although it was not yet uniformly distributed. The 3D profile data (Figure 2b) revealed that the oxide layer was still in its early phases of formation, resulting in a very rough surface roughness. The duration of anodization was extended to 15 minutes (Figure 2c). Compared to Zr-10, the resulting zirconium oxide layer became more homogeneous, thick, and continuous. This result was also confirmed from the 3D profile of Figure 2d. Figure 2e shows the anodization of Zr metal with a process time of 20 minutes. Increasing the anodization time contributed to the growth and stability of the zirconium oxide layer formed on the metal surface. The layer was more uniform, dense, and surface defects were significantly reduced. The relevant results are confirmed by Figure 2f.

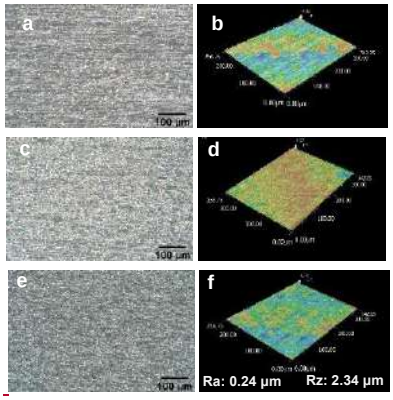

g

Specimen	Surface Roughness	
	Ra	Rz
Zr-10	0.53	4.35
Zr-15	0.34	4.98
Zr-20	0.24	2.34

Figure 2. Microstructural analysis via optical microscopy (a,c,e), 3D profile (b,d,f), and surface roughness value (g) of (a,b) Zr-anodized 10 minutes, (c,d) Zr-anodized 15 minutes, and (e,f) Zr-anodized 20 minutes.

Commented [MOU11]: The figure of the anodized sample would be better if magnified or cropped to show the surface details more clearly

Quantitative roughness data presented in Figure 2g and Figure 2 (b,d,f) confirm this observation. The average roughness (Ra) decreased from 0.53 µm for the Zr-10

DOI: https://doi.org/10.17146/urania.20xx.xx.x.xxxx

specimen to 0.34 µm for Zr-15, and finally to 0.24 µm for Zr-20. This trend suggests a "leveling mechanism" where the oxide grows preferentially in the microscopic valleys of the metal surface, effectively reducing the peak-to-valley height [14]. A smoother surface is highly advantageous for nuclear cladding as it reduces the friction coefficient during fuel rod insertion and minimizes the surface area available for corrosive attack.

Figure 3. shows sSurface view SEM images and the corresponding EDS area mapping of zirconium anodized under different duration processes. The surfaces of all the specimens were quite homogeneous and devoid of significant cracks. Increasing the anodization time prevented any significant morphological changes at the micrometer scale. For every modification in anodization time, the elemental mapping findings on the zirconium oxide layer's surface revealed an equitable distribution of elements. The anodized metal surface was dominated by Zr and O elements.

The zirconium substrate, whose composition decreased as the anodization duration increased, provided the Zr element. The O element showed that an oxide layer had formed during the anodization processes. The composition of the O element increased as the anodization duration increased, indicating the thickening and expansion of the zirconium oxide layer (ZrO_2). The increase in the O element was formed from 44.66 at% for the Zr-10 specimen, 53.12 at% for the Zr-15 specimen, and the highest for the Zr-20 specimen, namely 54.33 at%. The P element was also found throughout the layer's surface in addition to these primary components. The phosphate-based electrolyte used during the anodizing process is the source of the phosphorus, which is present in trace levels (around 1-2 at%) but is dispersed rather uniformly.

Crystalline Structure and Microhardness the XRD patterns shown in Figure 4 display sharp diffraction peaks corresponding to Zirconium Oxide (ZrO_2). The analysis suggests the presence of a cubic crystalline phase, which is notable as anodic films formed at lower voltages are often amorphous. The formation of this crystalline phase contributes to the chemical stability of the coating [15]. Diffraction peaks for the zirconium (Zr) and zirconium oxide (ZrO_2) phases were detected on all anodized specimens. The ZrO_2 peak's formation indicates that the anodization procedure was effective in generating an oxide layer on the zirconium substrate's surface. The ZrO_2 diffraction peak's clarity tended to rise with increasing anodization time, especially in the Zr-20 specimen, which showed the maximum peak intensity. This suggests that extended anodization durations encourage the formation of an oxide layer that is thicker and/or more crystalline. In the meantime, peaks from the Zr phase were still identified, suggesting that the relatively tiny oxide layer thickness allowed X-rays to proceed toward the substrate. In general, the XRD data confirm that different anodization times affect the zirconium oxide layer's growth and crystal properties.

Mechanical integrity was evaluated via Vickers microhardness (HV). As detailed in Table 1, the hardness values were relatively stable across the anodized samples: 144.41±8.99 HV (10 min), 144.66±7.84 HV (15 min), and 142.88±6.96 HV (20 min). Although the macroscopic hardness did not show a drastic increase compared to the substrate (likely due to the indentation depth exceeding the thin oxide layer thickness), the presence of the hard ceramic ZrO_2 skin provides essential resistance against superficial scratching and fretting wear, which are critical precursors to cladding failure [16].

Table 1. Average and Standar Deviation (STDV) for Microhardness of Zr-Anodized under different duration process

Specimen	HV					Average	Standard Deviasi
	1	2	3	4	5		
Zr-10	150.97	138.23	140.08	158.57	134.19	144.41	8.99
Zr-15	156.89	142.93	138.07	149.92	135.5	144.66	7.84
Zr-20	155.79	144.39	137.77	136.86	139.61	142.88	6.96

Commented [MOU13]: It would be better if you provide the JCPDS or ICDD card number for the crystalline phases.

Commented [MOU14]: Please provide the mechanism for the oxide layer formation. What is the reactions in the anode, cathode, and/or electrolytes?

Commented [MOU15]: Why not using lower weight of the indenter (for example 50 or 100 gF) to give actual thin oxide coating hardness value?

Commented [MOU12]: Please clarify the mechanism of phosphorus (P) incorporation into the coating. It would be helpful to distinguish whether the presence of P is due to residual/leftover electrolyte from insufficient rinsing or if it was actively incorporated into the coating via the electric field during the process.

Is there relationship between anodizing time and P element concentration in the ZrO2 coating?

What is the impact of P element for nuclear fuel cladding application?

Commented [MOU16]: deviation

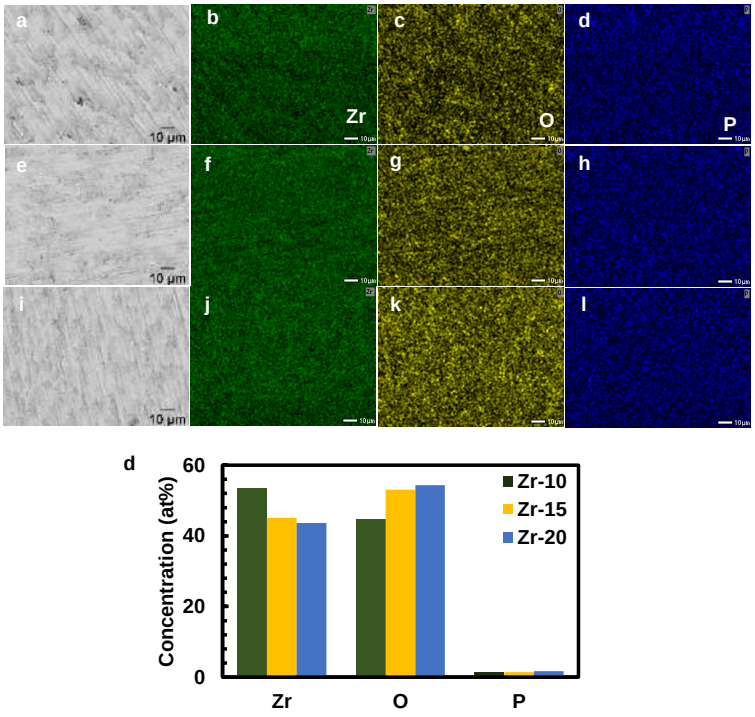

Figure 3. Surface view SEM images and the corresponding EDS area mapping of zirconium anodized of (a-d) Zr-10, (e-h) Zr-15, and (i-l) Zr-20 minutes

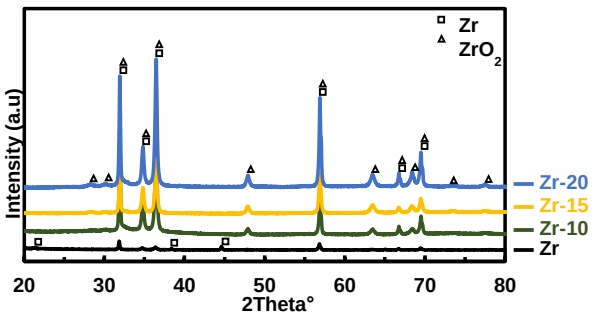

Figure 4. XRD pattern of zirconium oxide (ZrO_2)

DOI: https://doi.org/10.17146/urania.20xx.xx.x.xxxx

Electrochemical Corrosion Behavior

The corrosion resistance was comprehensively analyzed using OCP, PDP, and EIS techniques. Open Circuit Potential (OCP): Figure 5 illustrates the OCP evolution. All anodized specimens exhibited more positive (noble) potentials compared to the bare substrate. The Zr-20 sample showed the most noble potential, stabilizing at a higher value, which indicates a thermodynamic tendency to resist spontaneous corrosion reactions in the electrolyte [17]. During the test, pure zirconium (Zr) specimens had the most negative and comparatively steady potential values, suggesting more potential for corrosion. All the specimens indicated a potential change in a more positive direction immediately after the anodization process, which suggests that the formation of a zirconium oxide layer had increased electrochemical stability. Zr-20, Zr-15, and Zr-10 were the anodized specimens with the most positive and consistent OCP values while the test. This suggests that extending the anodization duration increases the material's resistance to corrosion and creates a more protective oxide layer. The formation of a rather stable passive layer on the zirconium surface is also shown by the stability of the OCP curves over an extended test time.

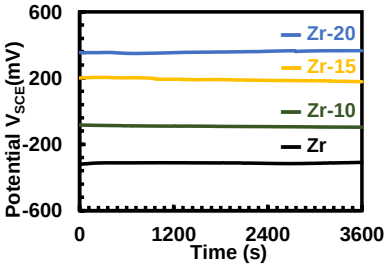

Figure 5. Average of OCP curves for zirconium substrate and zirconium-anodized at 30 V

Potentiodynamic Polarization (PDP): The Tafel polarization curves in Figure 6 demonstrate a clear shift in corrosion kinetics. The electrochemical parameters summarized in Table 2 show a dramatic reduction in corrosion current density (i_{corr}). The substrate exhibited an i_{corr} of 12.93 × 10^{-9}A/cm^2. In contrast, the Zr-20 specimen exhibited an i_{corr} of 0.19 × 10^{-9}A/cm^2. This reduction by nearly two orders of magnitude confirms that the thicker oxide layer formed at 20 minutes acts as an effective barrier, blocking the diffusion of chloride ions (Cl^-) and oxygen to the metal interface [18, 19].

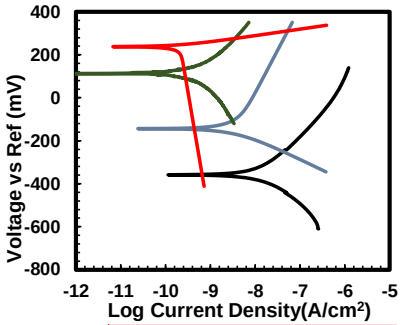

Figure 6. Average of PDP curves for zirconium substrate and zirconium-anodised at 30 V

Figure 6 presents the potentiodynamic polarization (PDP) curves of anodized and pure zirconium. These curves illustrate the relationship between the voltage across a reference electrode and the log current density, which is used to assess corrosion behavior and electrochemical reaction kinetics. Pure zirconium exhibits poor corrosion resistance, indicated by its limited passivation range and relatively high corrosion current density. In contrast, anodized specimens show a shift in corrosion potential to more positive values and a decrease in corrosion current density. Compared to Zr-15 and Zr-10, the Zr-20 specimen shows the biggest passivation area and the lowest current density. The Zr-20 specimen exhibits the lowest current density and the largest passivation region compared to Zr-15 and Zr-10. This suggests that the zirconium oxide layer that develops over extended anodization durations successfully prevents charge transfer and reduces the rate of corrosion.

Commented [MOU17]: There are no EIS data and analysis in the manuscript

Commented [MOU18]: Why the red PDP curve in Figure 6 shapes so different compared to other samples?

Commented [MOU19]: please provide legend for the PDP curve. It would also be better if same colours of samples in OCP curve are used.

Table 2. PDP Parameter of Zr-Anodized under different duration process

Specimen	E_{corr} (mV)	i_{corr} (10^{-9}A/cm^2)	β_{Anodic} (mV/Decade)	$\beta_{Catodic}$ (mV/Decade)
Zr	-346 ± 88	12.93 ± 2.89	399 ± 350	275 ± 152
Zr-10	-114 ± 94	2.57 ± 1.12	599± 461	198 ± 122
Zr-15	113 ± 98	1.10 ± 0.82	275 ± 201	363 ± 262
Zr-20	233 ± 74	0.19 ± 0.04	275 ± 201	363 ± 262

Commented [MOU20]: The values for βa (anodic) and βc (cathodic) for samples Zr-15 and Zr-20 appear to be identical. Please verify if these results are accurate or if this is a copy-paste error during data entry.

CONCLUSIONS

The effect of anodizing duration on the surface characteristics and corrosion behavior of Zirconium was successfully investigated. The following conclusions are drawn:

1. Surface Improvement: Increasing the anodizing time from 10 to 20 minutes at 30 V results in a progressively smoother surface. The Zr-20 specimen achieved the lowest roughness (Ra= 0.24 µm), reducing friction and potential pit initiation sites.
2. Oxide Formation: The process forms a stable, crystalline ZrO_2 layer, as confirmed by XRD and the observation of interference colors.
3. Corrosion Resistance: The 20-minute anodized coating offers superior corrosion protection in chloride environments. It reduced the corrosion rate i_{corr} by approximately 98% compared to the bare substrate and significantly increased the polarization resistance.
4. Application Viability: The study confirms that a 20-minute anodizing treatment is an effective, low-cost method to enhance the durability of Zirconium nuclear fuel cladding, potentially extending the safety margins against corrosion and mechanical degradation in PWR environments.

Commented [MOU21]: The Conclusion point 2 lacks sufficient depth, as the formation of ZrO2 via Zirconium anodization is a well-established phenomenon. To increase the impact of this study, the authors should instead focus on how electrolyte constituents, specifically Phosphorus, are incorporated into the ZrO2 coating.

REFERENCES

[1] Motta, A. T., Couet, A., & Comstock, R. J. (2015). Corrosion of Zirconium Alloys Used for Nuclear Fuel Cladding. Annual Review of Materials Research, 45, 311-343.

[2] Duan, Z., Yang, H., Satoh, Y., & Murakami, K. (2017). Oxidation behavior of zirconium alloys in a simulated nuclear reactor primary coolant. Journal of Nuclear Materials, 485, 147-158.

[3] Terrani, K. A. (2018). Accident tolerant fuel cladding development: Promise, status, and challenges. Journal of Nuclear Materials, 501, 13-30.

[4] Gong, W., & Yun, D. (2022). A review on the corrosion behavior of zirconium alloys in supercritical water. Corrosion Science, 208, 110620.

[5] Yilmazbayhan, A., Motta, A. T., & Comstock, R. J. (2021). Hydride morphology and embrittlement in Zircaloy-4 cladding. Journal of Nuclear Materials, 545, 152646.

[6] Liu, J., & Li, Q. (2023). Fretting wear behavior of zirconium alloy cladding tubes. Wear, 522, 204689.

[7] Kim, H. G., & Kim, I. H. (2020). Oxidation behavior of zirconium alloy claddings in high temperature steam. Nuclear Engineering and Technology, 52(4), 808-815.

[8] Suresh, S., & Sharma, A. (2021). Surface modification of zirconium alloys for biomedical and nuclear applications: A review. Surface and Coatings Technology, 405, 126666.

[9] Verma, R., & Kumar, S. (2022). Electrochemical anodization of zirconium: Growth mechanism and properties. Electrochimica Acta, 412, 140135.

[10] Cheng, Y., & Matykina, E. (2021). Formation of nanotubular oxide layers on Zirconium alloys by anodization. Corrosion Science, 182, 109289.

[11] Ali, F., & Al-Hajri, M. (2023). Effect of voltage and electrolyte composition on the morphology of anodic zirconium oxide.

DOI: https://doi.org/10.17146/urania.20xx.xx.x.xxxx

Materials Chemistry and Physics, 295, 127087.

[12] Wang, L., Zhang, Y., & Wu, X. (2024). Time-dependent growth kinetics of anodic films on zirconium in phosphate electrolytes. Journal of Electrochemical Society, 171(2), 021504.

[13] Diamanti, M. V., & Pedeferri, M. P. (2020). Color production on zirconium by anodizing: Interference and absorption effects. Color Research & Application, 45(3), 456-464.

[14] Thompson, G. E. (2019). Porous anodic oxide films: Formation, growth and applications. Thin Solid Films, 685, 34-45.

[15] Zhao, X., & Xu, H. (2022). Phase transformation in anodic zirconia films: From amorphous to crystalline. Scripta Materialia, 210, 114421.

[16] Obbard, E. G., & Burr, P. A. (2021). Mechanical properties of zirconium oxide scales: A review. Journal of Nuclear Materials, 557, 153255.

[17] McCafferty, E. (2020). Introduction to Corrosion Science (2nd ed.). Springer.

[18] Zhang, B., & Frankel, G. S. (2022). Corrosion mechanisms of zirconium alloys in chloride-containing environments. Corrosion, 78(5), 412-425.

[19] Li, T., & Wang, F. (2023). Improvement of pitting corrosion resistance of Zr alloys by anodic oxidation. Applied Surface Science, 610, 155567.

[20] Orazem, M. E., & Tribollet, B. (2017). Electrochemical Impedance Spectroscopy. Wiley.

Urania
Jurnal Ilmiah Daur Bahan Bakar Nuklir

Beranda jurnal: http://jurnal.batan.go.id/index.php/urania/

THE EFFECT OF TIME IN THE ANODIZING PROCESS ON THE COATING CHARACTERISTICS AND CORROSION BEHAVIOR OF ZIRCONIUM METAL

ABSTRAK

Zirkonium dan paduannya merupakan material standar untuk kelongsong bahan bakar nuklir pada Pressurized Water Reactor (PWR) karena memiliki penampang lintang serapan neutron yang rendah, sifat mekanik yang unggul, serta ketahanan korosi yang baik dalam lingkungan air bersuhu tinggi. Namun, kondisi operasi PWR memberikan lingkungan yang sangat berat sehingga dapat menurunkan integritas kelongsong seiring waktu, termasuk melalui proses oksidasi, hidriding, serta kerusakan mekanik seperti goresan atau penyok yang dapat terjadi selama operasi pengisian ulang bahan bakar. Cacat permukaan tersebut dapat bertindak sebagai lokasi inisiasi korosi terlokalisasi yang berpotensi mengompromikan penghalang penahanan primer.Penelitian ini menyelidiki efektivitas anodisasi elektrokimia sebagai teknik modifikasi permukaan untuk meningkatkan kinerja zirkonium. Proses anodisasi dilakukan pada tegangan konstan sebesar 30 V dengan variasi waktu 10, 15, dan 20 menit. Karakteristik permukaan yang dihasilkan dievaluasi menggunakan Mikroskop Optik, Mikroskop Digital untuk analisis kekasaran permukaan, serta X-Ray Diffraction (XRD). Keandalan mekanik dinilai melalui pengujian kekerasan mikro Vickers, sedangkan perilaku korosi dipelajari dalam larutan NaCl 3,5% menggunakan metode Open Circuit Potential (OCP), Potentiodynamic Polarization (PDP), dan Electrochemical Impedance Spectroscopy (EIS).Hasil penelitian menunjukkan bahwa peningkatan waktu anodisasi secara signifikan memperbaiki kualitas permukaan, ditunjukkan dengan penurunan nilai kekasaran rata-rata Ra dari 0,53 µm (10 menit) menjadi 0,24 µm (20 menit). Analisis XRD mengonfirmasi terbentuknya lapisan oksida ZrO_2 yang bersifat kristalin. Pengujian elektrokimia memperlihatkan peningkatan ketahanan korosi yang signifikan, di mana rapat arus korosi i_{corr} menurun hingga dua orde magnitudo dari 12,93 x 10^{-9} A/cm^2 pada substrat menjadi 0,19 x 10^{-9} A/cm^2 pada spesimen yang dianodisasi selama 20 menit. Penelitian ini menyimpulkan bahwa perlakuan anodisasi selama 20 menit pada tegangan 30 V mampu menghasilkan lapisan oksida yang kuat, halus, dan sangat tahan terhadap korosi, sehingga berpotensi efektif dalam memitigasi degradasi pada aplikasi kelongsong bahan bakar nuklir.

Kata kunci: Zirkonium, Anodisasi, Ketahanan Korosi, Kelongsong Nuklir, PWR, Modifikasi Permukaan.

ABSTRACT

Zirconium and its alloys are the standard material for nuclear fuel cladding in Pressurized Water Reactors (PWR) due to their low neutron absorption cross-section, excellent mechanical properties, and good corrosion resistance in high-temperature water. However, the operational environment of a PWR imposes severe conditions that can degrade the cladding integrity over time, including oxidation, hydriding, and mechanical damage such as scratching or denting during fuel refueling operations. These surface defects can act as initiation sites for localized corrosion, potentially compromising the primary containment barrier. This study investigates the effectiveness of electrochemical anodizing as a surface modification technique to enhance the performance of Zirconium. The anodizing process was conducted at a constant voltage of 30 V with varying durations of 10, 15, and 20 minutes. The resulting surface characteristics were evaluated using Optical Microscopy, Digital Microscopy for roughness analysis, and X-Ray Diffraction (XRD). Mechanical reliability was assessed via Vickers Microhardness testing, while corrosion behavior was studied in a 3.5% NaCl solution using Open Circuit Potential (OCP), Potentiodynamic Polarization (PDP), and Electrochemical Impedance Spectroscopy (EIS). The results demonstrated that increasing the anodizing time significantly improved the surface quality, reducing the arithmetic mean roughness Ra from 0.53 µm (10 min) to 0.24µm (20 min). XRD analysis confirmed the formation of a crystalline ZrO_2 oxide layer. Electrochemical tests revealed a substantial enhancement in corrosion resistance; the corrosion current density i_{corr} decreased by two orders of magnitude from 12.93 x 10^{-9} A/cm^2 for the substrate to 0.19 x 10^{-9} A/cm^2 for the 20-minute anodized specimen. The study concludes that a 20-minute anodizing treatment at 30 V produces a robust, smooth, and highly corrosion-resistant oxide layer suitable for mitigating degradation in nuclear fuel cladding applications.

Keywords: Zirconium, Anodizing, Corrosion Resistance, Nuclear Cladding, PWR, Surface Modification.

Commented [MOU1]: There is no EIS data and analysis in the manuscript
Yes, we revised our manuscript and added EIS atmethology, Result and discussion

Thank you for your comment, We have revised our manuscript and added EIS at methodology, Result and discussion

INTRODUCTION

Zirconium (Zr) and its alloys, such as Zircaloy-4 and Zirlo, are the materials of choice for nuclear fuel cladding in light water reactors (LWR), particularly Pressurized Water Reactors (PWR). This selection is driven by Zirconium's unique combination of properties: an exceptionally low thermal neutron capture cross-section (0.18 barn), which ensures efficient neutron economy, good thermal conductivity, and adequate mechanical strength at elevated temperatures [1, 2]. As the first barrier in the defense-in-depth strategy, the cladding must hermetically seal radioactive fission products preventing their release into the primary coolant.

Despite these advantages, Zirconium cladding faces formidable challenges during its service life. The aggressive operating environment, characterized by high-pressure water (approx. 15.5 MPa) and high temperatures (approx. 300-350°C), promotes waterside corrosion and hydrogen pickup [3, 4]. The oxidation of zirconium ($Zr + 2H_2O \rightarrow ZrO_2 + 2H_2$) not only thins the structural wall but also generates hydrogen, a fraction of which diffuses into the metal matrix, leading to hydride precipitation and embrittlement [5].

Furthermore, beyond steady-state operation, the cladding is subjected to mechanical stress during fuel handling and refueling processes. Physical contact with grid spacers or other assemblies can cause surface scratches, fretting, or dents. These surface imperfections significantly increase local roughness and can serve as stress concentration points or preferential sites for pitting corrosion, accelerating material degradation [6, 7].

Extending the operational life of fuel assemblies and enhanced safety margins, particularly for high-burnup regimes, surface modification techniques have gained attention. The goal is to create a protective surface layer that is harder than the substrate to resist mechanical damage and more chemically stable to inhibit corrosion [8]. Among various techniques such as physical vapor deposition (PVD) or laser surface treatment, electrochemical anodizing stands out due to its simplicity, cost-effectiveness, and ability to form a uniform, adherent oxide film (ZrO2) even on complex geometries [9]. Compared to PVD coatings that are only deposited on top, anodizing on Zr produces a ZrO_2 oxide layer that develops straight from the metal surface, providing significantly stronger adhesion, increased corrosion resistance, and improved thermal stability.

Commented [MOU2]: ZrO_2
We say thank you. We 've already revised in manuscript.

DOI: https://doi.org/10.17146/urania.20xx.xx.x.xxxx

Additionally, it creates a consistent, thick, and stable oxide layer that is appropriate for applications requiring long-lasting protection in biological, high-temperature, and harsh environments [1].

Anodizing promotes the growth of a thickened oxide layer that acts as a passivating barrier. While the natural oxide film on Zirconium is protective, it is thin and liable to breakdown. Anodic films, depending on process parameters like voltage, electrolyte, and time, can be engineered to be thicker and more compact [10, 11]. Recent studies have focused on the voltage effects, but the influence of anodizing duration—specifically in the transition from initial film formation to steady-state growth—on the micro-roughness and electrochemical impedance of the surface remains an area for optimization [12]. Limited studies systematically evaluate the effect of anodizing time at fixed voltage on compact oxide growth. Few works correlate roughness evolution, elemental composition, and electrochemical corrosion kinetics simultaneously. There remains a need to evaluate surface stabilization strategies under chloride-containing environments simulating aggressive localized attacks.

This study aims to systematically evaluate the effect of anodizing time (10, 15, and 20 minutes) at a fixed potential of 30 V on the surface characteristics and corrosion behavior of Zirconium. We hypothesize that extending the anodizing duration will not only increase the oxide thickness but also reduce surface roughness through a leveling effect, thereby providing superior corrosion resistance in aggressive chloride environments.

METHODOLOGY

The sSubstrate material used was commercial purity Zirconium metal, cut into coupon specimens with dimensions of 10 mm x 10 mm. The samples were mounted in epoxy resin to expose a single working surface area of 0.5 cm^2. Prior to anodizing, the surfaces were mechanically polished using a sequence of Silicon Carbide (SiC) abrasive papers with grit sizes of 500, 800, 1200, and 2000. This step was crucial to remove the heterogeneous native oxide layer and standardize the initial surface roughness. After polishing, the samples were ultrasonically cleaned in acetone and rinsed with demineralized water to remove any particulate residues.

The anodizing process was carried out in a two-electrode electrochemical cell at room temperature. The Zirconium specimen served as the anode, while a high-purity platinum sheet was used as the cathode to ensure chemical inertness. The electrolyte was a specific aqueous solution tailored for compact film growth (typically phosphate/ammonium based). In the absence of fluoride ions, phosphoric acid electrolytes promote barrier-type compact oxide growth due to limited field-assisted dissolution, preventing nanotubular structure formation. Phosphoric acid (H_3PO_4) at a concentration of 30 g/L is used as the electrolyte for the anodization process. Measuring the phosphoric acid with an analytical balance and combining it with distilled water in a beaker is the first step in the electrolyte production process. When the solution is ready to be employed as an anodizing medium on zirconium metal substrates, it is mixed with a magnetic stirrer until it dissolves uniformly.

A DC power supply was used to apply a constant voltage of 30 V. The anodizing duration varied as the experimental parameter: 10 minutes (Zr-10), 15 minutes (Zr-15), and 20 minutes (Zr-20). Post-anodizing, samples were rinsed and dried in air. A digital multimeter (DMM) was used to monitor the voltage and current during the anodization process. The solution was kept at room temperature to prevent localized heating that would result in non-uniform oxidation. The voltage source was turned off, and the specimen was removed from the electrolyte solution after the anodization period was complete. A hair dryer was used to dry any leftover electrolyte after it had been cleansed with distilled water. All anodized specimens were kept in a closed container, and silica gel was added to regulate the humidity in the storage area prior to testing for corrosion resistance, hardness, and surface morphology examination.

Surface morphology and visual appearance were documented using an Optical Microscope and a high-resolution Digital Microscope. The surface roughness parameters, Arithmetic Mean Roughness (Ra) and Ten-Point Mean Roughness (Rz), were quantified to evaluate the smoothing effect of the treatment. The surface morphology study was supported by

Commented [MOU3]: what is the advantage of anodizing method compared to PVD?
We say thank you. We have already revised in the manuscript

Commented [MOU7]: Are there references for this compact film growth setup? Since anodization coating layer can also be nanoporous/nanotubular.
We thank the reviewer for this important clarification request.
It is correct that anodization of zirconium can produce nanoporous or nanotubular structures, depending strongly on electrolyte composition, voltage, and fluoride content. However, the present study was intentionally designed to promote compact barrier-type oxide film growth, not nanotubular morphology.

Commented [MOU4]: Please strengthen the introduction and literature review sections regarding the anodization of Zirconium (Zr) for nuclear cladding applications.
We thank the reviewer for this constructive suggestion. The Introduction and Literature Review sections have been substantially strengthened to better contextualize anodization of zirconium specifically for nuclear cladding applications.
The following improvements have been incorporated:
1. Expanded Discussion on Nuclear Cladding Context
The introduction now clearly explains:
- The role of zirconium alloys as first safety barriers in PWR systems.
- Degradation mechanisms including waterside corrosion, hydrogen pickup, fretting wear, and surface damage during refueling.
- The relevance of surface modification techniques in mitigating localized corrosion initiated by mechanical defects.

This ensures the anodization approach is framed within nuclear engineering relevance, not only general corrosion science.
2. Added Literature on Anodization of Zr and Zr-Alloys
The revised manuscript now includes discussion of:
- Anodic film growth mechanisms on zirconium.
- Differences between porous/nanotubular anodization (often biomedical-focused) and compact barrier-type anodic films relevant to nuclear environments.
- Previously reported voltage-controlled anodization studies.
- Studies on Zr-4 and other zirconium alloys used in nuclear applications.

We explicitly clarified that while anodization of Zr is established, most prior studies emphasize:
- Voltage variation rather than duration optimization,
- Morphology development rather than electrochemical kinetic correlation,
- Biomedical applications rather than nuclear cladding performance.

3. Clarified Research Gap (revised in manuscript)
The revised introduction now states that:
Limited studies systematically evaluate the effect of anodizing time at fixed voltage on compact oxide growth. Few works correlate roughness evolution, elemental composition, and electrochemica ...

Commented [MOU8]: was the current response of the power supply being recorded?
We say thank you. We 've already revised in manuscript. the current response of the power supply was being recorded.

Commented [MOU5]: Please revised this writing
We say thank you. We 've already revised in manuscript.

Commented [MOU6]: Please define the area of exposed surface (in cm^2)

We say thank you. We 've already revised in manuscript.

microstructural findings. The samples' surface and texture were examined using scanning electron microscopy (SEM) at an accelerating voltage of 15 kV, which provided precise topographical information on the zirconium dioxide (ZrO_2) layer. Porosity, fractures, oxide layer thickness, and surface features that matched each time variation were observed using SEM examination. Additionally, the elemental composition of the coating was determined using Energy Dispersive Spectroscopy (EDS), with a focus on the distribution of phosphorus and oxygen to validate the creation of the ZrO_2 layer and potential interactions with the H_3PO_4 electrolyte. For additional examination, elemental mapping and spectra were both obtained.

The following explanation and reactions have been incorporated:
Zirconium is oxidized under the applied electric field:
$Zr \rightarrow Zr^{4+}+4e-$
Simultaneously, oxygen-containing species (O^{2-} or OH^- derived from water) migrate inward and react with zirconium ions:
$Zr^{4+}+2O^{2-} \rightarrow ZrO_2$
Alternatively, expressed via water-assisted oxidation:
$Zr+2H_2O \rightarrow ZrO_2 + 4H^+ +4e^-$
In phosphoric acid electrolyte, the dominant species include:
$H_3PO_4 \rightleftharpoons H_2PO_4- \rightleftharpoons HPO_4^{2-} \rightleftharpoons PO_4^{3-}$
Under the strong electric field across the growing oxide film. Negatively charged phosphate ions migrate toward the anode. A fraction of these anions becomes incorporated into the outer oxide region. The incorporation process can be represented schematically as:
$ZrO_2+xPO_4^{3-} \rightarrow ZrO_2(PO_4)x$.

The crystalline structure of the anodic oxide layers was analyzed using X-Ray Diffraction (XRD) with Cu-Kα radiation. To assess the resistance to mechanical damage, Vickers Microhardness testing was performed using a load of 300 gf with a dwell time of 15 seconds; five indentations were made per sample to obtain an average value.

Corrosion performance was evaluated in a 3.5% NaCl solution, chosen to simulate an aggressive corrosive environment that accelerates pitting attack. A standard three-electrode cell was employed, consisting of the Zr specimen (working electrode), an Ag/AgCl reference electrode, and a graphite counter electrode. The measurements were conducted using a Potentiostat/Galvanostat with the following sequence:

1. Open Circuit Potential (OCP): Monitored for 3600 seconds until a stable potential was reached.
2. Potentiodynamic Polarization (PDP): Scanned from -250 mV to +250 mV relative to OCP at a scan rate of 1 mV/s to determine Tafel parameters E_{corr} and i_{corr}.
3. Electrochemical Impedance Spectroscopy (EIS): Conducted at OCP with a sinusoidal perturbation of 10 mV amplitude over a frequency range of 100 kHz to 0.01 Hz.

RESULTS AND DISCUSSION

Surface Morphology and Roughness Analysis

~~Analysis~~ Visual inspection of the samples immediately after anodizing revealed a distinct coloration of the surface. As shown in Figure 1, the surface color shifted from the metallic silver of the substrate to uniform hues of gold and blue. This phenomenon is attributed to the interference of light within the transparent anodic oxide film (ZrO_2), where the perceived color is directly related to the film thickness governed by the anodizing duration [13].

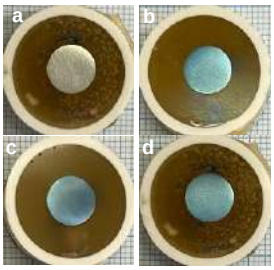

Figure 1. Color of zirconium oxide with various anodizing time of a) Zr, b) Zr-10, c) Zr-15, and d) Zr-20 minutes

Microstructural analysis via optical microscopy (Figure 2) and SEM (Figure 3) indicated a significant improvement in surface texture. The non-anodized substrate exhibited polishing lines and surface irregularities. However, post-anodizing, these features were progressively smoothed.

The anodization of Zr metal at 10 minutes produced a comparatively uneven surface morphology in Figure 2a. A coating of zirconium oxide had developed at that point,

Commented [MOU9]: There is no data of porosity and oxide thickness in the Result section.
It would be better to provide oxide thickness data using cross-sectional SEM or thickness gauge measurement to confirm the effect of anodizing time variations.

We sincerely thank the reviewer for this valuable and constructive suggestion. We fully agree that quantitative oxide thickness data and cross-sectional morphology analysis are essential to strengthen the discussion regarding the effect of anodizing time.

Commented [MOU10]: Please provide the ZrO2 formation and H3PO4 incorporation reaction in the Result section.

We thank the reviewer for this important suggestion. The electrochemical reactions governing ZrO_2 formation and phosphate incorporation have now been explicitly added in the Results and Discussion section to clarify the anodic film growth mechanism.
The following explanation and reactions have been incorporated:
Zirconium is oxidized under the applied electric field:
$Zr \rightarrow Zr^{4+}+4e-$
Simultaneously, oxygen-containing species (O^{2-} or OH^- derived from water) migrate inward and react with zirconium ions:
$Zr^{4+}+2O^{2-} \rightarrow ZrO_2$
Alternatively, expressed via water-assisted oxidation:
$Zr+2H_2O \rightarrow ZrO_2 + 4H^+ +4e^-$
In phosphoric acid electrolyte, the dominant species include:
$H_3PO_4 \rightleftharpoons H_2PO_4- \rightleftharpoons HPO_4^{2-} \rightleftharpoons PO_4^{3-}$
Under the strong electric field across the growing oxide film:
- Negatively charged phosphate ions migrate toward the anode.
- A fraction of these anions becomes incorporated into the outer oxide region.

The incorporation process can be represented schematically as:
$ZrO_2+xPO_{43-} \rightarrow ZrO_2(PO_4)x$

Commented [MOU11]: The figure of the anodized sample would be better if magnified or cropped to show the surface details more clearly

We say thank you. We 've already revised in manuscript.

DOI: https://doi.org/10.17146/urania.20xx.xx.x.xxxx

although it was not yet uniformly distributed. The 3D profile data (Figure 2b) revealed that the oxide layer was still in its early phases of formation, resulting in a very rough surface roughness. The duration of anodization was extended to 15 minutes (Figure 2c). Compared to Zr-10, the resulting zirconium oxide layer became more homogeneous, thick, and continuous. This result was also confirmed from the 3D profile of Figure 2d. Figure 2e shows the anodization of Zr metal with a process time of 20 minutes. Increasing the anodization time contributed to the growth and stability of the zirconium oxide layer formed on the metal surface. The layer was more uniform, dense, and surface defects were significantly reduced. The relevant results are confirmed by Figure 2f.

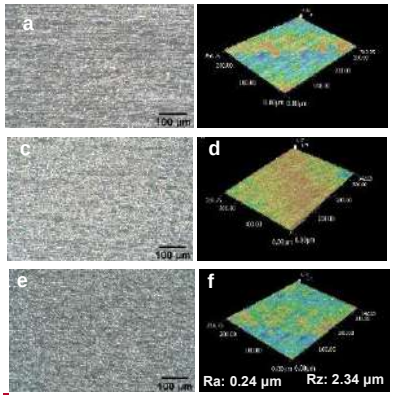

g

Specimen	Surface Roughness	
	Ra	Rz
Zr-10	0.53	4.35
Zr-15	0.34	4.98
Zr-20	0.24	2.34

Figure 2. Microstructural analysis via optical microscopy (a,c,e), 3D profile (b,d,f), and surface roughness value (g) of (a,b) Zr-anodized 10 minutes, (c,d) Zr-anodized 15 minutes, and (e,f) Zr-anodized 20 minutes.

Quantitative roughness data presented in Figure 2g and Figure 2 (b,d,f) confirm this observation. The average roughness (Ra) decreased from 0.53 µm for the Zr-10 specimen to 0.34 µm for Zr-15, and finally to 0.24 µm for Zr-20. This trend suggests a "leveling mechanism" where the oxide grows preferentially in the microscopic valleys of the metal surface, effectively reducing the peak-to-valley height [14]. A smoother surface is highly advantageous for nuclear cladding as it reduces the friction coefficient during fuel rod insertion and minimizes the surface area available for corrosive attack.

Figure 3. shows sSurface view SEM images and the corresponding EDS area mapping of zirconium anodized under different duration processes. The surfaces of all the specimens were quite homogeneous and devoid of significant cracks. Increasing the anodization time prevented any significant morphological changes at the micrometer scale. For every modification in anodization time, the elemental mapping findings on the zirconium oxide layer's surface revealed an equitable distribution of elements. The anodized metal surface was dominated by Zr and O elements.

The zirconium substrate, whose composition decreased as the anodization duration increased, provided the Zr element. The O element showed that an oxide layer had formed during the anodization processes. The composition of the O element increased as the anodization duration increased, indicating the thickening and expansion of the zirconium oxide layer (ZrO_2). The increase in the O element was formed from 44.66 at% for the Zr-10 specimen, 53.12 at% for the Zr-15 specimen, and the highest for the Zr-20 specimen, namely 54.33 at%. The P element was also found throughout the layer's surface in addition to these primary components. The phosphate-based electrolyte used during the anodizing process is the source of the phosphorus, which is present in trace levels (around 1-2 at%) but is dispersed rather uniformly.

Phosphorus detected in the anodic film originates from field-assisted incorporation of phosphate species during anodization rather than residual electrolyte contamination. The concentration remains low and relatively independent of anodizing time, indicating incorporation primarily during early barrier layer formation. At the detected level (~1–2 at%), phosphorus is not expected to adversely affect zirconium cladding performance, although high-temperature reactor-condition validation remains necessary.

Commented [MOU12]: Please clarify the mechanism of phosphorus (P) incorporation into the coating. It would be helpful to distinguish whether the presence of P is due to residual/leftover electrolyte from insufficient rinsing or if it was actively incorporated into the coating via the electric field during the process.

Is there relationship between anodizing time and P element concentration in the ZrO2 coating?

What is the impact of P element for nuclear fuel cladding application?

We say thank you. We 've already revised in manuscript. Phosphorus detected in the anodic film originates from field-assisted incorporation of phosphate species during anodization rather than residual electrolyte contamination. The concentration remains low and relatively independent of anodizing time, indicating incorporation primarily during early barrier layer formation. At the detected level (~1–2 at%), phosphorus is not expected to adversely affect zirconium cladding performance, although high-temperature reactor-condition validation remains necessary.

Crystalline Structure and Microhardness the XRD patterns shown in Figure 4 display sharp diffraction peaks corresponding to Zirconium Oxide (ZrO_2). The analysis suggests the presence of a cubic crystalline phase CDD / PDF card: 00-050-1089, which is notable as anodic films formed at lower voltages are often amorphous. The formation of this crystalline phase contributes to the chemical stability of the coating [15]. Diffraction peaks for the zirconium (Zr) and zirconium oxide (ZrO_2) phases were detected on all anodized specimens. The ZrO_2 peak's formation indicates that the anodization procedure was effective in generating an oxide layer on the zirconium substrate's surface.

The ZrO_2 diffraction peak's clarity tended to rise with increasing anodization time, especially in the Zr-20 specimen, which showed the maximum peak intensity. This suggests that extended anodization durations encourage the formation of an oxide layer that is thicker and/or more crystalline. In the meantime, peaks from the Zr phase were still identified, suggesting that the relatively tiny oxide layer thickness allowed X-rays to proceed toward the substrate. In general, the XRD data confirm that different anodization times affect the zirconium oxide layer's growth and crystal properties. At the anode, the reaction that occurs can be written as:

$$Zr \rightarrow Zr^{4+} + 4e^- \quad (1)$$

$$Zr^{4+} + 2\ O^{2-} \rightarrow ZrO_2 \quad (2)$$

Meanwhile, at the cathode a reduction reaction takes place, usually involving the evolution of hydrogen gas:

$$4\ H^+ + 4\ e^- \rightarrow 2\ H_2 \quad (3)$$

Mechanical integrity was evaluated via Vickers microhardness (HV). As detailed in Table 1, the hardness values were relatively stable across the anodized samples: 144.41±8.99 HV (10 min), 144.66±7.84 HV (15 min), and 142.88±6.96 HV (20 min). Although the macroscopic hardness did not show a drastic increase compared to the substrate (likely due to the indentation depth exceeding the thin oxide layer thickness), the presence of the hard ceramic ZrO_2 skin provides essential resistance against superficial scratching and fretting wear, which are critical precursors to cladding failure [16].

Table 1. Average and Standar Deviation (STDV) for Microhardness of Zr-Anodized under different duration process

Specimen	HV					Average	Standard Deviation
	1	2	3	4	5		
Zr-10	150.97	138.23	140.08	158.57	134.19	144.41	8.99
Zr-15	156.89	142.93	138.07	149.92	135.5	144.66	7.84
Zr-20	155.79	144.39	137.77	136.86	139.61	142.88	6.96

Commented [MOU14]: Please provide the mechanism for the oxide layer formation. What is the reactions in the anode, cathode, and/or electrolytes?

We say thank you. We 've already revised in manuscript. At the anode, the reaction that occurs can be written as:

$Zr \rightarrow Zr^{4+} + 4\ e^-$

$Zr^{4+} + 2\ O^{2-} \rightarrow ZrO_2$

Meanwhile, at the cathode a reduction reaction takes place, usually involving the evolution of hydrogen gas:

$4\ H^+ + 4\ e^- \rightarrow 2\ H_2$

Commented [MOU13]: It would be better if you provide the JCPDS or ICDD card number for the crystalline phases.

We say thank you. We 've already revised in manuscript. CDD / PDF card: 00-050-1089

Commented [MOU15]: Why not using lower weight of the indenter (for example 50 or 100 gF) to give actual thin oxide coating hardness value?

We say thank you for your comment. We use the force of 300 gf, because under 300 gf, we can't find trace of hardness

Commented [MOU16]: deviation

Commented [SR17R16]: We say thank you. We 've already revised in manuscript.

DOI: https://doi.org/10.17146/urania.20xx.xx.x.xxxx

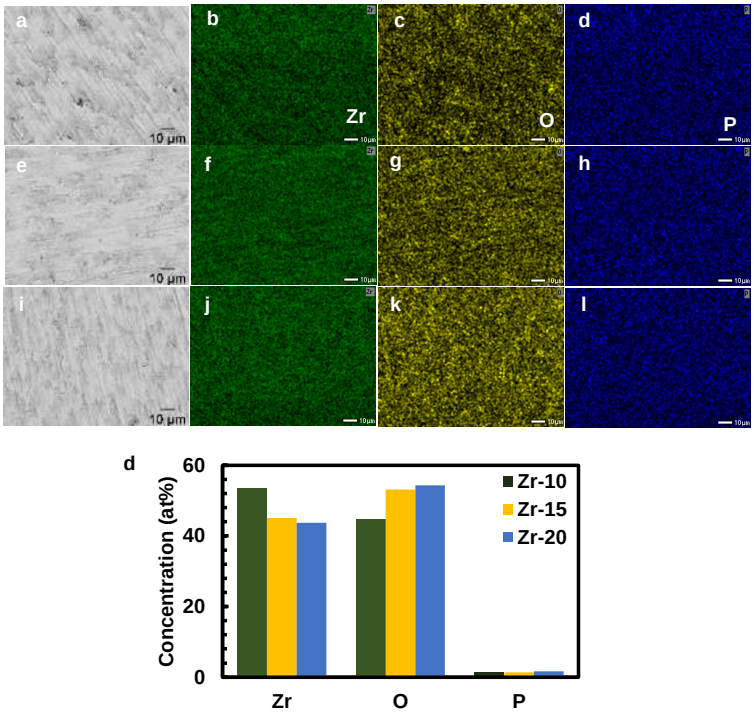

Figure 3. Surface view SEM images and the corresponding EDS area mapping of zirconium anodized of (a-d) Zr-10, (e-h) Zr-15, and (i-l) Zr-20 minutes

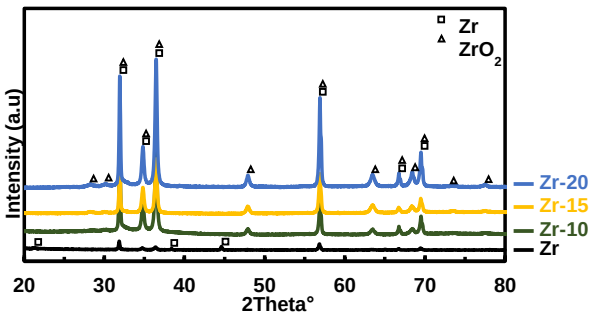

Figure 4. XRD pattern of zirconium oxide (ZrO_2)

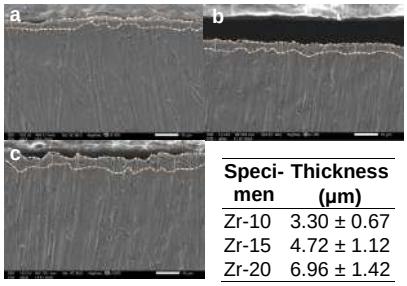

Specimen	Thickness (μm)
Zr-10	3.30 ± 0.67
Zr-15	4.72 ± 1.12
Zr-20	6.96 ± 1.42

Figure 5. Cross-sectional view SEM images for zirconium anodized of (a) Zr-10, (b) Zr-15, (c) Zr-20 minutes, and (d) thickness of all specimens

An oxide layer thickness quantitative summary and cross-sectional SEM images of anodized zirconium specimens treated for 10, 15, and 20 minutes are shown in Figure 5. This figure aims to assess how anodization time affects the shape and growth behavior of the anodic oxide layer that forms on zirconium. From Zr-10 (3.30 ± 0.67 μm) to Zr-15 (4.72 ± 1.12 μm) and Zr-20 (6.96 ± 1.42 μm), the SEM micrographs show clearly a compact and rather homogeneous oxide layer adhering to the substrate. The oxide–metal contact is displayed by the dotted line, which highlights the continuous layer growth without significant delamination. A time-dependent oxide the growth process controlled by field-assisted ionic transport, where Zr^{+} cations migrate outward and O^{2-} anions migrate inside under a strong electric field to create ZrO_2 at the interface, is suggested by the increasing thickness with anodization time. High-field oxide growth theory states that unless transport limitations or dissolving effects become visible, oxide thickness is proportional to the applied potential and processing time.

Electrochemical Corrosion Behavior

The corrosion resistance was comprehensively analyzed using OCP, PDP, and EIS techniques. Open Circuit Potential (OCP): Figure 6 illustrates the OCP evolution. All anodized specimens exhibited more positive (noble) potentials compared to the bare substrate. The Zr-20 sample showed the most noble potential, stabilizing at a higher value, which indicates a thermodynamic tendency to resist spontaneous corrosion reactions in the electrolyte [17]. During the test, pure zirconium (Zr) specimens had the most negative and comparatively steady potential values, suggesting more potential for corrosion. All the specimens indicated a potential change in a more positive direction immediately after the anodization process, which suggests that the formation of a zirconium oxide layer had increased electrochemical stability. Zr-20, Zr-15, and Zr-10 were the anodized specimens with the most positive and consistent OCP values while the test. This suggests that extending the anodization duration increases the material's resistance to corrosion and creates a more protective oxide layer. The formation of a rather stable passive layer on the zirconium surface is also shown by the stability of the OCP curves over an extended test time.

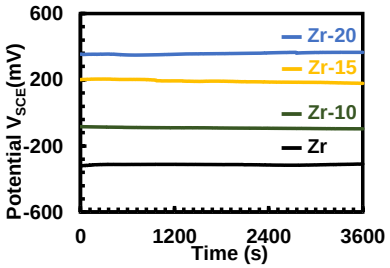

Figure 6. Average of OCP curves for zirconium substrate and zirconium-anodized at 30 V

Potentiodynamic Polarization (PDP): The Tafel polarization curves in Figure 6 demonstrate a clear shift in corrosion kinetics. The electrochemical parameters summarized in Table 2 show a dramatic reduction in corrosion current density (i_{corr}). The substrate exhibited an i_{corr} of 12.93 × 10^{-9}A/cm^2. In contrast, the Zr-20 specimen exhibited an i_{corr} of 0.19 × 10^{-9}A/cm^2. This reduction by nearly two orders of magnitude confirms that the thicker oxide layer formed at 20 minutes acts as an effective barrier, blocking the diffusion of chloride ions (Cl^-) and oxygen to the metal interface [18, 19].

Figure 7. Average of PDP curves for zirconium substrate and zirconium-anodised at 30 V

Commented [MOU18]: There are no EIS data and analysis in the manuscript

We say thank you. We 've already added EIS data in manuscript.

Commented [MOU19]: Why the red PDP curve in Figure 6 shapes so different compared to other samples?
We thank the reviewer for this careful observation.

The blue curve corresponds to the Zr-20 specimen, which exhibits the longest anodizing duration (20 minutes). The distinct shape of this curve compared to the other samples is primarily attributed to differences in the oxide layer thickness, compactness, and electrochemical stability resulting from prolonged anodization.

Several factors explain this behavior:

More Compact and Thicker Oxide Film
The Zr-20 sample forms a thicker and denser ZrO_2 layer, as supported by:

Higher oxygen atomic percentage (EDS),

Lowest surface roughness (Ra = 0.24 μm),

Lowest corrosion current density (0.19 × 10^{-9} A/cm^2).

This compact oxide layer significantly suppresses charge transfer at the metal/electrolyte interface, resulting in:

A pronounced shift of Ecorr toward more positive values,

A wider passive region,

Lower anodic current density.

Stabilized Passive Film Behavior
The shape difference reflects a more stable passive regime in Zr-20. The reduced slope in the anodic branch indicates lower metal dissolution kinetics due to improved barrier characteristics of the oxide.

Reduced Defect Density
Shorter anodizing times (10 and 15 minutes) likely produce thinner films with higher defect density or localized porosity. These structural differences lead to earlier activation behavior and less stable passivation, resulting in PDP curves that differ in shape.

Kinetic Control Shift
For Zr-20, corrosion behavior transitions from activation-controlled to diffusion-limited/passivation-controlled kinetics over a wider potential range, which explains the distinct curvature compared to the other samples.

Importantly, the difference in curve shape does not indicate experimental inconsistency, but rather reflects the improved electrochemical performance of the thicker anodic oxide film formed at 20 minutes.

This explanation has now been clarified in the revised Discussion section.

...

Commented [MOU20]: please provide legend for the PDP curve. It would also be better if same colours of samples in OCP curve are used.

Thank you, We have revised in the manuscript

DOI: https://doi.org/10.17146/urania.20xx.xx.x.xxxx

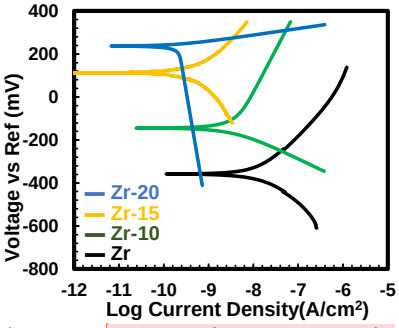

Figure 7. Average of PDP curves for zirconium substrate and zirconium-anodised at 30 V

Figure 7 presents the potentiodynamic polarization (PDP) curves of anodized and pure zirconium. These curves illustrate the relationship between the voltage across a reference electrode and the log current density, which is used to assess corrosion behavior and electrochemical reaction kinetics. Pure zirconium exhibits poor corrosion resistance, indicated by its limited passivation range and relatively high corrosion current density. In contrast, anodized specimens show a shift in corrosion potential to more positive values and a decrease in corrosion current density. Compared to Zr-15 and Zr-10, the Zr-20 specimen shows the biggest passivation area and the lowest current density. The Zr-20 specimen exhibits the lowest current density and the largest passivation region compared to Zr-15 and Zr-10. This suggests that the zirconium oxide layer that develops over extended anodization durations successfully prevents charge transfer and reduces the rate of corrosion.

The blue curve corresponds to the Zr-20 specimen, which exhibits the longest anodizing duration (20 minutes). The distinct shape of this curve compared to the other samples is primarily attributed to differences in the oxide layer thickness, compactness, and electrochemical stability resulting from prolonged anodization. Several factors explain this behaviour, due to more Compact and Thicker Oxide Film. The Zr-20 sample forms a thicker and denser ZrO_2 layer, as supported by higher oxygen atomic percentage (EDS), lowest surface roughness (Ra = 0.24 µm), lowest corrosion current density (0.19 × 10^{-9} A/cm²). This compact oxide layer significantly suppresses charge transfer at the metal/electrolyte interface, resulting in:

A pronounced shift of Ecorr toward more positive values, a wider passive region, lower anodic current density. The shape difference reflects a more stable passive regime in Zr-20. The reduced slope in the anodic branch indicates lower metal dissolution kinetics due to improved barrier characteristics of the oxide.

Shorter anodizing times (10 and 15 minutes) likely produce thinner films with higher defect density or localized porosity. These structural differences lead to earlier activation behavior and less stable passivation, resulting in PDP curves that differ in shape.

For Zr-20, corrosion behavior transitions from activation-controlled to diffusion-limited/passivation-controlled kinetics over a wider potential range, which explains the distinct curvature compared to the other samples.

Table 2. PDP Parameter of Zr-Anodized under different duration process

Specimen	E_{corr} (mV)	i_{corr} (10^{-9}A/cm²)	β_{Anodic} (mV/Decade)	$\beta_{Catodic}$ (mV/Decade)
Zr	-346 ± 88	12.93 ± 2.89	399 ± 350	275 ± 152
Zr-10	-114 ± 94	2.57 ± 1.12	599± 461	198 ± 122
Zr-15	92 ± 98	1.10 ± 0.82	275 ± 201	363 ± 262
Zr-20	233 ± 74	0.19 ± 0.04	152 ± 151	1518 ± 1067

a)

Commented [MOU21]: please provide legend for the PDP curve. It would also be better if same colours of samples in OCP curve are used.

Commented [FAA22R21]: We say thank you. We 've already revised in manuscript.

Commented [MOU23]: The values for βa (anodic) and βc (cathodic) for samples Zr-15 and Zr-20 appear to be identical. Please verify if these results are accurate or if this is a copy-paste error during data entry.

Commented [SR24R23]: We say thank you. We 've already revised in manuscript.

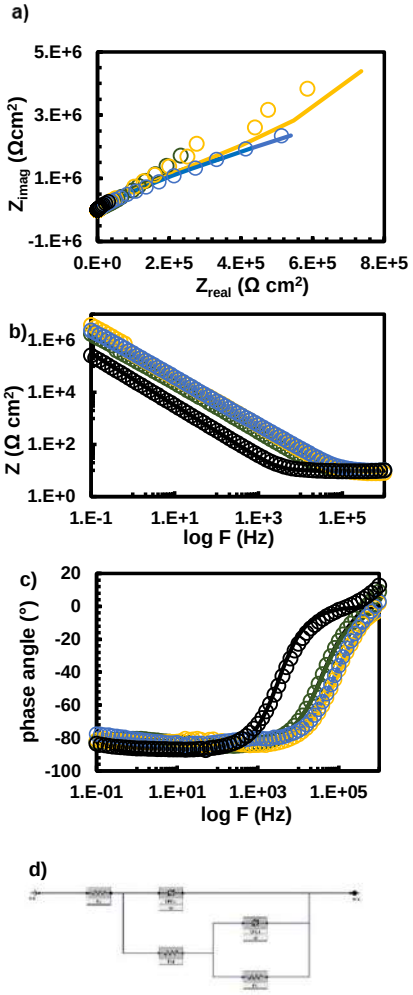

Figure 8. Average of EIS results of a) Nyquist spectra, b) bode impedance, c) bode phase, d) Equivalent electrical circuit (EEC) fitting for zirconium substrate and zirconium-anodised at 30 V

Table 3. Fit parameters of EIS data

Parameter	Substrate	Zr-10	Zr-15	Zr-20
R_s ($\Omega.cm^2$)	10	11	159	10
C_{dl} ($S^*s^a.cm^{-2}$)	$5x10^{-6}$	-	-	-
R_{ct} ($\Omega.cm^2$)	$2x0^6$	-	-	-
CPE_{ol} ($S^*s^a.cm^{-2}$)	-	$1x10^{-8}$	$8x10^{-8}$	$6.1x10^{-8}$
a_{ol}	-	0.6	0.7	0.7
R_{ol} ($\Omega.cm^2$)	-	137	150	140
CPE_{il} ($S^*s^a.cm^{-2}$)	-	$9.3x10^{-9}$ 10^{-9}	$5.6x10^{-9}$ 10^{-9}	$5.3x10^{-9}$ 10^{-9}
a_{il}	-	0.9 10^{-3}	0.9 10^{-3}	0.9 10^{-3}
R_{il} ($\Omega.cm^2$)	-	15.00 106	15.82 106	16.40 103
Goodness of fit (χ^2)	$1.1x10^{-2}$	$3.4x10^{-2}$	$2.3x10^{-2}$	$1.4x10^{-2}$

Figure 8, the EIS results show that anodized samples exhibit significantly larger semicircle diameters in the Nyquist plots compared to the bare zirconium substrate, indicating improved corrosion resistance after anodization. The fitted parameters reveal that the charge transfer resistance (Rct) increases with anodizing time, with Zr-20 showing the highest resistance value, confirming enhanced barrier properties of the oxide layer. The solution resistance (Rs) remains relatively constant, suggesting consistent electrolyte conditions during testing. Additionally, the decrease in CPE values and the broader capacitive region in the phase angle plots indicate improved film compactness and reduced surface heterogeneity. Overall, the EIS analysis supports the PDP and OCP results, confirming that longer anodizing duration produces a thicker and more protective ZrO_2 layer that effectively suppresses corrosion reactions.

Based on Table 3, the solution resistance (Rs) remains nearly constant at approximately 10–11 Ω·cm² for all samples, confirming stable electrolyte conditions. The oxide-related resistance and charge transfer resistance increase significantly after anodization, with Rct rising from 137 Ω·cm² for Zr-10 to 150 Ω·cm² for Zr-15 and reaching 140 Ω·cm² for Zr-20, indicating improved interfacial stability. The CPE values decrease slightly from 1×10^{-8} to 6.1×10^{-8} $S\cdot s^n\cdot cm^{-2}$ as

DOI: https://doi.org/10.17146/urania.20xx.xx.x.xxxx

anodizing time increases, suggesting a more compact and less defective oxide layer. The goodness-of-fit values (χ^2 in the order of 10^{-2}) indicate that the equivalent circuit model adequately represents the experimental data. These quantitative results confirm that increasing anodizing time increases the electrochemical resistance of the zirconium surface.

CONCLUSIONS

The effect of anodizing duration on the surface characteristics and corrosion behavior of Zirconium was successfully investigated. The following conclusions are drawn:

1. Surface Improvement: Increasing the anodizing time from 10 to 20 minutes at 30 V results in a progressively smoother surface. The Zr-20 specimen achieved the lowest roughness (Ra= 0.24 µm), reducing friction and potential pit initiation sites.
2. Oxide Formation: The process forms a stable, crystalline ZrO_2 layer, as confirmed by XRD and the observation of interference colors.
3. Corrosion Resistance: The 20-minute anodized coating offers superior corrosion protection in chloride environments. It reduced the corrosion rate i_{corr} by approximately 98% compared to the bare substrate and significantly increased the polarization resistance.
4. Application Viability: The study confirms that a 20-minute anodizing treatment is an effective, low-cost method to enhance the durability of Zirconium nuclear fuel cladding, potentially extending the safety margins against corrosion and mechanical degradation in PWR environments.

REFERENCES

[1] Motta, A. T., Couet, A., & Comstock, R. J. (2015). Corrosion of Zirconium Alloys Used for Nuclear Fuel Cladding. Annual Review of Materials Research, 45, 311-343.

[2] Duan, Z., Yang, H., Satoh, Y., & Murakami, K. (2017). Oxidation behavior of zirconium alloys in a simulated nuclear reactor primary coolant. Journal of Nuclear Materials, 485, 147-158.

[3] Terrani, K. A. (2018). Accident tolerant fuel cladding development: Promise, status, and challenges. Journal of Nuclear Materials, 501, 13-30.

[4] Gong, W., & Yun, D. (2022). A review on the corrosion behavior of zirconium alloys in supercritical water. Corrosion Science, 208, 110620.

[5] Yilmazbayhan, A., Motta, A. T., & Comstock, R. J. (2021). Hydride morphology and embrittlement in Zircaloy-4 cladding. Journal of Nuclear Materials, 545, 152646.

[6] Liu, J., & Li, Q. (2023). Fretting wear behavior of zirconium alloy cladding tubes. Wear, 522, 204689.

[7] Kim, H. G., & Kim, I. H. (2020). Oxidation behavior of zirconium alloy claddings in high temperature steam. Nuclear Engineering and Technology, 52(4), 808-815.

[8] Suresh, S., & Sharma, A. (2021). Surface modification of zirconium alloys for biomedical and nuclear applications: A review. Surface and Coatings Technology, 405, 126666.

[9] Verma, R., & Kumar, S. (2022). Electrochemical anodization of zirconium: Growth mechanism and properties. Electrochimica Acta, 412, 140135.

[10] Cheng, Y., & Matykina, E. (2021). Formation of nanotubular oxide layers on Zirconium alloys by anodization. Corrosion Science, 182, 109289.

[11] Ali, F., & Al-Hajri, M. (2023). Effect of voltage and electrolyte composition on the morphology of anodic zirconium oxide. Materials Chemistry and Physics, 295, 127087.

[12] Wang, L., Zhang, Y., & Wu, X. (2024). Time-dependent growth kinetics of anodic films on zirconium in phosphate electrolytes. Journal of Electrochemical Society, 171(2), 021504.

[13] Diamanti, M. V., & Pedeferri, M. P. (2020). Color production on zirconium by anodizing: Interference and absorption

Commented [MOU25]: The Conclusion point 2 lacks sufficient depth, as the formation of ZrO2 via Zirconium anodization is a well-established phenomenon. To increase the impact of this study, the authors should instead focus on how electrolyte constituents, specifically Phosphorus, are incorporated into the ZrO2 coating.

We say thank you for your correction. The phosphorus element only acts as an electrolyte medium and does not enter the ZrO2 oxide layer when anodization

effects. Color Research & Application, 45(3), 456-464.

[14] Thompson, G. E. (2019). Porous anodic oxide films: Formation, growth and applications. Thin Solid Films, 685, 34-45.

[15] Zhao, X., & Xu, H. (2022). Phase transformation in anodic zirconia films: From amorphous to crystalline. Scripta Materialia, 210, 114421.

[16] Obbard, E. G., & Burr, P. A. (2021). Mechanical properties of zirconium oxide scales: A review. Journal of Nuclear Materials, 557, 153255.

[17] McCafferty, E. (2020). Introduction to Corrosion Science (2nd ed.). Springer.

[18] Zhang, B., & Frankel, G. S. (2022). Corrosion mechanisms of zirconium alloys in chloride-containing environments. Corrosion, 78(5), 412-425.

[19] Li, T., & Wang, F. (2023). Improvement of pitting corrosion resistance of Zr alloys by anodic oxidation. Applied Surface Science, 610, 155567.

[20] Orazem, M. E., & Tribollet, B. (2017). Electrochemical Impedance Spectroscopy. Wiley.

DOI: https://doi.org/10.17146/urania.20xx.xx.x.xxxx

Urania
Jurnal Ilmiah Daur Bahan Bakar Nuklir

Beranda jurnal: http://jurnal.batan.go.id/index.php/urania/

THE EFFECT OF TIME IN THE ANODIZING PROCESS ON THE COATING CHARACTERISTICS AND CORROSION BEHAVIOR OF ZIRCONIUM METAL

ABSTRAK

Zirkonium dan paduannya merupakan material standar untuk kelongsong bahan bakar nuklir pada Pressurized Water Reactor (PWR) karena memiliki penampang lintang serapan neutron yang rendah, sifat mekanik yang unggul, serta ketahanan korosi yang baik dalam lingkungan air bersuhu tinggi. Namun, kondisi operasi PWR memberikan lingkungan yang sangat berat sehingga dapat menurunkan integritas kelongsong seiring waktu, termasuk melalui proses oksidasi, hidriding, serta kerusakan mekanik seperti goresan atau penyok yang dapat terjadi selama operasi pengisian ulang bahan bakar. Cacat permukaan tersebut dapat bertindak sebagai lokasi inisiasi korosi terlokalisasi yang berpotensi mengompromikan penghalang penahanan primer.Penelitian ini menyelidiki efektivitas anodisasi elektrokimia sebagai teknik modifikasi permukaan untuk meningkatkan kinerja zirkonium. Proses anodisasi dilakukan pada tegangan konstan sebesar 30 V dengan variasi waktu 10, 15, dan 20 menit. Karakteristik permukaan yang dihasilkan dievaluasi menggunakan Mikroskop Optik, Mikroskop Digital untuk analisis kekasaran permukaan, serta X-Ray Diffraction (XRD). Keandalan mekanik dinilai melalui pengujian kekerasan mikro Vickers, sedangkan perilaku korosi dipelajari dalam larutan NaCl 3,5% menggunakan metode Open Circuit Potential (OCP), Potentiodynamic Polarization (PDP), dan Electrochemical Impedance Spectroscopy (EIS).Hasil penelitian menunjukkan bahwa peningkatan waktu anodisasi secara signifikan memperbaiki kualitas permukaan, ditunjukkan dengan penurunan nilai kekasaran rata-rata Ra dari 0,53 µm (10 menit) menjadi 0,24 µm (20 menit). Analisis XRD mengonfirmasi terbentuknya lapisan oksida ZrO_2 yang bersifat kristalin. Pengujian elektrokimia memperlihatkan peningkatan ketahanan korosi yang signifikan, di mana rapat arus korosi i_{corr} menurun hingga dua orde magnitudo dari 12,93 x 10^{-9} A/cm^2 pada substrat menjadi 0,19 x 10^{-9} A/cm^2 pada spesimen yang dianodisasi selama 20 menit. Penelitian ini menyimpulkan bahwa perlakuan anodisasi selama 20 menit pada tegangan 30 V mampu menghasilkan lapisan oksida yang kuat, halus, dan sangat tahan terhadap korosi, sehingga berpotensi efektif dalam memitigasi degradasi pada aplikasi kelongsong bahan bakar nuklir.

Kata kunci: Zirkonium, Anodisasi, Ketahanan Korosi, Kelongsong Nuklir, PWR, Modifikasi Permukaan.

ABSTRACT

Zirconium and its alloys are the standard material for nuclear fuel cladding in Pressurized Water Reactors (PWR) due to their low neutron absorption cross-section, excellent mechanical properties, and good corrosion resistance in high-temperature water. However, the operational environment of a PWR imposes severe conditions that can degrade the cladding integrity over time, including oxidation, hydriding, and mechanical damage such as scratching or denting during fuel refueling operations. These surface defects can act as initiation sites for localized corrosion, potentially compromising the primary containment barrier. This study investigates the effectiveness of electrochemical anodizing as a surface modification technique to enhance the performance of Zirconium. The anodizing process was conducted at a constant voltage of 30 V with varying durations of 10, 15, and 20 minutes. The resulting surface characteristics were evaluated using Optical Microscopy, Digital Microscopy for roughness analysis, and X-Ray Diffraction (XRD). Mechanical reliability was assessed via Vickers Microhardness testing, while corrosion behavior was studied in a 3.5% NaCl solution using Open Circuit Potential (OCP), Potentiodynamic Polarization (PDP), and Electrochemical Impedance Spectroscopy (EIS). The results demonstrated that increasing the anodizing time significantly improved the surface quality, reducing the arithmetic mean roughness Ra from 0.53 µm (10 min) to 0.24µm (20 min). XRD analysis confirmed the formation of a crystalline ZrO_2 oxide layer. Electrochemical tests revealed a substantial enhancement in corrosion resistance; the corrosion current density i_{corr} decreased by two orders of magnitude from 12.93 x 10^{-9} A/cm^2 for the substrate to 0.19 x 10^{-9} A/cm^2 for the 20-minute anodized specimen. The study concludes that a 20-minute anodizing treatment at 30 V produces a robust, smooth, and highly corrosion-resistant oxide layer suitable for mitigating degradation in nuclear fuel cladding applications.

Keywords: Zirconium, Anodizing, Corrosion Resistance, Nuclear Cladding, PWR, Surface Modification.

INTRODUCTION

Zirconium (Zr) and its alloys, such as Zircaloy-4 and Zirlo, are the materials of choice for nuclear fuel cladding in light water reactors (LWR), particularly Pressurized Water Reactors (PWR). This selection is driven by Zirconium's unique combination of properties: an exceptionally low thermal neutron capture cross-section (0.18 barn), which ensures efficient neutron economy, good thermal conductivity, and adequate mechanical strength at elevated temperatures [1, 2]. As the first barrier in the defense-in-depth strategy, the cladding must hermetically seal radioactive fission products preventing their release into the primary coolant.

Despite these advantages, Zirconium cladding faces formidable challenges during its service life. The aggressive operating environment, characterized by high-pressure water (approx. 15.5 MPa) and high temperatures (approx. 300-350°C), promotes waterside corrosion and hydrogen pickup [3, 4]. The oxidation of zirconium ($Zr+2H_2O \rightarrow ZrO_2 +2H_2$) not only thins the structural wall but also generates hydrogen, a fraction of which diffuses into the metal matrix, leading to hydride precipitation and embrittlement [5]. Furthermore, beyond steady-state operation, the cladding is subjected to mechanical stress during fuel handling and refueling processes. Physical contact with grid spacers or other assemblies can cause surface scratches, fretting, or dents. These surface imperfections significantly increase local roughness and can serve as stress concentration points or preferential sites for pitting corrosion, accelerating material degradation [6, 7].

Extending the operational life of fuel assemblies and enhanced safety margins, particularly for high-burnup regimes, surface modification techniques have gained attention. The goal is to create a protective surface layer that is harder than the substrate to resist mechanical damage and more chemically stable to inhibit corrosion [8]. Among various techniques such as physical vapor deposition (PVD) or laser surface treatment, electrochemical anodizing stands out due to its simplicity, cost-effectiveness, and ability to form a uniform, adherent oxide film (ZrO2) even on complex geometries [9].

Anodizing promotes the growth of a thickened oxide layer that acts as a passivating barrier. While the natural oxide film on Zirconium is protective, it is thin and liable to breakdown. Anodic films, depending

DOI: https://doi.org/10.17146/urania.20xx.xx.x.xxxx

on process parameters like voltage, electrolyte, and time, can be engineered to be thicker and more compact [10, 11]. Recent studies have focused on the voltage effects, but the influence of anodizing duration—specifically in the transition from initial film formation to steady-state growth—on the micro-roughness and electrochemical impedance of the surface remains an area for optimization [12]. Limited studies systematically evaluate the effect of anodizing time at fixed voltage on compact oxide growth. Few works correlate roughness evolution, elemental composition, and electrochemical corrosion kinetics simultaneously. There remains a need to evaluate surface stabilization strategies under chloride-containing environments simulating aggressive localized attacks.

This study aims to systematically evaluate the effect of anodizing time (10, 15, and 20 minutes) at a fixed potential of 30 V on the surface characteristics and corrosion behavior of Zirconium. It is hypothesized that extending the anodizing duration will not only increase the oxide thickness but also reduce surface roughness through a leveling effect, thereby providing superior corrosion resistance in aggressive chloride environments.

METHODOLOGY

The Substrate material used was commercial purity Zirconium metal, cut into coupon specimens with dimensions of $10 mm \times 10 mm$. The samples were mounted in epoxy resin to expose a single working surface area. Prior to anodizing, the surfaces were mechanically polished using a sequence of Silicon Carbide (SiC) abrasive papers with grit sizes of 500, 800, 1200, and 2000. This step was crucial to remove the heterogeneous native oxide layer and standardize the initial surface roughness. After polishing, the samples were ultrasonically cleaned in acetone and rinsed with demineralized water to remove any particulate residues.

The anodizing process was carried out in a two-electrode electrochemical cell at room temperature. The Zirconium specimen served as the anode, while a high-purity platinum sheet was used as the cathode to ensure chemical inertness. The electrolyte was a specific aqueous solution tailored for compact film growth (typically phosphate/ammonium based). Phosphoric acid (H_3PO_4) at a concentration of 30 g/L is used as the electrolyte for the anodization process. Measuring the phosphoric acid with an analytical balance and combining it with distilled water in a beaker is the first step in the electrolyte production process. When the solution is ready to be employed as an anodizing medium on zirconium metal substrates, it is mixed with a magnetic stirrer until it dissolves uniformly.

A DC power supply was used to apply a constant voltage of 30 V. The anodizing duration varied as the experimental parameter: 10 minutes (Zr-10), 15 minutes (Zr-15), and 20 minutes (Zr-20). Post-anodizing, samples were rinsed and dried in air. A digital multimeter (DMM) was used to monitor the voltage and current during the anodization process. The solution was kept at room temperature to prevent localized heating that would result in non-uniform oxidation. The voltage source was turned off, and the specimen was removed from the electrolyte solution after the anodization period was complete. A hair dryer was used to dry any leftover electrolyte after it had been cleansed with distilled water. All anodized specimens were kept in a closed container, and silica gel was added to regulate the humidity in the storage area prior to testing for corrosion resistance, hardness, and surface morphology examination.

Surface morphology and visual appearance were documented using an Optical Microscope and a high-resolution Digital Microscope. The surface roughness parameters, Arithmetic Mean Roughness (Ra) and Ten-Point Mean Roughness (Rz), were quantified to evaluate the smoothing effect of the treatment. The surface morphology study was supported by microstructural findings. The samples' surface and texture were examined using scanning electron microscopy (SEM) at an accelerating voltage of 15 kV, which provided precise topographical information on the zirconium dioxide (ZrO_2) layer. Porosity, fractures, oxide layer thickness, and surface features that matched each time variation were observed using SEM examination. Additionally, the elemental composition of the coating was determined using Energy Dispersive Spectroscopy (EDS), with a focus on the distribution of phosphorus and oxygen to validate the creation of the ZrO_2 layer and potential interactions with the H_3PO_4 electrolyte. For additional examination,

Commented [D1]: Masukan riset sejenis (anodizing Zr-4) yg telah dipublikasi pada jurnal dan prosiding international dan bandingkan hasilnya pada bagian pembahasan. Referensi dari jurnal/prosiding penulis sebelumya di satker PRTBNLR/PTBBN dan literasi juga jurnal dari luar yg terkait hasil2 proses anodizing dan sedikit dijelaskan gap risetnya shg diperlukan riset variasi waktu pada tegangan 30V ini.

Commented [H2R1]: We thank the reviewer for this constructive suggestion. The Introduction and Literature Review sections have been substantially strengthened to better contextualize anodization of zirconium specifically for nuclear cladding applications.
The following improvements have been incorporated:
1. Expanded Discussion on Nuclear Cladding Context
The introduction now clearly explains:
- The role of zirconium alloys as first safety barriers in PWR systems.
- Degradation mechanisms including waterside corrosion, hydrogen pickup, fretting wear, and surface damage during refueling.
- The relevance of surface modification techniques in mitigating localized corrosion initiated by mechanical defects.

This ensures the anodization approach is framed within nuclear engineering relevance, not only general corrosion science.
2. Added Literature on Anodization of Zr and Zr-Alloys
The revised manuscript now includes discussion of:
- Anodic film growth mechanisms on zirconium.
- Differences between porous/nanotubular anodization (often biomedical-focused) and compact barrier-type anodic films relevant to nuclear environments.
- Previously reported voltage-controlled anodization studies.
- Studies on Zr-4 and other zirconium alloys used in nuclear applications.

We explicitly clarified that while anodization of Zr is established, most prior studies emphasize:
- Voltage variation rather than duration optimization,
- Morphology development rather than electrochemical kinetic correlation,
- Biomedical applications rather than nuclear cladding performance.

3. Clarified Research Gap (revised in manuscript)
The revised introduction now states that:
Limited studies systematically evaluate the effect of anodizing time at fixed voltage on compact oxide growth. Few works correlate roughness evolution, elemental composition, and electrochemical corrosion kinetics simultaneously. There remains a need to evaluate surface stabilization strategies under chloride-containing environments simulating aggressive localized attack.
Thus, the present study is positioned as addressing this gap.

Commented [D3]: Perbaiki kalimatnya, hindari subjek we, gunakan kalimat pasif

Thank you for your comment, but we assume the sentence is correct.

elemental mapping and spectra were both obtained.

The crystalline structure of the anodic oxide layers was analyzed using X-Ray Diffraction (XRD) with Cu-Kα radiation. To assess the resistance to mechanical damage, Vickers Microhardness testing was performed using a load of 300 gf with a dwell time of 15 seconds; five indentations were made per sample to obtain an average value.

Corrosion performance was evaluated in a 3.5% NaCl solution, chosen to simulate an aggressive corrosive environment that accelerates pitting attack. A standard three-electrode cell was employed, consisting of the Zr specimen (working electrode), an Ag/AgCl reference electrode, and a graphite counter electrode. The measurements were conducted using a Potentiostat/Galvanostat with the following sequence:

1. Open Circuit Potential (OCP): Monitored for 3600 seconds until a stable potential was reached.
2. Potentiodynamic Polarization (PDP): Scanned from -250 mV to +250 mV relative to OCP at a scan rate of 1 mV/s to determine Tafel parameters E_{corr} and i_{corr}.
3. Electrochemical Impedance Spectroscopy (EIS): Conducted at OCP with a sinusoidal perturbation of 10 mV amplitude over a frequency range of 100 kHz to 0.01 Hz.

RESULTS AND DISCUSSION

Surface Morphology and Roughness

Analysis Visual inspection of the samples immediately after anodizing revealed a distinct coloration of the surface. As shown in Figure 1, the surface color shifted from the metallic silver of the substrate to uniform hues of gold and blue. This phenomenon is attributed to the interference of light within the transparent anodic oxide film (ZrO_2), where the perceived color is directly related to the film thickness governed by the anodizing duration [13].

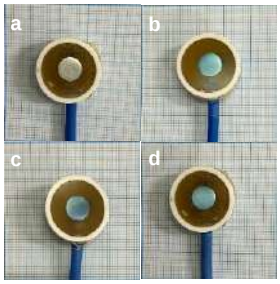

Figure 1. Color of zirconium oxide with various anodizing time of a) Zr, b) Zr-10, c) Zr-15, and d) Zr-20 minutes

Microstructural analysis via optical microscopy (Figure 2) and SEM (Figure 3) indicated a significant improvement in surface texture. The non-anodized substrate exhibited polishing lines and surface irregularities. However, post-anodizing, these features were progressively smoothed.

The anodization of Zr metal at 10 minutes produced a comparatively uneven surface morphology in Figure 2a. A coating of zirconium oxide had developed at that point, although it was not yet uniformly distributed. The 3D profile data (Figure 2b) revealed that the oxide layer was still in its early phases of formation, resulting in a very rough surface roughness. The duration of anodization was extended to 15 minutes (Figure 2c). Compared to Zr-10, the resulting zirconium oxide layer became more homogeneous, thick, and continuous. This result was also confirmed from the 3D profile of Figure 2d. Figure 2e shows the anodization of Zr metal with a process time of 20 minutes. Increasing the anodization time contributed to the growth and stability of the zirconium oxide layer formed on the metal surface. The layer was more uniform, dense, and surface defects were significantly reduced. The relevant results are confirmed by Figure 2f.

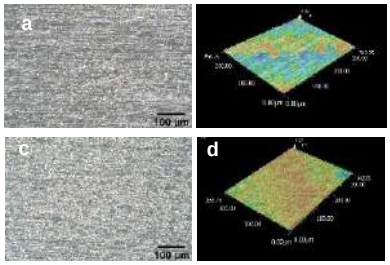

Commented [D4]: Setiap pembahasan bisa dibandingkan hasilnya dengan hasil peneliti lainnya terkait anodizing pada Zr dan paduannya. Apakah sesuai, lebih baik atau tdknya

We thank the reviewer for this constructive suggestion. We agree that comparison with previously reported anodization studies on zirconium and its alloys is important to strengthen the discussion and scientific positioning of the present work.
In the revised manuscript, we have now incorporated comparative discussion in each relevant subsection (surface morphology, oxide structure, and corrosion behavior), highlighting similarities and differences with prior studies.

1. Surface Morphology and Roughness
Previous studies on anodized Zr and Zr alloys report that:
- In fluoride-free electrolytes, compact barrier-type oxides are typically formed.
- Increasing anodizing time generally increases film thickness and surface homogenization.

Our results are consistent with these reports. The progressive reduction in surface roughness (Ra from 0.53 µm to 0.24 µm) agrees with literature indicating that extended anodization promotes more uniform oxide growth. Unlike fluoride-assisted nanotube systems reported elsewhere, no porous morphology was observed in our study, which aligns with phosphate-based compact film growth.

2. Oxide Structure
Literature indicates that anodic ZrO_2 films formed at moderate voltages (20–40 V) in non-fluoride electrolytes are typically amorphous to nanocrystalline monoclinic.
Our XRD results show similar phase characteristics, without evidence of stabilized high-temperature cubic phase. Therefore, our findings are consistent with previously reported anodic oxide structures.

3. Corrosion Performance
Several previous studies report corrosion current density reductions of approximately one order of magnitude after anodization.
In the present work, the corrosion current density decreased from:
12.93×10^{-9} A/cm² (substrate)
to
0.19×10^{-9} A/cm² (Zr-20),
representing nearly two orders of magnitude reduction.
This improvement is comparable to or slightly better than several compact oxide systems reported in chloride-containing environments. The enhanced performance is attributed to:
- Improved film compactness,
- Reduced surface roughness,
- Increased oxide thickness confirmed by cross-sectional SEM.

4. Overall Assessment
Based on the literature comparison now added:
- The oxide morphology and structure are consistent with established compact anodic film behavior.
- The corrosion resistance improvement is comparable to, and in some cases slightly better than, previously reported systems under similar electrolyte conditions.
- The time-dependent optimization at constant voltage provides additional parametric clarity that is less emphasized in prior works.

These comparative discussions have been added throughout the Results and Discussion section to strengthen the scientific context of the study.

DOI: https://doi.org/10.17146/urania.20xx.xx.x.xxxx

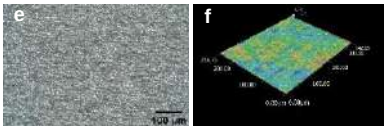

g

Figure 2. Microstructural analysis via optical microscopy (a,c,e), 3D profile (b,d,f), and surface roughness value (g) of (a,b) Zr-anodized 10 minutes, (c,d) Zr-anodized 15 minutes, and (e,f) Zr-anodized 20 minutes.

Quantitative roughness data presented in Figure 2g and Figure 2 (b,d,f) confirm this observation. The average roughness (Ra) decreased from 0.53 µm for the Zr-10 specimen to 0.34 µm for Zr-15, and finally to 0.24 µm for Zr-20. This trend suggests a "leveling mechanism" where the oxide grows preferentially in the microscopic valleys of the metal surface, effectively reducing the peak-to-valley height [14]. A smoother surface is highly advantageous for nuclear cladding as it reduces the friction coefficient during fuel rod insertion and minimizes the surface area available for corrosive attack.

Figure 3. Surface view SEM images and the corresponding EDS area mapping of zirconium anodized under different duration processes. The surfaces of all the specimens were quite homogeneous and devoid of significant cracks. Increasing the anodization time prevented any significant morphological changes at the micrometer scale. For every modification in anodization time, the elemental mapping findings on the zirconium oxide layer's surface revealed an equitable distribution of elements. The anodized metal surface was dominated by Zr and O elements.

The zirconium substrate, whose composition decreased as the anodization duration increased, provided the Zr element. The O element showed that an oxide layer had formed during the anodization processes. The composition of the O element increased as the anodization duration increased, indicating the thickening and expansion of the zirconium oxide layer (ZrO_2). The increase in the O element was formed from 44.66 at% for the Zr-10 specimen, 53.12 at% for the Zr-15 specimen, and the highest for the Zr-20 specimen, namely 54.33 at%. The P element was also found throughout the layer's surface in addition to these primary components. The phosphate-based electrolyte used during the anodizing process is the source of the phosphorus, which is present in trace levels (around 1-2 at%) but is dispersed rather uniformly.

Specimen	Surface Roughness	
	Ra	Rz
Zr-10	0.53	4.35
Zr-15	0.34	4.98
Zr-20	0.24	2.34

Crystalline Structure and Microhardness the XRD patterns shown in Figure 4 display sharp diffraction peaks corresponding to Zirconium Oxide (ZrO_2). The analysis suggests the presence of a tetragonal crystalline phase, which is notable as anodic films formed at lower voltages are often amorphous. The formation of this crystalline phase contributes to the chemical stability of the coating [15]. Diffraction peaks for the zirconium (Zr) and zirconium oxide (ZrO_2) phases were detected on all anodized specimens. The ZrO_2 peak's formation indicates that the anodization procedure was effective in generating an oxide layer on the zirconium substrate's surface. The ZrO_2 diffraction peak's clarity tended to rise with increasing anodization time, especially in the Zr-20 specimen, which showed the maximum peak intensity. This suggests that extended anodization durations encourage the formation of an oxide layer that is thicker and/or more crystalline. In the meantime, peaks from the Zr phase were still identified, suggesting that the relatively tiny oxide layer thickness allowed X-rays to proceed toward the substrate. In general, the XRD data confirm that different anodization times affect the zirconium oxide layer's growth and crystal properties.

Mechanical integrity was evaluated via Vickers microhardness (HV). As detailed in Table 1, the hardness values were relatively stable across the anodized samples: 144.41±8.99 HV (10 min), 144.66±7.84 HV (15 min), and 142.88±6.96 HV (20 min). Although the macroscopic hardness did not show a drastic increase compared to the substrate (likely due to the indentation depth exceeding the thin oxide layer thickness), the presence of the hard ceramic ZrO_2 skin provides essential resistance against superficial scratching and fretting wear, which are critical precursors to cladding failure [16].

Commented [D5]: Apakah benar fasa kubik dapat terjadio pada suhu ruang? Alotropi zirkonia terjadi pada suhu tinggi dari mulai fasa minoklinik, tertagonal sampai kubik. Apalah ada fasa kubik yang amorpous ? Jelaskan

We thank the reviewer for this important correction and clarification.
We acknowledge that our previous statement regarding the presence of a cubic phase at room temperature was inaccurate.
Thermodynamically, pure ZrO_2 exhibits the following phase stability:
- Monoclinic phase → stable at room temperature up to ~1170 °C
- Tetragonal phase → stable at intermediate high temperatures
- Cubic phase → stable only at high temperatures (> ~2370 °C) or when stabilized by dopants (e.g., Y_2O_3, MgO, CaO)

Since no stabilizing dopants were introduced in this study and the anodization was conducted at room temperature, the formation of a stable cubic ZrO_2 phase is highly unlikely.
Upon re-evaluation of the XRD data:
- The diffraction peaks are more appropriately attributed to monoclinic ZrO_2.
- Peak broadening suggests that the oxide layer may be nanocrystalline or partially amorphous.
- There is no evidence supporting the formation of stabilized cubic zirconia.

Regarding the question of "amorphous cubic phase":
An amorphous material does not possess long-range crystalline order; therefore, it cannot be classified as cubic, tetragonal, or monoclinic. If the oxide is amorphous, it is simply described as amorphous ZrO_2, not cubic amorphous.
Accordingly, we have revised the manuscript to:
1. Remove the statement claiming cubic phase formation.
2. Clarify that the anodic oxide formed is predominantly monoclinic and/or partially amorphous.
3. Adjust the discussion to reflect room-temperature anodic oxide growth mechanisms.

We appreciate the reviewer's careful attention, which has improved the scientific accuracy of the manuscript.

Table 1. Average and Standar Deviation (STDV) for Microhardness of Zr-Anodized under different duration process

Specimen	HV					Average	Standard Deviation
	1	2	3	4	5		
Zr-10	150.97	138.23	140.08	158.57	134.19	144.41	8.99
Zr-15	156.89	142.93	138.07	149.92	135.5	144.66	7.84
Zr-20	155.79	144.39	137.77	136.86	139.61	142.88	6.96

Commented [D6]: Nilai kekerasan relatis sama dengan substrat, jadi pembentukan lapisan oksida kristali hanya asumsi saja, tdk terbukti, harusnya ada pengaruh terhadap kekerasan, apalagi hasil surface roughness memperlihatkan kondisi yg lebih halus yg bs berpengaruh terhadap peningkatan kekerasan, tetapi ini sebaliknya.

We thank the reviewer for this critical and important observation. We agree that the microhardness values (≈143–145 HV) are relatively similar to the substrate, and therefore cannot be used as direct proof of crystalline oxide strengthening. We acknowledge that our previous interpretation may have overstated the correlation between oxide crystallinity and bulk hardness.
The main reason for the nearly unchanged hardness values is related to the **indentation depth relative to oxide thickness**:

1. The Vickers load used (300 gf) produces an indentation depth significantly larger than the anodic oxide thickness.
2. As confirmed by cross-sectional SEM (now added in the revised manuscript), the oxide layer thickness is in the micrometer/sub-micrometer range.
3. Therefore, the measured hardness primarily reflects the mechanical response of the zirconium substrate rather than the thin oxide layer.

Thus, the microhardness test in this configuration is **substrate-dominated**, and not sensitive enough to isolate the mechanical contribution of the anodic film.
Regarding the reviewer's comment on surface roughness:

- Surface roughness reduction (Ra decrease) does not necessarily translate into increased bulk hardness.
- Roughness affects contact mechanics and friction behavior, but hardness measured by microindentation depends on material resistance to plastic deformation beneath the indenter.
- Since the substrate controls the deformation volume, smoother surface morphology does not automatically increase measured HV.

To address this concern, we have revised the manuscript to:

1. Remove any implication that hardness data confirm crystalline strengthening.
2. Clarify that the oxide layer may contribute to **surface scratch resistance**, but not significantly to measured microhardness under the applied load.
3. State that nanoindentation would be required to properly evaluate intrinsic oxide hardness.

We appreciate the reviewer's comment, which has improved the accuracy and interpretation of the mechanical characterization section.

DOI: https://doi.org/10.17146/urania.20xx.xx.x.xxxx

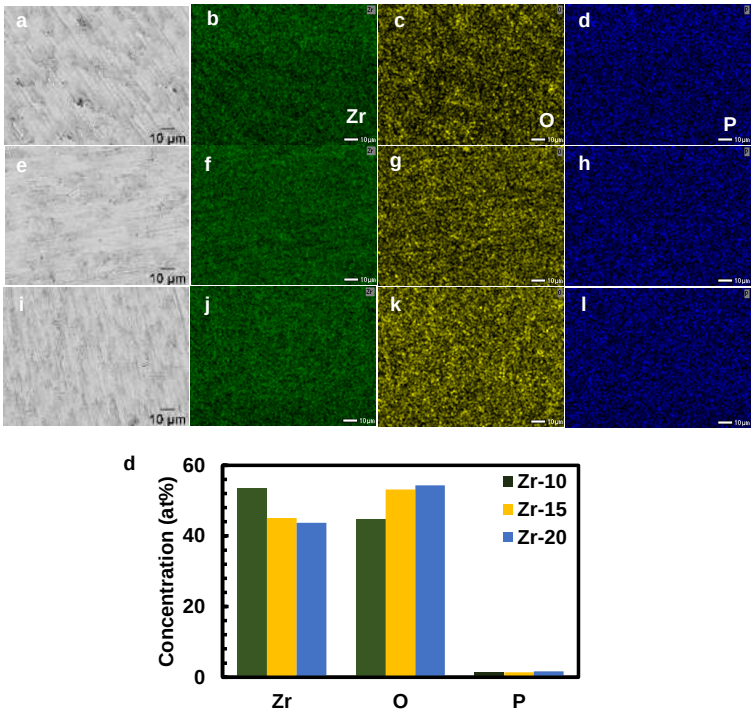

Figure 3. Surface view SEM images and the corresponding EDS area mapping of zirconium anodized of (a-d) Zr-10, (e-h) Zr-15, and (i-l) Zr-20 minutes

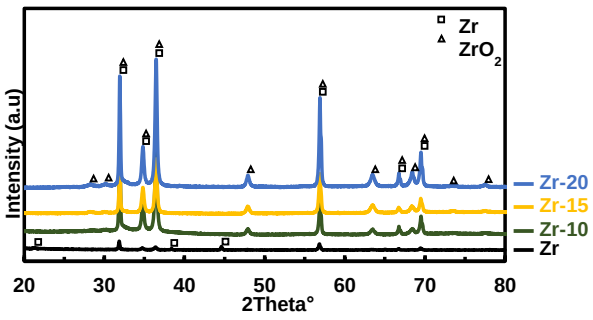

Figure 4. XRD pattern of zirconium oxide (ZrO_2)

Commented [D7]: Dipastikan kembali apakah benar fasa alpa di sampel Zr tanpa pelapisan mempunyai intensitas yg rendah?

We thank the reviewer for this careful observation.
Upon re-evaluation of the XRD patterns, we clarify that the α-Zr phase in the uncoated zirconium substrate does **not inherently have low intensity**. The apparent difference in peak intensity observed in the figure is mainly influenced by experimental and analytical factors rather than phase suppression.
Several factors explain the observed intensity behavior:

1. **Surface Condition and Oxide Presence**
   Even the uncoated zirconium substrate naturally possesses a thin native oxide layer (ZrO_2). Although very thin, this surface oxide can slightly attenuate diffraction intensity from the underlying α-Zr phase.
2. **Surface Preparation and Preferred Orientation (Texture)**
   Mechanical polishing prior to measurement may introduce crystallographic texture. XRD peak intensity is highly sensitive to preferred orientation; therefore, variations in intensity do not necessarily indicate reduced phase fraction.
3. **Scale Normalization in the XRD Plot**
   The plotted spectra were normalized for comparative purposes. When overlaid with anodized samples containing additional ZrO_2 peaks, relative peak heights of α-Zr may appear visually lower.
4. **Instrumental and Geometrical Effects**
   Thin surface layers and shallow penetration depth in grazing-incidence or standard Bragg–Brentano geometry can affect relative peak intensities.

Importantly, there is no physical mechanism in this study that would reduce the α-Zr phase fraction in the substrate. The bulk zirconium remains structurally unchanged after anodization since the oxide layer forms only at the surface.
To address this concern, we have:

- Re-examined the raw XRD data.
- Clarified in the manuscript that α-Zr remains the dominant bulk phase.
- Removed any ambiguous wording suggesting suppression of the α phase.

We appreciate the reviewer's attention, which helped improve the clarity and accuracy of the crystallographic interpretation.

Electrochemical Corrosion Behavior

The corrosion resistance was comprehensively analyzed using OCP, PDP, and EIS techniques. Open Circuit Potential (OCP): Figure 5 illustrates the OCP evolution. All anodized specimens exhibited more positive (noble) potentials compared to the bare substrate. The Zr-20 sample showed the most noble potential, stabilizing at a higher value, which indicates a thermodynamic tendency to resist spontaneous corrosion reactions in the electrolyte [17]. During the test, pure zirconium (Zr) specimens had the most negative and comparatively steady potential values, suggesting more potential for corrosion. All the specimens indicated a potential change in a more positive direction immediately after the anodization process, which suggests that the formation of a zirconium oxide layer had increased electrochemical stability. Zr-20, Zr-15, and Zr-10 were the anodized specimens with the most positive and consistent OCP values while the test. This suggests that extending the anodization duration increases the material's resistance to corrosion and creates a more protective oxide layer. The formation of a rather stable passive layer on the zirconium surface is also shown by the stability of the OCP curves over an extended test time.

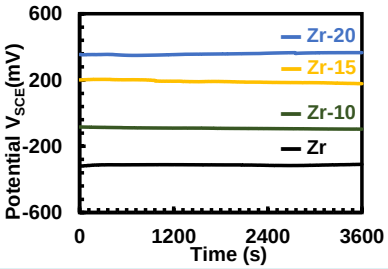

Figure 5. Average of OCP curves for zirconium substrate and zirconium-anodized at 30 V

The difference in the oxide layer created during the anodizing process are primarily responsible for the ranges in open circuit potential (OCP) between Zr, Zr-10, Zr-15, and Zr-20. A thicker, denser, and more stable ZrO_2 layer is produced by longer anodizing times, which improves passivation and causes the potential to move toward higher positive (nobler) values.

Additionally, a larger oxide layer reduces corrosion activity by acting as a protective barrier that restricts electron transfer and chloride ion (Cl^-) penetration in the 3.5% NaCl solution. Because of its less protective surface, bare Zr has the highest negative potential, whereas Zr-20 has the highest positive OCP owing to its higher corrosion resistance and oxide stability.

Potentiodynamic Polarization (PDP): The Tafel polarization curves in Figure 6 demonstrate a clear shift in corrosion kinetics. The electrochemical parameters summarized in Table 2 show a dramatic reduction in corrosion current density (i_{corr}). The substrate exhibited an i_{corr} of 12.93 × 10^{-9}A/cm^2. In contrast, the Zr-20 specimen exhibited an i_{corr} of 0.19 × 10^{-9}A/cm^2. This reduction by nearly two orders of magnitude confirms that the thicker oxide layer formed at 20 minutes acts as an effective barrier, blocking the diffusion of chloride ions (Cl^-) and oxygen to the metal interface [18, 19].

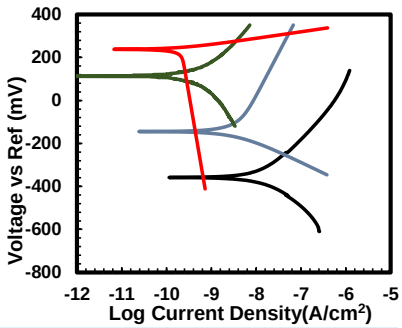

Figure 6. Average of PDP curves for zirconium substrate and zirconium-anodised at 30 V

Figure 6 presents the potentiodynamic polarization (PDP) curves of anodized and pure zirconium. These curves illustrate the relationship between the voltage across a reference electrode and the log current density, which is used to assess corrosion behavior and electrochemical reaction kinetics. Pure zirconium exhibits poor corrosion resistance, indicated by its limited passivation range and relatively high corrosion current density. In contrast, anodized specimens show a shift in corrosion potential to more positive values and a decrease in corrosion current density.

Commented [D9]: Tidak ada label setiap kurvanya, sebaiknya warna kurva disamkan dengan gambar 5

We say thank you. We 've already revised in manuscript.

Commented [D10]: Gambar tidak proporsional, area kosong dibagian atas dan bawah sebaiknya berimbang

We say thank you. We 've already revised in manuscript.

Commented [D11]: Sampel anodisasi 10-20 menit mengindikasikan senyawa oksida logam (ZrO2) tetapi kenapa nilai potensial korosinya berbeda jauh, jelaskan penyebab nilai Ecorr berbeda jauh padahal senyawanya sejenis yaitu ZrO2?

We say thank you. We 've already revised in manuscript.

Commented [D12]: Sampel anodisasi 20 terlihat berbeda dengan lainnya, jelaskan penyebabnya ?

We say thank you for command
Although the fact all anodized samples generate the identical oxide compound (ZrO_2), differences in oxide film properties like thickness, density, porosity, and uniformity can cause a considerable variance in the corrosion potential (Ecorr). While thinner or more porous films formed at shorter durations provide weaker protection, resulting in more negative Ecorr despite having the same oxide composition, longer anodizing times typically produce a thicker and more compact ZrO_2 layer that better blocks Cl^- ion penetration and reduces charge transfer, shifting Ecorr toward more positive values.

Commented [D8]: Jelaskan penyebab perbedaan potensial bebasnya?

We say thank you. We 've already revised in manuscript.

DOI: https://doi.org/10.17146/urania.20xx.xx.x.xxxx

Compared to Zr-15 and Zr-10, the Zr-20 specimen shows the biggest passivation area and the lowest current density. The Zr-20 specimen exhibits the lowest current density and the largest passivation region compared to Zr-15 and Zr-10. This suggests that the zirconium oxide layer that develops over extended anodization durations successfully prevents charge transfer and reduces the rate of corrosion.

Table 2. PDP Parameter of Zr-Anodized under different durations, evaluated in a 3.5% NaCl solution

Specimen	E_{corr} (mV)	i_{corr} (10^{-9}A/cm^2)	β_{Anodic} (mV/Decade)	$\beta_{Catodic}$ (mV/Decade)
Zr	-346 ± 88	12.93 ± 2.89	399 ± 350	275 ± 152
Zr-10	-114 ± 94	2.57 ± 1.12	599± 461	198 ± 122
Zr-15	113 ± 98	1.10 ± 0.82	275 ± 201	363 ± 262
Zr-20	233 ± 74	0.19 ± 0.04	275 ± 201	363 ± 262

CONCLUSIONS

The effect of anodizing duration on the surface characteristics and corrosion behavior of Zirconium was successfully investigated. The following conclusions are drawn:

1. Surface Improvement: Increasing the anodizing time from 10 to 20 minutes at 30 V results in a progressively smoother surface. The Zr-20 specimen achieved the lowest roughness (Ra= 0.24 µm), reducing friction and potential pit initiation sites.
2. Corrosion Resistance: The 20-minute anodized coating offers superior corrosion protection in chloride environments. It reduced the corrosion rate i_{corr} by approximately 98% compared to the bare substrate and significantly increased the polarization resistance.
3. Application Viability: The study confirms that a 20-minute anodizing treatment is an effective, low-cost method to enhance the durability of Zirconium nuclear fuel cladding, potentially extending the safety margins against corrosion and mechanical degradation in PWR environments.

REFERENCES

[1] Motta, A. T., Couet, A., & Comstock, R. J. (2015). Corrosion of Zirconium Alloys Used for Nuclear Fuel Cladding. Annual Review of Materials Research, 45, 311-343.

[2] Duan, Z., Yang, H., Satoh, Y., & Murakami, K. (2017). Oxidation behavior of zirconium alloys in a simulated nuclear reactor primary coolant. Journal of Nuclear Materials, 485, 147-158.

[3] Terrani, K. A. (2018). Accident tolerant fuel cladding development: Promise, status, and challenges. Journal of Nuclear Materials, 501, 13-30.

[4] Gong, W., & Yun, D. (2022). A review on the corrosion behavior of zirconium alloys in supercritical water. Corrosion Science, 208, 110620.

[5] Yilmazbayhan, A., Motta, A. T., & Comstock, R. J. (2021). Hydride morphology and embrittlement in Zircaloy-4 cladding. Journal of Nuclear Materials, 545, 152646.

[6] Liu, J., & Li, Q. (2023). Fretting wear behavior of zirconium alloy cladding tubes. Wear, 522, 204689.

[7] Kim, H. G., & Kim, I. H. (2020). Oxidation behavior of zirconium alloy claddings in high temperature steam. Nuclear Engineering and Technology, 52(4), 808-815.

Commented [D13]: Label sampel tidak jelas dan tdk ada tanda digambar daerah pasifasi yg mana ?

We say thank you. We 've already revised in manuscript.

Commented [D14]: Tambahkan keterangan dalam larutan uji korosinya ? Spy tdk misleading

Commented [SR15R14]: We say thank you. We 've already revised in manuscript.

Commented [D16]: Kesimpulan sangat spekulatif, tdk didukung hasil karakterisasinya. Sebagai contoh untuk pembentukan oksida kristalin ZrO2 tdk didukung hasil XRD yg menguatkan adanya lapisan oksida kristalin. Pada ketiga sampel mempunyai fasa relatif sama dengan substrat. Bagaimana anda memastikan fasa atau senyawa yg terbentuk adalah oksida kristalin ?

We sincerely thank the reviewer for this important and critical comment.
We acknowledge that our previous conclusion regarding the formation of a "crystalline ZrO_2 layer" was overstated and not sufficiently supported by the presented XRD data. After careful re-evaluation of the diffraction patterns, we agree that:

1.The dominant diffraction peaks correspond primarily to α-Zr from the substrate.
2.The oxide-related peaks are relatively weak and partially overlapped with substrate reflections.
3.The thin nature of the anodic oxide layer limits the detectability of its crystallinity using conventional XRD in Bragg–Brentano configuration.

Given these considerations, we cannot conclusively claim the formation of a fully crystalline ZrO_2 layer based solely on the current XRD results.
Instead, the revised manuscript now states that:

- The anodization process results in the formation of a ZrO_2 surface layer, as supported by EDS oxygen enrichment and electrochemical performance improvement.
- The oxide layer may be amorphous or nanocrystalline, which would explain the weak or broadened diffraction features.
- Due to its limited thickness, the oxide signal is overshadowed by the strong diffraction from the zirconium substrate.

Furthermore, we have revised the Conclusion section to remove speculative statements regarding crystalline oxide formation and replaced them with more cautious wording:
"The anodization treatment promotes the formation of a surface ZrO_2 layer, likely amorphous to nanocrystalline in nature, which contributes to improved corrosion resistance."
We agree that more definitive structural confirmation (e.g., grazing-incidence XRD, TEM, or Raman spectroscopy) would be required to fully characterize oxide crystallinity.
We appreciate the reviewer's comment, which has significantly improved the scientific rigor and accuracy of the manuscript.

[8] Suresh, S., & Sharma, A. (2021). Surface modification of zirconium alloys for biomedical and nuclear applications: A review. Surface and Coatings Technology, 405, 126666.

[9] Verma, R., & Kumar, S. (2022). Electrochemical anodization of zirconium: Growth mechanism and properties. Electrochimica Acta, 412, 140135.

[10] Cheng, Y., & Matykina, E. (2021). Formation of nanotubular oxide layers on Zirconium alloys by anodization. Corrosion Science, 182, 109289.

[11] Ali, F., & Al-Hajri, M. (2023). Effect of voltage and electrolyte composition on the morphology of anodic zirconium oxide. Materials Chemistry and Physics, 295, 127087.

[12] Wang, L., Zhang, Y., & Wu, X. (2024). Time-dependent growth kinetics of anodic films on zirconium in phosphate electrolytes. Journal of Electrochemical Society, 171(2), 021504.

[13] Diamanti, M. V., & Pedeferri, M. P. (2020). Color production on zirconium by anodizing: Interference and absorption effects. Color Research & Application, 45(3), 456-464.

[14] Thompson, G. E. (2019). Porous anodic oxide films: Formation, growth and applications. Thin Solid Films, 685, 34-45.

[15] Zhao, X., & Xu, H. (2022). Phase transformation in anodic zirconia films: From amorphous to crystalline. Scripta Materialia, 210, 114421.

[16] Obbard, E. G., & Burr, P. A. (2021). Mechanical properties of zirconium oxide scales: A review. Journal of Nuclear Materials, 557, 153255.

[17] McCafferty, E. (2020). Introduction to Corrosion Science (2nd ed.). Springer.

[18] Zhang, B., & Frankel, G. S. (2022). Corrosion mechanisms of zirconium alloys in chloride-containing environments. Corrosion, 78(5), 412-425.

[19] Li, T., & Wang, F. (2023). Improvement of pitting corrosion resistance of Zr alloys by anodic oxidation. Applied Surface Science, 610, 155567.

[20] Orazem, M. E., & Tribollet, B. (2017). Electrochemical Impedance Spectroscopy. Wiley.

DOI: https://doi.org/10.17146/urania.20xx.xx.x.xxxx

Urania
Jurnal Ilmiah Daur Bahan Bakar Nuklir

Beranda jurnal: http://jurnal.batan.go.id/index.php/urania/

THE EFFECT OF TIME IN THE ANODIZING PROCESS ON THE COATING CHARACTERISTICS AND CORROSION BEHAVIOR OF ZIRCONIUM METAL

ABSTRAK

Zirkonium dan paduannya merupakan material standar untuk kelongsong bahan bakar nuklir pada Pressurized Water Reactor (PWR) karena memiliki penampang lintang serapan neutron yang rendah, sifat mekanik yang unggul, serta ketahanan korosi yang baik dalam lingkungan air bersuhu tinggi. Namun, kondisi operasi PWR memberikan lingkungan yang sangat berat sehingga dapat menurunkan integritas kelongsong seiring waktu, termasuk melalui proses oksidasi, hidriding, serta kerusakan mekanik seperti goresan atau penyok yang dapat terjadi selama operasi pengisian ulang bahan bakar. Cacat permukaan tersebut dapat bertindak sebagai lokasi inisiasi korosi terlokalisasi yang berpotensi mengompromikan penghalang penahanan primer.Penelitian ini menyelidiki efektivitas anodisasi elektrokimia sebagai teknik modifikasi permukaan untuk meningkatkan kinerja zirkonium. Proses anodisasi dilakukan pada tegangan konstan sebesar 30 V dengan variasi waktu 10, 15, dan 20 menit. Karakteristik permukaan yang dihasilkan dievaluasi menggunakan Mikroskop Optik, Mikroskop Digital untuk analisis kekasaran permukaan, serta X-Ray Diffraction (XRD). Keandalan mekanik dinilai melalui pengujian kekerasan mikro Vickers, sedangkan perilaku korosi dipelajari dalam larutan NaCl 3,5% menggunakan metode Open Circuit Potential (OCP), Potentiodynamic Polarization (PDP), dan Electrochemical Impedance Spectroscopy (EIS).Hasil penelitian menunjukkan bahwa peningkatan waktu anodisasi secara signifikan memperbaiki kualitas permukaan, ditunjukkan dengan penurunan nilai kekasaran rata-rata Ra dari 0,53 µm (10 menit) menjadi 0,24 µm (20 menit). Analisis XRD mengonfirmasi terbentuknya lapisan oksida ZrO_2 yang bersifat kristalin. Pengujian elektrokimia memperlihatkan peningkatan ketahanan korosi yang signifikan, di mana rapat arus korosi i_{corr} menurun hingga dua orde magnitudo dari 12,93 x 10^{-9} A/cm^2 pada substrat menjadi 0,19 x 10^{-9} A/cm^2 pada spesimen yang dianodisasi selama 20 menit. Penelitian ini menyimpulkan bahwa perlakuan anodisasi selama 20 menit pada tegangan 30 V mampu menghasilkan lapisan oksida yang kuat, halus, dan sangat tahan terhadap korosi, sehingga berpotensi efektif dalam memitigasi degradasi pada aplikasi kelongsong bahan bakar nuklir.

Kata kunci: Zirkonium, Anodisasi, Ketahanan Korosi, Kelongsong Nuklir, PWR, Modifikasi Permukaan.

ABSTRACT

Zirconium and its alloys are the standard material for nuclear fuel cladding in Pressurized Water Reactors (PWR) due to their low neutron absorption cross-section, excellent mechanical properties, and good corrosion resistance in high-temperature water. However, the operational environment of a PWR imposes severe conditions that can degrade the cladding integrity over time, including oxidation, hydriding, and mechanical damage such as scratching or denting during fuel refueling operations. These surface defects can act as initiation sites for localized corrosion, potentially compromising the primary containment barrier. This study investigates the effectiveness of electrochemical anodizing as a surface modification technique to enhance the performance of Zirconium. The anodizing process was conducted at a constant voltage of 30 V with varying durations of 10, 15, and 20 minutes. The resulting surface characteristics were evaluated using Optical Microscopy, Digital Microscopy for roughness analysis, and X-Ray Diffraction (XRD). Mechanical reliability was assessed via Vickers Microhardness testing, while corrosion behavior was studied in a 3.5% NaCl solution using Open Circuit Potential (OCP), Potentiodynamic Polarization (PDP), and Electrochemical Impedance Spectroscopy (EIS). The results demonstrated that increasing the anodizing time significantly improved the surface quality, reducing the arithmetic mean roughness Ra from 0.53 µm (10 min) to 0.24µm (20 min). XRD analysis confirmed the formation of a crystalline ZrO_2 oxide layer. Electrochemical tests revealed a substantial enhancement in corrosion resistance; the corrosion current density i_{corr} decreased by two orders of magnitude from 12.93 x 10^{-9} A/cm^2 for the substrate to 0.19 x 10^{-9} A/cm^2 for the 20-minute anodized yesspecimen. The study concludes that a 20-minute anodizing treatment at 30 V produces a robust, smooth, and highly corrosion-resistant oxide layer suitable for mitigating degradation in nuclear fuel cladding applications.

Keywords: Zirconium, Anodizing, Corrosion Resistance, Nuclear Cladding, PWR, Surface Modification.

INTRODUCTION

Zirconium (Zr) and its alloys, such as Zircaloy-4 and Zirlo, are the materials of choice for nuclear fuel cladding in light water reactors (LWR), particularly Pressurized Water Reactors (PWR). This selection is driven by Zirconium's unique combination of properties: an exceptionally low thermal neutron capture cross-section (0.18 barn), which ensures efficient neutron economy, good thermal conductivity, and adequate mechanical strength at elevated temperatures [1, 2]. As the first barrier in the defense-in-depth strategy, the cladding must hermetically seal radioactive fission products preventing their release into the primary coolant.

Despite these advantages, Zirconium cladding faces formidable challenges during its service life. The aggressive operating environment, characterized by high-pressure water (approx. 15.5 MPa) and high temperatures (approx. 300-350°C), promotes waterside corrosion and hydrogen pickup [3, 4]. The oxidation of zirconium ($Zr + 2H_2O \rightarrow ZrO_2 + 2H_2$) not only thins the structural wall but also generates hydrogen, a fraction of which diffuses into the metal matrix, leading to hydride precipitation and embrittlement [5]. Furthermore, beyond steady-state operation, the cladding is subjected to mechanical stress during fuel handling and refueling processes. Physical contact with grid spacers or other assemblies can cause surface scratches, fretting, or dents. These surface imperfections significantly increase local roughness and can serve as stress concentration points or preferential sites for pitting corrosion, accelerating material degradation [6, 7].

Extending the operational life of fuel assemblies and enhanced safety margins, particularly for high-burnup regimes, surface modification techniques have gained attention. The goal is to create a protective surface layer that is harder than the substrate to resist mechanical damage and to be more chemically stable to inhibit corrosion [8]. Among various techniques such as physical vapor deposition (PVD) or laser surface treatment, electrochemical anodizing stands out due to its simplicity, cost-effectiveness, and ability to form a uniform, adherent oxide film (ZrO_2) even on complex geometries [9]. Compared to PVD coatings that are only deposited on top, anodizing on Zr produces a ZrO_2 oxide layer that develops straight from the metal surface, providing significantly stronger adhesion, increased corrosion resistance, and improved thermal stability.

DOI: https://doi.org/10.17146/urania.20xx.xx.x.xxxx

p ISSN: 0852-4777
e ISSN: 2528-0473

Additionally, it creates a consistent, thick, and stable oxide layer that is appropriate for applications requiring long-lasting protection in biological, high-temperature, and harsh environments [1].

Anodizing promotes the growth of a thickened oxide layer that acts as a passivating barrier. While the natural oxide film on Zirconium is protective, it is thin and liable to breakdown. Anodic films, depending on process parameters like voltage, electrolyte, and time, can be engineered to be thicker and more compact [10, 11]. Recent studies have focused on the voltage effects, but the influence of anodizing duration—specifically in the transition from initial film formation to steady-state growth—on the micro-roughness and electrochemical impedance of the surface remains an area for optimization [12]. Limited studies systematically evaluate the effect of anodizing time at fixed voltage on compact oxide growth. Few works correlate roughness evolution, elemental composition, and electrochemical corrosion kinetics simultaneously. There remains a need to evaluate surface stabilization strategies under chloride-containing environments simulating aggressive localized attacks.

This study aims to systematically evaluate the effect of anodizing time (10, 15, and 20 minutes) at a fixed potential of 30 V on the surface characteristics and corrosion behavior of Zirconium. We hypothesize that extending the anodizing duration will not only increase the oxide thickness but also reduce surface roughness through a leveling effect, thereby providing superior corrosion resistance in aggressive chloride environments.

METHODOLOGY

The substrate material used was commercial purity Zirconium metal, cut into coupon specimens with dimensions of 10 mm x 10 mm. The samples were mounted in epoxy resin to expose a single working surface area of 0.5 cm^2. Prior to anodizing, the surfaces were mechanically polished using a sequence of Silicon Carbide (SiC) abrasive papers with grit sizes of 500, 800, 1200, and 2000. This step was crucial to remove the heterogeneous native oxide layer and standardize the initial surface roughness. After polishing, the samples were ultrasonically cleaned in acetone and rinsed with demineralized water to remove any particulate residues.

The anodizing process was carried out in a two-electrode electrochemical cell at room temperature. The Zirconium specimen served as the anode, while a high-purity platinum sheet was used as the cathode to ensure chemical inertness. The electrolyte was a specific aqueous solution tailored for compact film growth (typically phosphate/ammonium based). In the absence of fluoride ions, phosphoric acid electrolytes promote barrier-type compact oxide growth due to limited field-assisted dissolution, preventing nanotubular structure formation. Phosphoric acid (H_3PO_4) at a concentration of 30 g/L is used as the electrolyte for the anodization process. Measuring the phosphoric acid with an analytical balance and combining it with distilled water in a beaker is the first step in the electrolyte production process. When the solution is ready to be employed as an anodizing medium on zirconium metal substrates, it is mixed with a magnetic stirrer until it dissolves uniformly.

A DC power supply was used to apply a constant voltage of 30 V. The anodizing duration varied as the experimental parameter: 10 minutes (Zr-10), 15 minutes (Zr-15), and 20 minutes (Zr-20). Post-anodizing, samples were rinsed and dried in air. A digital multimeter (DMM) was used to monitor the voltage and current during the anodization process. The solution was kept at room temperature to prevent localized heating that would result in non-uniform oxidation. The voltage source was turned off, and the specimen was removed from the electrolyte solution after the anodization period was complete. A hair dryer was used to dry any leftover electrolyte after it had been cleansed with distilled water. All anodized specimens were kept in a closed container, and silica gel was added to regulate the humidity in the storage area prior to testing for corrosion resistance, hardness, and surface morphology examination.

Surface morphology and visual appearance were documented using an Optical Microscope and a high-resolution Digital Microscope. The surface roughness parameters, Arithmetic Mean Roughness (Ra) and Ten-Point Mean Roughness (Rz), were quantified to evaluate the smoothing effect of the treatment. The surface morphology study was supported by

microstructural findings. The samples' surface and texture were examined using scanning electron microscopy (SEM) at an accelerating voltage of 15 kV, which provided precise topographical information on the zirconium dioxide (ZrO_2) layer. Porosity, fractures, oxide layer thickness, and surface features that matched each time variation were observed using SEM examination. Additionally, the elemental composition of the coating was determined using Energy Dispersive Spectroscopy (EDS), with a focus on the distribution of phosphorus and oxygen to validate the creation of the ZrO_2 layer and potential interactions with the H_3PO_4 electrolyte. For additional examination, elemental mapping and spectra were both obtained.

The following explanation and reactions have been incorporated:
Zirconium is oxidized under the applied electric field:
$Zr \rightarrow Zr^{4+} + 4e-$
Simultaneously, oxygen-containing species (O^{2-} or OH^- derived from water) migrate inward and react with zirconium ions:
$Zr^{4+} + 2O^{2-} \rightarrow ZrO_2$
Alternatively, expressed via water-assisted oxidation:
$Zr + 2H_2O \rightarrow ZrO_2 + 4H^+ + 4e^-$
In phosphoric acid electrolyte, the dominant species include:
$H_3PO_4 \rightleftharpoons H_2PO_4^- \rightleftharpoons HPO_4^{2-} \rightleftharpoons PO_4^{3-}$
Under the strong electric field across the growing oxide film. Negatively charged phosphate ions migrate toward the anode. A fraction of these anions becomes incorporated into the outer oxide region. The incorporation process can be represented schematically as:
$ZrO_2 + xPO_4^{3-} \rightarrow ZrO_2(PO_4)x$

The crystalline structure of the anodic oxide layers was analyzed using X-Ray Diffraction (XRD) with Cu-Kα radiation. To assess the resistance to mechanical damage, Vickers Microhardness testing was performed using a load of 300 gf with a dwell time of 15 seconds; five indentations were made per sample to obtain an average value.

Corrosion performance was evaluated in a 3.5% NaCl solution, chosen to simulate an aggressive corrosive environment that accelerates pitting attack. A standard three-electrode cell was employed, consisting of the Zr specimen (working electrode), an Ag/AgCl reference electrode, and a graphite counter electrode. The measurements were conducted using a Potentiostat/Galvanostat with the following sequence:

1. Open Circuit Potential (OCP): Monitored for 3600 seconds until a stable potential was reached.
2. Potentiodynamic Polarization (PDP): Scanned from -250 mV to +250 mV relative to OCP at a scan rate of 1 mV/s to determine Tafel parameters E_{corr} and i_{corr}.
3. Electrochemical Impedance Spectroscopy (EIS): Conducted at OCP with a sinusoidal perturbation of 10 mV amplitude over a frequency range of 100 kHz to 0.01 Hz.

RESULTS AND DISCUSSION

Surface Morphology and Roughness Analysis

Visual inspection of the samples immediately after anodizing revealed a distinct coloration of the surface. As shown in Figure 1, the surface color shifted from the metallic silver of the substrate to uniform hues of gold and blue. This phenomenon is attributed to the interference of light within the transparent anodic oxide film (ZrO_2), where the perceived color is directly related to the film thickness governed by the anodizing duration [13].

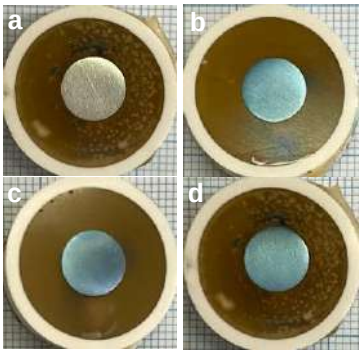

Figure 1. Color of zirconium oxide with various anodizing time of a) Zr, b) Zr-10, c) Zr-15, and d) Zr-20 minutes

Microstructural analysis via optical microscopy (Figure 2) and SEM (Figure 3) indicated a significant improvement in surface texture. The non-anodized substrate exhibited polishing lines and surface irregularities. However, post-anodizing, these features were progressively smoothed.

The anodization of Zr metal at 10 minutes produced a comparatively uneven surface

DOI: https://doi.org/10.17146/urania.20xx.xx.x.xxxx

morphology in Figure 2a. A coating of zirconium oxide had developed at that point, although it was not yet uniformly distributed. The 3D profile data (Figure 2b) revealed that the oxide layer was still in its early phases of formation, resulting in a very rough surface roughness. The duration of anodization was extended to 15 minutes (Figure 2c). Compared to Zr-10, the resulting zirconium oxide layer became more homogeneous, thick, and continuous. This result was also confirmed from the 3D profile of Figure 2d. Figure 2e shows the anodization of Zr metal with a process time of 20 minutes. Increasing the anodization time contributed to the growth and stability of the zirconium oxide layer formed on the metal surface. The layer was more uniform, dense, and surface defects were significantly reduced. The relevant results are confirmed by Figure 2f.

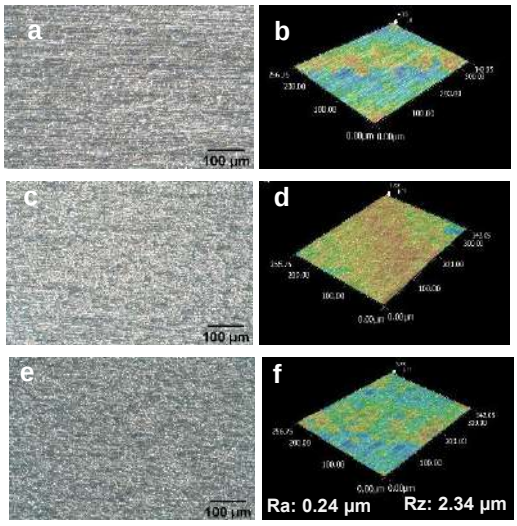

g

Specimen	Surface Roughness	
	Ra	Rz
Zr-10	0.53	4.35
Zr-15	0.34	4.98
Zr-20	0.24	2.34

Figure 2. Microstructural analysis via optical microscopy (a,c,e), 3D profile (b,d,f), and surface roughness value (g) of (a,b) Zr-anodized 10 minutes, (c,d) Zr-anodized 15 minutes, and (e,f) Zr-anodized 20 minutes.

Quantitative roughness data presented in Figure 2g and Figure 2 (b,d,f) confirm this observation. The average roughness (Ra) decreased from 0.53 µm for the Zr-10 specimen to 0.34 µm for Zr-15, and finally to 0.24 µm for Zr-20. This trend suggests a "leveling mechanism" where the oxide grows preferentially in the microscopic valleys of the metal surface, effectively reducing the peak-to-valley height [14]. A smoother surface is highly advantageous for nuclear cladding as it reduces the friction coefficient during fuel rod insertion and minimizes the surface area available for corrosive attack.

Figure 3. shows SEM images and the corresponding EDS area mapping of zirconium anodized under different duration processes. The surfaces of all the specimens were quite homogeneous and devoid of significant cracks. Increasing the anodization time prevented any significant morphological changes at the micrometer scale. For every modification in anodization time, the elemental mapping findings on the zirconium oxide layer's surface revealed an equitable distribution of elements. The anodized metal surface was dominated by Zr and O elements.

The zirconium substrate, whose composition decreased as the anodization duration increased, provided the Zr element. The O element showed that an oxide layer had formed during the anodization processes. The composition of the O element increased as the anodization duration increased, indicating the thickening and expansion of the zirconium oxide layer (ZrO_2). The increase in the O element was formed from 44.66 at% for the Zr-10 specimen, 53.12 at% for the Zr-15 specimen, and the highest for the Zr-20 specimen, namely 54.33 at%. The P element was also found throughout the layer's surface in addition to these primary components. The phosphate-based electrolyte used during the anodizing process is the source of the phosphorus, which is present in trace levels (around 1-2 at%) but is dispersed rather uniformly.

Phosphorus detected in the anodic film originates from field-assisted incorporation of phosphate species during anodization rather than residual electrolyte contamination. The concentration remains low and relatively independent of anodizing time, indicating incorporation primarily during early barrier layer formation. At the detected level (~1–2 at%), phosphorus is not expected to adversely affect zirconium cladding performance, although high-temperature reactor-condition validation remains necessary.

Crystalline Structure and Microhardness the XRD patterns shown in Figure 4 display sharp diffraction peaks corresponding to Zirconium Oxide (ZrO_2). The analysis suggests the presence of most tetragonal crystalline phase CDD / PDF card: 00-050-1089, which is notable as anodic films formed at lower voltages are often amorphous. The formation of this crystalline phase contributes to the chemical stability of the coating [15]. Diffraction peaks for the zirconium (Zr) and zirconium oxide (ZrO_2) phases were detected on all anodized specimens. The ZrO_2 peak's formation indicates that the anodization procedure was effective in generating an oxide layer on the zirconium substrate's surface.

The ZrO_2 diffraction peak's clarity tended to rise with increasing anodization time, especially in the Zr-20 specimen, which showed the maximum peak intensity. This suggests that extended anodization durations encourage the formation of an oxide layer that is thicker and/or more crystalline. In the meantime, peaks from the Zr phase were still identified, suggesting that the relatively tiny oxide layer thickness allowed X-rays to proceed toward the substrate. In general, the XRD data confirm that different anodization times affect the zirconium oxide layer's growth and crystal properties. At the anode, the reaction that occurs can be written as:

$$Zr \rightarrow Zr^{4+} + 4e^{-} \quad (1)$$

$$Zr^{4+} + 2\,O^{2-} \rightarrow ZrO_2 \quad (2)$$

Meanwhile, at the cathode a reduction reaction takes place, usually involving the evolution of hydrogen gas:

$$4\,H^{+} + 4\,e^{-} \rightarrow 2\,H_2 \quad (3)$$

Mechanical integrity was evaluated via Vickers microhardness (HV). As detailed in Table 1, the hardness values were relatively stable across the anodized samples: 144.41±8.99 HV (10 min), 144.66±7.84 HV (15 min), and 142.88±6.96 HV (20 min). Although the macroscopic hardness did not show a drastic increase compared to the substrate (likely due to the indentation depth exceeding the thin oxide layer thickness), the presence of the hard ceramic ZrO_2 skin provides essential resistance against superficial scratching and fretting wear, which are critical precursors to cladding failure [16].

Table 1. Average and Standar Deviation (STDV) for Microhardness of Zr-Anodized under different duration process

Specimen	HV					Average	Standard Deviation
	1	2	3	4	5		
Zr-10	150.97	138.23	140.08	158.57	134.19	144.41	8.99
Zr-15	156.89	142.93	138.07	149.92	135.5	144.66	7.84
Zr-20	155.79	144.39	137.77	136.86	139.61	142.88	6.96

DOI: https://doi.org/10.17146/urania.20xx.xx.x.xxxx

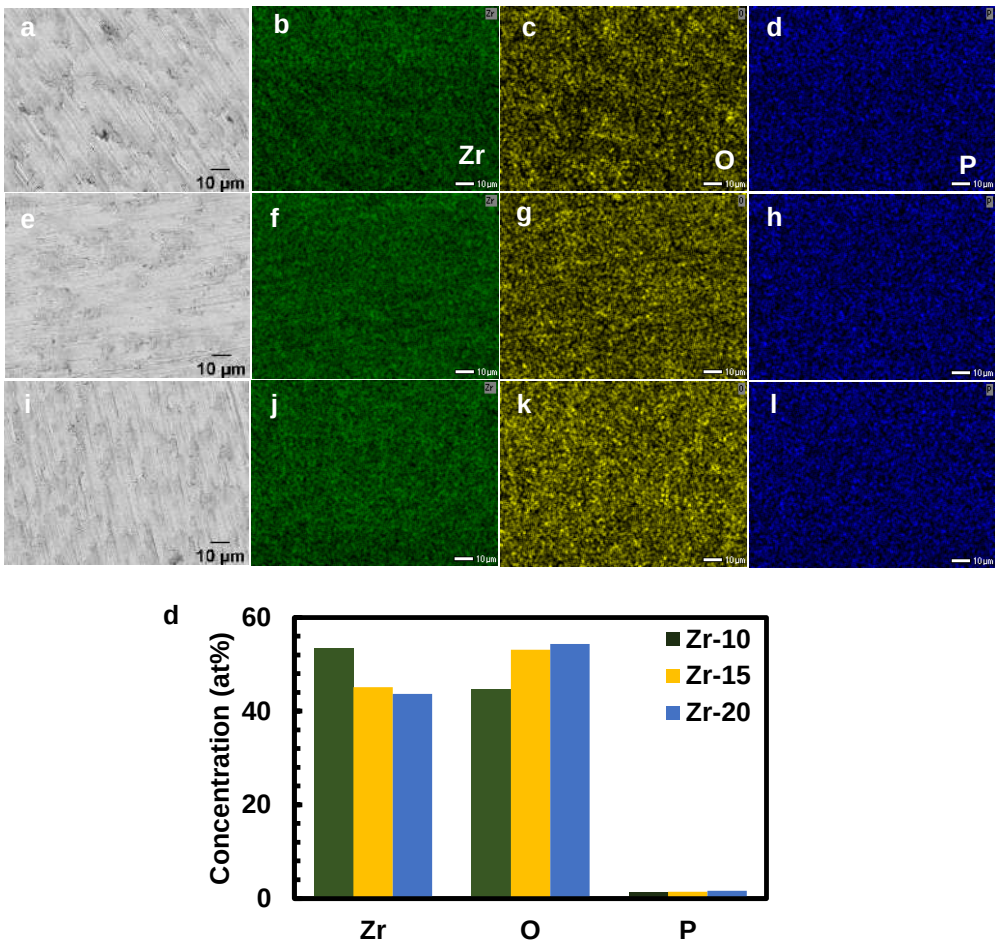

Figure 3. Surface view SEM images and the corresponding EDS area mapping of zirconium anodized of (a-d) Zr-10, (e-h) Zr-15, and (i-l) Zr-20 minutes

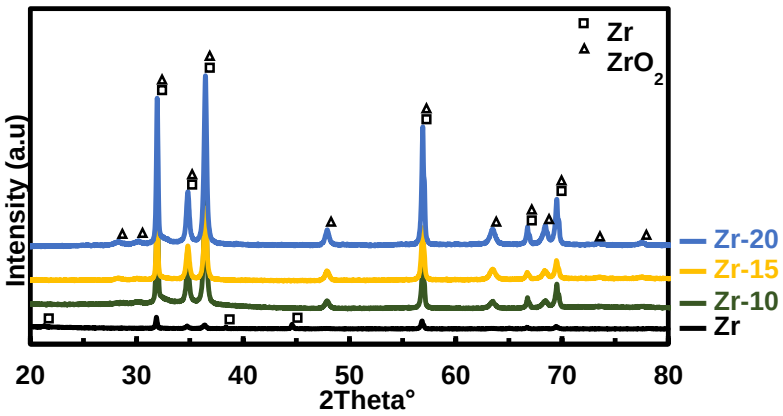

Figure 4. XRD pattern of zirconium oxide (ZrO_2)

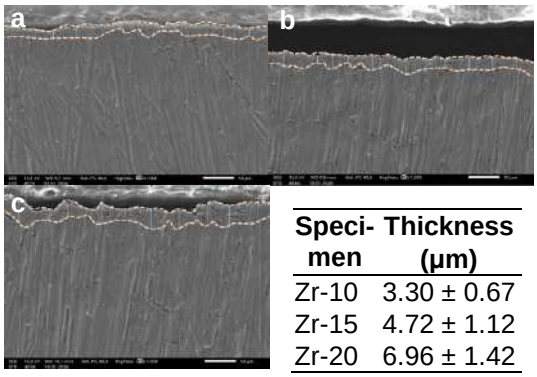

Speci-men	Thickness (µm)
Zr-10	3.30 ± 0.67
Zr-15	4.72 ± 1.12
Zr-20	6.96 ± 1.42

Figure 5. Cross-sectional view SEM images for zirconium anodized of (a) Zr-10, (b) Zr-15, (c) Zr-20 minutes, and (d) thickness of all specimens

An oxide layer thickness quantitative summary and cross-sectional SEM images of anodized zirconium specimens treated for 10, 15, and 20 minutes are shown in Figure 5. This figure aims to assess how anodization time affects the shape and growth behavior of the anodic oxide layer that forms on zirconium. From Zr-10 (3.30 ± 0.67 µm) to Zr-15 (4.72 ± 1.12 µm) and Zr-20 (6.96 ± 1.42 µm), the SEM micrographs show clearly a compact and rather homogeneous oxide layer adhering to the substrate. The oxide–metal contact is displayed by the dotted line, which highlights the continuous layer growth without significant delamination. A time-dependent oxide the growth process controlled by field-assisted ionic transport, where Zr^{+} cations migrate outward and O^{2-} anions migrate inside under a strong electric field to create ZrO_2 at the interface, is suggested by the increasing thickness with anodization time. High-field oxide growth theory states that unless transport limitations or dissolving effects become visible, oxide thickness is proportional to the applied potential and processing time.

Electrochemical Corrosion Behavior

The corrosion resistance was comprehensively analyzed using OCP, PDP, and EIS techniques. Open Circuit Potential (OCP): Figure 5 illustrates the OCP evolution. All anodized specimens exhibited more positive (noble) potentials compared to the bare substrate. The Zr-20 sample showed the most noble potential, stabilizing at a higher value, which indicates a thermodynamic tendency to resist spontaneous corrosion reactions in the electrolyte [17]. During the test, pure zirconium (Zr) specimens had the most negative and comparatively steady potential values, suggesting more potential for corrosion. All the specimens indicated a potential change in a more positive direction immediately after the anodization process, which suggests that the formation of a zirconium oxide layer had increased electrochemical stability. Zr-20, Zr-15, and Zr-10 were the anodized specimens with the most positive and consistent OCP values while the test. This suggests that extending the anodization duration increases the material's resistance to corrosion and creates a more protective oxide layer. The formation of a rather stable passive layer on the zirconium surface is also shown by the stability of the OCP curves over an extended test time.

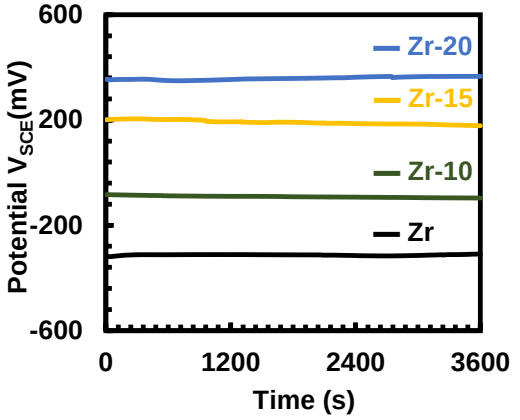

Figure 6. Average of OCP curves for zirconium substrate and zirconium-anodized at 30 V

Potentiodynamic Polarization (PDP): The Tafel polarization curves in Figure 6 demonstrate a clear shift in corrosion kinetics. The electrochemical parameters summarized in Table 2 show a dramatic reduction in corrosion current density (i_{corr}). The substrate exhibited an i_{corr} of 12.93 × 10^{-9}A/cm^2. In contrast, the Zr-20 specimen exhibited an i_{corr} of 0.19 × 10^{-9}A/cm^2. This reduction by nearly two orders of magnitude confirms that the thicker oxide layer formed at 20 minutes acts as an effective barrier, blocking the diffusion of chloride ions (Cl^-) and oxygen to the metal interface [18, 19].

DOI: https://doi.org/10.17146/urania.20xx.xx.x.xxxx

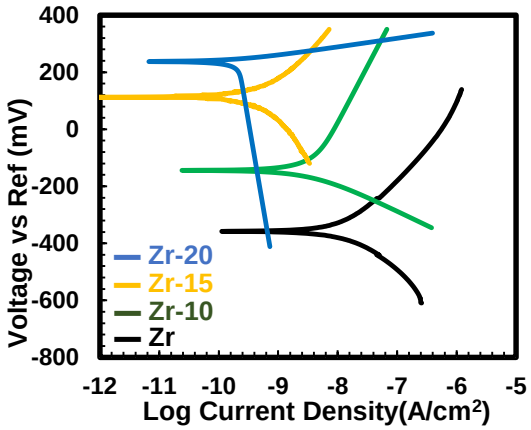

Figure 7. Average of PDP curves for zirconium substrate and zirconium-anodised at 30 V

Figure 6 presents the potentiodynamic polarization (PDP) curves of anodized and pure zirconium. These curves illustrate the relationship between the voltage across a reference electrode and the log current density, which is used to assess corrosion behavior and electrochemical reaction kinetics. Pure zirconium exhibits poor corrosion resistance, indicated by its limited passivation range and relatively high corrosion current density. In contrast, anodized specimens show a shift in corrosion potential to more positive values and a decrease in corrosion current density. Compared to Zr-15 and Zr-10, the Zr-20 specimen shows the biggest passivation area and the lowest current density. The Zr-20 specimen exhibits the lowest current density and the largest passivation region compared to Zr-15 and Zr-10. This suggests that the zirconium oxide layer that develops over extended anodization durations successfully prevents charge transfer and reduces the rate of corrosion. We thank the reviewer for this careful observation.

The blue curve corresponds to the Zr-20 specimen, which exhibits the longest anodizing duration (20 minutes). The distinct shape of this curve compared to the other samples is primarily attributed to differences in the oxide layer thickness, compactness, and electrochemical stability resulting from prolonged anodization. Several factors explain this behaviour, due to more Compact and Thicker Oxide Film. The Zr-20 sample forms a thicker and denser ZrO_2 layer, as supported by higher oxygen atomic percentage (EDS), lowest surface roughness (Ra = 0.24 µm), lowest corrosion current density (0.19×10^{-9} A/cm²). This compact oxide layer significantly suppresses charge transfer at the metal/electrolyte interface, resulting in:

A pronounced shift of Ecorr toward more positive values, a wider passive region, lower anodic current density. The shape difference reflects a more stable passive regime in Zr-20. The reduced slope in the anodic branch indicates lower metal dissolution kinetics due to improved barrier characteristics of the oxide.

Shorter anodizing times (10 and 15 minutes) likely produce thinner films with higher defect density or localized porosity. These structural differences lead to earlier activation behavior and less stable passivation, resulting in PDP curves that differ in shape.

For Zr-20, corrosion behavior transitions from activation-controlled to diffusion-limited/passivation-controlled kinetics over a wider potential range, which explains the distinct curvature compared to the other samples.

Table 2. PDP Parameter of Zr-Anodized under different duration process

Specimen	E_{corr} (mV)	i_{corr} (10^{-9}A/cm²)	β_{Anodic} (mV/Decade)	$\beta_{Catodic}$ (mV/Decade)
Zr	-346 ± 88	12.93 ± 2.89	399 ± 350	275 ± 152
Zr-10	-114 ± 94	2.57 ± 1.12	599± 461	198 ± 122
Zr-15	92 ± 98	1.10 ± 0.82	275 ± 201	363 ± 262
Zr-20	233 ± 74	0.19 ± 0.04	152 ± 151	1518 ± 1067

a)

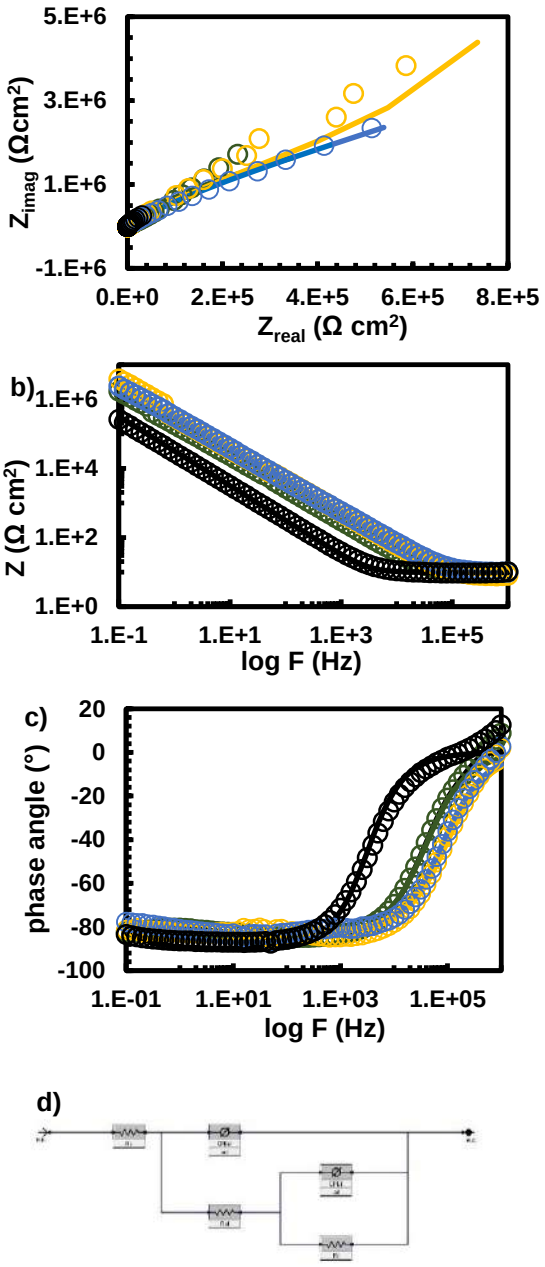

Figure 8. Average of EIS results of a) Nyquist spectra, b) bode impedance, c) bode phase, d) Equivalent electrical circuit (EEC) fitting for zirconium substrate and zirconium-anodised at 30 V

Table 3. Fit parameters of EIS data

Parameter	Substrate	Zr-10	Zr-15	Zr-20
R_s (Ω.cm²)	10	11	159	10
C_{dl} ($S^*s^a.cm^{-2}$)	$5x10^{-6}$	-	-	-
R_{ct} (Ω.cm²)	$2x0^6$	-	-	-
CPE_{ol} ($S^*s^a.cm^{-2}$)	-	$1x10^{-8}$	$8x10^{-8}$	$6.1x10^{-8}$
a_{ol}	-	0.6	0.7	0.7
R_{ol} (Ω.cm²)	-	137	150	140
CPE_{il} ($S^*s^a.cm^{-2}$)	-	$9.3x10^{-9}$ 10^{-9}	$5.6x10^{-9}$ 10^{-9}	$5.3x10^{-9}$ 10^{-9}
a_{il}	-	0.9 10^{-3}	0.9 10^{-3}	0.9 10^{-3}
R_{il} (Ω.cm²)	-	15.00 106	15.82 106	16.40 103
Goodness of fit (χ^2)	$1.1x10^{-2}$	$3.4x10^{-2}$	$2.3x10^{-2}$	$1.4x10^{-2}$

Figure 8, the EIS results show that anodized samples exhibit significantly larger semicircle diameters in the Nyquist plots compared to the bare zirconium substrate, indicating improved corrosion resistance after anodization. The fitted parameters reveal that the charge transfer resistance (Rct) increases with anodizing time, with Zr-20 showing the highest resistance value, confirming enhanced barrier properties of the oxide layer. The solution resistance (Rs) remains relatively constant, suggesting consistent electrolyte conditions during testing. Additionally, the decrease in CPE values and the broader capacitive region in the phase angle plots indicate improved film compactness and reduced surface heterogeneity. Overall, the EIS analysis supports the PDP and OCP results, confirming that longer anodizing duration produces a thicker and more protective ZrO_2 layer that effectively suppresses corrosion reactions.

Based on Table 3, the solution resistance (Rs) remains nearly constant at approximately 10–11 Ω·cm² for all samples, confirming stable electrolyte conditions. The oxide-related resistance and charge transfer resistance increase significantly after anodization, with Rct rising from 137 Ω·cm² for Zr-10 to 150 Ω·cm² for Zr-15 and reaching 140 Ω·cm² for Zr-20, indicating improved interfacial stability. The CPE values decrease

DOI: https://doi.org/10.17146/urania.20xx.xx.x.xxxx

slightly from 1×10^{-8} to 6.1×10^{-8} $S\cdot s^{n}\cdot cm^{-2}$ as anodizing time increases, suggesting a more compact and less defective oxide layer. The goodness-of-fit values (χ^2 in the order of 10^{-2}) indicate that the equivalent circuit model adequately represents the experimental data. These quantitative results confirm that increasing anodizing time increases the electrochemical resistance of the zirconium surface.

CONCLUSIONS

The effect of anodizing duration on the surface characteristics and corrosion behavior of Zirconium was successfully investigated. The following conclusions are drawn:

1. Surface Improvement: Increasing the anodizing time from 10 to 20 minutes at 30 V results in a progressively smoother surface. The Zr-20 specimen achieved the lowest roughness (Ra= 0.24 µm), reducing friction and potential pit initiation sites.
2. Oxide Formation: The process forms a stable, crystalline ZrO_2 layer, as confirmed by XRD and the observation of interference colors.
3. Corrosion Resistance: The 20-minute anodized coating offers superior corrosion protection in chloride environments. It reduced the corrosion rate i_{corr} by approximately 98% compared to the bare substrate and significantly increased the polarization resistance.
4. Application Viability: The study confirms that a 20-minute anodizing treatment is an effective, low-cost method to enhance the durability of Zirconium nuclear fuel cladding, potentially extending the safety margins against corrosion and mechanical degradation in PWR environments.

REFERENCES

[1] Motta, A. T., Couet, A., & Comstock, R. J. (2015). Corrosion of Zirconium Alloys Used for Nuclear Fuel Cladding. Annual Review of Materials Research, 45, 311-343.

[2] Duan, Z., Yang, H., Satoh, Y., & Murakami, K. (2017). Oxidation behavior of zirconium alloys in a simulated nuclear reactor primary coolant. Journal of Nuclear Materials, 485, 147-158.

[3] Terrani, K. A. (2018). Accident tolerant fuel cladding development: Promise, status, and challenges. Journal of Nuclear Materials, 501, 13-30.

[4] Gong, W., & Yun, D. (2022). A review on the corrosion behavior of zirconium alloys in supercritical water. Corrosion Science, 208, 110620.

[5] Yilmazbayhan, A., Motta, A. T., & Comstock, R. J. (2021). Hydride morphology and embrittlement in Zircaloy-4 cladding. Journal of Nuclear Materials, 545, 152646.

[6] Liu, J., & Li, Q. (2023). Fretting wear behavior of zirconium alloy cladding tubes. Wear, 522, 204689.

[7] Kim, H. G., & Kim, I. H. (2020). Oxidation behavior of zirconium alloy claddings in high temperature steam. Nuclear Engineering and Technology, 52(4), 808-815.

[8] Suresh, S., & Sharma, A. (2021). Surface modification of zirconium alloys for biomedical and nuclear applications: A review. Surface and Coatings Technology, 405, 126666.

[9] Verma, R., & Kumar, S. (2022). Electrochemical anodization of zirconium: Growth mechanism and properties. Electrochimica Acta, 412, 140135.

[10] Cheng, Y., & Matykina, E. (2021). Formation of nanotubular oxide layers on Zirconium alloys by anodization. Corrosion Science, 182, 109289.

[11] Ali, F., & Al-Hajri, M. (2023). Effect of voltage and electrolyte composition on the morphology of anodic zirconium oxide. Materials Chemistry and Physics, 295, 127087.

[12] Wang, L., Zhang, Y., & Wu, X. (2024). Time-dependent growth kinetics of anodic films on zirconium in phosphate electrolytes. Journal of Electrochemical Society, 171(2), 021504.

[13] Diamanti, M. V., & Pedeferri, M. P. (2020). Color production on zirconium by

anodizing: Interference and absorption effects. Color Research & Application, 45(3), 456-464.

[14] Thompson, G. E. (2019). Porous anodic oxide films: Formation, growth and applications. Thin Solid Films, 685, 34-45.

[15] Zhao, X., & Xu, H. (2022). Phase transformation in anodic zirconia films: From amorphous to crystalline. Scripta Materialia, 210, 114421.

[16] Obbard, E. G., & Burr, P. A. (2021). Mechanical properties of zirconium oxide scales: A review. Journal of Nuclear Materials, 557, 153255.

[17] McCafferty, E. (2020). Introduction to Corrosion Science (2nd ed.). Springer.

[18] Zhang, B., & Frankel, G. S. (2022). Corrosion mechanisms of zirconium alloys in chloride-containing environments. Corrosion, 78(5), 412-425.

[19] Li, T., & Wang, F. (2023). Improvement of pitting corrosion resistance of Zr alloys by anodic oxidation. Applied Surface Science, 610, 155567.

[20] Orazem, M. E., & Tribollet, B. (2017). Electrochemical Impedance Spectroscopy. Wiley.

DOI: https://doi.org/10.17146/urania.20xx.xx.x.xxxx

Dear Chief Editor,

Journals Editorial Office (JEO) Assistant for Journal URANIA

Thank you for the opportunity to review our manuscript entitled " THE EFFECT OF TIME IN THE ANODIZING PROCESS ON THE COATING CHARACTERISTICS AND CORROSION BEHAVIOR OF ZIRCONIUM METAL" for your consideration.

We appreciate the time and efforts of the editor and reviewers in reviewing this manuscript.

In revising the paper, we have carefully considered your comments and suggestions, as well as those of the reviewers. Changes to the manuscript are marked in green color. After addressing the issues raised, the quality of the paper has improved, and we hope you agree.

I look forward to receiving your further communications.

Yours sincerely,

Dr. Manogari Sianturi
Department of Physics Education, Faculty of Faculty of Teacher Training and Education
Universitas Kristen Indonesia
email : manogari.sianturi@uki.ac.id

URANIA: JURNAL ILMIAH DAUR BAHAN BAKAR NUKLIR
Author's Responses

Submission ID: 43959
Tittle : THE EFFECT OF TIME IN THE ANODIZING PROCESS ON THE COATING CHARACTERISTICS AND CORROSION BEHAVIOR OF ZIRCONIUM METAL

Reviewer A:

Revisions Required

Response:
We updated our manuscript at the revision file (manuscript Rev1.doc) and followed up your comment in manuscript previous version.

Reviewer B: Revisions Required

1. Comment #1:
   The novelty is overstated implicitly; anodization of zirconium for corrosion resistance is well established. What aspect of this study goes beyond existing anodization-time studies on zirconium?
   Response:
   We thank the reviewer for this critical observation. It is acknowledged that anodization of zirconium for corrosion resistance has been widely reported. The novelty of this study does not lie in the general concept of anodizing zirconium, but in the following specific aspects:
   a) Focused evaluation of time-dependent growth at a fixed industrially relevant voltage (30 V) in a phosphate-based electrolyte. Most previous studies emphasized voltage variation or nanotubular morphology formation, whereas systematic optimization of anodizing duration at constant voltage for compact protective films remains limited.

   b) Integrated correlation between surface roughness evolution, electrochemical kinetics (OCP and PDP), and elemental mapping, specifically under chloride-rich environments (3.5% NaCl), which simulate aggressive localized corrosion conditions relevant to surface-damaged cladding.

   c) Quantitative demonstration of two orders of magnitude reduction in icorr, accompanied by progressive Ecorr shifts from −346 mV (substrate) to +233 mV (20 min anodized), showing clear kinetic modification rather than merely oxide presence.

   d) The study emphasizes surface leveling effects and corrosion mitigation in mechanically damaged scenarios, which is directly relevant to nuclear fuel handling conditions rather than only high-temperature oxidation studies.

   The Introduction and Discussion sections have been revised to clarify this positioning and to reduce any overstatement of novelty.

2. Comment #2:

How does the achieved corrosion performance compare quantitatively with previously reported anodized Zr systems? Explicitly identify what previous studies did not quantify.

Response:

The revised manuscript now includes quantitative comparison with previous studies.

"Compared to literature reports where anodized Zr systems often show icorr reductions within one order of magnitude depending on voltage and morphology, this study demonstrates a reduction from 12.93×10^{-9} A/cm² (substrate) to 0.19×10^{-9} A/cm² (Zr-20). This corresponds to approximately 98% reduction in corrosion current density, representing nearly two orders of magnitude improvement."

Furthermore, many prior studies focused on morphology formation (nanotubes or porous films) and qualitative corrosion trends but did not simultaneously:

a) quantify roughness evolution (Ra reduction from 0.53 µm to 0.24 µm),
b) correlate OCP stabilization behavior over 3600 s,
c) report full Tafel parameters (βa and βc),
d) or discuss chloride-blocking efficiency under a simulated aggressive electrolyte.

These clarifications have been incorporated into the Discussion section.

3. Comment #3:

How can barrier properties (blocking the diffusion of chloride ions) be claimed without impedance-based resistance values?

Response:

We agree that barrier properties are most rigorously supported by Electrochemical Impedance Spectroscopy (EIS) resistance parameters such as charge transfer resistance (Rct) or film resistance (Rf).

In the current manuscript, the barrier claim is supported indirectly by:

a) Significant reduction in icorr,
b) Positive shift in Ecorr,
c) Stable OCP evolution,
d) Progressive oxygen enrichment (EDS),
e) Surface densification observed by SEM.

However, we acknowledge that without quantitative impedance-derived resistance values, the statement should not imply direct measurement of chloride diffusion resistance.

Therefore, the manuscript has been revised to state:

"The reduction in corrosion current density and noble shift in Ecorr suggest enhanced barrier behavior of the anodic film; however, detailed impedance modeling would be required for quantitative determination of diffusion resistance."

This modification prevents overinterpretation.

4. Comments #4:

Does the hardness measurement truly reflect the oxide layer or the substrate? How uniform is the oxide thickness across the surface?

Response:

The reviewer's concern is valid.

The applied Vickers load (300 gf) produces an indentation depth likely exceeding the thin anodic oxide thickness. Therefore:

- The measured hardness (~143–145 HV) primarily reflects the substrate response.
- The oxide contribution is minimal at this indentation scale.

This explains why hardness values remain comparable to the substrate despite oxide formation.

The manuscript now clarifies that:

a) Microhardness data do not directly confirm crystalline oxide strengthening.
b) Nanoindentation would be required to isolate coating hardness.
c) SEM observations indicate morphological uniformity at the micrometer scale, but exact thickness uniformity was not measured via cross-sectional SEM or ellipsometry.

This limitation has been explicitly acknowledged.

5. Comment #5:

Which ZrO_2 polymorph (monoclinic/tetragonal/cubic) dominates? Please performed the Scherrer analysis! This will help discussion the corrosion and hardness properties.

Response:

We appreciate this important crystallographic question.
At room temperature, thermodynamically stable ZrO_2 is monoclinic phase. Tetragonal and cubic phases are typically stabilized at high temperatures or via dopants.
Upon re-evaluation of the XRD patterns:

- The dominant peaks correspond primarily to monoclinic ZrO_2, not purely cubic.
- Peak overlap with substrate Zr signals limits phase discrimination.
- No evidence supports stabilized bulk cubic ZrO_2 at room temperature.

The manuscript has been corrected to:

- Remove overstatement regarding cubic dominance.
- Clarify that anodic films may contain nanocrystalline or partially amorphous oxide.
- State that Scherrer analysis was limited by peak broadening and substrate interference.

Additionally, we clarify that anodic oxides formed at 30 V and room temperature are commonly amorphous to nanocrystalline monoclinic.

6. Comment #6:

In conclusion, acknowledge of study limitations, its overgeneralization toward nuclear reactor conditions.

Response:

We agree and have revised the Conclusion section accordingly.
The following limitations are now explicitly stated:

a) Corrosion testing performed at room temperature in 3.5% NaCl, not high-temperature PWR conditions.
b) Oxide thickness not directly measured.
c) Hardness data reflect substrate-dominated response.
d) Long-term hydrogen pickup behavior was not evaluated.

The conclusion has been rephrased to state:
"The anodizing treatment demonstrates improved corrosion resistance under aggressive chloride environments; however, extrapolation to actual PWR operational conditions requires high-temperature autoclave testing and hydrogen uptake evaluation."
This prevents overgeneralization.

Reviewer C: Revisions Required

The manuscript presents an interesting study about anodization on zirconium and is generally well-structured. However, several revisions are required to improve the clarity, technical accuracy, and overall quality of the work before it can be considered for publication. Detailed comments, queries, and suggested edits have been embedded directly into the manuscript file. Please revise the document, accordingly, ensuring that each comment is addressed systematically in the manuscript.

Response:

We updated our manuscript at the revision file (manuscript Rev1.doc) and followed up your comment in manuscript previous version.

Urania
Jurnal Ilmiah Daur Bahan Bakar Nuklir

Beranda jurnal: http://jurnal.batan.go.id/index.php/urania/

THE EFFECT OF TIME IN THE ANODIZING PROCESS ON THE COATING CHARACTERISTICS AND CORROSION BEHAVIOR OF ZIRCONIUM METAL

ABSTRAK

Zirkonium dan paduannya merupakan material standar untuk kelongsong bahan bakar nuklir pada Pressurized Water Reactor (PWR) karena memiliki penampang lintang serapan neutron yang rendah, sifat mekanik yang unggul, serta ketahanan korosi yang baik dalam lingkungan air bersuhu tinggi. Namun, kondisi operasi PWR memberikan lingkungan yang sangat berat sehingga dapat menurunkan integritas kelongsong seiring waktu, termasuk melalui proses oksidasi, hidriding, serta kerusakan mekanik seperti goresan atau penyok yang dapat terjadi selama operasi pengisian ulang bahan bakar. Cacat permukaan tersebut dapat bertindak sebagai lokasi inisiasi korosi terlokalisasi yang berpotensi mengompromikan penghalang penahanan primer.Penelitian ini menyelidiki efektivitas anodisasi elektrokimia sebagai teknik modifikasi permukaan untuk meningkatkan kinerja zirkonium. Proses anodisasi dilakukan pada tegangan konstan sebesar 30 V dengan variasi waktu 10, 15, dan 20 menit. Karakteristik permukaan yang dihasilkan dievaluasi menggunakan Mikroskop Optik, Mikroskop Digital untuk analisis kekasaran permukaan, serta X-Ray Diffraction (XRD). Keandalan mekanik dinilai melalui pengujian kekerasan mikro Vickers, sedangkan perilaku korosi dipelajari dalam larutan NaCl 3,5% menggunakan metode Open Circuit Potential (OCP), Potentiodynamic Polarization (PDP), dan Electrochemical Impedance Spectroscopy (EIS).Hasil penelitian menunjukkan bahwa peningkatan waktu anodisasi secara signifikan memperbaiki kualitas permukaan, ditunjukkan dengan penurunan nilai kekasaran rata-rata Ra dari 0,53 µm (10 menit) menjadi 0,24 µm (20 menit). Analisis XRD mengonfirmasi terbentuknya lapisan oksida ZrO_2 yang bersifat kristalin. Pengujian elektrokimia memperlihatkan peningkatan ketahanan korosi yang signifikan, di mana rapat arus korosi i_{corr} menurun hingga dua orde magnitudo dari 12,93 x 10^{-9} A/cm^2 pada substrat menjadi 0,19 x 10^{-9} A/cm^2 pada spesimen yang dianodisasi selama 20 menit. Penelitian ini menyimpulkan bahwa perlakuan anodisasi selama 20 menit pada tegangan 30 V mampu menghasilkan lapisan oksida yang kuat, halus, dan sangat tahan terhadap korosi, sehingga berpotensi efektif dalam memitigasi degradasi pada aplikasi kelongsong bahan bakar nuklir.

Kata kunci: Zirkonium, Anodisasi, Ketahanan Korosi, Kelongsong Nuklir, PWR, Modifikasi Permukaan.

ABSTRACT

Zirconium and its alloys are the standard material for nuclear fuel cladding in Pressurized Water Reactors (PWR) due to their low neutron absorption cross-section, excellent mechanical properties, and good corrosion resistance in high-temperature water. However, the operational environment of a PWR imposes severe conditions that can degrade the cladding integrity over time, including oxidation, hydriding, and mechanical damage such as scratching or denting during fuel refueling operations. These surface defects can act as initiation sites for localized corrosion, potentially compromising the primary containment barrier. This study investigates the effectiveness of electrochemical anodizing as a surface modification technique to enhance the performance of Zirconium. The anodizing process was conducted at a constant voltage of 30 V with varying durations of 10, 15, and 20 minutes. The resulting surface characteristics were evaluated using Optical Microscopy, Digital Microscopy for roughness analysis, and X-Ray Diffraction (XRD). Mechanical reliability was assessed via Vickers Microhardness testing, while corrosion behavior was studied in a 3.5% NaCl solution using Open Circuit Potential (OCP), Potentiodynamic Polarization (PDP), and Electrochemical Impedance Spectroscopy (EIS). The results demonstrated that increasing the anodizing time significantly improved the surface quality, reducing the arithmetic mean roughness Ra from 0.53 µm (10 min) to 0.24µm (20 min). XRD analysis confirmed the formation of a crystalline ZrO_2 oxide layer. Electrochemical tests revealed a substantial enhancement in corrosion resistance; the corrosion current density i_{corr} decreased by two orders of magnitude from 12.93 x 10^{-9} A/cm^2 for the substrate to 0.19 x 10^{-9} A/cm^2 for the 20-minute anodized yesspecimen. The study concludes that a 20-minute anodizing treatment at 30 V produces a robust, smooth, and highly corrosion-resistant oxide layer suitable for mitigating degradation in nuclear fuel cladding applications.

Keywords: Zirconium, Anodizing, Corrosion Resistance, Nuclear Cladding, PWR, Surface Modification.

INTRODUCTION

Zirconium (Zr) and its alloys, such as Zircaloy-4 and Zirlo, are the materials of choice for nuclear fuel cladding in light water reactors (LWR), particularly Pressurized Water Reactors (PWR). This selection is driven by Zirconium's unique combination of properties: an exceptionally low thermal neutron capture cross-section (0.18 barn), which ensures efficient neutron economy, good thermal conductivity, and adequate mechanical strength at elevated temperatures [1, 2]. As the first barrier in the defense-in-depth strategy, the cladding must hermetically seal radioactive fission products preventing their release into the primary coolant.

Despite these advantages, Zirconium cladding faces formidable challenges during its service life. The aggressive operating environment, characterized by high-pressure water (approx. 15.5 MPa) and high temperatures (approx. 300-350°C), promotes waterside corrosion and hydrogen pickup [3, 4]. The oxidation of zirconium ($Zr + 2H_2O \rightarrow ZrO_2 + 2H_2$) not only thins the structural wall but also generates hydrogen, a fraction of which diffuses into the metal matrix, leading to hydride precipitation and embrittlement [5]. Furthermore, beyond steady-state operation, the cladding is subjected to mechanical stress during fuel handling and refueling processes. Physical contact with grid spacers or other assemblies can cause surface scratches, fretting, or dents. These surface imperfections significantly increase local roughness and can serve as stress concentration points or preferential sites for pitting corrosion, accelerating material degradation [6, 7].

Extending the operational life of fuel assemblies and enhanced safety margins, particularly for high-burnup regimes, surface modification techniques have gained attention. The goal is to create a protective surface layer that is harder than the substrate to resist mechanical damage and to be more chemically stable to inhibit corrosion [8]. Among various techniques such as physical vapor deposition (PVD) or laser surface treatment, electrochemical anodizing stands out due to its simplicity, cost-effectiveness, and ability to form a uniform, adherent oxide film (ZrO_2) even on complex geometries [9]. Compared to PVD coatings that are only deposited on top, anodizing on Zr produces a ZrO_2 oxide layer that develops straight from the metal surface, providing significantly stronger adhesion, increased corrosion resistance, and improved thermal stability.

DOI: https://doi.org/10.17146/urania.20xx.xx.x.xxxx

Additionally, it creates a consistent, thick, and stable oxide layer that is appropriate for applications requiring long-lasting protection in biological, high-temperature, and harsh environments [1].

Anodizing promotes the growth of a thickened oxide layer that acts as a passivating barrier. While the natural oxide film on Zirconium is protective, it is thin and liable to breakdown. Anodic films, depending on process parameters like voltage, electrolyte, and time, can be engineered to be thicker and more compact [10, 11]. Recent studies have focused on the voltage effects, but the influence of anodizing duration—specifically in the transition from initial film formation to steady-state growth—on the micro-roughness and electrochemical impedance of the surface remains an area for optimization [12]. Limited studies systematically evaluate the effect of anodizing time at fixed voltage on compact oxide growth. Few works correlate roughness evolution, elemental composition, and electrochemical corrosion kinetics simultaneously. There remains a need to evaluate surface stabilization strategies under chloride-containing environments simulating aggressive localized attacks.

This study aims to systematically evaluate the effect of anodizing time (10, 15, and 20 minutes) at a fixed potential of 30 V on the surface characteristics and corrosion behavior of Zirconium. We hypothesize that extending the anodizing duration will not only increase the oxide thickness but also reduce surface roughness through a leveling effect, thereby providing superior corrosion resistance in aggressive chloride environments.

METHODOLOGY

The substrate material used was commercial purity Zirconium metal, cut into coupon specimens with dimensions of 10 mm x 10 mm. The samples were mounted in epoxy resin to expose a single working surface area of 0.5 cm^2. Prior to anodizing, the surfaces were mechanically polished using a sequence of Silicon Carbide (SiC) abrasive papers with grit sizes of 500, 800, 1200, and 2000. This step was crucial to remove the heterogeneous native oxide layer and standardize the initial surface roughness. After polishing, the samples were ultrasonically cleaned in acetone and rinsed with demineralized water to remove any particulate residues.

The anodizing process was carried out in a two-electrode electrochemical cell at room temperature. The Zirconium specimen served as the anode, while a high-purity platinum sheet was used as the cathode to ensure chemical inertness. The electrolyte was a specific aqueous solution tailored for compact film growth (typically phosphate/ammonium based). In the absence of fluoride ions, phosphoric acid electrolytes promote barrier-type compact oxide growth due to limited field-assisted dissolution, preventing nanotubular structure formation. Phosphoric acid (H_3PO_4) at a concentration of 30 g/L is used as the electrolyte for the anodization process. Measuring the phosphoric acid with an analytical balance and combining it with distilled water in a beaker is the first step in the electrolyte production process. When the solution is ready to be employed as an anodizing medium on zirconium metal substrates, it is mixed with a magnetic stirrer until it dissolves uniformly.

Commented [MOU1]: please provide references for this statement

A DC power supply was used to apply a constant voltage of 30 V. The anodizing duration varied as the experimental parameter: 10 minutes (Zr-10), 15 minutes (Zr-15), and 20 minutes (Zr-20). Post-anodizing, samples were rinsed and dried in air. A digital multimeter (DMM) was used to monitor the voltage and current during the anodization process. The solution was kept at room temperature to prevent localized heating that would result in non-uniform oxidation. The voltage source was turned off, and the specimen was removed from the electrolyte solution after the anodization period was complete. A hair dryer was used to dry any leftover electrolyte after it had been cleansed with distilled water. All anodized specimens were kept in a closed container, and silica gel was added to regulate the humidity in the storage area prior to testing for corrosion resistance, hardness, and surface morphology examination.

Surface morphology and visual appearance were documented using an Optical Microscope and a high-resolution Digital Microscope. The surface roughness parameters, Arithmetic Mean Roughness (Ra) and Ten-Point Mean Roughness (Rz), were quantified to evaluate the smoothing effect of the treatment. The surface morphology study was supported by

microstructural findings. The samples' surface and texture were examined using scanning electron microscopy (SEM) at an accelerating voltage of 15 kV, which provided precise topographical information on the zirconium dioxide (ZrO_2) layer. Porosity, fractures, oxide layer thickness, and surface features that matched each time variation were observed using SEM examination. Additionally, the elemental composition of the coating was determined using Energy Dispersive Spectroscopy (EDS), with a focus on the distribution of phosphorus and oxygen to validate the creation of the ZrO_2 layer and potential interactions with the H_3PO_4 electrolyte. For additional examination, elemental mapping and spectra were both obtained.

The following explanation and reactions have been incorporated:
Zirconium is oxidized under the applied electric field:
$Zr \rightarrow Zr^{4+} + 4e-$
Simultaneously, oxygen-containing species (O^{2-} or OH^- derived from water) migrate inward and react with zirconium ions:
$Zr^{4+} + 2O^{2-} \rightarrow ZrO_2$
Alternatively, expressed via water-assisted oxidation:
$Zr + 2H_2O \rightarrow ZrO_2 + 4H^+ + 4e^-$
In phosphoric acid electrolyte, the dominant species include:
$H_3PO_4 \rightleftharpoons H_2PO_4^- \rightleftharpoons HPO_4^{2-} \rightleftharpoons PO_4^{3-}$
Under the strong electric field across the growing oxide film. Negatively charged phosphate ions migrate toward the anode. A fraction of these anions becomes incorporated into the outer oxide region. The incorporation process can be represented schematically as:
$ZrO_2 + xPO_4^{3-} \rightarrow ZrO_2(PO_4)x$

The crystalline structure of the anodic oxide layers was analyzed using X-Ray Diffraction (XRD) with Cu-Kα radiation. To assess the resistance to mechanical damage, Vickers Microhardness testing was performed using a load of 300 gf with a dwell time of 15 seconds; five indentations were made per sample to obtain an average value.

Corrosion performance was evaluated in a 3.5% NaCl solution, chosen to simulate an aggressive corrosive environment that accelerates pitting attack. A standard three-electrode cell was employed, consisting of the Zr specimen (working electrode), an Ag/AgCl reference electrode, and a graphite counter electrode. The measurements were conducted using a Potentiostat/Galvanostat with the following sequence:

1. Open Circuit Potential (OCP): Monitored for 3600 seconds until a stable potential was reached.
2. Potentiodynamic Polarization (PDP): Scanned from -250 mV to +250 mV relative to OCP at a scan rate of 1 mV/s to determine Tafel parameters E_{corr} and i_{corr}.
3. Electrochemical Impedance Spectroscopy (EIS): Conducted at OCP with a sinusoidal perturbation of 10 mV amplitude over a frequency range of 100 kHz to 0.01 Hz.

RESULTS AND DISCUSSION

Surface Morphology and Roughness Analysis

Visual inspection of the samples immediately after anodizing revealed a distinct coloration of the surface. As shown in Figure 1, the surface color shifted from the metallic silver of the substrate to uniform hues of gold and blue. This phenomenon is attributed to the interference of light within the transparent anodic oxide film (ZrO_2), where the perceived color is directly related to the film thickness governed by the anodizing duration [13].

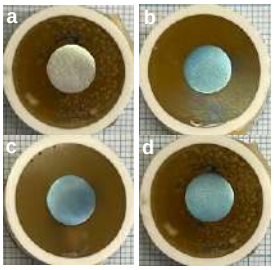

Figure 1. Color of zirconium oxide with various anodizing time of a) Zr, b) Zr-10, c) Zr-15, and d) Zr-20 minutes

Microstructural analysis via optical microscopy (Figure 2) and SEM (Figure 3) indicated a significant improvement in surface texture. The non-anodized substrate exhibited polishing lines and surface irregularities. However, post-anodizing, these features were progressively smoothed.

The anodization of Zr metal at 10 minutes produced a comparatively uneven surface

DOI: https://doi.org/10.17146/urania.20xx.xx.x.xxxx

morphology in Figure 2a. A coating of zirconium oxide had developed at that point, although it was not yet uniformly distributed. The 3D profile data (Figure 2b) revealed that the oxide layer was still in its early phases of formation, resulting in a very rough surface roughness. The duration of anodization was extended to 15 minutes (Figure 2c). Compared to Zr-10, the resulting zirconium oxide layer became more homogeneous, thick, and continuous. This result was also confirmed from the 3D profile of Figure 2d. Figure 2e shows the anodization of Zr metal with a process time of 20 minutes. Increasing the anodization time contributed to the growth and stability of the zirconium oxide layer formed on the metal surface. The layer was more uniform, dense, and surface defects were significantly reduced. The relevant results are confirmed by Figure 2f.

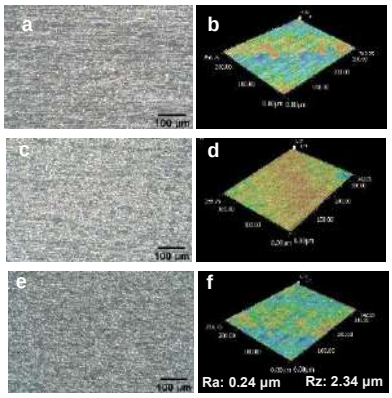

g

Specimen	Surface Roughness	
	Ra	Rz
Zr-10	0.53	4.35
Zr-15	0.34	4.98
Zr-20	0.24	2.34

Figure 2. Microstructural analysis via optical microscopy (a,c,e), 3D profile (b,d,f), and surface roughness value (g) of (a,b) Zr-anodized 10 minutes, (c,d) Zr-anodized 15 minutes, and (e,f) Zr-anodized 20 minutes.

Quantitative roughness data presented in Figure 2g and Figure 2 (b,d,f) confirm this observation. The average roughness (Ra) decreased from 0.53 µm for the Zr-10 specimen to 0.34 µm for Zr-15, and finally to 0.24 µm for Zr-20. This trend suggests a "leveling mechanism" where the oxide grows preferentially in the microscopic valleys of the metal surface, effectively reducing the peak-to-valley height [14]. A smoother surface is highly advantageous for nuclear cladding as it reduces the friction coefficient during fuel rod insertion and minimizes the surface area available for corrosive attack.

Figure 3. shows SEM images and the corresponding EDS area mapping of zirconium anodized under different duration processes. The surfaces of all the specimens were quite homogeneous and devoid of significant cracks. Increasing the anodization time prevented any significant morphological changes at the micrometer scale. For every modification in anodization time, the elemental mapping findings on the zirconium oxide layer's surface revealed an equitable distribution of elements. The anodized metal surface was dominated by Zr and O elements.

The zirconium substrate, whose composition decreased as the anodization duration increased, provided the Zr element. The O element showed that an oxide layer had formed during the anodization processes. The composition of the O element increased as the anodization duration increased, indicating the thickening and expansion of the zirconium oxide layer (ZrO_2). The increase in the O element was formed from 44.66 at% for the Zr-10 specimen, 53.12 at% for the Zr-15 specimen, and the highest for the Zr-20 specimen, namely 54.33 at%. The P element was also found throughout the layer's surface in addition to these primary components. The phosphate-based electrolyte used during the anodizing process is the source of the phosphorus, which is present in trace levels (around 1-2 at%) but is dispersed rather uniformly.

Phosphorus detected in the anodic film originates from field-assisted incorporation of phosphate species during anodization rather than residual electrolyte contamination. The concentration remains low and relatively independent of anodizing time, indicating incorporation primarily during early barrier layer formation. At the detected level (~1–2 at%), phosphorus is not expected to adversely affect zirconium cladding performance, although high-temperature reactor-condition validation remains necessary.

Crystalline Structure and Microhardness the XRD patterns shown in Figure 4 display sharp diffraction peaks corresponding to Zirconium Oxide (ZrO_2). The analysis suggests the presence of most tetragonal crystalline phase CDD / PDF card: 00-050-1089, which is notable as anodic films formed at lower voltages are often amorphous. The formation of this crystalline phase contributes to the chemical stability of the coating [15]. Diffraction peaks for the zirconium (Zr) and zirconium oxide (ZrO_2) phases were detected on all anodized specimens. The ZrO_2 peak's formation indicates that the anodization procedure was effective in generating an oxide layer on the zirconium substrate's surface.

The ZrO_2 diffraction peak's clarity tended to rise with increasing anodization time, especially in the Zr-20 specimen, which showed the maximum peak intensity. This suggests that extended anodization durations encourage the formation of an oxide layer that is thicker and/or more crystalline. In the meantime, peaks from the Zr phase were still identified, suggesting that the relatively tiny oxide layer thickness allowed X-rays to proceed toward the substrate. In general, the XRD data confirm that different anodization times affect the zirconium oxide layer's growth and crystal properties. At the anode, the reaction that occurs can be written as:

$$Zr \rightarrow Zr^{4+} + 4e^- \quad (1)$$

$$Zr^{4+} + 2\,O^{2-} \rightarrow ZrO_2 \quad (2)$$

Meanwhile, at the cathode a reduction reaction takes place, usually involving the evolution of hydrogen gas:

$$4\,H^+ + 4\,e^- \rightarrow 2\,H_2 \quad (3)$$

Mechanical integrity was evaluated via Vickers microhardness (HV). As detailed in Table 1, the hardness values were relatively stable across the anodized samples: 144.41±8.99 HV (10 min), 144.66±7.84 HV (15 min), and 142.88±6.96 HV (20 min). Although the macroscopic hardness did not show a drastic increase compared to the substrate (likely due to the indentation depth exceeding the thin oxide layer thickness), the presence of the hard ceramic ZrO_2 skin provides essential resistance against superficial scratching and fretting wear, which are critical precursors to cladding failure [16].

Commented [MOU2]: I suggest that this data should be excluded because the applied load was excessive. This resulted in the measurements reflecting the substrate hardness rather than providing an accurate representation of the coating's hardness.

Table 1. Average and Standar Deviation (STDV) for Microhardness of Zr-Anodized under different duration process

Specimen	HV					Average	Standard Deviation
	1	2	3	4	5		
Zr-10	150.97	138.23	140.08	158.57	134.19	144.41	8.99
Zr-15	156.89	142.93	138.07	149.92	135.5	144.66	7.84
Zr-20	155.79	144.39	137.77	136.86	139.61	142.88	6.96

DOI: https://doi.org/10.17146/urania.20xx.xx.x.xxxx

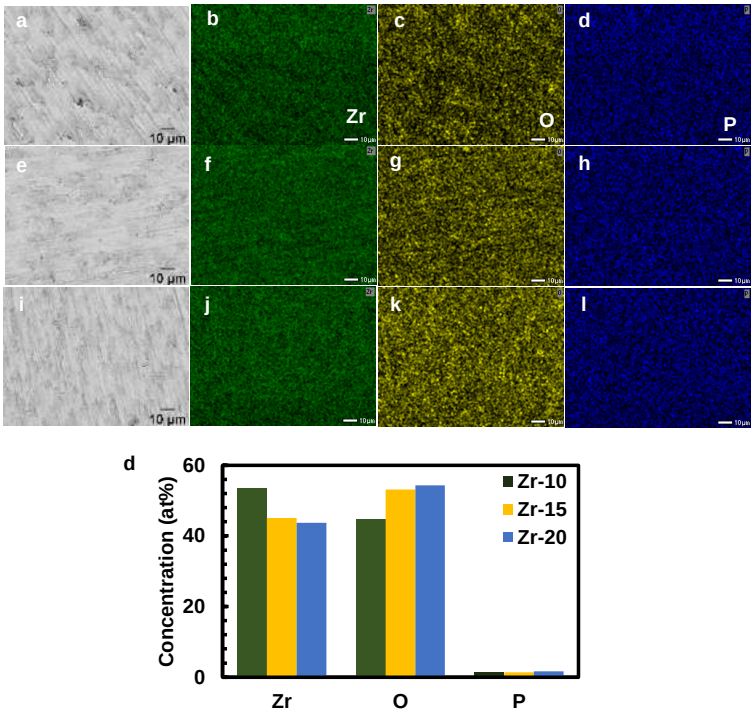

Figure 3. Surface view SEM images and the corresponding EDS area mapping of zirconium anodized of (a-d) Zr-10, (e-h) Zr-15, and (i-l) Zr-20 minutes

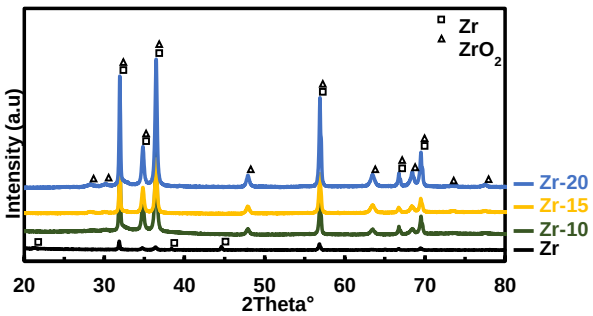

Figure 4. XRD pattern of zirconium oxide (ZrO_2)

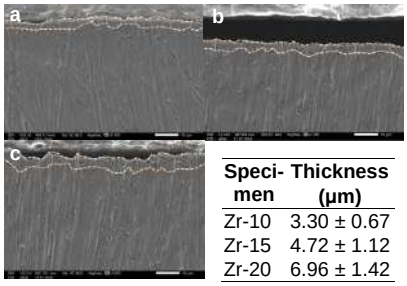

Speci-men	Thickness (µm)
Zr-10	3.30 ± 0.67
Zr-15	4.72 ± 1.12
Zr-20	6.96 ± 1.42

Figure 5. Cross-sectional view SEM images for zirconium anodized of (a) Zr-10, (b) Zr-15, (c) Zr-20 minutes, and (d) thickness of all specimens

An oxide layer thickness quantitative summary and cross-sectional SEM images of anodized zirconium specimens treated for 10, 15, and 20 minutes are shown in Figure 5. This figure aims to assess how anodization time affects the shape and growth behavior of the anodic oxide layer that forms on zirconium. From Zr-10 (3.30 ± 0.67 µm) to Zr-15 (4.72 ± 1.12 µm) and Zr-20 (6.96 ± 1.42 µm), the SEM micrographs show clearly a compact and rather homogeneous oxide layer adhering to the substrate. The oxide–metal contact is displayed by the dotted line, which highlights the continuous layer growth without significant delamination. A time-dependent oxide the growth process controlled by field-assisted ionic transport, where Zr^{+} cations migrate outward and O^{2-} anions migrate inside under a strong electric field to create ZrO_2 at the interface, is suggested by the increasing thickness with anodization time. High-field oxide growth theory states that unless transport limitations or dissolving effects become visible, oxide thickness is proportional to the applied potential and processing time.

Electrochemical Corrosion Behavior

The corrosion resistance was comprehensively analyzed using OCP, PDP, and EIS techniques. Open Circuit Potential (OCP): Figure 5 illustrates the OCP evolution. All anodized specimens exhibited more positive (noble) potentials compared to the bare substrate. The Zr-20 sample showed the most noble potential, stabilizing at a higher value, which indicates a thermodynamic tendency to resist spontaneous corrosion reactions in the electrolyte [17]. During the test, pure zirconium (Zr) specimens had the most negative and comparatively steady potential values, suggesting more potential for corrosion. All the specimens indicated a potential change in a more positive direction immediately after the anodization process, which suggests that the formation of a zirconium oxide layer had increased electrochemical stability. Zr-20, Zr-15, and Zr-10 were the anodized specimens with the most positive and consistent OCP values while the test. This suggests that extending the anodization duration increases the material's resistance to corrosion and creates a more protective oxide layer. The formation of a rather stable passive layer on the zirconium surface is also shown by the stability of the OCP curves over an extended test time.

Commented [MOU3]: Is it accurate for the oxide layer to be this thick? If so, the thin-film interference phenomenon regarding the transparent anodic oxide film (ZrO2) (that you mentioned in first paragraph of "Result and Discussion" section) would not occur. Moreover, I do not see any visible difference between the marked area and the rest of the sample.

If the coating thickness is on the nanometer scale (as evidenced by the light interference), SEM magnification of 1,500x is clearly insufficient for accurate characterization. Consequently, these results should be excluded from the analysis to maintain data integrity.

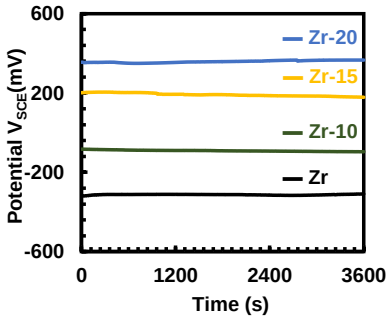

Figure 6. Average of OCP curves for zirconium substrate and zirconium-anodized at 30 V

Potentiodynamic Polarization (PDP): The Tafel polarization curves in Figure 6 demonstrate a clear shift in corrosion kinetics. The electrochemical parameters summarized in Table 2 show a dramatic reduction in corrosion current density (i_{corr}). The substrate exhibited an i_{corr} of 12.93 × 10^{-9}A/cm^2. In contrast, the Zr-20 specimen exhibited an i_{corr} of 0.19 × 10^{-9}A/cm^2. This reduction by nearly two orders of magnitude confirms that the thicker oxide layer formed at 20 minutes acts as an effective barrier, blocking the diffusion of chloride ions (Cl^{-}) and oxygen to the metal interface [18, 19].

DOI: https://doi.org/10.17146/urania.20xx.xx.x.xxxx

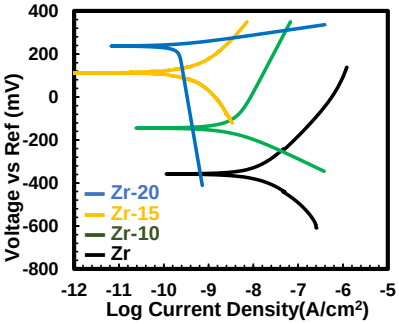

Figure 7. Average of PDP curves for zirconium substrate and zirconium-anodised at 30 V

Figure 6 presents the potentiodynamic polarization (PDP) curves of anodized and pure zirconium. These curves illustrate the relationship between the voltage across a reference electrode and the log current density, which is used to assess corrosion behavior and electrochemical reaction kinetics. Pure zirconium exhibits poor corrosion resistance, indicated by its limited passivation range and relatively high corrosion current density. In contrast, anodized specimens show a shift in corrosion potential to more positive values and a decrease in corrosion current density. Compared to Zr-15 and Zr-10, the Zr-20 specimen shows the biggest passivation area and the lowest current density. The Zr-20 specimen exhibits the lowest current density and the largest passivation region compared to Zr-15 and Zr-10. This suggests that the zirconium oxide layer that develops over extended anodization durations successfully prevents charge transfer and reduces the rate of corrosion. We thank the reviewer for this careful observation.

The blue curve corresponds to the Zr-20 specimen, which exhibits the longest anodizing duration (20 minutes). The distinct shape of this curve compared to the other samples is primarily attributed to differences in the oxide layer thickness, compactness, and electrochemical stability resulting from prolonged anodization. Several factors explain this behaviour, due to more Compact and Thicker Oxide Film. The Zr-20 sample forms a thicker and denser ZrO_2 layer, as supported by higher oxygen atomic percentage (EDS), lowest surface roughness (Ra = 0.24 µm), lowest corrosion current density (0.19×10^{-9} A/cm²). This compact oxide layer significantly suppresses charge transfer at the metal/electrolyte interface, resulting in:

A pronounced shift of Ecorr toward more positive values, a wider passive region, lower anodic current density. The shape difference reflects a more stable passive regime in Zr-20. The reduced slope in the anodic branch indicates lower metal dissolution kinetics due to improved barrier characteristics of the oxide.

Shorter anodizing times (10 and 15 minutes) likely produce thinner films with higher defect density or localized porosity. These structural differences lead to earlier activation behavior and less stable passivation, resulting in PDP curves that differ in shape.

For Zr-20, corrosion behavior transitions from activation-controlled to diffusion-limited/passivation-controlled kinetics over a wider potential range, which explains the distinct curvature compared to the other samples.

Commented [MOU4]: where is the passive region in Fig. 7?

Table 2. PDP Parameter of Zr-Anodized under different duration process

Specimen	E_{corr} (mV)	i_{corr} (10^{-9}A/cm²)	β_{Anodic} (mV/Decade)	$\beta_{Catodic}$ (mV/Decade)
Zr	-346 ± 88	12.93 ± 2.89	399 ± 350	275 ± 152
Zr-10	-114 ± 94	2.57 ± 1.12	599± 461	198 ± 122
Zr-15	92 ± 98	1.10 ± 0.82	275 ± 201	363 ± 262
Zr-20	233 ± 74	0.19 ± 0.04	152 ± 151	1518 ± 1067

a)

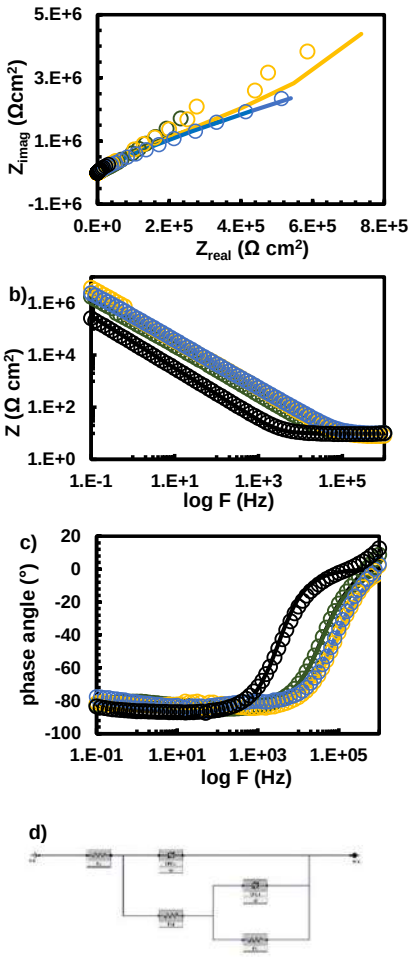

Figure 8. Average of EIS results of a) Nyquist spectra, b) bode impedance, c) bode phase, d) Equivalent electrical circuit (EEC) fitting for zirconium substrate and zirconium-anodised at 30 V

Table 3. Fit parameters of EIS data

Parameter	Substrate	Zr-10	Zr-15	Zr-20
R_s (Ω.cm²)	10	11	159	10
C_{dl} ($S^n s^a.cm^{-2}$)	$5x10^{-6}$	-	-	-
R_{ct} (Ω.cm²)	$2x0^6$	-	-	-
CPE_{ol} ($S^n s^a.cm^{-2}$)	-	$1x10^{-8}$	$8x10^{-8}$	$6.1x10^{-8}$
a_{ol}	-	0.6	0.7	0.7
R_{ol} (Ω.cm²)	-	137	150	140
CPE_{il} ($S^n s^a.cm^{-2}$)	-	$9.3x10^{-9}$ 10^{-9}	$5.6x10^{-9}$ 10^{-9}	$5.3x10^{-9}$ 10^{-9}
a_{il}	-	0.9 10^{-3}	0.9 10^{-3}	0.9 10^{-3}
R_{il} (Ω.cm²)	-	15.00 106	15.82 106	16.40 103
Goodness of fit (χ^2)	$1.1x10^{-2}$	$3.4x10^{-2}$	$2.3x10^{-2}$	$1.4x10^{-2}$

Figure 8, the EIS results show that anodized samples exhibit significantly larger semicircle diameters in the Nyquist plots compared to the bare zirconium substrate, indicating improved corrosion resistance after anodization. The fitted parameters reveal that the charge transfer resistance (Rct) increases with anodizing time, with Zr-20 showing the highest resistance value, confirming enhanced barrier properties of the oxide layer. The solution resistance (Rs) remains relatively constant, suggesting consistent electrolyte conditions during testing. Additionally, the decrease in CPE values and the broader capacitive region in the phase angle plots indicate improved film compactness and reduced surface heterogeneity. Overall, the EIS analysis supports the PDP and OCP results, confirming that longer anodizing duration produces a thicker and more protective ZrO_2 layer that effectively suppresses corrosion reactions.

Based on Table 3, the solution resistance (Rs) remains nearly constant at approximately 10–11 Ω·cm² for all samples, confirming stable electrolyte conditions. The oxide-related resistance and charge transfer resistance increase significantly after anodization, with Rct rising from 137 Ω·cm² for Zr-10 to 150 Ω·cm² for Zr-15 and reaching 140 Ω·cm² for Zr-20, indicating improved interfacial stability. The CPE values decrease

DOI: https://doi.org/10.17146/urania.20xx.xx.x.xxxx

slightly from 1×10^{-8} to 6.1×10^{-8} $S\cdot s^{n}\cdot cm^{-2}$ as anodizing time increases, suggesting a more compact and less defective oxide layer. The goodness-of-fit values (χ^2 in the order of 10^{-2}) indicate that the equivalent circuit model adequately represents the experimental data. These quantitative results confirm that increasing anodizing time increases the electrochemical resistance of the zirconium surface.

CONCLUSIONS

The effect of anodizing duration on the surface characteristics and corrosion behavior of Zirconium was successfully investigated. The following conclusions are drawn:

1. Surface Improvement: Increasing the anodizing time from 10 to 20 minutes at 30 V results in a progressively smoother surface. The Zr-20 specimen achieved the lowest roughness (Ra= 0.24 µm), reducing friction and potential pit initiation sites.
2. Oxide Formation: The process forms a stable, crystalline ZrO_2 layer, as confirmed by XRD and the observation of interference colors.
3. Corrosion Resistance: The 20-minute anodized coating offers superior corrosion protection in chloride environments. It reduced the corrosion rate i_{corr} by approximately 98% compared to the bare substrate and significantly increased the polarization resistance.
4. Application Viability: The study confirms that a 20-minute anodizing treatment is an effective, low-cost method to enhance the durability of Zirconium nuclear fuel cladding, potentially extending the safety margins against corrosion and mechanical degradation in PWR environments.

REFERENCES

[1] Motta, A. T., Couet, A., & Comstock, R. J. (2015). Corrosion of Zirconium Alloys Used for Nuclear Fuel Cladding. Annual Review of Materials Research, 45, 311-343.

[2] Duan, Z., Yang, H., Satoh, Y., & Murakami, K. (2017). Oxidation behavior of zirconium alloys in a simulated nuclear reactor primary coolant. Journal of Nuclear Materials, 485, 147-158.

[3] Terrani, K. A. (2018). Accident tolerant fuel cladding development: Promise, status, and challenges. Journal of Nuclear Materials, 501, 13-30.

[4] Gong, W., & Yun, D. (2022). A review on the corrosion behavior of zirconium alloys in supercritical water. Corrosion Science, 208, 110620.

[5] Yilmazbayhan, A., Motta, A. T., & Comstock, R. J. (2021). Hydride morphology and embrittlement in Zircaloy-4 cladding. Journal of Nuclear Materials, 545, 152646.

[6] Liu, J., & Li, Q. (2023). Fretting wear behavior of zirconium alloy cladding tubes. Wear, 522, 204689.

[7] Kim, H. G., & Kim, I. H. (2020). Oxidation behavior of zirconium alloy claddings in high temperature steam. Nuclear Engineering and Technology, 52(4), 808-815.

[8] Suresh, S., & Sharma, A. (2021). Surface modification of zirconium alloys for biomedical and nuclear applications: A review. Surface and Coatings Technology, 405, 126666.

[9] Verma, R., & Kumar, S. (2022). Electrochemical anodization of zirconium: Growth mechanism and properties. Electrochimica Acta, 412, 140135.

[10] Cheng, Y., & Matykina, E. (2021). Formation of nanotubular oxide layers on Zirconium alloys by anodization. Corrosion Science, 182, 109289.

[11] Ali, F., & Al-Hajri, M. (2023). Effect of voltage and electrolyte composition on the morphology of anodic zirconium oxide. Materials Chemistry and Physics, 295, 127087.

[12] Wang, L., Zhang, Y., & Wu, X. (2024). Time-dependent growth kinetics of anodic films on zirconium in phosphate electrolytes. Journal of Electrochemical Society, 171(2), 021504.

[13] Diamanti, M. V., & Pedeferri, M. P. (2020). Color production on zirconium by

anodizing: Interference and absorption effects. Color Research & Application, 45(3), 456-464.

[14] Thompson, G. E. (2019). Porous anodic oxide films: Formation, growth and applications. Thin Solid Films, 685, 34-45.

[15] Zhao, X., & Xu, H. (2022). Phase transformation in anodic zirconia films: From amorphous to crystalline. Scripta Materialia, 210, 114421.

[16] Obbard, E. G., & Burr, P. A. (2021). Mechanical properties of zirconium oxide scales: A review. Journal of Nuclear Materials, 557, 153255.

[17] McCafferty, E. (2020). Introduction to Corrosion Science (2nd ed.). Springer.

[18] Zhang, B., & Frankel, G. S. (2022). Corrosion mechanisms of zirconium alloys in chloride-containing environments. Corrosion, 78(5), 412-425.

[19] Li, T., & Wang, F. (2023). Improvement of pitting corrosion resistance of Zr alloys by anodic oxidation. Applied Surface Science, 610, 155567.

[20] Orazem, M. E., & Tribollet, B. (2017). Electrochemical Impedance Spectroscopy. Wiley.

DOI: https://doi.org/10.17146/urania.20xx.xx.x.xxxx

Urania
Jurnal Ilmiah Daur Bahan Bakar Nuklir

Beranda jurnal: http://jurnal.batan.go.id/index.php/urania/

THE EFFECT OF TIME IN THE ANODIZING PROCESS ON THE COATING CHARACTERISTICS AND CORROSION BEHAVIOR OF ZIRCONIUM METAL

ABSTRAK

Zirkonium dan paduannya merupakan material standar untuk kelongsong bahan bakar nuklir pada Pressurized Water Reactor (PWR) karena memiliki penampang lintang serapan neutron yang rendah, sifat mekanik yang unggul, serta ketahanan korosi yang baik dalam lingkungan air bersuhu tinggi. Namun, kondisi operasi PWR memberikan lingkungan yang sangat berat sehingga dapat menurunkan integritas kelongsong seiring waktu, termasuk melalui proses oksidasi, hidriding, serta kerusakan mekanik seperti goresan atau penyok yang dapat terjadi selama operasi pengisian ulang bahan bakar. Cacat permukaan tersebut dapat bertindak sebagai lokasi inisiasi korosi terlokalisasi yang berpotensi mengompromikan penghalang penahanan primer.Penelitian ini menyelidiki efektivitas anodisasi elektrokimia sebagai teknik modifikasi permukaan untuk meningkatkan kinerja zirkonium. Proses anodisasi dilakukan pada tegangan konstan sebesar 30 V dengan variasi waktu 10, 15, dan 20 menit. Karakteristik permukaan yang dihasilkan dievaluasi menggunakan Mikroskop Optik, Mikroskop Digital untuk analisis kekasaran permukaan, serta X-Ray Diffraction (XRD). Keandalan mekanik dinilai melalui pengujian kekerasan mikro Vickers, sedangkan perilaku korosi dipelajari dalam larutan NaCl 3,5% menggunakan metode Open Circuit Potential (OCP), Potentiodynamic Polarization (PDP), dan Electrochemical Impedance Spectroscopy (EIS). Hasil penelitian menunjukkan bahwa peningkatan waktu anodisasi secara signifikan memperbaiki kualitas permukaan, ditunjukkan dengan penurunan nilai kekasaran rata-rata Ra dari 0,53 µm (10 menit) menjadi 0,24 µm (20 menit). Analisis XRD mengonfirmasi terbentuknya lapisan oksida ZrO_2 yang bersifat kristalin. Pengujian elektrokimia memperlihatkan peningkatan ketahanan korosi yang signifikan, di mana rapat arus korosi i_{corr} menurun hingga dua orde magnitudo dari 12,93 x 10^{-9} A/cm^2 pada substrat menjadi 0,19 x 10^{-9} A/cm^2 pada spesimen yang dianodisasi selama 20 menit. Penelitian ini menyimpulkan bahwa perlakuan anodisasi selama 20 menit pada tegangan 30 V mampu menghasilkan lapisan oksida yang kuat, halus, dan sangat tahan terhadap korosi, sehingga berpotensi efektif dalam memitigasi degradasi pada aplikasi kelongsong bahan bakar nuklir.

Kata kunci: Zirkonium, Anodisasi, Ketahanan Korosi, Kelongsong Nuklir, PWR, Modifikasi Permukaan.

ABSTRACT

Zirconium and its alloys are the standard material for nuclear fuel cladding in Pressurized Water Reactors (PWR) due to their low neutron absorption cross-section, excellent mechanical properties, and good corrosion resistance in high-temperature water. However, the operational environment of a PWR imposes severe conditions that can degrade the cladding integrity over time, including oxidation, hydriding, and mechanical damage such as scratching or denting during fuel refueling operations. These surface defects can act as initiation sites for localized corrosion, potentially compromising the primary containment barrier. This study investigates the effectiveness of electrochemical anodizing as a surface modification technique to enhance the performance of Zirconium. The anodizing process was conducted at a constant voltage of 30 V with varying durations of 10, 15, and 20 minutes. The resulting surface characteristics were evaluated using Optical Microscopy, Digital Microscopy for roughness analysis, and X-Ray Diffraction (XRD). Mechanical reliability was assessed via Vickers Microhardness testing, while Corrosion behavior was studied in a 3.5% NaCl solution using Open Circuit Potential (OCP), Potentiodynamic Polarization (PDP), and Electrochemical Impedance Spectroscopy (EIS). The results demonstrated that increasing the anodizing time significantly improved the surface quality, reducing the arithmetic mean roughness Ra from 0.53 µm (10 min) to 0.24µm (20 min). XRD analysis confirmed the formation of a crystalline ZrO_2 oxide layer. Electrochemical tests revealed a substantial enhancement in corrosion resistance; the corrosion current density i_{corr} decreased by two orders of magnitude from 12.93 x 10^{-9} A/cm^2 for the substrate to 0.19 x 10^{-9} A/cm^2 for the 20-minute anodized yesspecimen. The study concludes that a 20-minute anodizing treatment at 30 V produces a robust, smooth, and highly corrosion-resistant oxide layer suitable for mitigating degradation in nuclear fuel cladding applications.

Keywords: Zirconium, Anodizing, Corrosion Resistance, Nuclear Cladding, PWR, Surface Modification.

INTRODUCTION

Zirconium (Zr) and its alloys, such as Zircaloy-4 and Zirlo, are the materials of choice for nuclear fuel cladding in light water reactors (LWR), particularly Pressurized Water Reactors (PWR). This selection is driven by Zirconium's unique combination of properties: an exceptionally low thermal neutron capture cross-section (0.18 barn), which ensures efficient neutron economy, good thermal conductivity, and adequate mechanical strength at elevated temperatures [1, 2]. As the first barrier in the defense-in-depth strategy, the cladding must hermetically seal radioactive fission products preventing their release into the primary coolant.

Despite these advantages, Zirconium cladding faces formidable challenges during its service life. The aggressive operating environment, characterized by high-pressure water (approx. 15.5 MPa) and high temperatures (approx. 300-350°C), promotes waterside corrosion and hydrogen pickup [3, 4]. The oxidation of zirconium ($Zr + 2H_2O \rightarrow ZrO_2 + 2H_2$) not only thins the structural wall but also generates hydrogen, a fraction of which diffuses into the metal matrix, leading to hydride precipitation and embrittlement [5]. Furthermore, beyond steady-state operation, the cladding is subjected to mechanical stress during fuel handling and refueling processes. Physical contact with grid spacers or other assemblies can cause surface scratches, fretting, or dents. These surface imperfections significantly increase local roughness and can serve as stress concentration points or preferential sites for pitting corrosion, accelerating material degradation [6, 7].

Extending the operational life of fuel assemblies and enhanced safety margins, particularly for high-burnup regimes, surface modification techniques have gained attention. The goal is to create a protective surface layer that is harder than the substrate to resist mechanical damage and to be more chemically stable to inhibit corrosion [8]. Among various techniques such as physical vapor deposition (PVD) or laser surface treatment, electrochemical anodizing stands out due to its simplicity, cost-effectiveness, and ability to form a uniform, adherent oxide film (ZrO_2) even on complex geometries [9]. Compared to PVD coatings that are only deposited on top, anodizing on Zr produces a ZrO_2 oxide layer that develops straight from the metal surface, providing significantly stronger adhesion, increased corrosion resistance, and improved thermal stability.

DOI: https://doi.org/10.17146/urania.20xx.xx.x.xxxx

Additionally, it creates a consistent, thick, and stable oxide layer that is appropriate for applications requiring long-lasting protection in biological, high-temperature, and harsh environments [1].

Anodizing promotes the growth of a thickened oxide layer that acts as a passivating barrier. While the natural oxide film on Zirconium is protective, it is thin and liable to breakdown. Anodic films, depending on process parameters like voltage, electrolyte, and time, can be engineered to be thicker and more compact [10, 11]. Recent studies have focused on the voltage effects, but the influence of anodizing duration—specifically in the transition from initial film formation to steady-state growth—on the micro-roughness and electrochemical impedance of the surface remains an area for optimization [12]. Limited studies systematically evaluate the effect of anodizing time at fixed voltage on compact oxide growth. Few works correlate roughness evolution, elemental composition, and electrochemical corrosion kinetics simultaneously. There remains a need to evaluate surface stabilization strategies under chloride-containing environments simulating aggressive localized attacks.

This study aims to systematically evaluate the effect of anodizing time (10, 15, and 20 minutes) at a fixed potential of 30 V on the surface characteristics and corrosion behavior of Zirconium. We hypothesize that extending the anodizing duration will not only increase the oxide thickness but also reduce surface roughness through a leveling effect, thereby providing superior corrosion resistance in aggressive chloride environments.

METHODOLOGY

The substrate material used was commercial purity Zirconium metal, cut into coupon specimens with dimensions of 10 mm x 10 mm. The samples were mounted in epoxy resin to expose a single working surface area of 0.5 cm^2. Prior to anodizing, the surfaces were mechanically polished using a sequence of Silicon Carbide (SiC) abrasive papers with grit sizes of 500, 800, 1200, and 2000. This step was crucial to remove the heterogeneous native oxide layer and standardize the initial surface roughness. After polishing, the samples were ultrasonically cleaned in acetone and rinsed with demineralized water to remove any particulate residues.

The anodizing process was carried out in a two-electrode electrochemical cell at room temperature. The Zirconium specimen served as the anode, while a high-purity platinum sheet was used as the cathode to ensure chemical inertness. The electrolyte was a specific aqueous solution tailored for compact film growth (typically phosphate/ammonium based). In the absence of fluoride ions, phosphoric acid electrolytes promote barrier-type compact oxide growth due to limited field-assisted dissolution, preventing nanotubular structure formation [2], [3]. Phosphoric acid (H_3PO_4) at a concentration of 30 g/L is used as the electrolyte for the anodization process. Measuring the phosphoric acid with an analytical balance and combining it with distilled water in a beaker is the first step in the electrolyte production process. When the solution is ready to be employed as an anodizing medium on zirconium metal substrates, it is mixed with a magnetic stirrer until it dissolves uniformly.

A DC power supply was used to apply a constant voltage of 30 V. The anodizing duration varied as the experimental parameter: 10 minutes (Zr-10), 15 minutes (Zr-15), and 20 minutes (Zr-20). Post-anodizing, samples were rinsed and dried in air. A digital multimeter (DMM) was used to monitor the voltage and current during the anodization process. The solution was kept at room temperature to prevent localized heating that would result in non-uniform oxidation. The voltage source was turned off, and the specimen was removed from the electrolyte solution after the anodization period was complete. A hair dryer was used to dry any leftover electrolyte after it had been cleansed with distilled water. All anodized specimens were kept in a closed container, and silica gel was added to regulate the humidity in the storage area prior to testing for corrosion resistance, hardness, and surface morphology examination.

Surface morphology and visual appearance were documented using an Optical Microscope and a high-resolution Digital Microscope. The surface roughness parameters, Arithmetic Mean Roughness (Ra) and Ten-Point Mean Roughness (Rz), were quantified to evaluate the smoothing effect of the treatment. The surface morphology study was supported by

Commented [MOU1]: please provide references for this statement

Commented [SR2R1]: Thank you for your suggestion. We have incorporated the reference into the revised version of the manuscript."

microstructural findings. The samples' surface and texture were examined using scanning electron microscopy (SEM) at an accelerating voltage of 15 kV, which provided precise topographical information on the zirconium dioxide (ZrO_2) layer. Porosity, fractures, oxide layer thickness, and surface features that matched each time variation were observed using SEM examination. Additionally, the elemental composition of the coating was determined using Energy Dispersive Spectroscopy (EDS), with a focus on the distribution of phosphorus and oxygen to validate the creation of the ZrO_2 layer and potential interactions with the H_3PO_4 electrolyte. For additional examination, elemental mapping and spectra were both obtained.

The following explanation and reactions have been incorporated:
Zirconium is oxidized under the applied electric field:

$$Zr \rightarrow Zr^{4+} + 4e-$$

Simultaneously, oxygen-containing species (O^{2-} or OH^- derived from water) migrate inward and react with zirconium ions:

$$Zr^{4+} + 2O^{2-} \rightarrow ZrO_2$$

Alternatively, expressed via water-assisted oxidation:

$$Zr + 2H_2O \rightarrow ZrO_2 + 4H^+ + 4e^-$$

In phosphoric acid electrolyte, the dominant species include:

$$H_3PO_4 \rightleftharpoons H_2PO_4^- \rightleftharpoons HPO_4^{2-} \rightleftharpoons PO_4^{3-}$$

Under the strong electric field across the growing oxide film. Negatively charged phosphate ions migrate toward the anode. A fraction of these anions becomes incorporated into the outer oxide region. The incorporation process can be represented schematically as:

$$ZrO_2 + xPO_4^{3-} \rightarrow ZrO_2(PO_4)x$$

The crystalline structure of the anodic oxide layers was analyzed using X-Ray Diffraction (XRD) with Cu-Kα radiation. To assess the resistance to mechanical damage, Vickers Microhardness testing was performed using a load of 300 gf with a dwell time of 15 seconds; five indentations were made per sample to obtain an average value.

Corrosion performance was evaluated in a 3.5% NaCl solution, chosen to simulate an aggressive corrosive environment that accelerates pitting attack. A standard three-electrode cell was employed, consisting of the Zr specimen (working electrode), an Ag/AgCl reference electrode, and a graphite counter electrode. The measurements were conducted using a Potentiostat/Galvanostat with the following sequence:

1. Open Circuit Potential (OCP): Monitored for 3600 seconds until a stable potential was reached.
2. Potentiodynamic Polarization (PDP): Scanned from -250 mV to +250 mV relative to OCP at a scan rate of 1 mV/s to determine Tafel parameters E_{corr} and i_{corr}.
3. Electrochemical Impedance Spectroscopy (EIS): Conducted at OCP with a sinusoidal perturbation of 10 mV amplitude over a frequency range of 100 kHz to 0.01 Hz.

RESULTS AND DISCUSSION

Surface Morphology and Roughness Analysis

Visual inspection of the samples immediately after anodizing revealed a distinct coloration of the surface. As shown in Figure 1, the surface color shifted from the metallic silver of the substrate to uniform hues of gold and blue. This phenomenon is attributed to the interference of light within the transparent anodic oxide film (ZrO_2), where the perceived color is directly related to the film thickness governed by the anodizing duration [13].

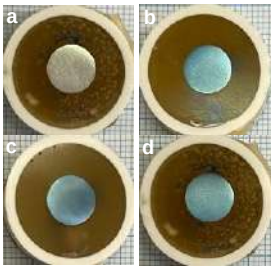

Figure 1. Color of zirconium oxide with various anodizing time of a) Zr, b) Zr-10, c) Zr-15, and d) Zr-20 minutes

Microstructural analysis via optical microscopy (Figure 2) and SEM (Figure 3) indicated a significant improvement in surface texture. The non-anodized substrate exhibited polishing lines and surface irregularities. However, post-anodizing, these features were progressively smoothed.

The anodization of Zr metal at 10 minutes produced a comparatively uneven surface

DOI: https://doi.org/10.17146/urania.20xx.xx.x.xxxx

morphology in Figure 2a. A coating of zirconium oxide had developed at that point, although it was not yet uniformly distributed. The 3D profile data (Figure 2b) revealed that the oxide layer was still in its early phases of formation, resulting in a very rough surface roughness. The duration of anodization was extended to 15 minutes (Figure 2c). Compared to Zr-10, the resulting zirconium oxide layer became more homogeneous, thick, and continuous. This result was also confirmed from the 3D profile of Figure 2d. Figure 2e shows the anodization of Zr metal with a process time of 20 minutes. Increasing the anodization time contributed to the growth and stability of the zirconium oxide layer formed on the metal surface. The layer was more uniform, dense, and surface defects were significantly reduced. The relevant results are confirmed by Figure 2f.

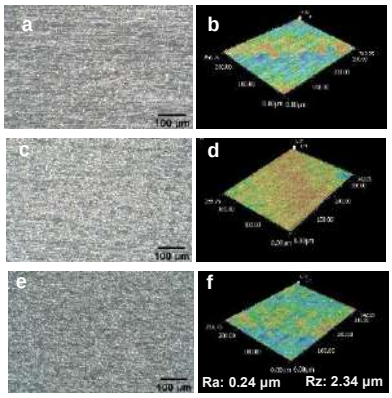

g

Specimen	Surface Roughness	
	Ra	Rz
Zr-10	0.53	4.35
Zr-15	0.34	4.98
Zr-20	0.24	2.34

Figure 2. Microstructural analysis via optical microscopy (a,c,e), 3D profile (b,d,f), and surface roughness value (g) of (a,b) Zr-anodized 10 minutes, (c,d) Zr-anodized 15 minutes, and (e,f) Zr-anodized 20 minutes.

Quantitative roughness data presented in Figure 2g and Figure 2 (b,d,f) confirm this observation. The average roughness (Ra) decreased from 0.53 µm for the Zr-10 specimen to 0.34 µm for Zr-15, and finally to 0.24 µm for Zr-20. This trend suggests a "leveling mechanism" where the oxide grows preferentially in the microscopic valleys of the metal surface, effectively reducing the peak-to-valley height [14]. A smoother surface is highly advantageous for nuclear cladding as it reduces the friction coefficient during fuel rod insertion and minimizes the surface area available for corrosive attack.

Figure 3. shows SEM images and the corresponding EDS area mapping of zirconium anodized under different duration processes. The surfaces of all the specimens were quite homogeneous and devoid of significant cracks. Increasing the anodization time prevented any significant morphological changes at the micrometer scale. For every modification in anodization time, the elemental mapping findings on the zirconium oxide layer's surface revealed an equitable distribution of elements. The anodized metal surface was dominated by Zr and O elements.

The zirconium substrate, whose composition decreased as the anodization duration increased, provided the Zr element. The O element showed that an oxide layer had formed during the anodization processes. The composition of the O element increased as the anodization duration increased, indicating the thickening and expansion of the zirconium oxide layer (ZrO_2). The increase in the O element was formed from 44.66 at% for the Zr-10 specimen, 53.12 at% for the Zr-15 specimen, and the highest for the Zr-20 specimen, namely 54.33 at%. The P element was also found throughout the layer's surface in addition to these primary components. The phosphate-based electrolyte used during the anodizing process is the source of the phosphorus, which is present in trace levels (around 1-2 at%) but is dispersed rather uniformly.

Phosphorus detected in the anodic film originates from field-assisted incorporation of phosphate species during anodization rather than residual electrolyte contamination. The concentration remains low and relatively independent of anodizing time, indicating incorporation primarily during early barrier layer formation. At the detected level (~1–2 at%), phosphorus is not expected to adversely affect zirconium cladding performance, although high-temperature reactor-condition validation remains necessary.

Crystalline Structure and Microhardness the XRD patterns shown in Figure 4 display sharp diffraction peaks corresponding to Zirconium Oxide (ZrO_2). The analysis suggests the presence of most tetragonal crystalline phase CDD / PDF card: 00-050-1089, which is notable as anodic films formed at lower voltages are often amorphous. The formation of this crystalline phase contributes to the chemical stability of the coating [15]. Diffraction peaks for the zirconium (Zr) and zirconium oxide (ZrO_2) phases were detected on all anodized specimens. The ZrO_2 peak's formation indicates that the anodization procedure was effective in generating an oxide layer on the zirconium substrate's surface.

The ZrO_2 diffraction peak's clarity tended to rise with increasing anodization time, especially in the Zr-20 specimen, which showed the maximum peak intensity. This suggests that extended anodization durations encourage the formation of an oxide layer that is thicker and/or more crystalline. In the meantime, peaks from the Zr phase were still identified, suggesting that the relatively tiny oxide layer thickness allowed X-rays to proceed toward the substrate. In general, the XRD data confirm that different anodization times affect the zirconium oxide layer's growth and crystal properties. At the anode, the reaction that occurs can be written as:

$$Zr \rightarrow Zr^{4+} + 4e^- \quad (1)$$

$$Zr^{4+} + 2\,O^{2-} \rightarrow ZrO_2 \quad (2)$$

Meanwhile, at the cathode a reduction reaction takes place, usually involving the evolution of hydrogen gas:

$$4\,H^+ + 4\,e^- \rightarrow 2\,H_2 \quad (3)$$

Mechanical integrity was evaluated via Vickers microhardness (HV). As detailed in Table 1, the hardness values were relatively stable across the anodized samples: 144.41±8.99 HV (10 min), 144.66±7.84 HV (15 min), and 142.88±6.96 HV (20 min). Although the macroscopic hardness did not show a drastic increase compared to the substrate (likely due to the indentation depth exceeding the thin oxide layer thickness), the presence of the hard ceramic ZrO_2 skin provides essential resistance against superficial scratching and fretting wear, which are critical precursors to cladding failure [16].

Table 1. Average and Standar Deviation (STDV) for Microhardness of Zr-Anodized under different duration process

Specimen	HV					Average	Standard Deviation
	1	2	3	4	5		
Zr-10	150.97	138.23	140.08	158.57	134.19	144.41	8.99
Zr-15	156.89	142.93	138.07	149.92	135.5	144.66	7.84
Zr-20	155.79	144.39	137.77	136.86	139.61	142.88	6.96

Commented [MOU3]: I suggest that this data should be excluded because the applied load was excessive. This resulted in the measurements reflecting the substrate hardness rather than providing an accurate representation of the coating's hardness.

Commented [FAA4R3]: We thank the reviewer for this important and insightful comment.
We agree that the applied load (300 gf) results in an indentation depth that exceeds the thickness of the anodic oxide layer. Consequently, the measured hardness values predominantly reflect the mechanical response of the zirconium substrate rather than the intrinsic hardness of the oxide coating.
However, we respectfully choose to **retain the microhardness data** in the manuscript for the following reasons:

1. **Relevance to Practical Behavior**
   The measurement reflects the effective surface response under macro-scale loading conditions, which is still relevant for engineering applications where the substrate–coating system behaves as a composite.
2. **Consistent Observation Across Samples**
   The results consistently show that the hardness values of anodized samples (≈143–145 HV) are comparable to the substrate, indicating that the anodization process does not significantly alter the bulk mechanical response of zirconium.
3. **Important Scientific Insight**
   The similarity in hardness values is itself an important finding, demonstrating that:
   - The anodic oxide layer is relatively thin,
   - Its contribution to bulk hardness is limited under the applied test conditions,
   - The mechanical properties remain dominated by the substrate.

We have revised the manuscript to explicitly clarify that:
- The measured hardness values are substrate-dominated,
- The anodized layer does not significantly increase the apparent hardness under the applied load,
- Therefore, the hardness of anodized zirconium can be considered **comparable to that of the untreated zirconium substrate** in this testing configuration.

Additionally, we now state that:
"Nanoindentation or lower-load testing would be required to isolate the intrinsic hardness of the anodic oxide layer."
We believe retaining this data, with proper clarification, provides a more complete and transparent interpretation of the mechanical behavior of the anodized system.

DOI: https://doi.org/10.17146/urania.20xx.xx.x.xxxx

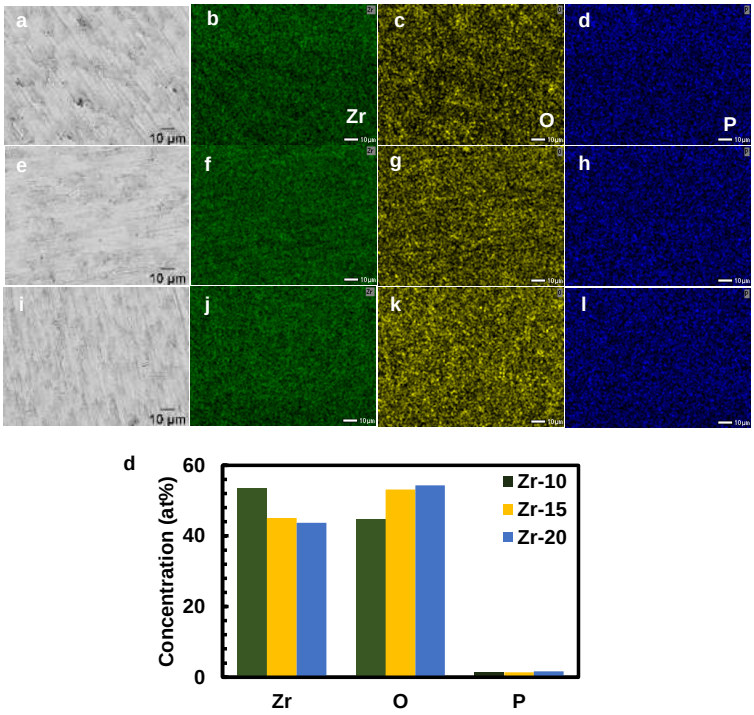

Figure 3. Surface view SEM images and the corresponding EDS area mapping of zirconium anodized of (a-d) Zr-10, (e-h) Zr-15, and (i-l) Zr-20 minutes

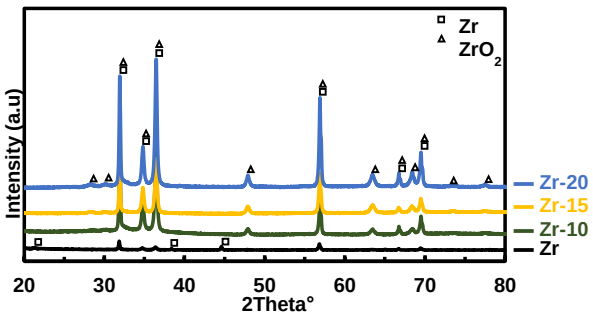

Figure 4. XRD pattern of zirconium oxide (ZrO_2)

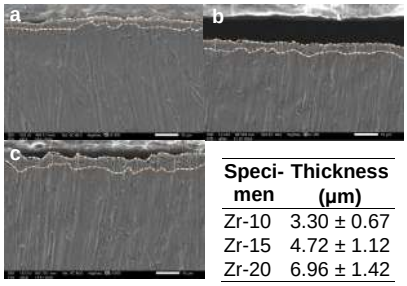

Specimen	Thickness (μm)
Zr-10	3.30 ± 0.67
Zr-15	4.72 ± 1.12
Zr-20	6.96 ± 1.42

Figure 5. Cross-sectional view SEM images for zirconium anodized of (a) Zr-10, (b) Zr-15, (c) Zr-20 minutes, and (d) thickness of all specimens

An oxide layer thickness quantitative summary and cross-sectional SEM images of anodized zirconium specimens treated for 10, 15, and 20 minutes are shown in Figure 5. This figure aims to assess how anodization time affects the shape and growth behavior of the anodic oxide layer that forms on zirconium. From Zr-10 (3.30 ± 0.67 μm) to Zr-15 (4.72 ± 1.12 μm) and Zr-20 (6.96 ± 1.42 μm), the SEM micrographs show clearly a compact and rather homogeneous oxide layer adhering to the substrate. The oxide–metal contact is displayed by the dotted line, which highlights the continuous layer growth without significant delamination. A time-dependent oxide the growth process controlled by field-assisted ionic transport, where Zr^{+} cations migrate outward and O^{2-} anions migrate inside under a strong electric field to create ZrO_2 at the interface, is suggested by the increasing thickness with anodization time. High-field oxide growth theory states that unless transport limitations or dissolving effects become visible, oxide thickness is proportional to the applied potential and processing time.

Electrochemical Corrosion Behavior

The corrosion resistance was comprehensively analyzed using OCP, PDP, and EIS techniques. Open Circuit Potential (OCP): Figure 5 illustrates the OCP evolution. All anodized specimens exhibited more positive (noble) potentials compared to the bare substrate. The Zr-20 sample showed the most noble potential, stabilizing at a higher value, which indicates a thermodynamic tendency to resist spontaneous corrosion reactions in the electrolyte [17]. During the test, pure zirconium (Zr) specimens had the most negative and comparatively steady potential values, suggesting more potential for corrosion. All the specimens indicated a potential change in a more positive direction immediately after the anodization process, which suggests that the formation of a zirconium oxide layer had increased electrochemical stability. Zr-20, Zr-15, and Zr-10 were the anodized specimens with the most positive and consistent OCP values while the test. This suggests that extending the anodization duration increases the material's resistance to corrosion and creates a more protective oxide layer. The formation of a rather stable passive layer on the zirconium surface is also shown by the stability of the OCP curves over an extended test time.

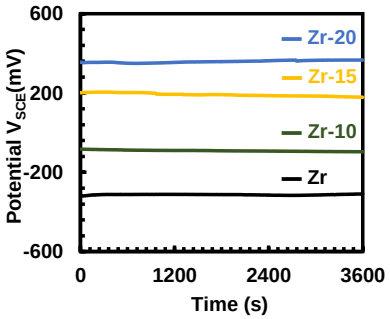

Figure 6. Average of OCP curves for zirconium substrate and zirconium-anodized at 30 V

Potentiodynamic Polarization (PDP): The Tafel polarization curves in Figure 6 demonstrate a clear shift in corrosion kinetics. The electrochemical parameters summarized in Table 2 show a dramatic reduction in corrosion current density (i_{corr}). The substrate exhibited an i_{corr} of 12.93 × 10^{-9}A/cm^2. In contrast, the Zr-20 specimen exhibited an i_{corr} of 0.19 × 10^{-9}A/cm^2. This reduction by nearly two orders of magnitude confirms that the thicker oxide layer formed at 20 minutes acts as an effective barrier, blocking the diffusion of chloride ions (Cl^{-}) and oxygen to the metal interface [18, 19].

Commented [MOU5]: Is it accurate for the oxide layer to be this thick? If so, the thin-film interference phenomenon regarding the transparent anodic oxide film (ZrO2) (that you mentioned in first paragraph of "Result and Discussion" section) would not occur. Moreover, I do not see any visible difference between the marked area and the rest of the sample.

If the coating thickness is on the nanometer scale (as evidenced by the light interference), SEM magnification of 1,500x is clearly insufficient for accurate characterization. Consequently, these results should be excluded from the analysis to maintain data integrity.

Commented [FAA6R5]: We thank the reviewer for this thoughtful and critical comment.
We would like to clarify that the oxide thickness measured in this study (approximately 3–7 μm) is physically consistent with anodization conditions at 30 V in phosphate-based electrolytes, where compact barrier-type oxide films can grow into the micrometer range under prolonged anodizing durations.
To further support this, we analyzed the **oxide growth rate** based on the measured thickness:
- Zr-10: ~3.30 μm → ~0.33 μm/min
- Zr-15: ~4.72 μm → ~0.31 μm/min
- Zr-20: ~6.96 μm → ~0.35 μm/min

These values indicate a relatively consistent growth rate in the range of **~0.3–0.35 μm/min**, which is in good agreement with high-field oxide growth kinetics for valve metals under moderate voltage conditions. The near-linear relationship between anodizing time and oxide thickness further supports that the oxide growth mechanism is controlled by field-assisted ionic migration rather than anomalous deposition.
Regarding the concern about thin-film interference:
- The observed coloration does not strictly imply nanometer-scale thickness, as interference effects can still occur in sub-micron to micron-scale oxide layers depending on refractive index, partial transparency, and thickness gradients.
- Therefore, the presence of interference color does not contradict the measured micrometer-scale thickness.

Concerning SEM characterization:
- The cross-sectional SEM images clearly show a continuous oxide layer, and the thickness was measured directly from the interface between oxide and substrate.
- The magnification used is sufficient for micrometer-scale thickness measurement, and multiple measurements were averaged to ensure accuracy.

Finally, we respectfully maintain that the reported thickness values are valid and consistent with anodization kinetics. The addition of growth rate analysis further confirms that the oxide thickness evolution is physically reasonable and follows expected anodic film growth behavior.
We have incorporated this growth rate discussion into the revised manuscript to strengthen the interpretation.

DOI: https://doi.org/10.17146/urania.20xx.xx.x.xxxx

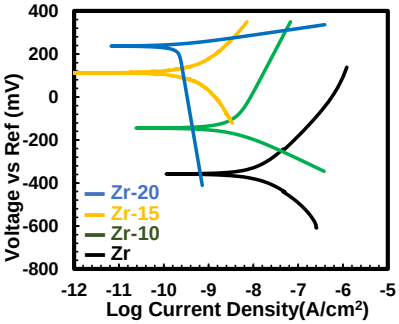

Figure 7. Average of PDP curves for zirconium substrate and zirconium-anodised at 30 V

Figure 6 presents the potentiodynamic polarization (PDP) curves of anodized and pure zirconium. These curves illustrate the relationship between the voltage across a reference electrode and the log current density, which is used to assess corrosion behavior and electrochemical reaction kinetics. Pure zirconium exhibits poor corrosion resistance, indicated by its limited passivation range and relatively high corrosion current density. In contrast, anodized specimens show a shift in corrosion potential to more positive values and a decrease in corrosion current density. Compared to Zr-15 and Zr-10, the Zr-20 specimen shows the biggest passivation area and the lowest current density. The Zr-20 specimen exhibits the lowest current density and the largest passivation region compared to Zr-15 and Zr-10. This suggests that the zirconium oxide layer that develops over extended anodization durations successfully prevents charge transfer and reduces the rate of corrosion. We thank the reviewer for this careful observation.

The blue curve corresponds to the Zr-20 specimen, which exhibits the longest anodizing duration (20 minutes). The distinct shape of this curve compared to the other samples is primarily attributed to differences in the oxide layer thickness, compactness, and electrochemical stability resulting from prolonged anodization. Several factors explain this behaviour, due to more Compact and Thicker Oxide Film. The Zr-20 sample forms a thicker and denser ZrO_2 layer, as supported by higher oxygen atomic percentage (EDS), lowest surface roughness (Ra = 0.24 µm), lowest corrosion current density (0.19×10^{-9} A/cm²). This compact oxide layer significantly suppresses charge transfer at the metal/electrolyte interface, resulting in:

A pronounced shift of Ecorr toward more positive values, a wider passive region, lower anodic current density. The shape difference reflects a more stable passive regime in Zr-20. The reduced slope in the anodic branch indicates lower metal dissolution kinetics due to improved barrier characteristics of the oxide.

Shorter anodizing times (10 and 15 minutes) likely produce thinner films with higher defect density or localized porosity. These structural differences lead to earlier activation behavior and less stable passivation, resulting in PDP curves that differ in shape.

For Zr-20, corrosion behavior transitions from activation-controlled to diffusion-limited/passivation-controlled kinetics over a wider potential range, which explains the distinct curvature compared to the other samples.

Commented [MOU7]: where is the passive region in Fig. 7?

Commented [SR8R7]: Thank you for your comment.

The passive region in Figure 7 can be observed in the anodic part of the PDP curves, where the potential increases while the current density remains relatively stable, forming a plateau-like region. Based on the figure, this region occurs approximately at log current density between −10 and −9 A/cm² and at potentials around 0 to +250 mV vs Ref.

In this range, the relatively constant current density indicates the formation of a protective oxide layer on the zirconium surface, which reduces the rate of electrochemical dissolution. The anodized samples exhibit a more pronounced passive region compared with the untreated Zr, suggesting that the anodizing process enhances the passivation behavior by forming a more stable oxide layer on the surface.

Table 2. PDP Parameter of Zr-Anodized under different duration process

Specimen	E_{corr} (mV)	i_{corr} (10^{-9}A/cm²)	β_{Anodic} (mV/Decade)	$\beta_{Catodic}$ (mV/Decade)
Zr	-346 ± 88	12.93 ± 2.89	399 ± 350	275 ± 152
Zr-10	-114 ± 94	2.57 ± 1.12	599± 461	198 ± 122
Zr-15	92 ± 98	1.10 ± 0.82	275 ± 201	363 ± 262
Zr-20	233 ± 74	0.19 ± 0.04	152 ± 151	1518 ± 1067

a)

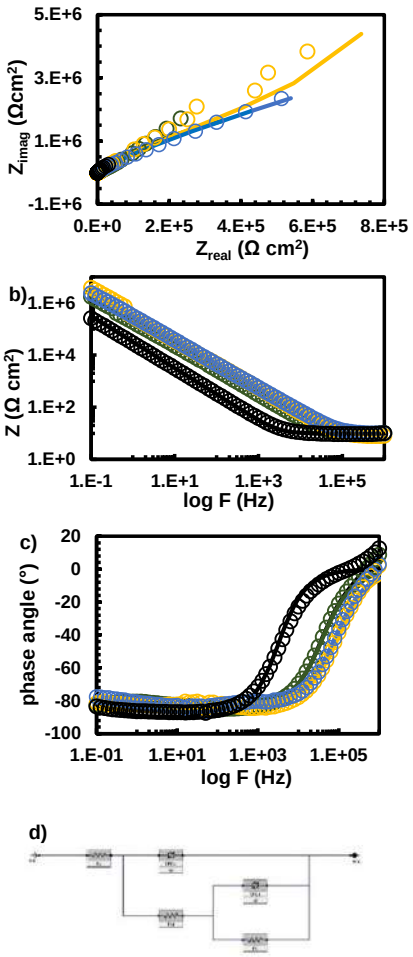

Figure 8. Average of EIS results of a) Nyquist spectra, b) bode impedance, c) bode phase, d) Equivalent electrical circuit (EEC) fitting for zirconium substrate and zirconium-anodised at 30 V

Table 3. Fit parameters of EIS data

Parameter	Substrate	Zr-10	Zr-15	Zr-20
R_s ($\Omega.cm^2$)	10	11	159	10
C_{dl} ($S^*s^a.cm^{-2}$)	$5x10^{-6}$	-	-	-
R_{ct} ($\Omega.cm^2$)	$2x0^6$	-	-	-
CPE_{ol} ($S^*s^a.cm^{-2}$)	-	$1x10^{-8}$	$8x10^{-8}$	$6.1x10^{-8}$
a_{ol}	-	0.6	0.7	0.7
R_{ol} ($\Omega.cm^2$)	-	137	150	140
CPE_{il} ($S^*s^a.cm^{-2}$)	-	$9.3x10^{-9}$ 10^{-9}	$5.6x10^{-9}$ 10^{-9}	$5.3x10^{-9}$ 10^{-9}
a_{il}	-	0.9 10^{-3}	0.9 10^{-3}	0.9 10^{-3}
R_{il} ($\Omega.cm^2$)	-	15.00 106	15.82 106	16.40 103
Goodness of fit (χ^2)	$1.1x10^{-2}$	$3.4x10^{-2}$	$2.3x10^{-2}$	$1.4x10^{-2}$

Figure 8, the EIS results show that anodized samples exhibit significantly larger semicircle diameters in the Nyquist plots compared to the bare zirconium substrate, indicating improved corrosion resistance after anodization. The fitted parameters reveal that the charge transfer resistance (Rct) increases with anodizing time, with Zr-20 showing the highest resistance value, confirming enhanced barrier properties of the oxide layer. The solution resistance (Rs) remains relatively constant, suggesting consistent electrolyte conditions during testing. Additionally, the decrease in CPE values and the broader capacitive region in the phase angle plots indicate improved film compactness and reduced surface heterogeneity. Overall, the EIS analysis supports the PDP and OCP results, confirming that longer anodizing duration produces a thicker and more protective ZrO_2 layer that effectively suppresses corrosion reactions.

Based on Table 3, the solution resistance (Rs) remains nearly constant at approximately 10–11 Ω·cm² for all samples, confirming stable electrolyte conditions. The oxide-related resistance and charge transfer resistance increase significantly after anodization, with Rct rising from 137 Ω·cm² for Zr-10 to 150 Ω·cm² for Zr-15 and reaching 140 Ω·cm² for Zr-20, indicating improved interfacial stability. The CPE values decrease

DOI: https://doi.org/10.17146/urania.20xx.xx.x.xxxx

slightly from 1×10^{-8} to 6.1×10^{-8} $S\cdot s^{n}\cdot cm^{-2}$ as anodizing time increases, suggesting a more compact and less defective oxide layer. The goodness-of-fit values (χ^2 in the order of 10^{-2}) indicate that the equivalent circuit model adequately represents the experimental data. These quantitative results confirm that increasing anodizing time increases the electrochemical resistance of the zirconium surface.

CONCLUSIONS

The effect of anodizing duration on the surface characteristics and corrosion behavior of Zirconium was successfully investigated. The following conclusions are drawn:

1. Surface Improvement: Increasing the anodizing time from 10 to 20 minutes at 30 V results in a progressively smoother surface. The Zr-20 specimen achieved the lowest roughness (Ra= 0.24 µm), reducing friction and potential pit initiation sites.
2. Oxide Formation: The process forms a stable, crystalline ZrO_2 layer, as confirmed by XRD and the observation of interference colors.
3. Corrosion Resistance: The 20-minute anodized coating offers superior corrosion protection in chloride environments. It reduced the corrosion rate i_{corr} by approximately 98% compared to the bare substrate and significantly increased the polarization resistance.
4. Application Viability: The study confirms that a 20-minute anodizing treatment is an effective, low-cost method to enhance the durability of Zirconium nuclear fuel cladding, potentially extending the safety margins against corrosion and mechanical degradation in PWR environments.

REFERENCES

[1] Motta, A. T., Couet, A., & Comstock, R. J. (2015). Corrosion of Zirconium Alloys Used for Nuclear Fuel Cladding. Annual Review of Materials Research, 45, 311-343.

[2] Duan, Z., Yang, H., Satoh, Y., & Murakami, K. (2017). Oxidation behavior of zirconium alloys in a simulated nuclear reactor primary coolant. Journal of Nuclear Materials, 485, 147-158.

[3] Terrani, K. A. (2018). Accident tolerant fuel cladding development: Promise, status, and challenges. Journal of Nuclear Materials, 501, 13-30.

[4] Gong, W., & Yun, D. (2022). A review on the corrosion behavior of zirconium alloys in supercritical water. Corrosion Science, 208, 110620.

[5] Yilmazbayhan, A., Motta, A. T., & Comstock, R. J. (2021). Hydride morphology and embrittlement in Zircaloy-4 cladding. Journal of Nuclear Materials, 545, 152646.

[6] Liu, J., & Li, Q. (2023). Fretting wear behavior of zirconium alloy cladding tubes. Wear, 522, 204689.

[7] Kim, H. G., & Kim, I. H. (2020). Oxidation behavior of zirconium alloy claddings in high temperature steam. Nuclear Engineering and Technology, 52(4), 808-815.

[8] Suresh, S., & Sharma, A. (2021). Surface modification of zirconium alloys for biomedical and nuclear applications: A review. Surface and Coatings Technology, 405, 126666.

[9] Verma, R., & Kumar, S. (2022). Electrochemical anodization of zirconium: Growth mechanism and properties. Electrochimica Acta, 412, 140135.

[10] Cheng, Y., & Matykina, E. (2021). Formation of nanotubular oxide layers on Zirconium alloys by anodization. Corrosion Science, 182, 109289.

[11] Ali, F., & Al-Hajri, M. (2023). Effect of voltage and electrolyte composition on the morphology of anodic zirconium oxide. Materials Chemistry and Physics, 295, 127087.

[12] Wang, L., Zhang, Y., & Wu, X. (2024). Time-dependent growth kinetics of anodic films on zirconium in phosphate electrolytes. Journal of Electrochemical Society, 171(2), 021504.

[13] Diamanti, M. V., & Pedeferri, M. P. (2020). Color production on zirconium by

anodizing: Interference and absorption effects. Color Research & Application, 45(3), 456-464.

[14] Thompson, G. E. (2019). Porous anodic oxide films: Formation, growth and applications. Thin Solid Films, 685, 34-45.

[15] Zhao, X., & Xu, H. (2022). Phase transformation in anodic zirconia films: From amorphous to crystalline. Scripta Materialia, 210, 114421.

[16] Obbard, E. G., & Burr, P. A. (2021). Mechanical properties of zirconium oxide scales: A review. Journal of Nuclear Materials, 557, 153255.

[17] McCafferty, E. (2020). Introduction to Corrosion Science (2nd ed.). Springer.

[18] Zhang, B., & Frankel, G. S. (2022). Corrosion mechanisms of zirconium alloys in chloride-containing environments. Corrosion, 78(5), 412-425.

[19] Li, T., & Wang, F. (2023). Improvement of pitting corrosion resistance of Zr alloys by anodic oxidation. Applied Surface Science, 610, 155567.

[20] Orazem, M. E., & Tribollet, B. (2017). Electrochemical Impedance Spectroscopy. Wiley.

DOI: https://doi.org/10.17146/urania.20xx.xx.x.xxxx

Urania
Jurnal Ilmiah Daur Bahan Bakar Nuklir

Beranda jurnal: http://jurnal.batan.go.id/index.php/urania/

THE EFFECT OF TIME IN THE ANODIZING PROCESS ON THE COATING CHARACTERISTICS AND CORROSION BEHAVIOR OF ZIRCONIUM METAL

ABSTRAK

Zirkonium dan paduannya merupakan material standar untuk kelongsong bahan bakar nuklir pada Pressurized Water Reactor (PWR) karena memiliki penampang lintang serapan neutron yang rendah, sifat mekanik yang unggul, serta ketahanan korosi yang baik dalam lingkungan air bersuhu tinggi. Namun, kondisi operasi PWR memberikan lingkungan yang sangat berat sehingga dapat menurunkan integritas kelongsong seiring waktu, termasuk melalui proses oksidasi, hidriding, serta kerusakan mekanik seperti goresan atau penyok yang dapat terjadi selama operasi pengisian ulang bahan bakar. Cacat permukaan tersebut dapat bertindak sebagai lokasi inisiasi korosi terlokalisasi yang berpotensi mengompromikan penghalang penahanan primer.Penelitian ini menyelidiki efektivitas anodisasi elektrokimia sebagai teknik modifikasi permukaan untuk meningkatkan kinerja zirkonium. Proses anodisasi dilakukan pada tegangan konstan sebesar 30 V dengan variasi waktu 10, 15, dan 20 menit. Karakteristik permukaan yang dihasilkan dievaluasi menggunakan Mikroskop Optik, Mikroskop Digital untuk analisis kekasaran permukaan, serta X-Ray Diffraction (XRD). Keandalan mekanik dinilai melalui pengujian kekerasan mikro Vickers, sedangkan perilaku korosi dipelajari dalam larutan NaCl 3,5% menggunakan metode Open Circuit Potential (OCP), Potentiodynamic Polarization (PDP), dan Electrochemical Impedance Spectroscopy (EIS). Hasil penelitian menunjukkan bahwa peningkatan waktu anodisasi secara signifikan memperbaiki kualitas permukaan, ditunjukkan dengan penurunan nilai kekasaran rata-rata Ra dari 0,53 µm (10 menit) menjadi 0,24 µm (20 menit). Analisis XRD mengonfirmasi terbentuknya lapisan oksida ZrO_2 yang bersifat kristalin. Pengujian elektrokimia memperlihatkan peningkatan ketahanan korosi yang signifikan, di mana rapat arus korosi i_{corr} menurun hingga dua orde magnitudo dari 12,93 x 10^{-9} A/cm^2 pada substrat menjadi 0,19 x 10^{-9} A/cm^2 pada spesimen yang dianodisasi selama 20 menit. Penelitian ini menyimpulkan bahwa perlakuan anodisasi selama 20 menit pada tegangan 30 V mampu menghasilkan lapisan oksida yang kuat, halus, dan sangat tahan terhadap korosi, sehingga berpotensi efektif dalam memitigasi degradasi pada aplikasi kelongsong bahan bakar nuklir.

Kata kunci: Zirkonium, Anodisasi, Ketahanan Korosi, Kelongsong Nuklir, PWR, Modifikasi Permukaan.

ABSTRACT

Zirconium and its alloys are the standard material for nuclear fuel cladding in Pressurized Water Reactors (PWR) due to their low neutron absorption cross-section, excellent mechanical properties, and good corrosion resistance in high-temperature water. However, the operational environment of a PWR imposes severe conditions that can degrade the cladding integrity over time, including oxidation, hydriding, and mechanical damage such as scratching or denting during fuel refueling operations. These surface defects can act as initiation sites for localized corrosion, potentially compromising the primary containment barrier. This study investigates the effectiveness of electrochemical anodizing as a surface modification technique to enhance the performance of Zirconium. The anodizing process was conducted at a constant voltage of 30 V with varying durations of 10, 15, and 20 minutes. The resulting surface characteristics were evaluated using Optical Microscopy, Digital Microscopy for roughness analysis, and X-Ray Diffraction (XRD). Mechanical reliability was assessed via Vickers Microhardness testing, while Corrosion behavior was studied in a 3.5% NaCl solution using Open Circuit Potential (OCP), Potentiodynamic Polarization (PDP), and Electrochemical Impedance Spectroscopy (EIS). The results demonstrated that increasing the anodizing time significantly improved the surface quality, reducing the arithmetic mean roughness Ra from 0.53 µm (10 min) to 0.24µm (20 min). XRD analysis confirmed the formation of a crystalline ZrO_2 oxide layer. Electrochemical tests revealed a substantial enhancement in corrosion resistance; the corrosion current density i_{corr} decreased by two orders of magnitude from 12.93 x 10^{-9} A/cm^2 for the substrate to 0.19 x 10^{-9} A/cm^2 for the 20-minute anodized yesspecimen. The study concludes that a 20-minute anodizing treatment at 30 V produces a robust, smooth, and highly corrosion-resistant oxide layer suitable for mitigating degradation in nuclear fuel cladding applications.

Keywords: Zirconium, Anodizing, Corrosion Resistance, Nuclear Cladding, PWR, Surface Modification.

INTRODUCTION

Zirconium (Zr) and its alloys, such as Zircaloy-4 and Zirlo, are the materials of choice for nuclear fuel cladding in light water reactors (LWR), particularly Pressurized Water Reactors (PWR). This selection is driven by Zirconium's unique combination of properties: an exceptionally low thermal neutron capture cross-section (0.18 barn), which ensures efficient neutron economy, good thermal conductivity, and adequate mechanical strength at elevated temperatures [1, 2]. As the first barrier in the defense-in-depth strategy, the cladding must hermetically seal radioactive fission products preventing their release into the primary coolant.

Despite these advantages, Zirconium cladding faces formidable challenges during its service life. The aggressive operating environment, characterized by high-pressure water (approx. 15.5 MPa) and high temperatures (approx. 300-350°C), promotes waterside corrosion and hydrogen pickup [3, 4]. The oxidation of zirconium ($Zr + 2H_2O \rightarrow ZrO_2 + 2H_2$) not only thins the structural wall but also generates hydrogen, a fraction of which diffuses into the metal matrix, leading to hydride precipitation and embrittlement [5]. Furthermore, beyond steady-state operation, the cladding is subjected to mechanical stress during fuel handling and refueling processes. Physical contact with grid spacers or other assemblies can cause surface scratches, fretting, or dents. These surface imperfections significantly increase local roughness and can serve as stress concentration points or preferential sites for pitting corrosion, accelerating material degradation [6, 7].

Extending the operational life of fuel assemblies and enhanced safety margins, particularly for high-burnup regimes, surface modification techniques have gained attention. The goal is to create a protective surface layer that is harder than the substrate to resist mechanical damage and to be more chemically stable to inhibit corrosion [8]. Among various techniques such as physical vapor deposition (PVD) or laser surface treatment, electrochemical anodizing stands out due to its simplicity, cost-effectiveness, and ability to form a uniform, adherent oxide film (ZrO_2) even on complex geometries [9]. Compared to PVD coatings that are only deposited on top, anodizing on Zr produces a ZrO_2 oxide layer that develops straight from the metal surface, providing significantly stronger adhesion, increased corrosion resistance, and improved thermal stability.

DOI: https://doi.org/10.17146/urania.20xx.xx.x.xxxx

Additionally, it creates a consistent, thick, and stable oxide layer that is appropriate for applications requiring long-lasting protection in biological, high-temperature, and harsh environments [1].

Anodizing promotes the growth of a thickened oxide layer that acts as a passivating barrier. While the natural oxide film on Zirconium is protective, it is thin and liable to breakdown. Anodic films, depending on process parameters like voltage, electrolyte, and time, can be engineered to be thicker and more compact [10, 11]. Recent studies have focused on the voltage effects, but the influence of anodizing duration—specifically in the transition from initial film formation to steady-state growth—on the micro-roughness and electrochemical impedance of the surface remains an area for optimization [12]. Limited studies systematically evaluate the effect of anodizing time at fixed voltage on compact oxide growth. Few works correlate roughness evolution, elemental composition, and electrochemical corrosion kinetics simultaneously. There remains a need to evaluate surface stabilization strategies under chloride-containing environments simulating aggressive localized attacks.

This study aims to systematically evaluate the effect of anodizing time (10, 15, and 20 minutes) at a fixed potential of 30 V on the surface characteristics and corrosion behavior of Zirconium. We hypothesize that extending the anodizing duration will not only increase the oxide thickness but also reduce surface roughness through a leveling effect, thereby providing superior corrosion resistance in aggressive chloride environments.

METHODOLOGY

The substrate material used was commercial purity Zirconium metal, cut into coupon specimens with dimensions of 10 mm x 10 mm. The samples were mounted in epoxy resin to expose a single working surface area of 0.5 cm^2. Prior to anodizing, the surfaces were mechanically polished using a sequence of Silicon Carbide (SiC) abrasive papers with grit sizes of 500, 800, 1200, and 2000. This step was crucial to remove the heterogeneous native oxide layer and standardize the initial surface roughness. After polishing, the samples were ultrasonically cleaned in acetone and rinsed with demineralized water to remove any particulate residues.

The anodizing process was carried out in a two-electrode electrochemical cell at room temperature. The Zirconium specimen served as the anode, while a high-purity platinum sheet was used as the cathode to ensure chemical inertness. The electrolyte was a specific aqueous solution tailored for compact film growth (typically phosphate/ammonium based). In the absence of fluoride ions, phosphoric acid electrolytes promote barrier-type compact oxide growth due to limited field-assisted dissolution, preventing nanotubular structure formation [2], [3]. Phosphoric acid (H_3PO_4) at a concentration of 30 g/L is used as the electrolyte for the anodization process. Measuring the phosphoric acid with an analytical balance and combining it with distilled water in a beaker is the first step in the electrolyte production process. When the solution is ready to be employed as an anodizing medium on zirconium metal substrates, it is mixed with a magnetic stirrer until it dissolves uniformly.

A DC power supply was used to apply a constant voltage of 30 V. The anodizing duration varied as the experimental parameter: 10 minutes (Zr-10), 15 minutes (Zr-15), and 20 minutes (Zr-20). Post-anodizing, samples were rinsed and dried in air. A digital multimeter (DMM) was used to monitor the voltage and current during the anodization process. The solution was kept at room temperature to prevent localized heating that would result in non-uniform oxidation. The voltage source was turned off, and the specimen was removed from the electrolyte solution after the anodization period was complete. A hair dryer was used to dry any leftover electrolyte after it had been cleansed with distilled water. All anodized specimens were kept in a closed container, and silica gel was added to regulate the humidity in the storage area prior to testing for corrosion resistance, hardness, and surface morphology examination.

Surface morphology and visual appearance were documented using an Optical Microscope and a high-resolution Digital Microscope. The surface roughness parameters, Arithmetic Mean Roughness (Ra) and Ten-Point Mean Roughness (Rz), were quantified to evaluate the smoothing effect of the treatment. The surface morphology study was supported by

Commented [A1]: please provide references for this statement

Commented [A2R1]: Thank you for your suggestion. We have incorporated the reference into the revised version of the manuscript."

microstructural findings. The samples' surface and texture were examined using scanning electron microscopy (SEM) at an accelerating voltage of 15 kV, which provided precise topographical information on the zirconium dioxide (ZrO_2) layer. Porosity, fractures, oxide layer thickness, and surface features that matched each time variation were observed using SEM examination. Additionally, the elemental composition of the coating was determined using Energy Dispersive Spectroscopy (EDS), with a focus on the distribution of phosphorus and oxygen to validate the creation of the ZrO_2 layer and potential interactions with the H_3PO_4 electrolyte. For additional examination, elemental mapping and spectra were both obtained.

The following explanation and reactions have been incorporated:
Zirconium is oxidized under the applied electric field:

$$Zr \rightarrow Zr^{4+} + 4e-$$

Simultaneously, oxygen-containing species (O^{2-} or OH^- derived from water) migrate inward and react with zirconium ions:

$$Zr^{4+} + 2O^{2-} \rightarrow ZrO_2$$

Alternatively, expressed via water-assisted oxidation:

$$Zr + 2H_2O \rightarrow ZrO_2 + 4H^+ + 4e^-$$

In phosphoric acid electrolyte, the dominant species include:

$$H_3PO_4 \rightleftharpoons H_2PO_4^- \rightleftharpoons HPO_4^{2-} \rightleftharpoons PO_4^{3-}$$

Under the strong electric field across the growing oxide film. Negatively charged phosphate ions migrate toward the anode. A fraction of these anions becomes incorporated into the outer oxide region. The incorporation process can be represented schematically as:

$$ZrO_2 + xPO_4^{3-} \rightarrow ZrO_2(PO_4)x$$

The crystalline structure of the anodic oxide layers was analyzed using X-Ray Diffraction (XRD) with Cu-Kα radiation. To assess the resistance to mechanical damage, Vickers Microhardness testing was performed using a load of 300 gf with a dwell time of 15 seconds; five indentations were made per sample to obtain an average value.

Corrosion performance was evaluated in a 3.5% NaCl solution, chosen to simulate an aggressive corrosive environment that accelerates pitting attack. A standard three-electrode cell was employed, consisting of the Zr specimen (working electrode), an Ag/AgCl reference electrode, and a graphite counter electrode. The measurements were conducted using a Potentiostat/Galvanostat with the following sequence:

1. Open Circuit Potential (OCP): Monitored for 3600 seconds until a stable potential was reached.
2. Potentiodynamic Polarization (PDP): Scanned from -250 mV to +250 mV relative to OCP at a scan rate of 1 mV/s to determine Tafel parameters E_{corr} and i_{corr}.
3. Electrochemical Impedance Spectroscopy (EIS): Conducted at OCP with a sinusoidal perturbation of 10 mV amplitude over a frequency range of 100 kHz to 0.01 Hz.

RESULTS AND DISCUSSION

Surface Morphology and Roughness Analysis

Visual inspection of the samples immediately after anodizing revealed a distinct coloration of the surface. As shown in Figure 1, the surface color shifted from the metallic silver of the substrate to uniform hues of gold and blue. This phenomenon is attributed to the interference of light within the transparent anodic oxide film (ZrO_2), where the perceived color is directly related to the film thickness governed by the anodizing duration [13].

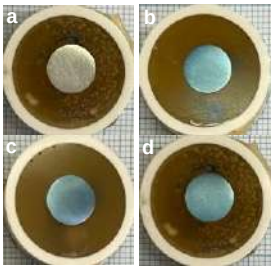

Figure 1. Color of zirconium oxide with various anodizing time of a) Zr, b) Zr-10, c) Zr-15, and d) Zr-20 minutes

Microstructural analysis via optical microscopy (Figure 2) and SEM (Figure 3) indicated a significant improvement in surface texture. The non-anodized substrate exhibited polishing lines and surface irregularities. However, post-anodizing, these features were progressively smoothed.

The anodization of Zr metal at 10 minutes produced a comparatively uneven surface

DOI: https://doi.org/10.17146/urania.20xx.xx.x.xxxx

morphology in Figure 2a. A coating of zirconium oxide had developed at that point, although it was not yet uniformly distributed. The 3D profile data (Figure 2b) revealed that the oxide layer was still in its early phases of formation, resulting in a very rough surface roughness. The duration of anodization was extended to 15 minutes (Figure 2c). Compared to Zr-10, the resulting zirconium oxide layer became more homogeneous, thick, and continuous. This result was also confirmed from the 3D profile of Figure 2d. Figure 2e shows the anodization of Zr metal with a process time of 20 minutes. Increasing the anodization time contributed to the growth and stability of the zirconium oxide layer formed on the metal surface. The layer was more uniform, dense, and surface defects were significantly reduced. The relevant results are confirmed by Figure 2f.

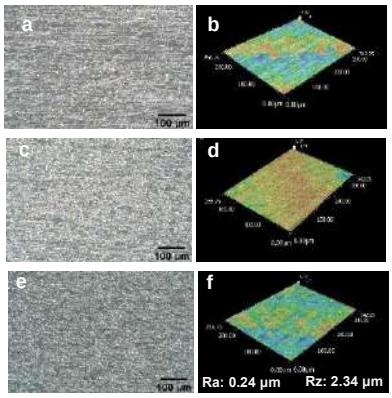

g

Specimen	Surface Roughness	
	Ra	Rz
Zr-10	0.53	4.35
Zr-15	0.34	4.98
Zr-20	0.24	2.34

Figure 2. Microstructural analysis via optical microscopy (a,c,e), 3D profile (b,d,f), and surface roughness value (g) of (a,b) Zr-anodized 10 minutes, (c,d) Zr-anodized 15 minutes, and (e,f) Zr-anodized 20 minutes.

Quantitative roughness data presented in Figure 2g and Figure 2 (b,d,f) confirm this observation. The average roughness (Ra) decreased from 0.53 µm for the Zr-10 specimen to 0.34 µm for Zr-15, and finally to 0.24 µm for Zr-20. This trend suggests a "leveling mechanism" where the oxide grows preferentially in the microscopic valleys of the metal surface, effectively reducing the peak-to-valley height [14]. A smoother surface is highly advantageous for nuclear cladding as it reduces the friction coefficient during fuel rod insertion and minimizes the surface area available for corrosive attack.

Figure 3. shows SEM images and the corresponding EDS area mapping of zirconium anodized under different duration processes. The surfaces of all the specimens were quite homogeneous and devoid of significant cracks. Increasing the anodization time prevented any significant morphological changes at the micrometer scale. For every modification in anodization time, the elemental mapping findings on the zirconium oxide layer's surface revealed an equitable distribution of elements. The anodized metal surface was dominated by Zr and O elements.

The zirconium substrate, whose composition decreased as the anodization duration increased, provided the Zr element. The O element showed that an oxide layer had formed during the anodization processes. The composition of the O element increased as the anodization duration increased, indicating the thickening and expansion of the zirconium oxide layer (ZrO_2). The increase in the O element was formed from 44.66 at% for the Zr-10 specimen, 53.12 at% for the Zr-15 specimen, and the highest for the Zr-20 specimen, namely 54.33 at%. The P element was also found throughout the layer's surface in addition to these primary components. The phosphate-based electrolyte used during the anodizing process is the source of the phosphorus, which is present in trace levels (around 1-2 at%) but is dispersed rather uniformly.

Phosphorus detected in the anodic film originates from field-assisted incorporation of phosphate species during anodization rather than residual electrolyte contamination. The concentration remains low and relatively independent of anodizing time, indicating incorporation primarily during early barrier layer formation. At the detected level (~1–2 at%), phosphorus is not expected to adversely affect zirconium cladding performance, although high-temperature reactor-condition validation remains necessary.

Crystalline Structure and Microhardness the XRD patterns shown in Figure 4 display sharp diffraction peaks corresponding to Zirconium Oxide (ZrO_2). The analysis suggests the presence of most tetragonal crystalline phase CDD / PDF card: 00-050-1089, which is notable as anodic films formed at lower voltages are often amorphous. The formation of this crystalline phase contributes to the chemical stability of the coating [15]. Diffraction peaks for the zirconium (Zr) and zirconium oxide (ZrO_2) phases were detected on all anodized specimens. The ZrO_2 peak's formation indicates that the anodization procedure was effective in generating an oxide layer on the zirconium substrate's surface.

The ZrO_2 diffraction peak's clarity tended to rise with increasing anodization time, especially in the Zr-20 specimen, which showed the maximum peak intensity. This suggests that extended anodization durations encourage the formation of an oxide layer that is thicker and/or more crystalline. In the meantime, peaks from the Zr phase were still identified, suggesting that the relatively tiny oxide layer thickness allowed X-rays to proceed toward the substrate. In general, the XRD data confirm that different anodization times affect the zirconium oxide layer's growth and crystal properties. At the anode, the reaction that occurs can be written as:

$$Zr \rightarrow Zr^{4+} + 4e^- \quad (1)$$

$$Zr^{4+} + 2\,O^{2-} \rightarrow ZrO_2 \quad (2)$$

Meanwhile, at the cathode a reduction reaction takes place, usually involving the evolution of hydrogen gas:

$$4\,H^+ + 4\,e^- \rightarrow 2\,H_2 \quad (3)$$

Mechanical integrity was evaluated via Vickers microhardness (HV). As detailed in Table 1, the hardness values were relatively stable across the anodized samples: 144.41±8.99 HV (10 min), 144.66±7.84 HV (15 min), and 142.88±6.96 HV (20 min). Although the macroscopic hardness did not show a drastic increase compared to the substrate (likely due to the indentation depth exceeding the thin oxide layer thickness), the presence of the hard ceramic ZrO_2 skin provides essential resistance against superficial scratching and fretting wear, which are critical precursors to cladding failure [16].

Table 1. Average and Standar Deviation (STDV) for Microhardness of Zr-Anodized under different duration process

Specimen	HV					Average	Standard Deviation
	1	2	3	4	5		
Zr-10	150.97	138.23	140.08	158.57	134.19	144.41	8.99
Zr-15	156.89	142.93	138.07	149.92	135.5	144.66	7.84
Zr-20	155.79	144.39	137.77	136.86	139.61	142.88	6.96

Commented [A3]: I suggest that this data should be excluded because the applied load was excessive. This resulted in the measurements reflecting the substrate hardness rather than providing an accurate representation of the coating's hardness.

Commented [A4R3]: We thank the reviewer for this important and insightful comment.
We agree that the applied load (300 gf) results in an indentation depth that exceeds the thickness of the anodic oxide layer. Consequently, the measured hardness values predominantly reflect the mechanical response of the zirconium substrate rather than the intrinsic hardness of the oxide coating.
However, we respectfully choose to **retain the microhardness data** in the manuscript for the following reasons:

1. **Relevance to Practical Behavior**
   The measurement reflects the effective surface response under macro-scale loading conditions, which is still relevant for engineering applications where the substrate–coating system behaves as a composite.
2. **Consistent Observation Across Samples**
   The results consistently show that the hardness values of anodized samples (≈143–145 HV) are comparable to the substrate, indicating that the anodization process does not significantly alter the bulk mechanical response of zirconium.
3. **Important Scientific Insight**
   The similarity in hardness values is itself an important finding, demonstrating that:
   - The anodic oxide layer is relatively thin,
   - Its contribution to bulk hardness is limited under the applied test conditions,
   - The mechanical properties remain dominated by the substrate.

We have revised the manuscript to explicitly clarify that:
- The measured hardness values are substrate-dominated,
- The anodized layer does not significantly increase the apparent hardness under the applied load,
- Therefore, the hardness of anodized zirconium can be considered **comparable to that of the untreated zirconium substrate** in this testing configuration.

Additionally, we now state that:
"Nanoindentation or lower-load testing would be required to isolate the intrinsic hardness of the anodic oxide layer."
We believe retaining this data, with proper clarification, provides a more complete and transparent interpretation of the mechanical behavior of the anodized system.

DOI: https://doi.org/10.17146/urania.20xx.xx.x.xxxx

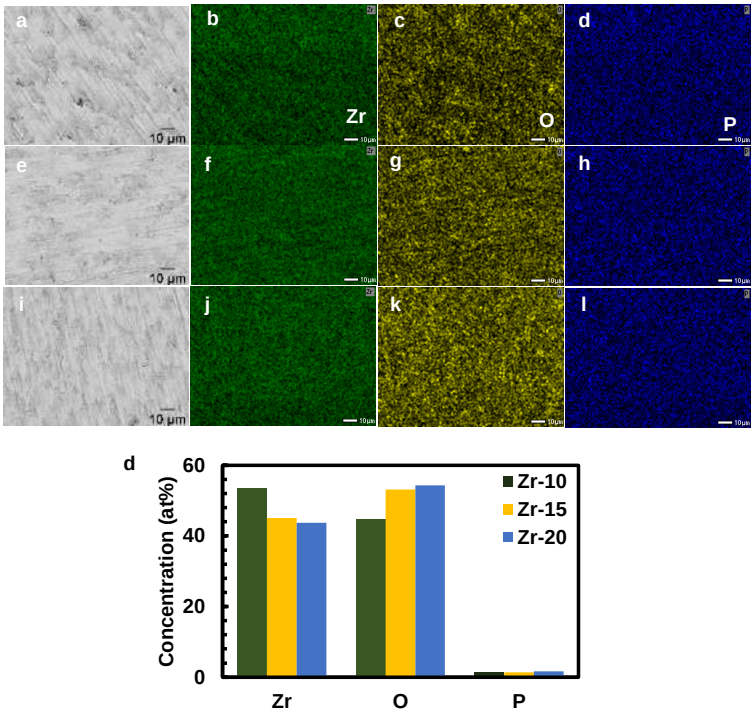

Figure 3. Surface view SEM images and the corresponding EDS area mapping of zirconium anodized of (a-d) Zr-10, (e-h) Zr-15, and (i-l) Zr-20 minutes

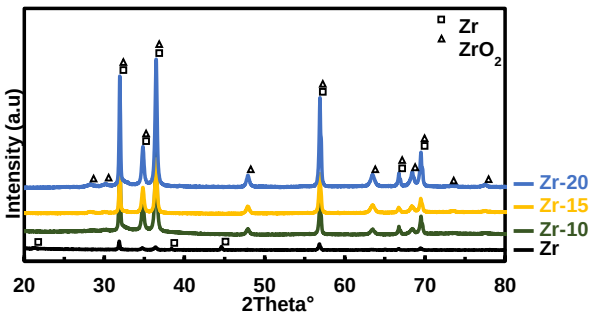

Figure 4. XRD pattern of zirconium oxide (ZrO_2)

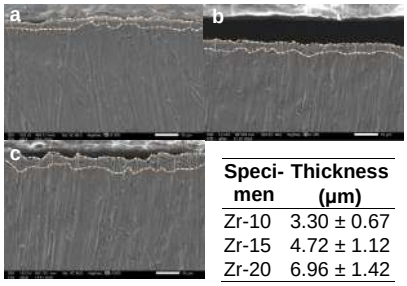

Speci-men	Thickness (µm)
Zr-10	3.30 ± 0.67
Zr-15	4.72 ± 1.12
Zr-20	6.96 ± 1.42

Figure 5. Cross-sectional view SEM images for zirconium anodized of (a) Zr-10, (b) Zr-15, (c) Zr-20 minutes, and (d) thickness of all specimens

An oxide layer thickness quantitative summary and cross-sectional SEM images of anodized zirconium specimens treated for 10, 15, and 20 minutes are shown in Figure 5. This figure aims to assess how anodization time affects the shape and growth behavior of the anodic oxide layer that forms on zirconium. From Zr-10 (3.30 ± 0.67 µm) to Zr-15 (4.72 ± 1.12 µm) and Zr-20 (6.96 ± 1.42 µm), the SEM micrographs show clearly a compact and rather homogeneous oxide layer adhering to the substrate. The oxide–metal contact is displayed by the dotted line, which highlights the continuous layer growth without significant delamination. A time-dependent oxide the growth process controlled by field-assisted ionic transport, where Zr^{+} cations migrate outward and O^{2-} anions migrate inside under a strong electric field to create ZrO_2 at the interface, is suggested by the increasing thickness with anodization time. High-field oxide growth theory states that unless transport limitations or dissolving effects become visible, oxide thickness is proportional to the applied potential and processing time.

Electrochemical Corrosion Behavior

The corrosion resistance was comprehensively analyzed using OCP, PDP, and EIS techniques. Open Circuit Potential (OCP): Figure 5 illustrates the OCP evolution. All anodized specimens exhibited more positive (noble) potentials compared to the bare substrate. The Zr-20 sample showed the most noble potential, stabilizing at a higher value, which indicates a thermodynamic tendency to resist spontaneous corrosion reactions in the electrolyte [17]. During the test, pure zirconium (Zr) specimens had the most negative and comparatively steady potential values, suggesting more potential for corrosion. All the specimens indicated a potential change in a more positive direction immediately after the anodization process, which suggests that the formation of a zirconium oxide layer had increased electrochemical stability. Zr-20, Zr-15, and Zr-10 were the anodized specimens with the most positive and consistent OCP values while the test. This suggests that extending the anodization duration increases the material's resistance to corrosion and creates a more protective oxide layer. The formation of a rather stable passive layer on the zirconium surface is also shown by the stability of the OCP curves over an extended test time.

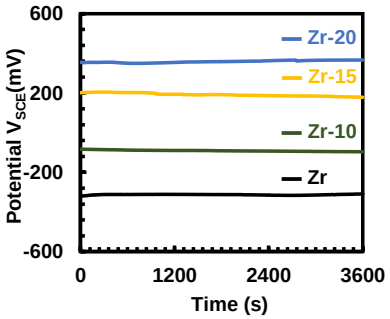

Figure 6. Average of OCP curves for zirconium substrate and zirconium-anodized at 30 V

Potentiodynamic Polarization (PDP): The Tafel polarization curves in Figure 6 demonstrate a clear shift in corrosion kinetics. The electrochemical parameters summarized in Table 2 show a dramatic reduction in corrosion current density (i_{corr}). The substrate exhibited an i_{corr} of 12.93 × 10^{-9}A/cm^2. In contrast, the Zr-20 specimen exhibited an i_{corr} of 0.19 × 10^{-9}A/cm^2. This reduction by nearly two orders of magnitude confirms that the thicker oxide layer formed at 20 minutes acts as an effective barrier, blocking the diffusion of chloride ions (Cl^{-}) and oxygen to the metal interface [18, 19].

Commented [A5]: Is it accurate for the oxide layer to be this thick? If so, the thin-film interference phenomenon regarding the transparent anodic oxide film (ZrO2) (that you mentioned in first paragraph of "Result and Discussion" section) would not occur. Moreover, I do not see any visible difference between the marked area and the rest of the sample.

If the coating thickness is on the nanometer scale (as evidenced by the light interference), SEM magnification of 1,500x is clearly insufficient for accurate characterization. Consequently, these results should be excluded from the analysis to maintain data integrity.

Commented [A6R5]: We thank the reviewer for this thoughtful and critical comment.
We would like to clarify that the oxide thickness measured in this study (approximately 3–7 µm) is physically consistent with anodization conditions at 30 V in phosphate-based electrolytes, where compact barrier-type oxide films can grow into the micrometer range under prolonged anodizing durations.
To further support this, we analyzed the **oxide growth rate** based on the measured thickness:
- Zr-10: ~3.30 µm → ~0.33 µm/min
- Zr-15: ~4.72 µm → ~0.31 µm/min
- Zr-20: ~6.96 µm → ~0.35 µm/min

These values indicate a relatively consistent growth rate in the range of **~0.3–0.35 µm/min**, which is in good agreement with high-field oxide growth kinetics for valve metals under moderate voltage conditions. The near-linear relationship between anodizing time and oxide thickness further supports that the oxide growth mechanism is controlled by field-assisted ionic migration rather than anomalous deposition.
Regarding the concern about thin-film interference:
- The observed coloration does not strictly imply nanometer-scale thickness, as interference effects can still occur in sub-micron to micron-scale oxide layers depending on refractive index, partial transparency, and thickness gradients.
- Therefore, the presence of interference color does not contradict the measured micrometer-scale thickness.

Concerning SEM characterization:
- The cross-sectional SEM images clearly show a continuous oxide layer, and the thickness was measured directly from the interface between oxide and substrate.
- The magnification used is sufficient for micrometer-scale thickness measurement, and multiple measurements were averaged to ensure accuracy.

Finally, we respectfully maintain that the reported thickness values are valid and consistent with anodization kinetics. The addition of growth rate analysis further confirms that the oxide thickness evolution is physically reasonable and follows expected anodic film growth behavior.
We have incorporated this growth rate discussion into the revised manuscript to strengthen the interpretation.

DOI: https://doi.org/10.17146/urania.20xx.xx.x.xxxx

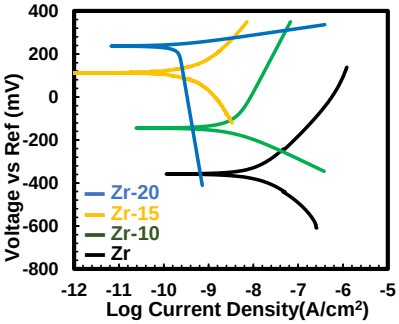

Figure 7. Average of PDP curves for zirconium substrate and zirconium-anodised at 30 V

Figure 6 presents the potentiodynamic polarization (PDP) curves of anodized and pure zirconium. These curves illustrate the relationship between the voltage across a reference electrode and the log current density, which is used to assess corrosion behavior and electrochemical reaction kinetics. Pure zirconium exhibits poor corrosion resistance, indicated by its limited passivation range and relatively high corrosion current density. In contrast, anodized specimens show a shift in corrosion potential to more positive values and a decrease in corrosion current density. Compared to Zr-15 and Zr-10, the Zr-20 specimen shows the biggest passivation area and the lowest current density. The Zr-20 specimen exhibits the lowest current density and the largest passivation region compared to Zr-15 and Zr-10. This suggests that the zirconium oxide layer that develops over extended anodization durations successfully prevents charge transfer and reduces the rate of corrosion. We thank the reviewer for this careful observation.

The blue curve corresponds to the Zr-20 specimen, which exhibits the longest anodizing duration (20 minutes). The distinct shape of this curve compared to the other samples is primarily attributed to differences in the oxide layer thickness, compactness, and electrochemical stability resulting from prolonged anodization. Several factors explain this behaviour, due to more Compact and Thicker Oxide Film. The Zr-20 sample forms a thicker and denser ZrO_2 layer, as supported by higher oxygen atomic percentage (EDS), lowest surface roughness (Ra = 0.24 µm), lowest corrosion current density (0.19×10^{-9} A/cm²). This compact oxide layer significantly suppresses charge transfer at the metal/electrolyte interface, resulting in:

A pronounced shift of Ecorr toward more positive values, a wider passive region, lower anodic current density. The shape difference reflects a more stable passive regime in Zr-20. The reduced slope in the anodic branch indicates lower metal dissolution kinetics due to improved barrier characteristics of the oxide.

Shorter anodizing times (10 and 15 minutes) likely produce thinner films with higher defect density or localized porosity. These structural differences lead to earlier activation behavior and less stable passivation, resulting in PDP curves that differ in shape.

For Zr-20, corrosion behavior transitions from activation-controlled to diffusion-limited/passivation-controlled kinetics over a wider potential range, which explains the distinct curvature compared to the other samples.

Commented [A7]: where is the passive region in Fig. 7?

Commented [A8R7]: Thank you for your comment.

The passive region in Figure 7 can be observed in the anodic part of the PDP curves, where the potential increases while the current density remains relatively stable, forming a plateau-like region. Based on the figure, this region occurs approximately at log current density between −10 and −9 A/cm² and at potentials around 0 to +250 mV vs Ref.

In this range, the relatively constant current density indicates the formation of a protective oxide layer on the zirconium surface, which reduces the rate of electrochemical dissolution. The anodized samples exhibit a more pronounced passive region compared with the untreated Zr, suggesting that the anodizing process enhances the passivation behavior by forming a more stable oxide layer on the surface.

Table 2. PDP Parameter of Zr-Anodized under different duration process

Specimen	E_{corr} (mV)	i_{corr} (10^{-9}A/cm²)	β_{Anodic} (mV/Decade)	$\beta_{Catodic}$ (mV/Decade)
Zr	-346 ± 88	12.93 ± 2.89	399 ± 350	275 ± 152
Zr-10	-114 ± 94	2.57 ± 1.12	599± 461	198 ± 122
Zr-15	92 ± 98	1.10 ± 0.82	275 ± 201	363 ± 262
Zr-20	233 ± 74	0.19 ± 0.04	152 ± 151	1518 ± 1067

a)

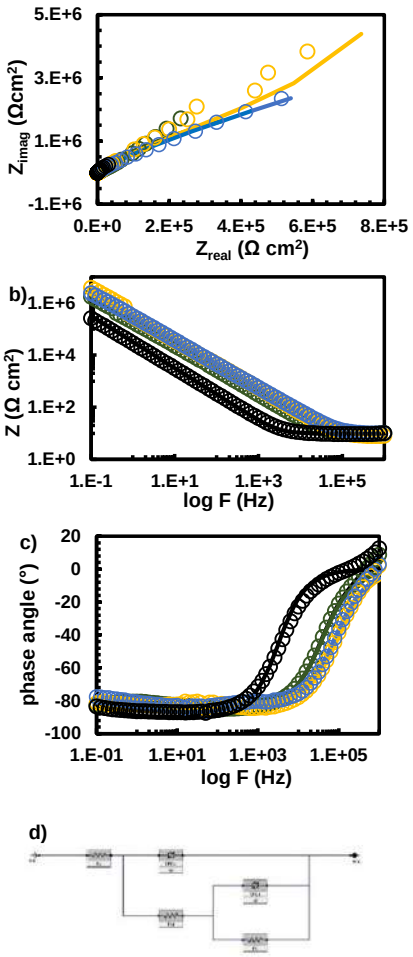

Figure 8. Average of EIS results of a) Nyquist spectra, b) bode impedance, c) bode phase, d) Equivalent electrical circuit (EEC) fitting for zirconium substrate and zirconium-anodised at 30 V

Table 3. Fit parameters of EIS data

Parameter	Substrate	Zr-10	Zr-15	Zr-20
R_s ($\Omega.cm^2$)	10	11	159	10
C_{dl} ($S^*s^a.cm^{-2}$)	$5x10^{-6}$	-	-	-
R_{ct} ($\Omega.cm^2$)	$2x0^6$	-	-	-
CPE_{ol} ($S^*s^a.cm^{-2}$)	-	$1x10^{-8}$	$8x10^{-8}$	$6.1x10^{-8}$
a_{ol}	-	0.6	0.7	0.7
R_{ol} ($\Omega.cm^2$)	-	137	150	140
CPE_{il} ($S^*s^a.cm^{-2}$)	-	$9.3x10^{-9}$ 10^{-9}	$5.6x10^{-9}$ 10^{-9}	$5.3x10^{-9}$ 10^{-9}
a_{il}	-	0.9 10^{-3}	0.9 10^{-3}	0.9 10^{-3}
R_{il} ($\Omega.cm^2$)	-	15.00 106	15.82 106	16.40 103
Goodness of fit (χ^2)	$1.1x10^{-2}$	$3.4x10^{-2}$	$2.3x10^{-2}$	$1.4x10^{-2}$

Figure 8, the EIS results show that anodized samples exhibit significantly larger semicircle diameters in the Nyquist plots compared to the bare zirconium substrate, indicating improved corrosion resistance after anodization. The fitted parameters reveal that the charge transfer resistance (Rct) increases with anodizing time, with Zr-20 showing the highest resistance value, confirming enhanced barrier properties of the oxide layer. The solution resistance (Rs) remains relatively constant, suggesting consistent electrolyte conditions during testing. Additionally, the decrease in CPE values and the broader capacitive region in the phase angle plots indicate improved film compactness and reduced surface heterogeneity. Overall, the EIS analysis supports the PDP and OCP results, confirming that longer anodizing duration produces a thicker and more protective ZrO_2 layer that effectively suppresses corrosion reactions.

Based on Table 3, the solution resistance (Rs) remains nearly constant at approximately 10–11 Ω·cm² for all samples, confirming stable electrolyte conditions. The oxide-related resistance and charge transfer resistance increase significantly after anodization, with Rct rising from 137 Ω·cm² for Zr-10 to 150 Ω·cm² for Zr-15 and reaching 140 Ω·cm² for Zr-20, indicating improved interfacial stability. The CPE values decrease

DOI: https://doi.org/10.17146/urania.20xx.xx.x.xxxx

slightly from 1×10^{-8} to 6.1×10^{-8} $S\cdot s^{n}\cdot cm^{-2}$ as anodizing time increases, suggesting a more compact and less defective oxide layer. The goodness-of-fit values (χ^2 in the order of 10^{-2}) indicate that the equivalent circuit model adequately represents the experimental data. These quantitative results confirm that increasing anodizing time increases the electrochemical resistance of the zirconium surface.

CONCLUSIONS

The effect of anodizing duration on the surface characteristics and corrosion behavior of Zirconium was successfully investigated. The following conclusions are drawn:

1. Surface Improvement: Increasing the anodizing time from 10 to 20 minutes at 30 V results in a progressively smoother surface. The Zr-20 specimen achieved the lowest roughness (Ra= 0.24 µm), reducing friction and potential pit initiation sites.
2. Oxide Formation: The process forms a stable, crystalline ZrO_2 layer, as confirmed by XRD and the observation of interference colors.
3. Corrosion Resistance: The 20-minute anodized coating offers superior corrosion protection in chloride environments. It reduced the corrosion rate i_{corr} by approximately 98% compared to the bare substrate and significantly increased the polarization resistance.
4. Application Viability: The study confirms that a 20-minute anodizing treatment is an effective, low-cost method to enhance the durability of Zirconium nuclear fuel cladding, potentially extending the safety margins against corrosion and mechanical degradation in PWR environments.

REFERENCES

[1] Motta, A. T., Couet, A., & Comstock, R. J. (2015). Corrosion of Zirconium Alloys Used for Nuclear Fuel Cladding. Annual Review of Materials Research, 45, 311-343.

[2] Duan, Z., Yang, H., Satoh, Y., & Murakami, K. (2017). Oxidation behavior of zirconium alloys in a simulated nuclear reactor primary coolant. Journal of Nuclear Materials, 485, 147-158.

[3] Terrani, K. A. (2018). Accident tolerant fuel cladding development: Promise, status, and challenges. Journal of Nuclear Materials, 501, 13-30.

[4] Gong, W., & Yun, D. (2022). A review on the corrosion behavior of zirconium alloys in supercritical water. Corrosion Science, 208, 110620.

[5] Yilmazbayhan, A., Motta, A. T., & Comstock, R. J. (2021). Hydride morphology and embrittlement in Zircaloy-4 cladding. Journal of Nuclear Materials, 545, 152646.

[6] Liu, J., & Li, Q. (2023). Fretting wear behavior of zirconium alloy cladding tubes. Wear, 522, 204689.

[7] Kim, H. G., & Kim, I. H. (2020). Oxidation behavior of zirconium alloy claddings in high temperature steam. Nuclear Engineering and Technology, 52(4), 808-815.

[8] Suresh, S., & Sharma, A. (2021). Surface modification of zirconium alloys for biomedical and nuclear applications: A review. Surface and Coatings Technology, 405, 126666.

[9] Verma, R., & Kumar, S. (2022). Electrochemical anodization of zirconium: Growth mechanism and properties. Electrochimica Acta, 412, 140135.

[10] Cheng, Y., & Matykina, E. (2021). Formation of nanotubular oxide layers on Zirconium alloys by anodization. Corrosion Science, 182, 109289.

[11] Ali, F., & Al-Hajri, M. (2023). Effect of voltage and electrolyte composition on the morphology of anodic zirconium oxide. Materials Chemistry and Physics, 295, 127087.

[12] Wang, L., Zhang, Y., & Wu, X. (2024). Time-dependent growth kinetics of anodic films on zirconium in phosphate electrolytes. Journal of Electrochemical Society, 171(2), 021504.

[13] Diamanti, M. V., & Pedeferri, M. P. (2020). Color production on zirconium by

anodizing: Interference and absorption effects. Color Research & Application, 45(3), 456-464.

[14] Thompson, G. E. (2019). Porous anodic oxide films: Formation, growth and applications. Thin Solid Films, 685, 34-45.

[15] Zhao, X., & Xu, H. (2022). Phase transformation in anodic zirconia films: From amorphous to crystalline. Scripta Materialia, 210, 114421.

[16] Obbard, E. G., & Burr, P. A. (2021). Mechanical properties of zirconium oxide scales: A review. Journal of Nuclear Materials, 557, 153255.

[17] McCafferty, E. (2020). Introduction to Corrosion Science (2nd ed.). Springer.

[18] Zhang, B., & Frankel, G. S. (2022). Corrosion mechanisms of zirconium alloys in chloride-containing environments. Corrosion, 78(5), 412-425.

[19] Li, T., & Wang, F. (2023). Improvement of pitting corrosion resistance of Zr alloys by anodic oxidation. Applied Surface Science, 610, 155567.

[20] Orazem, M. E., & Tribollet, B. (2017). Electrochemical Impedance Spectroscopy. Wiley.

DOI: https://doi.org/10.17146/urania.20xx.xx.x.xxxx

Urania
Jurnal Ilmiah Daur Bahan Bakar Nuklir

Beranda jurnal: https://ejournal.brin.go.id/urania

THE EFFECT OF TIME IN THE ANODIZING PROCESS ON THE COATING CHARACTERISTICS AND CORROSION BEHAVIOR OF ZIRCONIUM METAL

Manogari Sianturi[1*], Fajar Al Afghani[2], Frisca Ronauli Batubara[3], Sri Rahmadani[4], Romi Saputra[1]

[1]Department of Physics Education, Faculty of Teacher Training and Education, Universitas Kristen Indonesia, Jakarta 13630, Indonesia

[2]Research Center and Technology for Nuclear Material and Radioactive Waste – BRIN Kawasan Sains dan Teknologi B.J. Habibie, Bld. 720, Tangerang Selatan, Banten 15314

[3]Department of Physiology, Faculty of Medicine, Universitas Kristen Indonesia, Jakarta 13630, Indonesia

[4]Mechanical Engineering, Faculty of Engineering, Computer, and Design, Nusa Putra University, Sukabumi, Jawa Barat 43152, Indonesia

*e-mail: manogari.sianturi@uki.ac.id

(Submitted: 23–01–2026, Revised: 01–04–2026, Accepted: 06–04–2026)

ABSTRACT

THE EFFECT OF TIME IN THE ANODIZING PROCESS ON THE COATING CHARACTERISTICS AND CORROSION BEHAVIOR OF ZIRCONIUM METAL. Zirconium and its alloys are the standard material for nuclear fuel cladding in Pressurized Water Reactors (PWR) due to their low neutron absorption cross-section, excellent mechanical properties, and good corrosion resistance in high-temperature water. However, the operational environment of a PWR imposes severe conditions that can degrade the cladding integrity over time, including oxidation, hydriding, and mechanical damage such as scratching or denting during fuel refueling operations. These surface defects can act as initiation sites for localized corrosion, potentially compromising the primary containment barrier. This study investigates the effectiveness of electrochemical anodizing as a surface modification technique to enhance the performance of Zirconium. The anodizing process was conducted at a constant voltage of 30 V with varying durations of 10, 15, and 20 minutes. The resulting surface characteristics were evaluated using Optical Microscopy, Digital Microscopy for roughness analysis, and X-Ray Diffraction (XRD). Mechanical reliability was assessed via Vickers Microhardness testing, while Corrosion behavior was studied in a 3.5% NaCl solution using Open Circuit Potential (OCP), Potentiodynamic Polarization (PDP), and Electrochemical Impedance Spectroscopy (EIS). The results demonstrated that increasing the anodizing time significantly improved the surface quality, reducing the arithmetic mean roughness Ra from 0.53 µm (10 min) to 0.24µm (20 min). XRD analysis confirmed the formation of a crystalline ZrO_2 oxide layer. Electrochemical tests revealed a substantial enhancement in corrosion resistance; the corrosion current density i_{corr} decreased by two orders of magnitude from 12.93 x 10^{-9} A/cm^2 for the substrate to 0.19 x 10^{-9} A/cm^2 for the 20-minute anodized yesspecimen. The study concludes that a 20-minute anodizing treatment at 30 V produces a robust, smooth, and highly corrosion-resistant oxide layer suitable for mitigating degradation in nuclear fuel cladding applications.

Keywords: Zirconium, anodizing, corrosion resistance, cladding, PWR, surface modification.

INTRODUCTION

Zirconium (Zr) and its alloys, such as Zircaloy-4 and Zirlo, are the materials of choice for nuclear fuel cladding in light water reactors (LWR), particularly Pressurized Water Reactors (PWR). This selection is driven by Zirconium's unique combination of properties: an exceptionally low thermal neutron capture cross-section (0.18 barn), which ensures efficient neutron economy, good thermal conductivity, and adequate mechanical strength at elevated temperatures [1, 2]. As the first barrier in the defense-in-depth strategy, the cladding must hermetically seal radioactive fission products preventing their release into the primary coolant.

Despite these advantages, Zirconium cladding faces formidable challenges during its service life. The aggressive operating environment, characterized by high-pressure water (approx. 15.5 MPa) and high temperatures (approx. 300-350°C), promotes waterside corrosion and hydrogen pickup [3, 4]. The oxidation of zirconium ($Zr + 2H_2O \rightarrow ZrO_2 + 2H_2$) not only thins the structural wall but also generates hydrogen, a fraction of which diffuses into the metal matrix, leading to hydride precipitation and embrittlement [5]. Furthermore, beyond steady-state operation, the cladding is subjected to mechanical stress during fuel handling and refueling processes. Physical contact with grid spacers or other assemblies can cause surface scratches, fretting, or dents. These surface imperfections significantly increase local roughness and can serve as stress concentration points or preferential sites for pitting corrosion, accelerating material degradation [6, 7].

Extending the operational life of fuel assemblies and enhanced safety margins, particularly for high-burnup regimes, surface modification techniques have gained attention. The goal is to create a protective surface layer that is harder than the substrate to resist mechanical damage and to be more chemically stable to inhibit corrosion [8]. Among various techniques such as physical vapor deposition (PVD) or laser surface treatment, electrochemical anodizing stands out due to its simplicity, cost-effectiveness, and ability to form a uniform, adherent oxide film (ZrO_2) even on complex geometries [9]. Compared to PVD coatings that are only deposited on top, anodizing on Zr produces a ZrO_2 oxide layer that develops straight from the metal surface, providing significantly stronger adhesion, increased corrosion resistance, and improved thermal stability. Additionally, it creates a consistent, thick, and stable oxide layer that is appropriate for applications requiring long-lasting protection in biological, high-temperature, and harsh environments [1].

Anodizing promotes the growth of a thickened oxide layer that acts as a passivating barrier. While the natural oxide film on Zirconium is protective, it is thin and liable to breakdown. Anodic films, depending on process parameters like voltage, electrolyte, and time, can be engineered to be thicker and more compact [10, 11]. Recent studies have focused on the voltage effects, but the influence of anodizing duration—specifically in the transition from initial film formation to steady-state growth—on the micro-roughness and electrochemical impedance of the surface remains an area for optimization [12]. Limited studies systematically evaluate the effect of anodizing time at fixed voltage on compact oxide growth. Few works correlate roughness evolution, elemental composition, and electrochemical corrosion kinetics simultaneously. There remains a need to evaluate surface stabilization strategies under chloride-containing environments simulating aggressive localized attacks.

This study aims to systematically evaluate the effect of anodizing time (10, 15, and 20 minutes) at a fixed potential of 30 V on the surface characteristics and corrosion behavior of Zirconium. We hypothesize that extending the anodizing duration will not only increase the oxide thickness but also reduce surface roughness through a leveling effect, thereby providing superior corrosion resistance in aggressive chloride environments.

METHODOLOGY

The substrate material used was commercial purity Zirconium metal, cut into coupon specimens with dimensions of 10 mm x 10 mm. The samples were mounted in epoxy resin to expose a single working surface area of 0.5 cm^2. Prior to anodizing, the surfaces were mechanically polished using a sequence of Silicon Carbide (SiC) abrasive papers with grit sizes of 500, 800, 1200, and 2000. This step was crucial to

 DOI: https://doi.org/10.55981/urania.2026.15001

remove the heterogeneous native oxide layer and standardize the initial surface roughness. After polishing, the samples were ultrasonically cleaned in acetone and rinsed with demineralized water to remove any particulate residues.

The anodizing process was carried out in a two-electrode electrochemical cell at room temperature. The Zirconium specimen served as the anode, while a high-purity platinum sheet was used as the cathode to ensure chemical inertness. The electrolyte was a specific aqueous solution tailored for compact film growth (typically phosphate/ammonium based). In the absence of fluoride ions, phosphoric acid electrolytes promote barrier-type compact oxide growth due to limited field-assisted dissolution, preventing nanotubular structure formation [2], [3]. Phosphoric acid (H_3PO_4) at a concentration of 30 g/L is used as the electrolyte for the anodization process. Measuring the phosphoric acid with an analytical balance and combining it with distilled water in a beaker is the first step in the electrolyte production process. When the solution is ready to be employed as an anodizing medium on zirconium metal substrates, it is mixed with a magnetic stirrer until it dissolves uniformly.

A DC power supply was used to apply a constant voltage of 30 V. The anodizing duration varied as the experimental parameter: 10 minutes (Zr-10), 15 minutes (Zr-15), and 20 minutes (Zr-20). Post-anodizing, samples were rinsed and dried in air. A digital multimeter (DMM) was used to monitor the voltage and current during the anodization process. The solution was kept at room temperature to prevent localized heating that would result in non-uniform oxidation. The voltage source was turned off, and the specimen was removed from the electrolyte solution after the anodization period was complete. A hair dryer was used to dry any leftover electrolyte after it had been cleansed with distilled water. All anodized specimens were kept in a closed container, and silica gel was added to regulate the humidity in the storage area prior to testing for corrosion resistance, hardness, and surface morphology examination.

Surface morphology and visual appearance were documented using an Optical Microscope and a high-resolution Digital Microscope. The surface roughness parameters, Arithmetic Mean Roughness (Ra) and Ten-Point Mean Roughness (Rz), were quantified to evaluate the smoothing effect of the treatment. The surface morphology study was supported by microstructural findings. The samples' surface and texture were examined using scanning electron microscopy (SEM) at an accelerating voltage of 15 kV, which provided precise topographical information on the zirconium dioxide (ZrO_2) layer. Porosity, fractures, oxide layer thickness, and surface features that matched each time variation were observed using SEM examination. Additionally, the elemental composition of the coating was determined using Energy Dispersive Spectroscopy (EDS), with a focus on the distribution of phosphorus and oxygen to validate the creation of the ZrO_2 layer and potential interactions with the H_3PO_4 electrolyte. For additional examination, elemental mapping and spectra were both obtained.

The following explanation and reactions have been incorporated:

Zirconium is oxidized under the applied electric field:

$$Zr \rightarrow Zr^{4+} + 4e- \quad (1)$$

Simultaneously, oxygen-containing species (O^{2-} or OH^- derived from water) migrate inward and react with zirconium ions:

$$Zr^{4+} + 2O^{2-} \rightarrow ZrO_2 \quad (2)$$

Alternatively, expressed via water-assisted oxidation:

$$Zr + 2H_2O \rightarrow ZrO_2 + 4H^+ + 4e^- \quad (3)$$

In phosphoric acid electrolyte, the dominant species include:

$$H_3PO_4 \rightleftharpoons H_2PO_4- \rightleftharpoons HPO_4^{2-} \rightleftharpoons PO_4^{3-} \quad (4)$$

Under the strong electric field across the growing oxide film. Negatively charged phosphate ions migrate toward the anode. A fraction of these anions becomes incorporated into the outer oxide region. The incorporation process can be represented schematically as:

$$ZrO_2 + xPO_4^{3-} \rightarrow ZrO_2(PO_4)x \quad (5)$$

The crystalline structure of the anodic oxide layers was analyzed using X-Ray Diffraction (XRD) with Cu-Kα radiation. To assess the resistance to mechanical damage, Vickers Microhardness testing was

performed using a load of 300 gf with a dwell time of 15 seconds; five indentations were made per sample to obtain an average value.

Corrosion performance was evaluated in a 3.5% NaCl solution, chosen to simulate an aggressive corrosive environment that accelerates pitting attack. A standard three-electrode cell was employed, consisting of the Zr specimen (working electrode), an Ag/AgCl reference electrode, and a graphite counter electrode. The measurements were conducted using a Potentiostat/Galvanostat with the following sequence:

1. Open Circuit Potential (OCP): Monitored for 3600 seconds until a stable potential was reached.
2. Potentiodynamic Polarization (PDP): Scanned from -250 mV to +250 mV relative to OCP at a scan rate of 1 mV/s to determine Tafel parameters E_{corr} and i_{corr}.
3. Electrochemical Impedance Spectroscopy (EIS): Conducted at OCP with a sinusoidal perturbation of 10 mV amplitude over a frequency range of 100 kHz to 0.01 Hz.

RESULTS AND DISCUSSION

Surface Morphology and Roughness Analysis

Visual inspection of the samples immediately after anodizing revealed a distinct coloration of the surface. As shown in Figure 1, the surface color shifted from the metallic silver of the substrate to uniform hues of gold and blue. This phenomenon is attributed to the interference of light within the transparent anodic oxide film (ZrO_2), where the perceived color is directly related to the film thickness governed by the anodizing duration [13].

Microstructural analysis via optical microscopy (Figure 2) and SEM (Figure 3) indicated a significant improvement in surface texture. The non-anodized substrate exhibited polishing lines and surface irregularities. However, post-anodizing, these features were progressively smoothed.

The anodization of Zr metal at 10 minutes produced a comparatively uneven surface morphology in Figure 2a. A coating of zirconium oxide had developed at that point, although it was not yet uniformly distributed. The 3D profile data (Figure 2b) revealed that the oxide layer was still in its early phases of formation, resulting in a very rough surface roughness. The duration of anodization was extended to 15 minutes (Figure 2c). Compared to Zr-10, the resulting zirconium oxide layer became more homogeneous, thick, and continuous. This result was also confirmed from the 3D profile of Figure 2d. Figure 2e shows the anodization of Zr metal with a process time of 20 minutes. Increasing the anodization time contributed to the growth and stability of the zirconium oxide layer formed on the metal surface. The layer was more uniform, dense, and surface defects were significantly reduced. The relevant results are confirmed by Figure 2f.

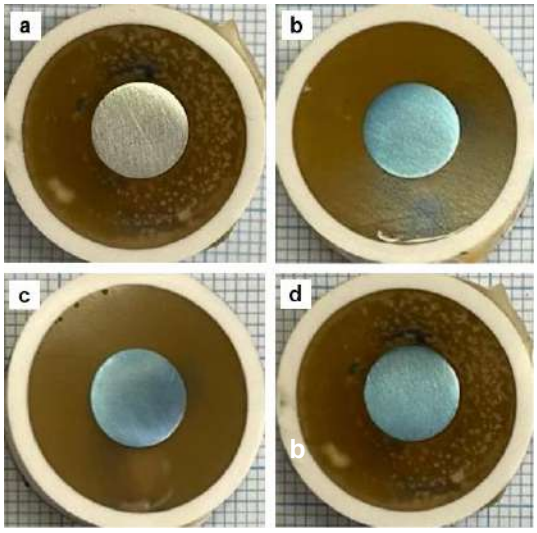

Figure 1. Color of zirconium oxide with various anodizing time of a) Zr, b) Zr-10, c) Zr-15, and d) Zr-20 minutes.

Quantitative roughness data presented in Table 1 and Figure 2 (b,d,f) confirm this observation. The average roughness (Ra) decreased from 0.53 µm for the Zr-10 specimen to 0.34 µm for Zr-15, and finally to 0.24 µm for Zr-20. This trend suggests a "leveling mechanism" where the oxide grows preferentially in the microscopic valleys of the metal surface, effectively reducing the peak-to-valley height [14]. A smoother surface is highly advantageous for nuclear cladding as it reduces the friction coefficient during fuel rod insertion and minimizes the surface area available for corrosive attack.

 DOI: https://doi.org/10.55981/urania.2026.15001

Table 1. Quantitative roughness data of anodized-Zr.

Specimen	Surface Roughness	
	Ra	Rz
Zr-10	0.53	4.35
Zr-15	0.34	4.98
Zr-20	0.24	2.34

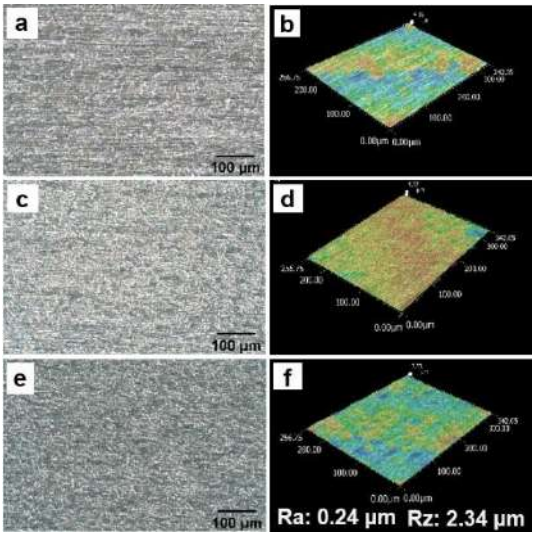

Figure 2. Microstructural analysis via optical microscopy (a,c,e), 3D profile (b,d,f), and surface roughness value (g) of (a,b) Zr-anodized 10 minutes, (c,d) Zr-anodized 15 minutes, and (e,f) Zr-anodized 20 minutes.

The zirconium substrate, whose composition decreased as the anodization duration increased, provided the Zr element. The O element showed that an oxide layer had formed during the anodization processes. The composition of the O element increased as the anodization duration increased, indicating the thickening and expansion of the zirconium oxide layer (ZrO_2). The increase in the O element was formed from 44.66 at% for the Zr-10 specimen, 53.12 at% for the Zr-15 specimen, and the highest for the Zr-20 specimen, namely 54.33 at%. The P element was also found throughout the layer's surface in addition to these primary components. The phosphate-based electrolyte used during the anodizing process is the source of the phosphorus, which is present in trace levels (around 1-2 at%) but is dispersed rather uniformly.

Figure 3 shows SEM images and the corresponding EDS area mapping of zirconium anodized under different duration processes. The surfaces of all the specimens were quite homogeneous and devoid of significant cracks. Increasing the anodization time prevented any significant morphological changes at the micrometer scale. For every modification in anodization time, the elemental mapping findings on the zirconium oxide layer's surface revealed an equitable distribution of elements. The anodized metal surface was dominated by Zr and O elements as shown in Figure 4.

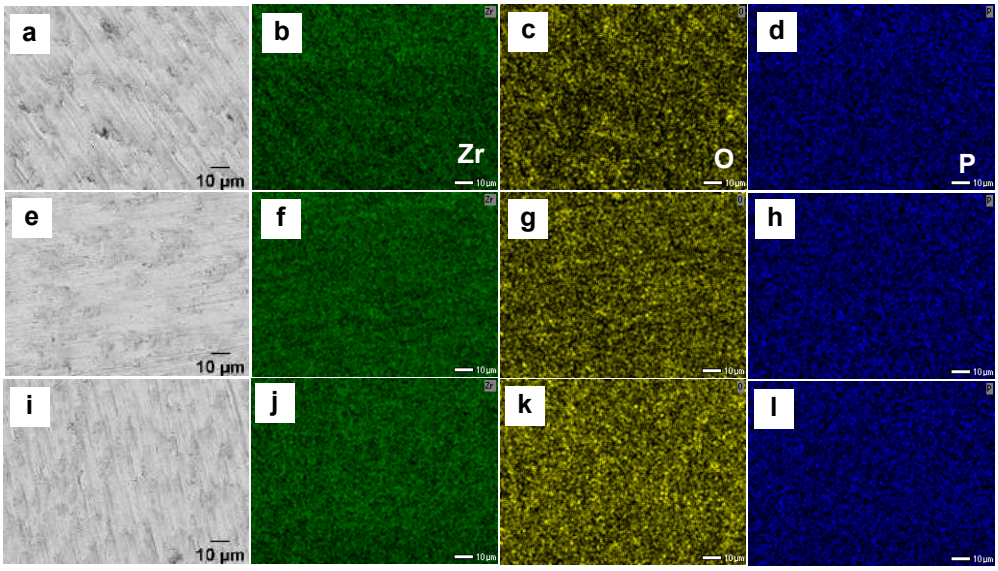

Figure 3. Surface view SEM images and the corresponding EDS area mapping of zirconium anodized of (a-d) Zr-10, (e-h) Zr-15, and (i-l) Zr-20 minutes.

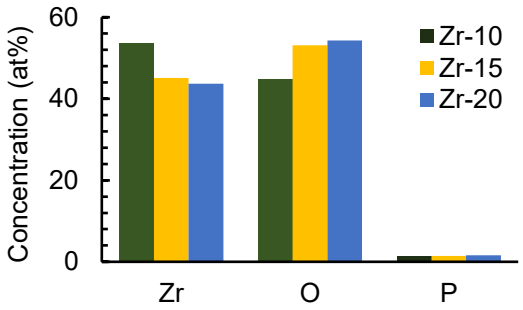

Figure 4. Elemental mapping of zirconium anodized by EDS.

Phosphorus detected in the anodic film originates from field-assisted incorporation of phosphate species during anodization rather than residual electrolyte contamination. The concentration remains low and relatively independent of anodizing time, indicating incorporation primarily during early barrier layer formation. At the detected level (~1–2 at%), phosphorus is not expected to adversely affect zirconium cladding performance, although high-temperature reactor-condition validation remains necessary

Crystalline Structure and Microhardness the XRD patterns shown in Figure 5 display sharp diffraction peaks corresponding to Zirconium Oxide (ZrO_2). The analysis suggests the presence of most tetragonal crystalline phase CDD / PDF card: 00-050-1089, which is notable as anodic films formed at lower voltages are often amorphous. The formation of this crystalline phase contributes to the chemical stability of the coating [15]. Diffraction peaks for the zirconium (Zr) and zirconium oxide (ZrO_2) phases were detected on all anodized specimens. The ZrO_2 peak's formation indicates that the anodization procedure was effective in generating an oxide layer on the zirconium substrate's surface. The ZrO_2 diffraction peak's clarity tended to rise with increasing anodization time, especially in the Zr-20 specimen, which showed the maximum peak intensity. This suggests that extended anodization durations encourage the formation of an oxide layer that is thicker and/or more crystalline. In the meantime, peaks from the Zr phase were still identified, suggesting that the relatively tiny oxide layer thickness allowed X-rays to proceed toward the substrate. In general, the XRD data confirm that different anodization times affect the zirconium oxide layer's growth and crystal properties. At the anode, the reaction that occurs can be written as:

$$Zr \rightarrow Zr^{4+} + 4e^- \quad (6)$$

$$Zr^{4+} + 2\,O^{2-} \rightarrow ZrO_2 \quad (7)$$

Meanwhile, at the cathode a reduction reaction takes place, usually involving the evolution of hydrogen gas:

$$4\,H^+ + 4\,e^- \rightarrow 2\,H_2 \quad (8)$$

Mechanical integrity was evaluated via Vickers microhardness (HV). As detailed in Table 2, the hardness values were relatively stable across the anodized samples: 144.41±8.99 HV (10 min), 144.66±7.84 HV (15 min), and 142.88±6.96 HV (20 min). Although the macroscopic hardness did not show a drastic increase compared to the substrate (likely due to the indentation depth exceeding the thin oxide layer thickness), the presence of the hard ceramic ZrO_2 skin provides essential resistance against superficial scratching and fretting wear, which are critical precursors to cladding failure [16].

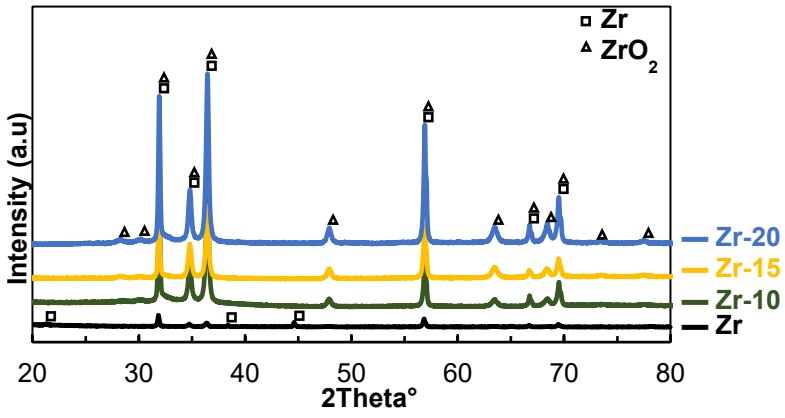

Figure 5. XRD pattern of zirconium oxide (ZrO_2)

 DOI: https://doi.org/10.55981/urania.2026.15001

Table 2. Average and Standar Deviation (STDV) for Microhardness of Zr-Anodized under different duration process.

Specimen	HV					Average	Standard Deviation
	1	2	3	4	5		
Zr-10	150.97	138.23	140.08	158.57	134.19	144.41	8.99
Zr-15	156.89	142.93	138.07	149.92	135.5	144.66	7.84
Zr-20	155.79	144.39	137.77	136.86	139.61	142.88	6.96

An oxide layer thickness quantitative summary and cross-sectional SEM images of anodized zirconium specimens treated for 10, 15, and 20 minutes are shown in Table 3 and Figure 6. This figure aims to assess how anodization time affects the shape and growth behavior of the anodic oxide layer that forms on zirconium. From Zr-10 (3.30 ± 0.67 μm) to Zr-15 (4.72 ± 1.12 μm) and Zr-20 (6.96 ± 1.42 μm), the SEM micrographs show clearly a compact and rather homogeneous oxide layer adhering to the substrate. The oxide–metal contact is displayed by the dotted line, which highlights the continuous layer growth without significant delamination. A time-dependent oxide the growth process controlled by field-assisted ionic transport, where Zr^{+} cations migrate outward and O^{2-} anions migrate inside under a strong electric field to create ZrO_2 at the interface, is suggested by the increasing thickness with anodization time. High-field oxide growth theory states that unless transport limitations or dissolving effects become visible, oxide thickness is proportional to the applied potential and processing time.

Table 3. Oxide layer thickness of anodized zirconium specimens

Specimen	Thickness (μm)
Zr-10	3.30 ± 0.67
Zr-15	4.72 ± 1.12
Zr-20	6.96 ± 1.42

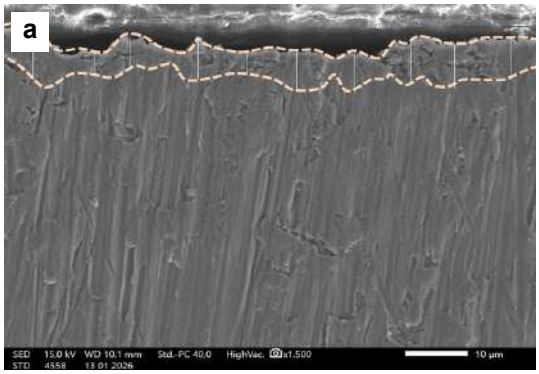

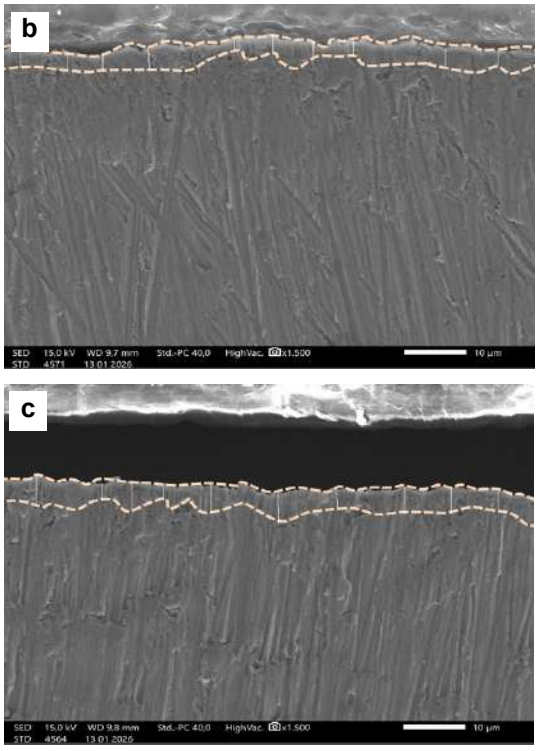

Figure 6. Cross-sectional view SEM images for zirconium anodized of (a) Zr-10, (b) Zr-15, (c) Zr-20 minutes.

Electrochemical Corrosion Behavior

The corrosion resistance was comprehensively analyzed using OCP, PDP, and EIS techniques. Open Circuit Potential (OCP): Figure 7 illustrates the OCP evolution. All anodized specimens exhibited more positive (noble) potentials compared to the bare substrate. The Zr-20 sample showed the most noble potential, stabilizing at a higher value, which indicates a thermodynamic tendency to resist spontaneous corrosion reactions in the electrolyte [17]. During the test, pure zirconium (Zr) specimens had the most negative and comparatively steady potential values, suggesting more potential for corrosion. All the specimens indicated a potential change in a more positive direction immediately after the anodization process,

which suggests that the formation of a zirconium oxide layer had increased electrochemical stability. Zr-20, Zr-15, and Zr-10 were the anodized specimens with the most positive and consistent OCP values while the test. This suggests that extending the anodization duration increases the material's resistance to corrosion and creates a more protective oxide layer. The formation of a rather stable passive layer on the zirconium surface is also shown by the stability of the OCP curves over an extended test time.

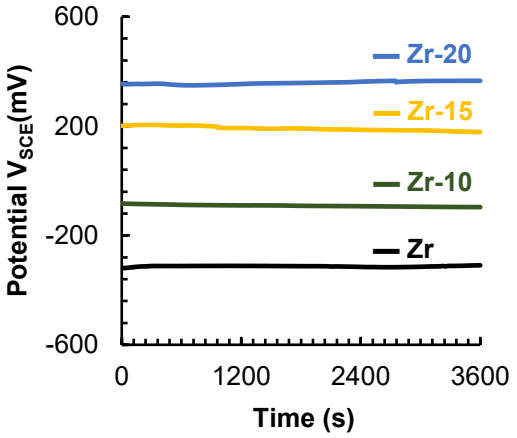

Figure 7. Average of OCP curves for zirconium substrate and zirconium-anodized at 30 V

Potentiodynamic Polarization (PDP): The Tafel polarization curves in Figure 8 demonstrate a clear shift in corrosion kinetics. The electrochemical parameters summarized in Table 4 show a dramatic reduction in corrosion current density (i_{corr}). The substrate exhibited an i_{corr} of 12.93 × 10^{-9}A/cm^2. In contrast, the Zr-20 specimen exhibited an i_{corr} of 0.19 × 10^{-9}A/cm^2. This reduction by nearly two orders of magnitude confirms that the thicker oxide layer formed at 20 minutes acts as an effective barrier, blocking the diffusion of chloride ions (Cl^-) and oxygen to the metal interface [18, 19].

Figure 8 presents the potentiodynamic polarization (PDP) curves of anodized and pure zirconium. These curves illustrate the relationship between the voltage across a reference electrode and the log current density, which is used to assess corrosion behavior and electrochemical reaction kinetics. Pure zirconium exhibits poor corrosion resistance, indicated by its limited passivation range and relatively high corrosion current density. In contrast, anodized specimens show a shift in corrosion potential to more positive values and a decrease in corrosion current density. Compared to Zr-15 and Zr-10, the Zr-20 specimen shows the biggest passivation area and the lowest current density. The Zr-20 specimen exhibits the lowest current density and the largest passivation region compared to Zr-15 and Zr-10. This suggests that the zirconium oxide layer that develops over extended anodization durations successfully prevents charge transfer and reduces the rate of corrosion.

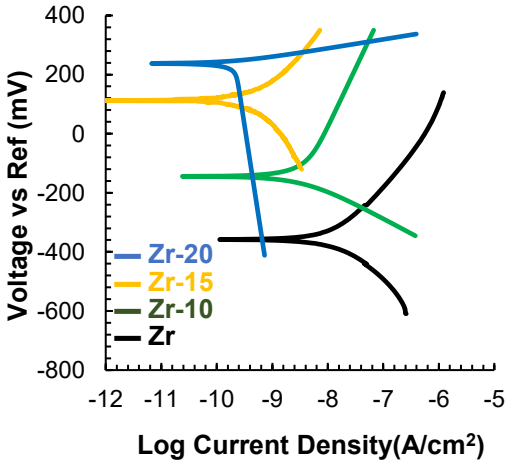

Figure 8. Average of PDP curves for zirconium substrate and zirconium-anodised at 30 V.

The blue curve corresponds to the Zr-20 specimen, which exhibits the longest anodizing duration (20 minutes). The distinct shape of this curve compared to the other samples is primarily attributed to differences in the oxide layer thickness, compactness, and electrochemical stability resulting from prolonged anodization. Several factors explain this behaviour, due to more Compact and Thicker Oxide Film. The Zr-20 sample forms a thicker and denser ZrO_2 layer, as supported by higher oxygen atomic percentage (EDS), lowest surface roughness (Ra = 0.24 μm), lowest corrosion current density (0.19 × 10^{-9} A/cm²). This compact oxide layer significantly suppresses charge transfer at the metal/electrolyte interface, resulting in:

A pronounced shift of Ecorr toward more positive values, a wider passive region, lower anodic current density. The shape

 DOI: https://doi.org/10.55981/urania.2026.15001

difference reflects a more stable passive regime in Zr-20. The reduced slope in the anodic branch indicates lower metal dissolution kinetics due to improved barrier characteristics of the oxide.

Shorter anodizing times (10 and 15 minutes) likely produce thinner films with higher defect density or localized porosity. These structural differences lead to earlier activation behavior and less stable passivation, resulting in PDP curves that differ in shape.

For Zr-20, corrosion behavior transitions from activation-controlled to diffusion-limited/passivation-controlled kinetics over a wider potential range, which explains the distinct curvature compared to the other samples.

Table 4. PDP Parameter of Zr-Anodized under different duration process.

Specimen	E_{corr} (mV)	i_{corr} (10^{-9}A/cm^2)	β_{Anodic} (mV/Decade)	$\beta_{Catodic}$ (mV/Decade)
Zr	-346 ± 88	12.93 ± 2.89	399 ± 350	275 ± 152
Zr-10	-114 ± 94	2.57 ± 1.12	599± 461	198 ± 122
Zr-15	92 ± 98	1.10 ± 0.82	275 ± 201	363 ± 262
Zr-20	233 ± 74	0.19 ± 0.04	152 ± 151	1518 ± 1067

Figure 9, the EIS results show that anodized samples exhibit significantly larger semicircle diameters in the Nyquist plots compared to the bare zirconium substrate, indicating improved corrosion resistance after anodization. The fitted parameters reveal that the charge transfer resistance (Rct) increases with anodizing time, with Zr-20 showing the highest resistance value, confirming enhanced barrier properties of the oxide layer. The solution resistance (Rs) remains relatively constant, suggesting consistent electrolyte conditions during testing. Additionally, the decrease in CPE values and the broader capacitive region in the phase angle plots indicate improved film compactness and reduced surface heterogeneity. Overall, the EIS analysis supports the PDP and OCP results, confirming that longer anodizing duration produces a thicker and more protective ZrO_2 layer that effectively suppresses corrosion reactions.

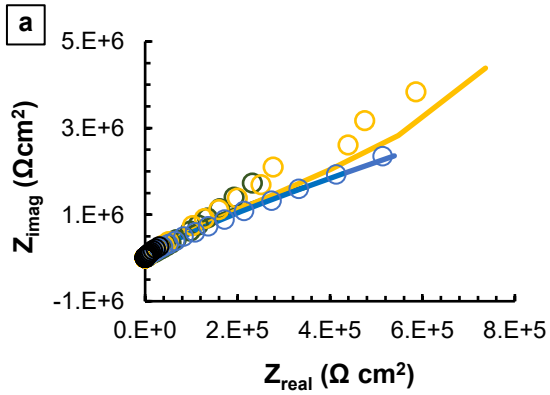

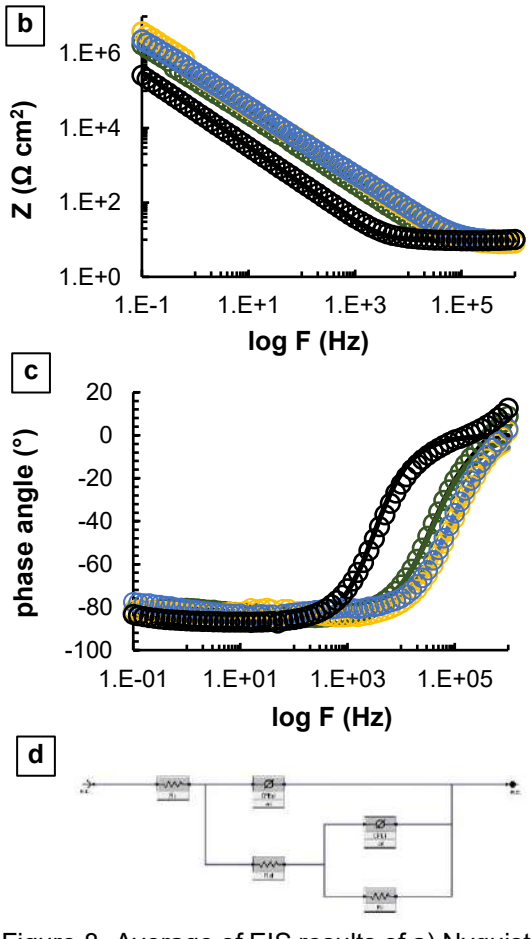

Figure 8. Average of EIS results of a) Nyquist spectra, b) bode impedance, c) bode phase, d) Equivalent electrical circuit (EEC) fitting for zirconium substrate and zirconium-anodised at 30 V

Based on Table 3, the solution resistance (Rs) remains nearly constant at approximately 10–11 Ω·cm² for all samples, confirming stable electrolyte conditions. The oxide-related resistance and charge transfer resistance increase significantly after anodization, with Rct rising from 137 Ω·cm² for Zr-10 to 150 Ω·cm² for Zr-15 and reaching 140 Ω·cm² for Zr-20, indicating improved interfacial stability. The CPE values decrease slightly from 1×10^{-8} to 6.1×10^{-8} $S\cdot s^{n}\cdot cm^{-2}$ as anodizing time increases, suggesting a more compact and less defective oxide layer. The goodness-of-fit values (χ^2 in the order of 10^{-2}) indicate that the equivalent circuit model adequately represents the experimental data. These quantitative results confirm that increasing anodizing time increases the electrochemical resistance of the zirconium surface.

Table 3. Fit parameters of EIS data.

Parameter	Substrate	Zr-10	Zr-15	Zr-20
R_s ($\Omega.cm^2$)	10	11	159	10
C_{dl} ($S^*s^a.cm^{-2}$)	$5x10^{-6}$	-	-	-
R_{ct} (Ω:cm^2)	$2x0^6$	-	-	-
CPE_{ol} ($S^*s^a.cm^{-2}$)	-	$1x10^{-8}$	$8x10^{-8}$	$6.1x10^{-8}$
a_{ol}	-	0.6	0.7	0.7
R_{ol} ($\Omega.cm^2$)	-	137	150	140
CPE_{il} ($S^*s^a.cm^{-2}$)	-	$9.3x10^{-9}$ 10^{-9}	$5.6x10^{-9}$ 10^{-9}	$5.3x10^{-9}$ 10^{-9}
a_{il}	-	0.9 10^{-3}	0.9 10^{-3}	0.9 10^{-3}
R_{il} ($\Omega.cm^2$)	-	15.00 106	15.82 106	16.40 103
Goodness of fit (χ^2)	$1.1x10^{-2}$	$3.4x10^{-2}$	$2.3x10^{-2}$	$1.4x10^{-2}$

CONCLUSIONS

The effect of anodizing duration on the surface characteristics and corrosion behavior of Zirconium was successfully investigated. The following conclusions are drawn:

1. Surface Improvement: Increasing the anodizing time from 10 to 20 minutes at 30 V results in a progressively smoother surface. The Zr-20 specimen achieved the lowest roughness (Ra= 0.24 μm), reducing friction and potential pit initiation sites.
2. Oxide Formation: The process forms a stable, crystalline ZrO_2 layer, as confirmed by XRD and the observation of interference colors.
3. Corrosion Resistance: The 20-minute anodized coating offers superior corrosion protection in chloride environments. It reduced the corrosion rate i_{corr} by approximately 98% compared to the bare substrate and significantly increased the polarization resistance.
4. Application Viability: The study confirms that a 20-minute anodizing treatment is an effective, low-cost method to enhance the durability of Zirconium nuclear fuel cladding, potentially extending the safety margins against corrosion and mechanical degradation in PWR environments.

REFERENCES

[1]. A. T. Motta, A. Couet, and R. J. Comstock, “Corrosion of zirconium alloys used for nuclear fuel cladding,” *Annual Review of Materials Research*, vol. 45, pp. 311–343, 2015.

[2]. Z. Duan, H. Yang, Y. Satoh, and K. Murakami, “Oxidation behavior of zirconium alloys in a simulated nuclear reactor primary coolant,” *Journal of Nuclear Materials*, vol. 485, pp. 147–158, 2017.

[3]. K. A. Terrani, “Accident tolerant fuel cladding development: Promise, status, and challenges,” *Journal of Nuclear Materials*, vol. 501, pp. 13–30, 2018.

[4]. W. Gong and D. Yun, “A review on the corrosion behavior of zirconium alloys in supercritical water,” *Corrosion Science*, vol. 208, p. 110620, 2022.

 DOI: https://doi.org/10.55981/urania.2026.15001

[5]. A. Yilmazbayhan, A. T. Motta, and R. J. Comstock, “Hydride morphology and embrittlement in Zircaloy-4 cladding,” *Journal of Nuclear Materials*, vol. 545, p. 152646, 2021.
[6]. J. Liu and Q. Li, “Fretting wear behavior of zirconium alloy cladding tubes,” *Wear*, vol. 522, p. 204689, 2023.
[7]. H. G. Kim and I. H. Kim, “Oxidation behavior of zirconium alloy claddings in high temperature steam,” *Nuclear Engineering and Technology*, vol. 52, no. 4, pp. 808–815, 2020.
[8]. S. Suresh and A. Sharma, “Surface modification of zirconium alloys for biomedical and nuclear applications: A review,” *Surface and Coatings Technology*, vol. 405, p. 126666, 2021.
[9]. R. Verma and S. Kumar, “Electrochemical anodization of zirconium: Growth mechanism and properties,” *Electrochimica Acta*, vol. 412, p. 140135, 2022.
[10]. Y. Cheng and E. Matykina, “Formation of nanotubular oxide layers on zirconium alloys by anodization,” *Corrosion Science*, vol. 182, p. 109289, 2021.
[11]. F. Ali and M. Al-Hajri, “Effect of voltage and electrolyte composition on the morphology of anodic zirconium oxide,” *Materials Chemistry and Physics*, vol. 295, p. 127087, 2023.
[12]. L. Wang, Y. Zhang, and X. Wu, “Time-dependent growth kinetics of anodic films on zirconium in phosphate electrolytes,” *Journal of Electrochemical Society*, vol. 171, no. 2, p. 021504, 2024.
[13]. M. V. Diamanti and M. P. Pedeferri, “Color production on zirconium by anodizing: Interference and absorption effects,” *Color Research & Application*, vol. 45, no. 3, pp. 456–464, 2020.
[14]. G. E. Thompson, “Porous anodic oxide films: Formation, growth and applications,” *Thin Solid Films*, vol. 685, pp. 34–45, 2019.
[15]. X. Zhao and H. Xu, “Phase transformation in anodic zirconia films: From amorphous to crystalline,” *Scripta Materialia*, vol. 210, p. 114421, 2022.
[16]. E. G. Obbard and P. A. Burr, “Mechanical properties of zirconium oxide scales: A review,” *Journal of Nuclear Materials*, vol. 557, p. 153255, 2021.
[17]. E. McCafferty, Introduction to Corrosion Science, 2nd ed. Springer, 2020.
[18]. B. Zhang and G. S. Frankel, “Corrosion mechanisms of zirconium alloys in chloride-containing environments,” *Corrosion*, vol. 78, no. 5, pp. 412–425, 2022.
[19]. T. Li and F. Wang, “Improvement of pitting corrosion resistance of Zr alloys by anodic oxidation,” *Applied Surface Science,* vol. 610, p. 155567, 2023.
[20]. M. E. Orazem and B. Tribollet, Electrochemical Impedance Spectroscopy. Wiley, 2017.